



Universiteit
Leiden
The Netherlands

Novel functions of MDMX and innovative therapeutic strategies for melanoma

Heijkants, R.C.

Citation

Heijkants, R. C. (2018, October 18). *Novel functions of MDMX and innovative therapeutic strategies for melanoma*. Retrieved from <https://hdl.handle.net/1887/66268>

Version: Not Applicable (or Unknown)

License: [Licence agreement concerning inclusion of doctoral thesis in the Institutional Repository of the University of Leiden](#)

Downloaded from: <https://hdl.handle.net/1887/66268>

Note: To cite this publication please use the final published version (if applicable).

Cover Page



Universiteit Leiden



The handle <http://hdl.handle.net/1887/66268> holds various files of this Leiden University dissertation.

Author: Heijkants, R.C.

Title: Novel functions of MDMX and innovative therapeutic strategies for melanoma

Issue Date: 2018-10-18

Novel functions of MDMX and innovative therapeutic strategies for melanoma

Renier C. Heijkants

Cover by: Linda van Zijp, StudioLIN.

Lay-out and print by: ProefschriftMaken // www.proefschriftmaken.nl

ISBN: -

Copyright 2018 by Renier C. Heijkants, Oss, The Netherlands. All rights reserved.

Copyright of individual chapters lies with the authors, except for chapters 3 and 5.

No part of this thesis may be reproduced, digitalized or transmitted in any form, by any means, electronic or mechanical, including photocopying, recording or by any information storage or retrieval system, without prior permission from the author.

Novel functions of MDMX and innovative therapeutic strategies for melanoma

Proefschrift

ter verkrijging van
de graad van Doctor aan de Universiteit Leiden,
op gezag van Rector Magnificus prof.mr. C.J.J.M. Stolker,
volgens besluit van het College voor Promoties
te verdedigen op donderdag 18 oktober 2018
klokke 13:45 uur

door

Renier C. Heijkants
geboren te Amersfoort
in 1989

Promotor

Prof. dr. P. ten Dijke

Co-promotor

Dr. A.G. Jochemsen

Promotiecommissie

Prof. dr. M.J. Jager

Prof. dr. B.M.T. Burgering (Universitair Medisch Centrum Utrecht)

Prof. dr. B.E. Snaar-Jagalska (Universiteit Leiden)

Dr. R. van Doorn

'Imagine'

John Lennon

9 oktober 1940 – 8 december 1980

Table of contents

Chapter 1	General introduction	9
Chapter 2	MDMX regulates transcriptional activity of p53 and FOXO	37
Chapter 3	Targeting MDMX and PKC δ to improve current uveal melanoma therapeutic strategies	77
Chapter 4	Combined EZH2 and HDAC inhibition as novel therapeutic intervention for metastasized uveal melanoma	103
Chapter 5	Combined inhibition of CDK and HDAC as a promising therapeutic strategy for both cutaneous and uveal metastatic melanoma	123
Chapter 6	General discussion	153
Appendix	Dutch summary	172
	Curriculum Vitae	180
	List of publications	181
	Acknowledgements	183
	List of abbreviations	185

CHAPTER 1

General introduction

1. THE P53 PROTEIN AND ITS REGULATORS MDM2 AND MDMX

1.1 p53

The p53 protein was originally discovered in 1979 as a target of the SV40 oncogenic DNA virus Large T-antigen [1, 2]. More than 3 decades later and over 92.000 scientific papers published mentioning p53, the p53 protein is recognized as a central node in cellular stress responses. The p53 protein functions as a transcription factor, which upon activation and stabilization controls the expression of many genes involved in multiple pathways including cell cycle, metabolism, apoptosis and angiogenesis [3-5]. Despite its central role in cellular responses to stress, p53-deficient mice develop almost normal, but are prone to develop malignancies of which lymphomas are most frequent [6, 7]. Mutations in the *p53* gene are found in proximally 50% of all human cancers, emphasizing the importance of the tumor suppressor function of p53 [8, 9]. A more detailed analysis shows that 95% of *p53* mutations are found in the exons encoding DNA binding domain, underlining its tumor suppressor function as transcription factor [10]. A mutation in the DNA binding domain renders p53 incapable of binding to its consensus DNA recognition sequence, losing its transcription regulatory function, rendering a cell sensitive for a malignant transformation and relatively resistant to stress induced apoptosis, cell cycle arrest or senescence, e.g. induced by chemotherapeutics, radiation or hypoxia.

Despite this high mutation frequency, incidence of *p53* mutations differs considerably between cancer types. *P53* mutations are found rarely (<1%) in, for example, uveal melanoma (UM) and thyroid cancer, while mutations are found commonly (>90%) in ovarian cancer and lung squamous cell carcinoma (Figure 1) [11]. It is believed that in tumors expressing wild-type p53 the tumor suppressor pathway of p53 is inhibited either upstream or downstream, implicating that all cancers have an attenuated p53 pathway [4].

1.2 Regulation of p53 by MDM2 and MDMX

The central and important functions of p53 in cell-fate determination imply that p53 activity should be tightly controlled, in which ubiquitin ligase mouse double minute (MDM) 2 and the structurally related MDMX play a pivotal role. The importance of the MDM2 and MDMX proteins for p53 regulation is best illustrated by the mouse KO models. Knockout of either *MDM2* or *MDMX* is embryonic lethal in a fully p53-dependent manner [12-14]. Whereas *MDM2* transgenic mice can rescue the *MDMX* knockout phenotype, high *MDMX* levels in *MDMX* transgenic mice cannot rescue the *MDM2* knockout [15, 16]. Although both *MDM2* and *MDMX* are crucial for embryonic development, in adult cells and tissues *MDM2* loss is still always lethal whereas

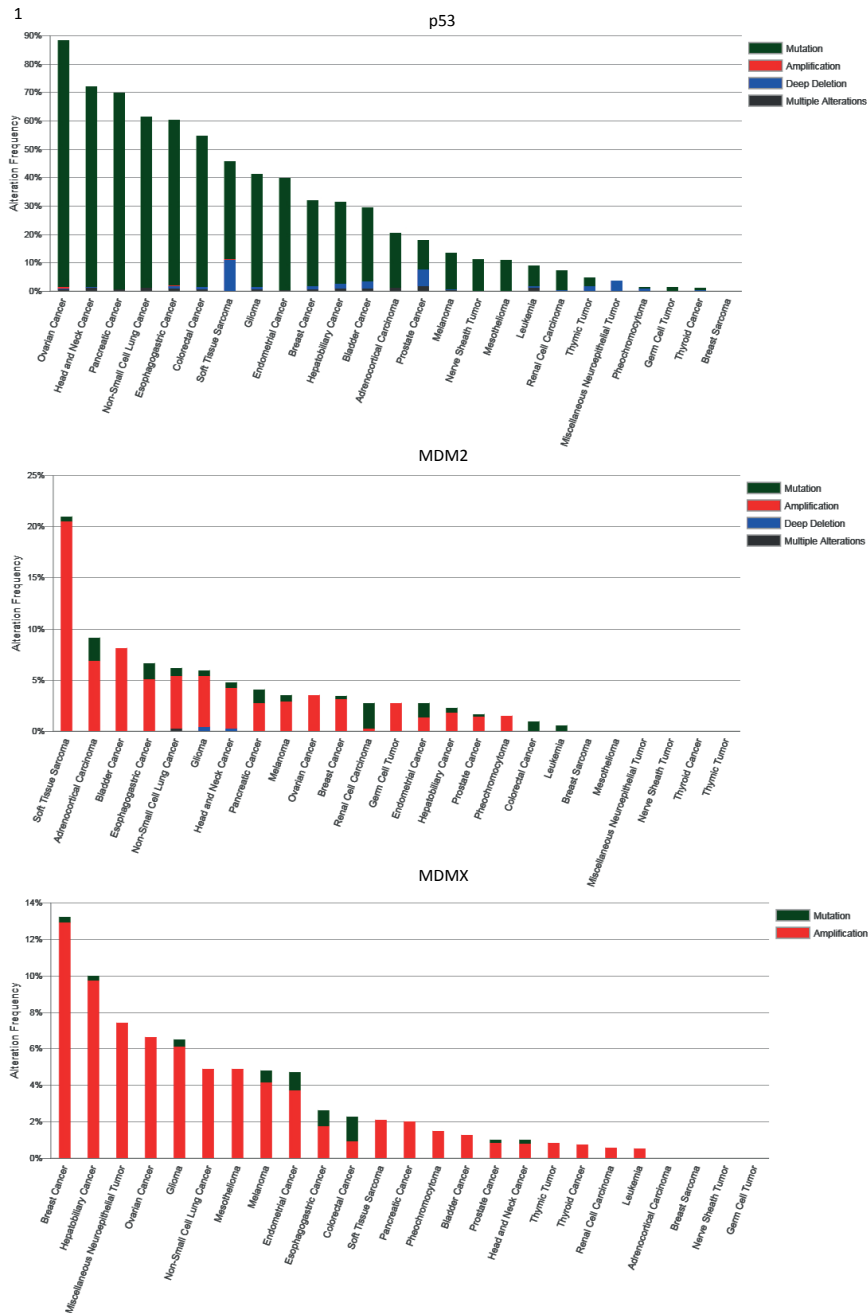


Figure 1. Genomic alterations affecting p53, MDM2 or MDMX in different cancers. Frequency of mutations (green), amplifications (red), deep deletions (blue) and multiple alterations (gray) are given per cancer. Data depicted is derived from www.cbioportal.org and only shows TCGA provisional data sets.

MDMX loss can be compatible with life, probably because in most adult tissues *MDMX* protein is not or hardly detectable anyway [17-23]. *MDM2* is an E3 ubiquitin ligase and has been shown to directly bind *p53* [24]. *MDM2* activity results in lysine-48 poly-ubiquitination of *p53*, which is consequently degraded by the proteasome [25]. Thereby *MDM2* effectively keeps the basal levels of *p53* low and thus promotes cell proliferation and survival. Both the RING finger domain and the central acidic domain of *MDM2* are essential for the *p53* ubiquitination [26, 27]. Although *MDM2* during animal development is mainly acting through the repression of *p53*, *MDM2* has been reported to have *p53*-independent functions and ubiquitination targets [28-31].

The essential *p53* inhibitor *MDMX* was initially discovered as a novel *p53* interactor with high sequence homology with *MDM2* [32]. *MDM2* and *MDMX* have great structural similarities of which the N-terminal hydrophobic pocket that binds the N-terminal alpha helix of *p53*, shielding the *p53* transactivation domain, is best conserved [33, 34]. Despite the high conservation of the RING finger domain and the central acidic domain *MDMX* does not have any E3 ubiquitin ligase activity and its main *p53* inhibitory function is shielding the *p53* transactivation domain [26, 27]. Despite the lack of intrinsic E3 ligase activity *MDMX* forms a heterodimer with *MDM2* [35], which is thought to promote *MDM2* E3 activity by providing a better scaffold for E2-enzyme binding, thus resulting in faster degradation of *p53* [36, 37]. Considering that the levels of *MDM2* and *MDMX* are crucial for cellular activity of *p53*, expression of these proteins should also be tightly controlled. *p53* has to be liberated from *MDM2* and *MDMX* to exert its function upon certain stress, for example in response to DNA damage. Several phosphorylation events on *MDM2*, mediated by serine/threonine kinase ATM, inhibit its ubiquitin ligase activity towards *p53* [38]. Upon stresses, *MDM2* both auto-ubiquitinates [38, 39] and ubiquitinates *MDMX* [40-42] sending both for proteasomal degradation. This cellular depletion of inhibitory proteins results in a feed forward loop in which *p53* is stabilized and activated. After cellular stress, for example induced by DNA damage, during the recovery phase a cell needs to re-constrain *p53*. It has been shown that both *MDM2* and *MDMX* are transcriptional targets of *p53* providing a negative feedback loop and thus re-establish *p53* inhibition [43, 44].

1.3 Reactivating *p53* in cancer

In order to become malignant cells need to lose or at least attenuate *p53* activity, for example by direct gene mutation [8, 9]. Therefore, specifically targeting *p53* mutated cancer cells would provide a very interesting therapeutic intervention, potentially benefitting half of all cancer patients. It was reasoned that cancer cells with mutated *p53* would remain sensitive for *p53*-induced apoptosis, since the downstream path-

way remains intact [45]. Therefore, various approaches were designed to reactivate mutant p53 [46]. One compound discovered to reactivate mutant p53 was named p53 reactivation and induction of massive apoptosis (PRIMA) [45], which binds the core domain the DNA binding domain of p53 and changes the conformation from mutant to wild-type, resulting in the induction of apoptosis [47, 48]. This biological effect induced by PRIMA has been suggested to be specific for p53 mutant cell lines [49]. However, evidence is accumulating that PRIMA induces anti-cancer effects regardless of the presence of p53 mutations [50, 51]. This could be explained, at least in part, by the observation that PRIMA also targets other p53 family members such as p63 and p73 [51-53]. Other approaches found to target p53 mutated cells include the cholesterol lowering drugs, the statins [54, 55]. Depletion of cells from mevalonate-5-phosphate by treatment with statins resulted in impairment of the mutant-p53 interaction with the chaperone protein DNAJA1/hsp40 which caused ubiquitin E3 ligase CHIP-mediated degradation of mutant p53 [55]. These studies have provided new insights with potential new strategies to specifically target mutant p53 cells.

Despite the frequent occurrence of *p53* mutations, the remaining half of human cancers had to find alternative mechanisms to attenuate p53 signaling [4]. Amplifications of the *MDM2* gene are frequently found in sarcoma [56-58] and esophageal cancer [59] (Figure 1). Similarly to *MDM2*, *MDMX* amplifications and overexpression are found in various cancers including glioblastoma [60], retinoblastoma [61] and breast cancer [62], in most cases correlating with wild-type *p53* status (Figure 1). The MDM2 interaction with the p53 transactivation domain is well defined by crystal structures [63]. These structures show that the hydrophobic pocket of MDM2 interacts with 3 side chains from a peptide derived from the p53 transactivation domain. This clearly defined pocket and interaction between MDM2 and p53 allowed for effective drug development. The first small molecule compound described to bind MDM2 in its p53-binding pocket was Nutlin-3 [64]. Antagonizing the MDM2-p53 interaction using Nutlin-3 resulted in stabilization of p53 in an MDM2-amplified osteosarcoma cell line, leading in cell cycle arrest and apoptosis, both *in vitro* and *in vivo*. Importantly, the p53 activation by Nutlin-3 was not due to DNA damage signaling [65, 66]. This mode of action resulted in the observation that mice treated with Nutlin-3 did not lose weight while p53 was being activated, indeed separating Nutlin-3 from DNA damaging agents and their associated adverse clinical effects [64]. This approach has spurred the development of various small molecule compounds targeting the MDM2-p53 interaction such as 1, 4-benzodiazepin-2, 5-dione [67], spiro-oxindoles [68] and RITA [69], all resulting in p53 stabilization and inducing cell cycle arrest and apoptosis. Although found in a screen to identify p53 re-activating compounds and thought originally to block the MDM2-p53 interaction, RITA elicits a DNA damage

response, rendering the anti-cancer effects not exclusive to the MDM2-p53 inhibition [70-72]. Furthermore, some evidence exists indicating that RITA does not block the MDM2-p53 interaction [73], implying that RITA targets cells expressing p53, but not by directly binding to p53.

Based on these promising results *in vitro* and in pre-clinical mouse models, a number of clinical trials were initiated using various compounds targeting the MDM2-p53 interaction [74]. RG7112, a Nutlin-3 analog, was initially tested in liposarcoma patients with *MDM2* amplifications. Of the 20 patients in this clinical trial 14 had stable disease and 1 patient had a partial response [75]. Besides its therapeutic potential RG7112 treatment elicited severe neutropenia and thrombocytopenia in these patients. In a phase 1 clinical trial assessing RG7112 in 116 patients with various hematological malignancies, similar to the sarcoma trial, 22% of the patients showed severe neutropenia [76]. Although MDM2 inhibition has a clinical benefit for these patients, the strong, on target, adverse effects need to be managed in order to continue long-term MDM2 inhibition [77]. In addition, resistance to MDM2 inhibition has been shown to occur via specific point mutations in *p53* [78, 79].

Antagonists for the MDMX-p53 interaction have been in development since *MDMX* amplification and/or overexpression in *p53* wildtype tumors was discovered. Despite the overall structural similarity between MDM2 and MDMX, some important differences were found in their p53 binding pocket [34, 80]. These slight changes in the p53-binding hydrophobic cleft reduce the binding capabilities of Nutlin-3 to MDMX approximately 40 fold, although Nutlin-3 can still clearly antagonize the interaction between MDMX and p53 [61]. The reduced efficacy of MDM2 inhibitors for MDMX suggested a window of specificity, which led to the pursue of an MDMX-specific inhibitor. SJ172550 was the first described small molecule specifically designed to block the MDMX-p53 interaction [81]. However, it has been described later that SJ172550 is not a simple inhibitor between MDMX and p53, but locks MDMX in a conformational state by covalent interaction that is unable to bind p53 [82]. Unfortunately, this conformational state change is dependent on many factors including the reducing potential of the media, hindering the further clinical development of SJ172550 [82]. Another study described molecules inhibiting MDMX transcription, e.g. XI-006 and XI-011 [83]. These compounds resulted in the cellular depletion of MDMX promoting p53 activation, reportedly without induction of double strands DNA breaks, providing treatment options for various cancers [84-86]. However, this MDMX depletion effect by XI-011 was later shown to be partly due to increased DNA damage signaling resulting in MDMX degradation and subsequent p53 activation [86, 87] and apoptosis induced by XI-006 in Ewing Sarcoma was even shown to be p53 independent [85]. It

thus appears that the design of small molecules specifically targeting MDMX without inducing DNA damage signaling is a difficult task. It could be that dual inhibitors of MDM2 and MDMX provide a solution [88]. By simultaneously inhibiting MDM2 and MDMX p53 activation is boosted, meaning that less MDM2 inhibition (and therefore less adverse effects) might be needed to achieve functional p53 activation.

Alternative approaches to target MDMX could involve other pathways, which have shown to play a role in overexpression of MDMX. It has been demonstrated that the receptor tyrosine kinases Her4 (also known as ErbB4) and AXL are capable of stabilizing MDMX in order to suppress p53 [89, 90]. Targeting these signaling pathways might be a potent way to destabilize MDMX, thus releasing p53 activity, possibly without inducing DNA damage signaling. However, these kinases have multiple targets and downstream effects independently of MDMX, which will make the analysis of these inhibitors on MDMX function especially difficult.

Alternative splicing is yet another mechanism by which the abundance of MDMX is reduced upon DNA damage [91]. The short isoform of MDMX, missing exon 6, is a naturally occurring transcript, which results in a short protein due to an early stop [92]. Mice that are lacking exon 6 are embryonic lethal in a p53-dependent manner [93]. By promoting the skipping of exon 6 using anti-sense oligonucleotides the splicing ratio could be altered favoring the short over the full length isoform, resulting in decreased MDMX protein levels [94]. MDMX has been shown to be a potent target in both melanoma [95] and wildtype p53 breast cancer [96]. Depletion of MDMX resulted in a cell cycle arrest and apoptosis in a partly p53-independent manner [87, 95]. The p53-independent cell cycle arrest could be explained, at least in part, by the p53-independent upregulation of the cyclin dependent kinase (CDK)-inhibitor p27 upon MDMX depletion [87]. These results suggest that MDMX might not only be a therapeutic target in wildtype p53 tumors, but also in p53 mutated tumor cells. Indeed, p53 mutated breast cancer cell lines expressing high levels of MDMX are dependent on continuous MDMX expression for proliferation [97].

2. MELANOMA

To study the functions of p53 and especially of MDMX, this thesis focusses on melanoma, a malignancy arising from melanocytes. In cutaneous melanoma p53 mutation frequency is low (10-20%) and UM cells essentially lack p53 mutations [98, 99]. Despite the absence of *MDM2* or *MDMX* amplification, melanoma cells frequently overexpress one or both of these p53 inhibitors, especially MDMX [87, 95]. Since melanoma

patients with distant metastases respond poorly to classical chemotherapy and, therefore, have a short overall survival, studying melanoma with a focus on the MDMX/p53 complex is highly clinically relevant [100]. Although melanoma encompasses only a low percentage of skin cancer, melanoma is a deadly form of cancer causing most of the skin cancer-associated deaths. The increased melanoma incidence found over the last decades emphasizes the importance of finding an effective cure for melanoma [101]. Due to advances in early detection of melanoma the primary tumors can be efficiently resected resulting in high survival rates. However, prognosis significantly worsens upon metastasis. Improvements have been made during the past decades in understanding melanoma and how to use this knowledge to target this malignancy. The main current treatments for melanoma are briefly discussed below.

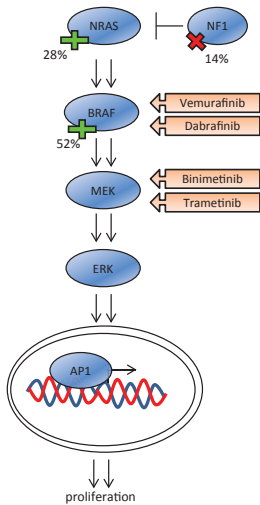
2.1 Cutaneous melanoma

2.1.1 Targeted therapy

Previous studies have already reported that the MAPK signaling pathway is activated in various cancer types including melanoma [102]. The most frequent and well described melanoma driver is an activating mutation in the serine/threonine kinase *BRAF* gene in up to 50% of melanomas. Most common mutation is the valine (V) substitution for glutamic acid (E) of codon 600 (V600E), feeding into the MAPK pathway and driving melanomagenesis [102]. Mutations upstream of *BRAF*, mainly in *NRAS*, are found in 10-25% of all cutaneous melanoma cases [103]. The most common activating *NRAS* mutation occurs at the codon for glutamine (Q) 61 [104]. These hotspot mutations in *BRAF* and *NRAS* rendering the proteins permanently active, and continuously stimulate the pro-proliferation MAPK pathway. Additionally, in 14% of cutaneous melanoma samples inactivating mutations are found in *NF1*, a GTPase-activating protein. By losing *NF1* expression RAS-GTP is much slower converted to its inactive GDP form, resulting in increased RAS activation and consequently an overactive MAPK pathway. Therefore, loss of *NF1* (14%), activating mutation in *NRAS* (28%) or in *BRAF* (52%) explains the activated MAPK signaling in 94% of all melanoma cases (Figure 2A) [104].

Recently, a novel classification was presented identifying four major subtypes of cutaneous melanoma; *BRAF*, *NRAS*, *NF1* and the so called triple-negative [104]. Interestingly, mutations in the gene encoding the receptor tyrosine kinase (RTK) *KIT* are enriched in the triple-negative subgroup. Although only 3% of all melanoma have *KIT* mutations or amplifications, these mutations are more commonly found in melanoma originating from mucosal, acral a chronically sun-damaged surface [105]. Like *BRAF* and *NRAS*, mutations in *KIT* focus on a 'hot-spot' with 30% of *KIT* mutations showing an activating L576P substitution, suggesting a potential therapeutic benefit of the

2A



B

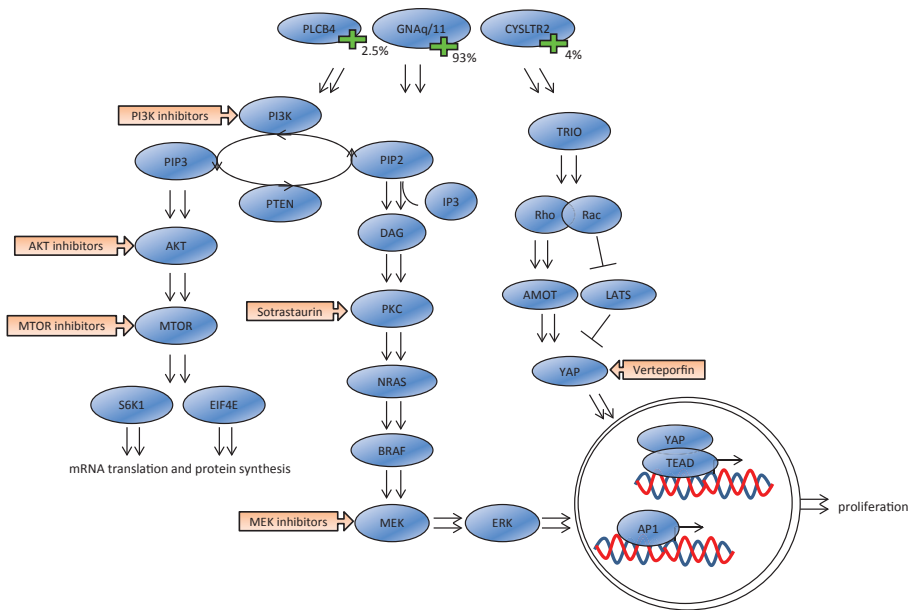


Figure 2. Melanoma signaling and therapeutic interventions. A) Cutaneous melanoma signaling driven by activating mutations in BRAF/NRAS or inactivating mutations in NF1. Therapeutic interventions consist of BRAF and MEK inhibition via Vemurafinib/Dabrafenib and Binimetinib/Trametinib respectively. B) Oncogenic mutations driving signaling in uveal melanoma. Activating mutations in PLCB4, GNAQ/11 and CYSLTR2 drive the PI3K/AKT/MTOR, PKC/MEK and the YAP pathway. Therapeutic interventions in uveal melanoma therefore consist of PI3K, AKT, MTOR, PKC, MEK and YAP inhibitors

use of RTK inhibitors in these patients [106]. When patients carrying a *KIT* mutation were treated with RTK inhibitory molecules, these cancer patients develop therapy resistance by acquiring secondary *NRAS* mutations [107].

Knowledge about *BRAF* and *NRAS* mutations have led to the development of mutant specific *BRAF*V600E inhibitors and MEK inhibitors, blocking the oncogenic MAPK pathway [108]. Despite single agent success to *BRAF* and MEK inhibition, most patients develop disease progression after 6 to 7 months and only a small portion remain disease free [109-112]. The major factor contributing to *BRAF* and MEK inhibitor resistance found was the reactivation of the same MEK/ERK pathway via alternative means, such as activation of other receptor tyrosine kinases or *NRAS* upregulation [113-119]. MEK inhibition and *NRAS* depletion both trigger an apoptotic program in *NRAS* mutated melanoma, whereas only *NRAS* depletion additionally resulted in a CDK inhibitory effect. Indeed combined MEK and CDK4 inhibition resulted in synergistic therapeutic effect [120]. These results suggest that CDK4 inhibition might result in increased patient survival in combination with MEK inhibition, which is currently being investigated in an ongoing clinical trial (identifier: NCT01781572).

2.1.2 Immunotherapy

In addition to *BRAF*- and MEK inhibitors [109, 121, 122] the FDA has also approved immunotherapies for melanoma treatment [123, 124]. The first immune checkpoint which could be effectively targeted and inhibited was cytotoxic T-lymphocyte antigen-4 (CTLA-4) [125]. The response of a T lymphocyte, upon binding of the T cell receptor to a peptide presenting MHC molecule, is the result of a balance of both stimulatory and inhibitory signals (reviewed by [126]). This balance consists of the stimulatory interaction between CD80/86 (on the antigen presenting cell) and CD28 and the inhibitory signals residing from an interaction between CD80/86 and CTLA-4. Cancer cells take advantage of these inhibitory signals by hiding them from tumor antigen-specific T-lymphocytes. Tumor-specific antigens arise as a consequence of genomic mutations. By blocking the inhibitory signals with CTLA-4 with monoclonal antibody Ipilimumab the T-lymphocytes are unleashed and shows convincing clinical efficacy [123, 127]. Moreover, Ipilimumab was the first treatment to prolong the survival of advanced melanoma patients, highlighting the clinical importance of these therapies [123, 127].

Another effective immunotherapeutic approach is by blocking PD-1 and/or PD-1L using monoclonal antibodies. PD1 is a receptor expressed on various activated immune cells such as T-, B-, natural killer- cells and T- regulatory cells [128]. When PD1 binds to its ligand PD-1L, presented by an antigen presenting cell, the efficacy of the activated

immune cell is attenuated [129]. Like CTLA-4, PD-1/PD-1L blocking results in increased progression free- and overall survival, with a manageable toxicity profile [130-133]. Interestingly, BRAF inhibition seems to enhance PD-1/PD-1L expression suggesting that down regulating the immune system is beneficial for the acquirement of BRAF resistance [134]. These data suggested already that combining BRAF inhibition with immunotherapy could boost the efficiency of each single therapy. And indeed, pre-clinical data have shown that combining BRAF inhibition with immunotherapy has significant additive effects over the single treatments [135, 136].

2.2 Uveal melanoma

Uveal melanoma (UM) accounts for approximately 5 % of total melanoma incidence and originates from the choroid (85%), iris (5%) or ciliary body (10%) [137, 138]. Driver mutations in UM are found in the α subunits of G-proteins *GNAQ* (50%) or *GNA11* (43%), mainly resulting in a Q209L substitution locking GNAQ/11 in a GTP-bound, active state [139-141]. Due to the high frequency of these activating mutations in GNAQ/11, like BRAF in cutaneous melanoma, targeting the mutant protein(s) could potentially serve as an interesting therapeutic intervention. Although a number of cyclic depsipeptides have been reported to selectively inhibit GNAQ, it has not been investigated properly whether these compounds can still bind the mutant GNAQ [141, 142]. UM without *GNAQ* or *GNA11* have mutual exclusive mutations in the G-protein coupled receptor encoding *Cysteinyl Leukotriene Receptor 2 (CYSLTR2)* (4%) or the downstream effector *Phospholipase C Beta 4 (PLCB4)* (2.5%) [143, 144]. Together these data demonstrate that constitutively active G-protein signaling is an important early event in UM.

Like with cutaneous melanoma, the primary UM tumor can be treated efficiently. However, once UM patients develop metastasis, which happens in about half of the patients within 15 years after primary tumor detection, median survival is reduced to only several months since no effective treatment exists [145-147]. Frequent chromosomal aberrations in UM are loss of one copy of chromosome 3, amplification of 8q, 6p or both. Less frequently 8p gain or loss of 1p, 6q and 16q is observed [148, 149]. Monosomy 3 strongly correlates with development of metastasis and therefore is a marker for poor prognosis [150, 151]. The *BAP1* gene residing at chromosome 3 frequently shows an inactivating mutation and the remaining wild type *BAP1* allele is often lost due the monosomy 3 [152]. Mutations in *BAP1* have a strong predictive power for the occurrence of metastasis in UM and 80-90% of the metastatic patients contain a *BAP1* mutation [152, 153]. *BAP1* functions as a de-ubiquitination enzyme and a regulator of cell cycle progression and DNA damage response [154-157]. It is thought that *BAP1* influences these processes by de-ubiquitination of one of its

primary targets, histone 2A [158]. Depletion of BAP1 *in vitro* results in a stem cell-like phenotype of UM cells [159]. In addition to monosomy 3 and loss of BAP1 expression, gain of 8q is associated with poor survival rates [160, 161]. Multiple potentially interesting genes residing on 8q could potentially explain the poor survival and/or provide interesting therapeutic targets, such as proto-oncogenes *PTP4A3*, *c-MYC*, *PVT1*, *LYN* and *MOS*.

In addition, mutations have been found in the *EIF1AX* gene, coding for Eukaryotic Translation Initiation Factor 1A X-linked, an essential component of translation initiation [162-164]. Mutations in *EIF1AX* occur for 20% in N-terminal end of the protein, which do not include inactivating mutations, such as frame shifts suggesting activating mutations [163, 165]. Mutations in *EIF1AX* are associated with good prognosis and subsequently correlate with disomy 3 [163]. Interestingly, only the mutant allele is expressed suggesting an oncogenic selection advantage [163]. Depletion of *EIF1AX* in wild type and mutant cell lines result in reduced cell viability, suggesting *EIF1AX* to be an essential gene [165]. Another gene often found mutated in UM in which two copies of chromosome 3 are retained is encoding the splicing factor 3B subunit 1 (*SF3B1*) and these mutations corrupt *SF3B1* functioning and are associated with a favorable prognosis [162, 166]. However, it has recently been shown that, although *SF3B1* mutations have a favorable prognosis compared to monosomy 3 tumors, these mutations are associated with metastasis development after 5 year [167], indicating that *SF3B1* mutations are a long term poor prognosis marker. Mutations in *SF3B1* are found in 10-21% of patients and mainly affect Arg625 [163, 166]. *SF3B1* has been shown to be an essential part of the spliceosome [168]. It is, therefore, not surprising that mutations in *SF3B1* resulted in alterations in the splicing of many genes [169, 170]. It remains unclear how *EIF1AX* and *SF3B1* mutations exactly contribute to melanoma formation and how their functions correlate with their respective prognostic implications. It could be hypothesized that due to the mutual exclusive pattern and functioning in RNA processing *EIF1AX* and *SF3B1* have partly overlapping functions in driving UM.

Most novel therapeutic interventions employed for metastasized UM focus on mutated G-protein signaling. G-protein coupled signaling feeds into the known oncogenic MAPK pathway via its important effector PLC- β , which hydrolyzes phosphatidylinositol 4,5-bisphosphate (PIP2) into inositol 1,4,5-trisphosphate (IP3) and diacylglycerol (DAG) [171]. IP3, via the increase of intracellular Ca^{2++} , and DAG act as second messengers to activate various protein kinase C (PKC) isoforms (Figure 2B) [172, 173]. Although multiple PKC isoforms are activated, PKC δ and ϵ were shown to be sufficient to activate MEK, mediated by RAS Guanyl Releasing Protein 3 (RASGRP3) activation,

which in turn promotes UM survival and proliferation [174]. Indicating that the growth inhibitory effects of other PKC isoforms is not mediated through MAPK inhibition. The insights into PKC activation have spurred investigations on PKC inhibitors such as Sotrastaurin. Indeed, UM cells are highly dependent on PKC and MEK signaling and were found to be sensitive to either MEK or PKC inhibition by small molecule compounds [175, 176]. A phase I clinical trial with UM patients was initiated using Sotrastaurin as PKC inhibitor. Sotrastaurin treatment resulted in progression free survival of 15 weeks in about 50% of the patients [177]. Interestingly, both MEK and PKC inhibition is required to completely abolish ERK phosphorylation and thereby cell proliferation and survival *in vitro* and *in vivo* [176]. Unfortunately, a clinical trial assessing the potency of dual MEK and PKC inhibition had to be terminated due to strong adverse effects [178]. Aside from the MAPK pathway the PI3K pathway is also activated by the continuous G-protein coupled signaling in UM (Figure 2B). Upon activation PI3K catalyzes the conversion of PIP2 into PIP3, which in turn mediates the activation of AKT [179]. Indeed, the inhibition of the PI3K/AKT pathway has been shown to reduce proliferation *in vitro* [180]. A downstream target of AKT in the PI3K pathway is MTOR, a kinase with downstream effectors 4E-BP1 and S6K1 regulating translation [181-185]. Although multiple effective MTOR inhibitors exist, the impact of mTOR inhibition on UM cell proliferation and survival appears to be far less potent when compared to BRAF mutant cells [180, 186, 187]. Mutated G-protein coupled signaling to cell proliferation and survival also involves the transcription regulators YAP and TAZ (Figure 2B). Mutated GNAQ/11 has been demonstrated to increase YAP/TAZ activity via Trio and downstream G-proteins Rho and Rac [188, 189]. The requirement of the YAP pathway for UM proliferation and survival was best illustrated by the knockdown of YAP in UM cells. Additionally, small molecule inhibition of YAP using Verteporfin demonstrated the clinical potential of targeting this pathway downstream of mutated GNAQ/11 [188-190]. Together these pathways provide a wide range of opportunities to find novel therapeutic interventions for patients with metastasized UM (Figure 2B).

3. AIM AND OUTLINE OF THIS THESIS

The focus of this thesis is uveal melanoma (UM), an ocular cancer which, once metastasized, is lethal due to lack of effective treatment options. UM is driven by an oncogenic activating mutation in the α subunit of G-proteins GNAQ or GNA11. Essentially no mutations are found in the tumor suppressor gene *p53* in UM. To represses *p53* activity approximately 65% of UM tumors express high levels of the *p53* inhibitory proteins MDMX or MDM2. MDMX is shown to act as *p53* inhibitor by binding to its transactivation domain, rendering it inactive as a transcription factor. Interestingly, it

has been demonstrated that the oncogenic function of MDMX reaches beyond that of p53 inhibition. The aim of this thesis is to unravel the oncogenic function of MDMX and provide new treatment options for patients with metastasized UM.

Chapter 2 describes the regulation of the transcriptome by MDMX in UM. We demonstrate here that MDMX affects the transcription of genes involved in cell cycle regulation or apoptosis. This chapter also describes novel p53-independent effects of MDMX in addition to p53 inhibition, i.e. FOXO inhibition. Furthermore, a novel p53 back-up mechanism with a potential therapeutic target is proposed in this chapter.

In chapter 3 the opportunities of a combined targeting of two common signaling pathways, GNAQ/11 mutations and wildtype p53, as therapeutic intervention for metastasized UM patients is investigated. Drugs targeting these pathways, PKC- and MDM2 inhibitors, are already known to elicit strong adverse effects in patients. Genetic interference with either MDMX or PKC δ expression or activity showed that beneficial effects can already be achieved by a more specific targeting, which is presumably less toxic to the patient.

In chapter 4 it is described, opposed to what has been reported before, that enhancer of zeste homolog 2 (EZH2) inhibition poses a valuable novel therapeutic invention for UM. However, since EZH2 inhibition might take too long to exert a clinical beneficial effect, it was investigated whether EZH2 targeting would sensitize UM cells for other therapeutic strategies. Indeed, interfering with EZH2 activity synergized with HDAC inhibition, thus providing a novel treatment option for metastasized UM.

In chapter 5 it is shown that combining two clinically approved drugs, the pan-histone deacetylase (HDAC) inhibitor Quisinostat and the pan-CDK inhibitor Flavopiridol, could serve as an effective therapeutic intervention for UM patients. In addition, this combination of compounds, effectively causing apoptotic cell death in UM cells, could serve as alternative treatment option for cutaneous melanoma patients as well.

In chapter 6 the results from the preceding chapters are summarized and discussed and implications for future research and clinical implementation provided.

References

1. Lane DP, Crawford LV. T antigen is bound to a host protein in SV40-transformed cells. *Nature*. 1979; 278: 261-3. doi:
2. Linzer DI, Levine AJ. Characterization of a 54K dalton cellular SV40 tumor antigen present in SV40-transformed cells and uninfected embryonal carcinoma cells. *Cell*. 1979; 17: 43-52. doi:
3. Fischer M. Census and evaluation of p53 target genes. *Oncogene*. 2017; 36: 3943-56. doi: 10.1038/onc.2016.502.
4. Vogelstein B, Lane D, Levine AJ. Surfing the p53 network. *Nature*. 2000; 408: 307-10. doi: 10.1038/35042675.
5. Biegging KT, Mello SS, Attardi LD. Unravelling mechanisms of p53-mediated tumour suppression. *Nat Rev Cancer*. 2014; 14: 359-70. doi: 10.1038/nrc3711.
6. Donehower LA, Harvey M, Slagle BL, McArthur MJ, Montgomery CA, Jr., Butel JS, Bradley A. Mice deficient for p53 are developmentally normal but susceptible to spontaneous tumours. *Nature*. 1992; 356: 215-21. doi: 10.1038/356215a0.
7. Jacks T, Remington L, Williams BO, Schmitt EM, Halachmi S, Bronson RT, Weinberg RA. Tumor spectrum analysis in p53-mutant mice. *Curr Biol*. 1994; 4: 1-7. doi:
8. Hainaut P, Hollstein M. p53 and human cancer: the first ten thousand mutations. *Adv Cancer Res*. 2000; 77: 81-137. doi:
9. Hollstein M, Sidransky D, Vogelstein B, Harris CC. p53 mutations in human cancers. *Science*. 1991; 253: 49-53. doi:
10. Martin AC, Facchiano AM, Cuff AL, Hernandez-Boussard T, Olivier M, Hainaut P, Thornton JM. Integrating mutation data and structural analysis of the TP53 tumor-suppressor protein. *Hum Mutat*. 2002; 19: 149-64. doi: 10.1002/humu.10032.
11. Gao J, Aksoy BA, Dogrusoz U, Dresdner G, Gross B, Sumer SO, Sun Y, Jacobsen A, Sinha R, Larsson E, Cerami E, Sander C, Schultz N. Integrative analysis of complex cancer genomics and clinical profiles using the cBioPortal. *Sci Signal*. 2013; 6: p11. doi: 10.1126/scisignal.2004088.
12. Okamoto K, Kashima K, Pereg Y, Ishida M, Yamazaki S, Nota A, Teunisse A, Migliorini D, Kitabayashi I, Marine JC, Prives C, Shiloh Y, Jochemsen AG, et al. DNA damage-induced phosphorylation of MdmX at serine 367 activates p53 by targeting MdmX for Mdm2-dependent degradation. *Mol Cell Biol*. 2005; 25: 9608-20. doi: 10.1128/MCB.25.21.9608-9620.2005.
13. Finch RA, Donoviel DB, Potter D, Shi M, Fan A, Freed DD, Wang CY, Zambrowicz BP, Ramirez-Solis R, Sands AT, Zhang N. mdmX is a negative regulator of p53 activity in vivo. *Cancer Res*. 2002; 62: 3221-5. doi:
14. Parant J, Chavez-Reyes A, Little NA, Yan W, Reinke V, Jochemsen AG, Lozano G. Rescue of embryonic lethality in Mdm4-null mice by loss of Trp53 suggests a nonoverlapping pathway with MDM2 to regulate p53. *Nat Genet*. 2001; 29: 92-5. doi: 10.1038/ng714.
15. Steinman HA, Hoover KM, Keeler ML, Sands AT, Jones SN. Rescue of Mdm4-deficient mice by Mdm2 reveals functional overlap of Mdm2 and Mdm4 in development. *Oncogene*. 2005; 24: 7935-40. doi: 10.1038/sj.onc.1208930.
16. De Clercq S, Gembarska A, Denecker G, Maetens M, Naessens M, Haigh K, Haigh JJ, Marine JC. Widespread overexpression of epitope-tagged Mdm4 does not accelerate tumor formation in vivo. *Mol Cell Biol*. 2010; 30: 5394-405. doi: 10.1128/MCB.00330-10.
17. Francoz S, Froment P, Bogaerts S, De Clercq S, Maetens M, Doumont G, Bellefroid E, Marine JC. Mdm4 and Mdm2 cooperate to inhibit p53 activity in proliferating and quiescent cells in vivo. *Proc Natl Acad Sci U S A*. 2006; 103: 3232-7. doi: 10.1073/pnas.0508476103.

18. Marine JC, Francoz S, Maetens M, Wahl G, Toledo F, Lozano G. Keeping p53 in check: essential and synergistic functions of Mdm2 and Mdm4. *Cell Death Differ.* 2006; 13: 927-34. doi: 10.1038/sj.cdd.4401912.
19. Valentin-Vega YA, Okano H, Lozano G. The intestinal epithelium compensates for p53-mediated cell death and guarantees organismal survival. *Cell Death Differ.* 2008; 15: 1772-81. doi: 10.1038/cdd.2008.109.
20. Valentin-Vega YA, Box N, Terzian T, Lozano G. Mdm4 loss in the intestinal epithelium leads to compartmentalized cell death but no tissue abnormalities. *Differentiation.* 2009; 77: 442-9. doi: 10.1016/j.diff.2009.03.001.
21. Grier JD, Xiong S, Elizondo-Fraire AC, Parant JM, Lozano G. Tissue-specific differences of p53 inhibition by Mdm2 and Mdm4. *Mol Cell Biol.* 2006; 26: 192-8. doi: 10.1128/MCB.26.1.192-198.2006.
22. Ringshausen I, O'Shea CC, Finch AJ, Swigart LB, Evan GI. Mdm2 is critically and continuously required to suppress lethal p53 activity in vivo. *Cancer Cell.* 2006; 10: 501-14. doi: 10.1016/j.ccr.2006.10.010.
23. Xiong S, Van Pelt CS, Elizondo-Fraire AC, Fernandez-Garcia B, Lozano G. Loss of Mdm4 results in p53-dependent dilated cardiomyopathy. *Circulation.* 2007; 115: 2925-30. doi: 10.1161/CIRCULATIONAHA.107.689901.
24. Haupt Y, Maya R, Kazaz A, Oren M. Mdm2 promotes the rapid degradation of p53. *Nature.* 1997; 387: 296-9. doi: 10.1038/387296a0.
25. Li M, Brooks CL, Wu-Baer F, Chen D, Baer R, Gu W. Mono- versus polyubiquitination: differential control of p53 fate by Mdm2. *Science.* 2003; 302: 1972-5. doi: 10.1126/science.1091362.
26. Kawai H, Wiederschain D, Yuan ZM. Critical contribution of the MDM2 acidic domain to p53 ubiquitination. *Mol Cell Biol.* 2003; 23: 4939-47. doi:
27. Meulmeester E, Frenk R, Stad R, de Graaf P, Marine JC, Vousden KH, Jochemsen AG. Critical role for a central part of Mdm2 in the ubiquitylation of p53. *Mol Cell Biol.* 2003; 23: 4929-38. doi:
28. Wade M, Wang YV, Wahl GM. The p53 orchestra: Mdm2 and Mdmx set the tone. *Trends Cell Biol.* 2010; 20: 299-309. doi: 10.1016/j.tcb.2010.01.009.
29. Bouska A, Eischen CM. Murine double minute 2: p53-independent roads lead to genome instability or death. *Trends Biochem Sci.* 2009; 34: 279-86. doi: 10.1016/j.tibs.2009.02.006.
30. Bouska A, Eischen CM. Mdm2 affects genome stability independent of p53. *Cancer Res.* 2009; 69: 1697-701. doi: 10.1158/0008-5472.CAN-08-3732.
31. Bouska A, Lushnikova T, Plaza S, Eischen CM. Mdm2 promotes genetic instability and transformation independent of p53. *Mol Cell Biol.* 2008; 28: 4862-74. doi: 10.1128/MCB.01584-07.
32. Shvarts A, Steegenga WT, Riteco N, van Laar T, Dekker P, Bazuine M, van Ham RC, van der Houven van Oordt W, Hateboer G, van der Eb AJ, Jochemsen AG. MDMX: a novel p53-binding protein with some functional properties of MDM2. *EMBO J.* 1996; 15: 5349-57. doi:
33. Marine JC, Jochemsen AG. Mdmx and Mdm2: brothers in arms? *Cell Cycle.* 2004; 3: 900-4. doi:
34. Bottger V, Bottger A, Garcia-Echeverria C, Ramos YF, van der Eb AJ, Jochemsen AG, Lane DP. Comparative study of the p53-mdm2 and p53-MDMX interfaces. *Oncogene.* 1999; 18: 189-99. doi: 10.1038/sj.onc.1202281.
35. Sharp DA, Kratowicz SA, Sank MJ, George DL. Stabilization of the MDM2 oncoprotein by interaction with the structurally related MDMX protein. *J Biol Chem.* 1999; 274: 38189-96. doi:
36. Gu J, Kawai H, Nie L, Kitao H, Wiederschain D, Jochemsen AG, Parant J, Lozano G, Yuan ZM. Mutual dependence of MDM2 and MDMX in their functional inactivation of p53. *J Biol Chem.* 2002; 277: 19251-4. doi: 10.1074/jbc.C200150200.

37. Linares LK, Hengstermann A, Ciechanover A, Muller S, Scheffner M. HdmX stimulates Hdm2-mediated ubiquitination and degradation of p53. *Proc Natl Acad Sci U S A*. 2003; 100: 12009-14. doi: 10.1073/pnas.2030930100.
38. Stommel JM, Wahl GM. Accelerated MDM2 auto-degradation induced by DNA-damage kinases is required for p53 activation. *EMBO J*. 2004; 23: 1547-56. doi: 10.1038/sj.emboj.7600145.
39. Fang S, Jensen JP, Ludwig RL, Vousden KH, Weissman AM. Mdm2 is a RING finger-dependent ubiquitin protein ligase for itself and p53. *J Biol Chem*. 2000; 275: 8945-51. doi:
40. de Graaf P, Little NA, Ramos YF, Meulmeester E, Letteboer SJ, Jochemsen AG. Hdmx protein stability is regulated by the ubiquitin ligase activity of Mdm2. *J Biol Chem*. 2003; 278: 38315-24. doi: 10.1074/jbc.M213034200.
41. Kawai H, Wiederschain D, Kitao H, Stuart J, Tsai KK, Yuan ZM. DNA damage-induced MDMX degradation is mediated by MDM2. *J Biol Chem*. 2003; 278: 45946-53. doi: 10.1074/jbc.M308295200.
42. Pan Y, Chen J. MDM2 promotes ubiquitination and degradation of MDMX. *Mol Cell Biol*. 2003; 23: 5113-21. doi:
43. Phillips A, Teunisse A, Lam S, Lodder K, Darley M, Emaduddin M, Wolf A, Richter J, de Lange J, Verlaan-de Vries M, Lenos K, Bohnke A, Bartel F, et al. HDMX-L is expressed from a functional p53-responsive promoter in the first intron of the HDMX gene and participates in an autoregulatory feedback loop to control p53 activity. *J Biol Chem*. 2010; 285: 29111-27. doi: 10.1074/jbc.M110.129726.
44. Pigolotti S, Krishna S, Jensen MH. Oscillation patterns in negative feedback loops. *Proc Natl Acad Sci U S A*. 2007; 104: 6533-7. doi: 10.1073/pnas.0610759104.
45. Bykov VJ, Issaeva N, Shilov A, Hultcrantz M, Pugacheva E, Chumakov P, Bergman J, Wiman KG, Selivanova G. Restoration of the tumor suppressor function to mutant p53 by a low-molecular-weight compound. *Nat Med*. 2002; 8: 282-8. doi: 10.1038/nm0302-282.
46. Selivanova G, Kawasaki T, Ryabchenko L, Wiman KG. Reactivation of mutant p53: a new strategy for cancer therapy. *Semin Cancer Biol*. 1998; 8: 369-78. doi:
47. Lambert JM, Gorzov P, Veprintsev DB, Soderqvist M, Segerback D, Bergman J, Fersht AR, Hainaut P, Wiman KG, Bykov VJ. PRIMA-1 reactivates mutant p53 by covalent binding to the core domain. *Cancer Cell*. 2009; 15: 376-88. doi: 10.1016/j.ccr.2009.03.003.
48. Lambert JM, Moshfegh A, Hainaut P, Wiman KG, Bykov VJ. Mutant p53 reactivation by PRIMA-1MET induces multiple signaling pathways converging on apoptosis. *Oncogene*. 2010; 29: 1329-38. doi: 10.1038/onc.2009.425.
49. Bykov VJ, Issaeva N, Selivanova G, Wiman KG. Mutant p53-dependent growth suppression distinguishes PRIMA-1 from known anticancer drugs: a statistical analysis of information in the National Cancer Institute database. *Carcinogenesis*. 2002; 23: 2011-8. doi:
50. Lu T, Zou Y, Xu G, Potter JA, Taylor GL, Duan Q, Yang Q, Xiong H, Qiu H, Ye D, Zhang P, Yu S, Yuan X, et al. PRIMA-1Met suppresses colorectal cancer independent of p53 by targeting MEK. *Oncotarget*. 2016; 7: 83017-30. doi: 10.18632/oncotarget.12940.
51. Teoh PJ, Bi C, Sintosebastian C, Tay LS, Fonseca R, Chng WJ. PRIMA-1 targets the vulnerability of multiple myeloma of deregulated protein homeostasis through the perturbation of ER stress via p73 demethylation. *Oncotarget*. 2016; 7: 61806-19. doi: 10.18632/oncotarget.11241.
52. Rokaeus N, Shen J, Eckhardt I, Bykov VJ, Wiman KG, Wilhelm MT. PRIMA-1(MET)/APR-246 targets mutant forms of p53 family members p63 and p73. *Oncogene*. 2010; 29: 6442-51. doi: 10.1038/onc.2010.382.
53. Saha MN, Jiang H, Yang Y, Reece D, Chang H. PRIMA-1Met/APR-246 displays high antitumor activity in multiple myeloma by induction of p73 and Noxa. *Mol Cancer Ther*. 2013; 12: 2331-41. doi: 10.1158/1535-7163.MCT-12-1166.

54. Turrell FK, Kerr EM, Gao M, Thorpe H, Doherty GJ, Cridge J, Shorthouse D, Speed A, Samarajiva S, Hall BA, Griffiths M, Martins CP. Lung tumors with distinct p53 mutations respond similarly to p53 targeted therapy but exhibit genotype-specific statin sensitivity. *Genes Dev.* 2017. doi: 10.1101/gad.298463.117.
55. Parrales A, Ranjan A, Iyer SV, Padhye S, Weir SJ, Roy A, Iwakuma T. DNAJA1 controls the fate of misfolded mutant p53 through the mevalonate pathway. *Nat Cell Biol.* 2016; 18: 1233-43. doi: 10.1038/ncb3427.
56. Panagopoulos I, Bjerkehagen B, Gorunova L, Berner JM, Boye K, Heim S. Several fusion genes identified by whole transcriptome sequencing in a spindle cell sarcoma with rearrangements of chromosome arm 12q and MDM2 amplification. *Int J Oncol.* 2014; 45: 1829-36. doi: 10.3892/ijo.2014.2605.
57. Ware PL, Snow AN, Gvalani M, Pettenati MJ, Qasem SA. MDM2 copy numbers in well-differentiated and dedifferentiated liposarcoma: characterizing progression to high-grade tumors. *Am J Clin Pathol.* 2014; 141: 334-41. doi: 10.1309/AJCLPLYU89XHSNHQO.
58. Momand J, Jung D, Wilczynski S, Niland J. The MDM2 gene amplification database. *Nucleic Acids Res.* 1998; 26: 3453-9. doi:
59. Michalk M, Meinrath J, Kunstlinger H, Koitzsch U, Drebber U, Merkelbach-Bruse S, Bollschweiler E, Kloth M, Hartmann W, Holscher A, Quaas A, Grimminger PP, Odenthal M. MDM2 gene amplification in esophageal carcinoma. *Oncol Rep.* 2016; 35: 2223-7. doi: 10.3892/or.2016.4578.
60. Riemenschneider MJ, Buschges R, Wolter M, Reifenberger J, Bostrom J, Kraus JA, Schlegel U, Reifenberger G. Amplification and overexpression of the MDM4 (MDMX) gene from 1q32 in a subset of malignant gliomas without TP53 mutation or MDM2 amplification. *Cancer Res.* 1999; 59: 6091-6. doi:
61. Laurie NA, Donovan SL, Shih CS, Zhang J, Mills N, Fuller C, Teunisse A, Lam S, Ramos Y, Mohan A, Johnson D, Wilson M, Rodriguez-Galindo C, et al. Inactivation of the p53 pathway in retinoblastoma. *Nature.* 2006; 444: 61-6. doi: 10.1038/nature05194.
62. Danovi D, Meulmeester E, Pasini D, Migliorini D, Capra M, Frenk R, de Graaf P, Francoz S, Gasparini P, Gobbi A, Helin K, Pelicci PG, Jochemsen AG, et al. Amplification of Mdmx (or Mdm4) directly contributes to tumor formation by inhibiting p53 tumor suppressor activity. *Mol Cell Biol.* 2004; 24: 5835-43. doi: 10.1128/MCB.24.13.5835-5843.2004.
63. Kussie PH, Gorina S, Marechal V, Elenbaas B, Moreau J, Levine AJ, Pavletich NP. Structure of the MDM2 oncoprotein bound to the p53 tumor suppressor transactivation domain. *Science.* 1996; 274: 948-53. doi:
64. Vassilev LT, Vu BT, Graves B, Carvajal D, Podlaski F, Filipovic Z, Kong N, Kammlott U, Lukacs C, Klein C, Fotouhi N, Liu EA. In vivo activation of the p53 pathway by small-molecule antagonists of MDM2. *Science.* 2004; 303: 844-8. doi: 10.1126/science.1092472.
65. Vassilev LT. MDM2 inhibitors for cancer therapy. *Trends Mol Med.* 2007; 13: 23-31. doi: 10.1016/j.molmed.2006.11.002.
66. de Lange J, Ly LV, Lodder K, Verlaan-de Vries M, Teunisse AF, Jager MJ, Jochemsen AG. Synergistic growth inhibition based on small-molecule p53 activation as treatment for intraocular melanoma. *Oncogene.* 2012; 31: 1105-16. doi: 10.1038/onc.2011.309.
67. Parks DJ, Lafrance LV, Calvo RR, Milkiewicz KL, Gupta V, Lattanze J, Ramachandren K, Carver TE, Petrella EC, Cummings MD, Maguire D, Grasberger BL, Lu T. 1,4-Benzodiazepine-2,5-diones as small molecule antagonists of the HDM2-p53 interaction: discovery and SAR. *Bioorg Med Chem Lett.* 2005; 15: 765-70. doi: 10.1016/j.bmcl.2004.11.009.
68. Ding K, Lu Y, Nikolovska-Coleska Z, Wang G, Qiu S, Shangary S, Gao W, Qin D, Stuckey J, Krajewski K, Roller PP, Wang S. Structure-based design of spiro-oxindoles as potent, specific small-molecule inhibitors of the MDM2-p53 interaction. *J Med Chem.* 2006; 49: 3432-5. doi: 10.1021/jm051122a.

69. Issaeva N, Bozko P, Enge M, Protopopova M, Verhoef LG, Masucci M, Pramanik A, Selivanova G. Small molecule RITA binds to p53, blocks p53-HDM-2 interaction and activates p53 function in tumors. *Nat Med.* 2004; 10: 1321-8. doi: 10.1038/nm1146.
70. Spinnler C, Hedstrom E, Li H, de Lange J, Nikulenkov F, Teunisse AF, Verlaan-de Vries M, Grinkevich V, Jochemsen AG, Selivanova G. Abrogation of Wip1 expression by RITA-activated p53 potentiates apoptosis induction via activation of ATM and inhibition of HdmX. *Cell Death Differ.* 2011; 18: 1736-45. doi: 10.1038/cdd.2011.45.
71. de Lange J, Verlaan-de Vries M, Teunisse AF, Jochemsen AG. Chk2 mediates RITA-induced apoptosis. *Cell Death Differ.* 2012; 19: 980-9. doi: 10.1038/cdd.2011.182.
72. Nieves-Neira W, Rivera MI, Kohlhagen G, Hursey ML, Pourquier P, Sausville EA, Pommier Y. DNA protein cross-links produced by NSC 652287, a novel thiophene derivative active against human renal cancer cells. *Mol Pharmacol.* 1999; 56: 478-84. doi:
73. Krajewski M, Ozdowy P, D'Silva L, Rothweiler U, Holak TA. NMR indicates that the small molecule RITA does not block p53-MDM2 binding in vitro. *Nat Med.* 2005; 11: 1135-6; author reply 6-7. doi: 10.1038/nm1105-1135.
74. Burgess A, Chia KM, Haupt S, Thomas D, Haupt Y, Lim E. Clinical Overview of MDM2/X-Targeted Therapies. *Front Oncol.* 2016; 6: 7. doi: 10.3389/fonc.2016.00007.
75. Ray-Coquard I, Blay JY, Italiano A, Le Cesne A, Penel N, Zhi J, Heil F, Rueger R, Graves B, Ding M, Geho D, Middleton SA, Vassilev LT, et al. Effect of the MDM2 antagonist RG7112 on the P53 pathway in patients with MDM2-amplified, well-differentiated or dedifferentiated liposarcoma: an exploratory proof-of-mechanism study. *Lancet Oncol.* 2012; 13: 1133-40. doi: 10.1016/S1470-2045(12)70474-6.
76. Andreeff M, Kelly KR, Yee K, Assouline S, Strair R, Popplewell L, Bowen D, Martinelli G, Drummond MW, Vyas P, Kirschbaum M, Iyer SP, Ruvolo V, et al. Results of the Phase I Trial of RG7112, a Small-Molecule MDM2 Antagonist in Leukemia. *Clin Cancer Res.* 2016; 22: 868-76. doi: 10.1158/1078-0432.CCR-15-0481.
77. Biswas S, Killick E, Jochemsen AG, Lunec J. The clinical development of p53-reactivating drugs in sarcomas - charting future therapeutic approaches and understanding the clinical molecular toxicology of Nutlins. *Expert Opin Investig Drugs.* 2014; 23: 629-45. doi: 10.1517/13543784.2014.892924.
78. Jones RJ, Bjorklund CC, Baladandayuthapani V, Kuhn DJ, Orlowski RZ. Drug resistance to inhibitors of the human double minute-2 E3 ligase is mediated by point mutations of p53, but can be overcome with the p53 targeting agent RITA. *Mol Cancer Ther.* 2012; 11: 2243-53. doi: 10.1158/1535-7163.MCT-12-0135.
79. Jung J, Lee JS, Dickson MA, Schwartz GK, Le Cesne A, Varga A, Bahleda R, Wagner AJ, Choy E, de Jonge MJ, Light M, Rowley S, Mace S, et al. TP53 mutations emerge with HDM2 inhibitor SAR405838 treatment in de-differentiated liposarcoma. *Nat Commun.* 2016; 7: 12609. doi: 10.1038/ncomms12609.
80. Popowicz GM, Czarna A, Holak TA. Structure of the human Mdmx protein bound to the p53 tumor suppressor transactivation domain. *Cell Cycle.* 2008; 7: 2441-3. doi: 10.4161/cc.6365.
81. Reed D, Shen Y, Shelat AA, Arnold LA, Ferreira AM, Zhu F, Mills N, Smithson DC, Regni CA, Bashford D, Cicero SA, Schulman BA, Jochemsen AG, et al. Identification and characterization of the first small molecule inhibitor of MDMX. *J Biol Chem.* 2010; 285: 10786-96. doi: 10.1074/jbc.M109.056747.
82. Bista M, Smithson D, Pecak A, Salinas G, Pustelny K, Min J, Pirog A, Finch K, Zdzalik M, Waddell B, Wladyka B, Kedracka-Krok S, Dyer MA, et al. On the mechanism of action of SJ-172550 in inhibiting the interaction of MDM4 and p53. *PLoS One.* 2012; 7: e37518. doi: 10.1371/journal.pone.0037518.
83. Wang H, Ma X, Ren S, Buolamwini JK, Yan C. A small-molecule inhibitor of MDMX activates p53 and induces apoptosis. *Mol Cancer Ther.* 2011; 10: 69-79. doi: 10.1158/1535-7163.MCT-10-0581.

84. Roh JL, Park JY, Kim EH. XI-011 enhances cisplatin-induced apoptosis by functional restoration of p53 in head and neck cancer. *Apoptosis*. 2014; 19: 1594-602. doi: 10.1007/s10495-014-1026-8.
85. Pishas KI, Adwal A, Neuhaus SJ, Clayer MT, Farshid G, Staudacher AH, Callen DF. XI-006 induces potent p53-independent apoptosis in Ewing sarcoma. *Sci Rep*. 2015; 5: 11465. doi: 10.1038/srep11465.
86. Wang H, Yan C. A small-molecule p53 activator induces apoptosis through inhibiting MDMX expression in breast cancer cells. *Neoplasia*. 2011; 13: 611-9. doi:
87. de Lange J, Teunisse AF, Vries MV, Lodder K, Lam S, Luyten GP, Bernal F, Jager MJ, Jochemsen AG. High levels of Hdmx promote cell growth in a subset of uveal melanomas. *Am J Cancer Res*. 2012; 2: 492-507. doi:
88. Graves B, Thompson T, Xia M, Janson C, Lukacs C, Deo D, Di Lello P, Fry D, Garvie C, Huang KS, Gao L, Tovar C, Lovey A, et al. Activation of the p53 pathway by small-molecule-induced MDM2 and MDMX dimerization. *Proc Natl Acad Sci U S A*. 2012; 109: 11788-93. doi: 10.1073/pnas.1203789109.
89. de Polo A, Luo Z, Gerarduzzi C, Chen X, Little JB, Yuan ZM. AXL receptor signalling suppresses p53 in melanoma through stabilization of the MDMX-MDM2 complex. *J Mol Cell Biol*. 2016. doi: 10.1093/jmcb/mjw045.
90. Gerarduzzi C, de Polo A, Liu XS, El Kharbili M, Little JB, Yuan ZM. Human epidermal growth factor receptor 4 (Her4) Suppresses p53 Protein via Targeting the MDMX-MDM2 Protein Complex: IMPLICATION OF A NOVEL MDMX SER-314 PHOSPHOSITE. *J Biol Chem*. 2016; 291: 25937-49. doi: 10.1074/jbc.M116.752303.
91. Boutz PL, Bhutkar A, Sharp PA. Detained introns are a novel, widespread class of post-transcriptionally spliced introns. *Genes Dev*. 2015; 29: 63-80. doi: 10.1101/gad.247361.114.
92. Rallapalli R, Strachan G, Cho B, Mercer WE, Hall DJ. A novel MDMX transcript expressed in a variety of transformed cell lines encodes a truncated protein with potent p53 repressive activity. *J Biol Chem*. 1999; 274: 8299-308. doi:
93. Bardot B, Bouarich-Bourimi R, Leemput J, Lejour V, Hamon A, Plancke L, Jochemsen AG, Simeonova I, Fang M, Toledo F. Mice engineered for an obligatory Mdm4 exon skipping express higher levels of the Mdm4-S isoform but exhibit increased p53 activity. *Oncogene*. 2015; 34: 2943-8. doi: 10.1038/onc.2014.230.
94. Dewaele M, Tabaglio T, Willekens K, Bezzi M, Teo SX, Low DH, Koh CM, Rambow F, Fiers M, Rogiers A, Radaelli E, Al-Haddawi M, Tan SY, et al. Antisense oligonucleotide-mediated MDM4 exon 6 skipping impairs tumor growth. *J Clin Invest*. 2016; 126: 68-84. doi: 10.1172/JCI82534.
95. Gembarska A, Luciani F, Fedele C, Russell EA, Dewaele M, Villar S, Zwolinska A, Haupt S, de Lange J, Yip D, Goydos J, Haigh JJ, Haupt Y, et al. MDM4 is a key therapeutic target in cutaneous melanoma. *Nat Med*. 2012; 18: 1239-47. doi: 10.1038/nm.2863.
96. Haupt S, Buckley D, Pang JM, Panimaya J, Paul PJ, Gamell C, Takano EA, Lee YY, Hiddingh S, Rogers TM, Teunisse AF, Herold MJ, Marine JC, et al. Targeting Mdmx to treat breast cancers with wild-type p53. *Cell Death Dis*. 2015; 6: e1821. doi: 10.1038/cddis.2015.173.
97. Jeffreena Miranda P, Buckley D, Raghu D, Pang JB, Takano EA, Vijayakumaran R, Teunisse AF, Posner A, Procter T, Herold MJ, Gamell C, Marine JC, Fox SB, et al. MDM4 is a rational target for treating breast cancers with mutant p53. *J Pathol*. 2017. doi: 10.1002/path.4877.
98. Hodis E, Watson IR, Kryukov GV, Arold ST, Imielinski M, Theurillat JP, Nickerson E, Auclair D, Li L, Place C, Dicara D, Ramos AH, Lawrence MS, et al. A landscape of driver mutations in melanoma. *Cell*. 2012; 150: 251-63. doi: 10.1016/j.cell.2012.06.024.
99. Chin L, Garraway LA, Fisher DE. Malignant melanoma: genetics and therapeutics in the genomic era. *Genes Dev*. 2006; 20: 2149-82. doi: 10.1101/gad.1437206.

100. Balch CM, Gershenwald JE, Soong SJ, Thompson JF, Atkins MB, Byrd DR, Buzaid AC, Cochran AJ, Coit DG, Ding S, Eggermont AM, Flaherty KT, Gimotty PA, et al. Final version of 2009 AJCC melanoma staging and classification. *J Clin Oncol*. 2009; 27: 6199-206. doi: 10.1200/JCO.2009.23.4799.
101. Garbe C, Leiter U. Melanoma epidemiology and trends. *Clin Dermatol*. 2009; 27: 3-9. doi: 10.1016/j.clindermatol.2008.09.001.
102. Davies H, Bignell GR, Cox C, Stephens P, Edkins S, Clegg S, Teague J, Woffendin H, Garnett MJ, Bottomley W, Davis N, Dicks E, Ewing R, et al. Mutations of the BRAF gene in human cancer. *Nature*. 2002; 417: 949-54. doi: 10.1038/nature00766.
103. Omholt K, Platz A, Kanter L, Ringborg U, Hansson J. NRAS and BRAF mutations arise early during melanoma pathogenesis and are preserved throughout tumor progression. *Clin Cancer Res*. 2003; 9: 6483-8. doi: 10.1158/1078-0432.CCR-03-0575.
104. Cancer Genome Atlas N. Genomic Classification of Cutaneous Melanoma. *Cell*. 2015; 161: 1681-96. doi: 10.1016/j.cell.2015.05.044.
105. Carvajal RD, Antonescu CR, Wolchok JD, Chapman PB, Roman RA, Teitcher J, Panageas KS, Busam KJ, Chmielowski B, Lutzky J, Pavlick AC, Fusco A, Cane L, et al. KIT as a therapeutic target in metastatic melanoma. *JAMA*. 2011; 305: 2327-34. doi: 10.1001/jama.2011.746.
106. Beadling C, Jacobson-Dunlop E, Hodi FS, Le C, Warrick A, Patterson J, Town A, Harlow A, Cruz F, 3rd, Azar S, Rubin BP, Muller S, West R, et al. KIT gene mutations and copy number in melanoma subtypes. *Clin Cancer Res*. 2008; 14: 6821-8. doi: 10.1158/1078-0432.CCR-08-0575.
107. Minor DR, Kashani-Sabet M, Garrido M, O'Day SJ, Hamid O, Bastian BC. Sunitinib therapy for melanoma patients with KIT mutations. *Clin Cancer Res*. 2012; 18: 1457-63. doi: 10.1158/1078-0432.CCR-11-1987.
108. Tsao H, Chin L, Garraway LA, Fisher DE. Melanoma: from mutations to medicine. *Genes Dev*. 2012; 26: 1131-55. doi: 10.1101/gad.191999.112.
109. Chapman PB, Hauschild A, Robert C, Haanen JB, Ascierto P, Larkin J, Dummer R, Garbe C, Testori A, Maio M, Hogg D, Lorigan P, Lebbe C, et al. Improved survival with vemurafenib in melanoma with BRAF V600E mutation. *N Engl J Med*. 2011; 364: 2507-16. doi: 10.1056/NEJMoa1103782.
110. Hauschild A, Grob JJ, Demidov LV, Jouary T, Gutzmer R, Millward M, Rutkowski P, Blank CU, Miller WH, Jr., Kaempgen E, Martin-Algarra S, Karaszewska B, Mauch C, et al. Dabrafenib in BRAF-mutated metastatic melanoma: a multicentre, open-label, phase 3 randomised controlled trial. *Lancet*. 2012; 380: 358-65. doi: 10.1016/S0140-6736(12)60868-X.
111. Flaherty KT, Puzanov I, Kim KB, Ribas A, McArthur GA, Sosman JA, O'Dwyer PJ, Lee RJ, Grippo JF, Nolop K, Chapman PB. Inhibition of mutated, activated BRAF in metastatic melanoma. *N Engl J Med*. 2010; 363: 809-19. doi: 10.1056/NEJMoa1002011.
112. Sosman JA, Kim KB, Schuchter L, Gonzalez R, Pavlick AC, Weber JS, McArthur GA, Hutson TE, Moschos SJ, Flaherty KT, Hersey P, Kefford R, Lawrence D, et al. Survival in BRAF V600-mutant advanced melanoma treated with vemurafenib. *N Engl J Med*. 2012; 366: 707-14. doi: 10.1056/NEJMoa1112302.
113. Girotti MR, Pedersen M, Sanchez-Laorden B, Viros A, Turajlic S, Niculescu-Duvaz D, Zamboni A, Sinclair J, Hayes A, Gore M, Lorigan P, Springer C, Larkin J, et al. Inhibiting EGF receptor or SRC family kinase signaling overcomes BRAF inhibitor resistance in melanoma. *Cancer Discov*. 2013; 3: 158-67. doi: 10.1158/2159-8290.CD-12-0386.
114. Johannessen CM, Boehm JS, Kim SY, Thomas SR, Wardwell L, Johnson LA, Emery CM, Stransky N, Cogdill AP, Barretina J, Caponigro G, Hieronymus H, Murray RR, et al. COT drives resistance to RAF inhibition through MAP kinase pathway reactivation. *Nature*. 2010; 468: 968-72. doi: 10.1038/nature09627.

115. Nazarian R, Shi H, Wang Q, Kong X, Koya RC, Lee H, Chen Z, Lee MK, Attar N, Sazegar H, Chodon T, Nelson SF, McArthur G, et al. Melanomas acquire resistance to B-RAF(V600E) inhibition by RTK or N-RAS upregulation. *Nature*. 2010; 468: 973-7. doi: 10.1038/nature09626.
116. Shi H, Moriceau G, Kong X, Lee MK, Lee H, Koya RC, Ng C, Chodon T, Scolyer RA, Dahlman KB, Sosman JA, Kefford RF, Long GV, et al. Melanoma whole-exome sequencing identifies (V600E)B-RAF amplification-mediated acquired B-RAF inhibitor resistance. *Nat Commun*. 2012; 3: 724. doi: 10.1038/ncomms1727.
117. Straussman R, Morikawa T, Shee K, Barzily-Rokni M, Qian ZR, Du J, Davis A, Mongare MM, Gould J, Frederick DT, Cooper ZA, Chapman PB, Solit DB, et al. Tumour micro-environment elicits innate resistance to RAF inhibitors through HGF secretion. *Nature*. 2012; 487: 500-4. doi: 10.1038/nature11183.
118. Vergani E, Vallacchi V, Frigerio S, Deho P, Mondellini P, Perego P, Cassinelli G, Lanzi C, Testi MA, Rivoltini L, Bongarzone I, Rodolfo M. Identification of MET and SRC activation in melanoma cell lines showing primary resistance to PLX4032. *Neoplasia*. 2011; 13: 1132-42. doi:
119. Villanueva J, Vultur A, Lee JT, Somasundaram R, Fukunaga-Kalabis M, Cipolla AK, Wubbenhorst B, Xu X, Gimotty PA, Kee D, Santiago-Walker AE, Letrero R, D'Andrea K, et al. Acquired resistance to BRAF inhibitors mediated by a RAF kinase switch in melanoma can be overcome by cotargeting MEK and IGF-1R/PI3K. *Cancer Cell*. 2010; 18: 683-95. doi: 10.1016/j.ccr.2010.11.023.
120. Kwong LN, Costello JC, Liu H, Jiang S, Helms TL, Langsdorf AE, Jakubosky D, Genovese G, Muller FL, Jeong JH, Bender RP, Chu GC, Flaherty KT, et al. Oncogenic NRAS signaling differentially regulates survival and proliferation in melanoma. *Nat Med*. 2012; 18: 1503-10. doi: 10.1038/nm.2941.
121. Flaherty KT, Infante JR, Daud A, Gonzalez R, Kefford RF, Sosman J, Hamid O, Schuchter L, Cebon J, Ibrahim N, Kudchadkar R, Burris HA, 3rd, Falchook G, et al. Combined BRAF and MEK inhibition in melanoma with BRAF V600 mutations. *N Engl J Med*. 2012; 367: 1694-703. doi: 10.1056/NEJMoa1210093.
122. Flaherty KT, Robert C, Hersey P, Nathan P, Garbe C, Milhem M, Demidov LV, Hassel JC, Rutkowski P, Mohr P, Dummer R, Trefzer U, Larkin JM, et al. Improved survival with MEK inhibition in BRAF-mutated melanoma. *N Engl J Med*. 2012; 367: 107-14. doi: 10.1056/NEJMoa1203421.
123. Hamid O, Robert C, Daud A, Hodi FS, Hwu WJ, Kefford R, Wolchok JD, Hersey P, Joseph RW, Weber JS, Dronca R, Gangadhar TC, Patnaik A, et al. Safety and tumor responses with lambrolizumab (anti-PD-1) in melanoma. *N Engl J Med*. 2013; 369: 134-44. doi: 10.1056/NEJMoa1305133.
124. Hodi FS, O'Day SJ, McDermott DF, Weber RW, Sosman JA, Haanen JB, Gonzalez R, Robert C, Schadendorf D, Hassel JC, Akerley W, van den Eertwegh AJ, Lutzky J, et al. Improved survival with ipilimumab in patients with metastatic melanoma. *N Engl J Med*. 2010; 363: 711-23. doi: 10.1056/NEJMoa1003466.
125. Leach DR, Krummel MF, Allison JP. Enhancement of antitumor immunity by CTLA-4 blockade. *Science*. 1996; 271: 1734-6. doi:
126. McCoy KD, Le Gros G. The role of CTLA-4 in the regulation of T cell immune responses. *Immunol Cell Biol*. 1999; 77: 1-10. doi: 10.1046/j.1440-1711.1999.00795.x.
127. Robert C, Thomas L, Bondarenko I, O'Day S, Weber J, Garbe C, Lebbe C, Baurain JF, Testori A, Grob JJ, Davidson N, Richards J, Maio M, et al. Ipilimumab plus dacarbazine for previously untreated metastatic melanoma. *N Engl J Med*. 2011; 364: 2517-26. doi: 10.1056/NEJMoa1104621.
128. Okazaki T, Chikuma S, Iwai Y, Fagarasan S, Honjo T. A rheostat for immune responses: the unique properties of PD-1 and their advantages for clinical application. *Nat Immunol*. 2013; 14: 1212-8. doi: 10.1038/ni.2762.
129. Sharpe AH, Wherry EJ, Ahmed R, Freeman GJ. The function of programmed cell death 1 and its ligands in regulating autoimmunity and infection. *Nat Immunol*. 2007; 8: 239-45. doi: 10.1038/ni1443.
130. Weber JS, D'Angelo SP, Minor D, Hodi FS, Gutzmer R, Neyns B, Hoeller C, Khusalani NI, Miller WH, Jr., Lao CD, Linette GP, Thomas L, Lorigan P, et al. Nivolumab versus chemotherapy in patients with

- advanced melanoma who progressed after anti-CTLA-4 treatment (CheckMate 037): a randomised, controlled, open-label, phase 3 trial. *Lancet Oncol.* 2015; 16: 375-84. doi: 10.1016/S1470-2045(15)70076-8.
131. Robert C, Schachter J, Long GV, Arance A, Grob JJ, Mortier L, Daud A, Carlino MS, McNeil C, Lotem M, Larkin J, Lorigan P, Neyns B, et al. Pembrolizumab versus Ipilimumab in Advanced Melanoma. *N Engl J Med.* 2015; 372: 2521-32. doi: 10.1056/NEJMoa1503093.
 132. Robert C, Long GV, Brady B, Dutriaux C, Maio M, Mortier L, Hassel JC, Rutkowski P, McNeil C, Kalinka-Warzocha E, Savage KJ, Hernberg MM, Lebbe C, et al. Nivolumab in previously untreated melanoma without BRAF mutation. *N Engl J Med.* 2015; 372: 320-30. doi: 10.1056/NEJMoa1412082.
 133. Ribas A, Puzanov I, Dummer R, Schadendorf D, Hamid O, Robert C, Hodi FS, Schachter J, Pavlick AC, Lewis KD, Cranmer LD, Blank CU, O'Day SJ, et al. Pembrolizumab versus investigator-choice chemotherapy for ipilimumab-refractory melanoma (KEYNOTE-002): a randomised, controlled, phase 2 trial. *Lancet Oncol.* 2015; 16: 908-18. doi: 10.1016/S1470-2045(15)00083-2.
 134. Jiang X, Zhou J, Giobbie-Hurder A, Wargo J, Hodi FS. The activation of MAPK in melanoma cells resistant to BRAF inhibition promotes PD-L1 expression that is reversible by MEK and PI3K inhibition. *Clin Cancer Res.* 2013; 19: 598-609. doi: 10.1158/1078-0432.CCR-12-2731.
 135. Wargo JA, Cooper ZA, Flaherty KT. Universes collide: combining immunotherapy with targeted therapy for cancer. *Cancer Discov.* 2014; 4: 1377-86. doi: 10.1158/2159-8290.CD-14-0477.
 136. Liu L, Mayes PA, Eastman S, Shi H, Yadavilli S, Zhang T, Yang J, Seestaller-Wehr L, Zhang SY, Hopson C, Tsvetkov L, Jing J, Zhang S, et al. The BRAF and MEK Inhibitors Dabrafenib and Trametinib: Effects on Immune Function and in Combination with Immunomodulatory Antibodies Targeting PD-1, PD-L1, and CTLA-4. *Clin Cancer Res.* 2015; 21: 1639-51. doi: 10.1158/1078-0432.CCR-14-2339.
 137. Shah SU, Mashayekhi A, Shields CL, Walia HS, Hubbard GB, 3rd, Zhang J, Shields JA. Uveal metastasis from lung cancer: clinical features, treatment, and outcome in 194 patients. *Ophthalmology.* 2014; 121: 352-7. doi: 10.1016/j.ophtha.2013.07.014.
 138. Singh AD, Bergman L, Seregard S. Uveal melanoma: epidemiologic aspects. *Ophthalmol Clin North Am.* 2005; 18: 75-84, viii. doi: 10.1016/j.ohc.2004.07.002.
 139. Van Raamsdonk CD, Bezrookove V, Green G, Bauer J, Gaugler L, O'Brien JM, Simpson EM, Barsh GS, Bastian BC. Frequent somatic mutations of GNAQ in uveal melanoma and blue naevi. *Nature.* 2009; 457: 599-602. doi: 10.1038/nature07586.
 140. Van Raamsdonk CD, Griewank KG, Crosby MB, Garrido MC, Vemula S, Wiesner T, Obenaus AC, Wackernagel W, Green G, Bouvier N, Sozen MM, Baimukanova G, Roy R, et al. Mutations in GNA11 in uveal melanoma. *N Engl J Med.* 2010; 363: 2191-9. doi: 10.1056/NEJMoa1000584.
 141. Chua V, Lapadula D, Randolph C, Benovic JL, Wedegaertner P, Aplin AE. Dysregulated GPCR Signaling and Therapeutic Options in Uveal Melanoma. *Mol Cancer Res.* 2017. doi: 10.1158/1541-7786.MCR-17-0007.
 142. Takasaki J, Saito T, Taniguchi M, Kawasaki T, Moritani Y, Hayashi K, Kobori M. A novel Galphaq/11-selective inhibitor. *J Biol Chem.* 2004; 279: 47438-45. doi: 10.1074/jbc.M408846200.
 143. Robertson AG, Shih J, Yau C, Gibb EA, Oba J, Mungall KL, Hess JM, Uzunangelov V, Walter V, Danilova L, Lichtenberg TM, Kucherlapati M, Kimes PK, et al. Integrative Analysis Identifies Four Molecular and Clinical Subsets in Uveal Melanoma. *Cancer Cell.* 2017; 32: 204-20 e15. doi: 10.1016/j.ccell.2017.07.003.
 144. Moore AR, Ceraudo E, Sher JJ, Guan Y, Shoushtari AN, Chang MT, Zhang JQ, Walczak EG, Kazmi MA, Taylor BS, Huber T, Chi P, Sakmar TP, et al. Recurrent activating mutations of G-protein-coupled receptor CYSLTR2 in uveal melanoma. *Nat Genet.* 2016; 48: 675-80. doi: 10.1038/ng.3549.

145. Augsburger JJ, Correa ZM, Shaikh AH. Effectiveness of treatments for metastatic uveal melanoma. *Am J Ophthalmol*. 2009; 148: 119-27. doi: 10.1016/j.ajo.2009.01.023.
146. Kivela T, Eskelin S, Kujala E. Metastatic uveal melanoma. *Int Ophthalmol Clin*. 2006; 46: 133-49. doi:
147. Rajpal S, Moore R, Karakousis CP. Survival in metastatic ocular melanoma. *Cancer*. 1983; 52: 334-6. doi:
148. Horsman DE, White VA. Cytogenetic analysis of uveal melanoma. Consistent occurrence of monosomy 3 and trisomy 8q. *Cancer*. 1993; 71: 811-9. doi:
149. Kilic E, van Gils W, Lodder E, Beverloo HB, van Til ME, Mooy CM, Paridaens D, de Klein A, Luyten GP. Clinical and cytogenetic analyses in uveal melanoma. *Invest Ophthalmol Vis Sci*. 2006; 47: 3703-7. doi: 10.1167/iovs.06-0101.
150. Prescher G, Bornfeld N, Horsthemke B, Becher R. Chromosomal aberrations defining uveal melanoma of poor prognosis. *Lancet*. 1992; 339: 691-2. doi:
151. Prescher G, Bornfeld N, Hirche H, Horsthemke B, Jockel KH, Becher R. Prognostic implications of monosomy 3 in uveal melanoma. *Lancet*. 1996; 347: 1222-5. doi:
152. Harbour JW, Onken MD, Roberson ED, Duan S, Cao L, Worley LA, Council ML, Matattal KA, Helms C, Bowcock AM. Frequent mutation of BAP1 in metastasizing uveal melanomas. *Science*. 2010; 330: 1410-3. doi: 10.1126/science.1194472.
153. van Essen TH, van Pelt SI, Versluis M, Bronkhorst IH, van Duinen SG, Marinkovic M, Kroes WG, Ruivenkamp CA, Shukla S, de Klein A, Kilic E, Harbour JW, Luyten GP, et al. Prognostic parameters in uveal melanoma and their association with BAP1 expression. *Br J Ophthalmol*. 2014; 98: 1738-43. doi: 10.1136/bjophthalmol-2014-305047.
154. Ventii KH, Devi NS, Friedrich KL, Chernova TA, Tighiouart M, Van Meir EG, Wilkinson KD. BRCA1-associated protein-1 is a tumor suppressor that requires deubiquitinating activity and nuclear localization. *Cancer Res*. 2008; 68: 6953-62. doi: 10.1158/0008-5472.CAN-08-0365.
155. Lee HS, Lee SA, Hur SK, Seo JW, Kwon J. Stabilization and targeting of INO80 to replication forks by BAP1 during normal DNA synthesis. *Nat Commun*. 2014; 5: 5128. doi: 10.1038/ncomms6128.
156. Yu H, Pak H, Hammond-Martel I, Ghram M, Rodrigue A, Daou S, Barbour H, Corbeil L, Hebert J, Drobetsky E, Masson JY, Di Noia JM, Affar el B. Tumor suppressor and deubiquitinase BAP1 promotes DNA double-strand break repair. *Proc Natl Acad Sci U S A*. 2014; 111: 285-90. doi: 10.1073/pnas.1309085110.
157. Eletr ZM, Wilkinson KD. An emerging model for BAP1's role in regulating cell cycle progression. *Cell Biochem Biophys*. 2011; 60: 3-11. doi: 10.1007/s12013-011-9184-6.
158. Sahtoe DD, van Dijk WJ, Ekkebus R, Ovaa H, Sixma TK. BAP1/ASXL1 recruitment and activation for H2A deubiquitination. *Nat Commun*. 2016; 7: 10292. doi: 10.1038/ncomms10292.
159. Matattal KA, Agapova OA, Onken MD, Worley LA, Bowcock AM, Harbour JW. BAP1 deficiency causes loss of melanocytic cell identity in uveal melanoma. *BMC Cancer*. 2013; 13: 371. doi: 10.1186/1471-2407-13-371.
160. Cassoux N, Rodrigues MJ, Plancher C, Asselain B, Levy-Gabriel C, Lumbroso-Le Rouic L, Piperno-Neumann S, Dendale R, Sastre X, Desjardins L, Couturier J. Genome-wide profiling is a clinically relevant and affordable prognostic test in posterior uveal melanoma. *Br J Ophthalmol*. 2014; 98: 769-74. doi: 10.1136/bjophthalmol-2013-303867.
161. Versluis M, de Lange MJ, van Pelt SI, Ruivenkamp CA, Kroes WG, Cao J, Jager MJ, Luyten GP, van der Velden PA. Digital PCR validates 8q dosage as prognostic tool in uveal melanoma. *PLoS One*. 2015; 10: e0116371. doi: 10.1371/journal.pone.0116371.

162. Harbour JW, Roberson ED, Anbunathan H, Onken MD, Worley LA, Bowcock AM. Recurrent mutations at codon 625 of the splicing factor SF3B1 in uveal melanoma. *Nat Genet.* 2013; 45: 133-5. doi: 10.1038/ng.2523.
163. Martin M, Masshofer L, Temming P, Rahmann S, Metz C, Bornfeld N, van de Nes J, Klein-Hitpass L, Hinnebusch AG, Horsthemke B, Lohmann DR, Zeschnick M. Exome sequencing identifies recurrent somatic mutations in EIF1AX and SF3B1 in uveal melanoma with disomy 3. *Nat Genet.* 2013; 45: 933-6. doi: 10.1038/ng.2674.
164. Pestova TV, Borukhov SI, Hellen CU. Eukaryotic ribosomes require initiation factors 1 and 1A to locate initiation codons. *Nature.* 1998; 394: 854-9. doi: 10.1038/29703.
165. Johnson CP, Kim IK, Esmaeli B, Amin-Mansour A, Treacy DJ, Carter SL, Hodis E, Wagle N, Seepo S, Yu X, Lane AM, Gragoudas ES, Vazquez F, et al. Systematic genomic and translational efficiency studies of uveal melanoma. *PLoS One.* 2017; 12: e0178189. doi: 10.1371/journal.pone.0178189.
166. Furney SJ, Pedersen M, Gentien D, Dumont AG, Rapinat A, Desjardins L, Turajlic S, Piperno-Neumann S, de la Grange P, Roman-Roman S, Stern MH, Marais R. SF3B1 mutations are associated with alternative splicing in uveal melanoma. *Cancer Discov.* 2013; 3: 1122-9. doi: 10.1158/2159-8290.CD-13-0330.
167. Yavuziyigitoglu S, Koopmans AE, Verdijk RM, Vaarwater J, Eussen B, van Bodegom A, Paridaens D, Kilic E, de Klein A, Rotterdam Ocular Melanoma Study G. Uveal Melanomas with SF3B1 Mutations: A Distinct Subclass Associated with Late-Onset Metastases. *Ophthalmology.* 2016; 123: 1118-28. doi: 10.1016/j.ophtha.2016.01.023.
168. Golas MM, Sander B, Will CL, Luhrmann R, Stark H. Molecular architecture of the multiprotein splicing factor SF3b. *Science.* 2003; 300: 980-4. doi: 10.1126/science.1084155.
169. Yoshida K, Sanada M, Shiraishi Y, Nowak D, Nagata Y, Yamamoto R, Sato Y, Sato-Otsubo A, Kon A, Nagasaki M, Chalkidis G, Suzuki Y, Shiosaka M, et al. Frequent pathway mutations of splicing machinery in myelodysplasia. *Nature.* 2011; 478: 64-9. doi: 10.1038/nature10496.
170. Quesada V, Conde L, Villamor N, Ordonez GR, Jares P, Bassaganyas L, Ramsay AJ, Bea S, Pinyol M, Martinez-Trillos A, Lopez-Guerra M, Colomer D, Navarro A, et al. Exome sequencing identifies recurrent mutations of the splicing factor SF3B1 gene in chronic lymphocytic leukemia. *Nat Genet.* 2011; 44: 47-52. doi: 10.1038/ng.1032.
171. Kalinec G, Nazarali AJ, Hermouet S, Xu N, Gutkind JS. Mutated alpha subunit of the Gq protein induces malignant transformation in NIH 3T3 cells. *Mol Cell Biol.* 1992; 12: 4687-93. doi:
172. Isakov N. Protein kinase C (PKC) isoforms in cancer, tumor promotion and tumor suppression. *Semin Cancer Biol.* 2017. doi: 10.1016/j.semcancer.2017.04.012.
173. Newton AC. Protein kinase C: structure, function, and regulation. *J Biol Chem.* 1995; 270: 28495-8. doi:
174. Chen X, Wu Q, Depeille P, Chen P, Thornton S, Kalirai H, Coupland SE, Roose JP, Bastian BC. RasGRP3 Mediates MAPK Pathway Activation in GNAQ Mutant Uveal Melanoma. *Cancer Cell.* 2017; 31: 685-96 e6. doi: 10.1016/j.ccell.2017.04.002.
175. Wu X, Li J, Zhu M, Fletcher JA, Hodi FS. Protein kinase C inhibitor AEB071 targets ocular melanoma harboring GNAQ mutations via effects on the PKC/Erk1/2 and PKC/NF-kappaB pathways. *Mol Cancer Ther.* 2012; 11: 1905-14. doi: 10.1158/1535-7163.MCT-12-0121.
176. Chen X, Wu Q, Tan L, Porter D, Jager MJ, Emery C, Bastian BC. Combined PKC and MEK inhibition in uveal melanoma with GNAQ and GNA11 mutations. *Oncogene.* 2014; 33: 4724-34. doi: 10.1038/onc.2013.418.
177. Piperno-Neumann S, Kapiteijn E, Larkin J, Carvajal RD, Luke JJ, Seifert H, Roozen I, Zoubir M, Yang L, Choudhury S, Yerramilli-Rao P, Hodi FS, Schwartz GK. (2014). Phase I dose-escalation study of the

- protein kinase C (PKC) inhibitor AEB071 in patients with metastatic uveal melanoma. ASCO annual meeting 2014: J. Clin. Oncol (abstr 9030)).
178. Carita G, Frisch-Dit-Leitz E, Dahmani A, Raymondie C, Cassoux N, Piperno-Neumann S, Nemati F, Laurent C, De Koning L, Halilovic E, Jeay S, Wylie A, Emery C, et al. Dual inhibition of protein kinase C and p53-MDM2 or PKC and mTORC1 are novel efficient therapeutic approaches for uveal melanoma. *European Journal of Cancer*. 2016; 68: S31-S. doi:
 179. Patel M, Smyth E, Chapman PB, Wolchok JD, Schwartz GK, Abramson DH, Carvajal RD. Therapeutic implications of the emerging molecular biology of uveal melanoma. *Clin Cancer Res*. 2011; 17: 2087-100. doi: 10.1158/1078-0432.CCR-10-3169.
 180. Babchia N, Calipel A, Mouriaux F, Faussat AM, Mascarelli F. The PI3K/Akt and mTOR/P70S6K signaling pathways in human uveal melanoma cells: interaction with B-Raf/ERK. *Invest Ophthalmol Vis Sci*. 2010; 51: 421-9. doi: 10.1167/iops.09-3974.
 181. Bjornsti MA, Houghton PJ. The TOR pathway: a target for cancer therapy. *Nat Rev Cancer*. 2004; 4: 335-48. doi: 10.1038/nrc1362.
 182. Hara K, Maruki Y, Long X, Yoshino K, Oshiro N, Hidayat S, Tokunaga C, Avruch J, Yonezawa K. Raptor, a binding partner of target of rapamycin (TOR), mediates TOR action. *Cell*. 2002; 110: 177-89. doi:
 183. Kim DH, Sarbassov DD, Ali SM, King JE, Latek RR, Erdjument-Bromage H, Tempst P, Sabatini DM. mTOR interacts with raptor to form a nutrient-sensitive complex that signals to the cell growth machinery. *Cell*. 2002; 110: 163-75. doi:
 184. Oshiro N, Yoshino K, Hidayat S, Tokunaga C, Hara K, Eguchi S, Avruch J, Yonezawa K. Dissociation of raptor from mTOR is a mechanism of rapamycin-induced inhibition of mTOR function. *Genes Cells*. 2004; 9: 359-66. doi: 10.1111/j.1356-9597.2004.00727.x.
 185. Sancak Y, Thoreen CC, Peterson TR, Lindquist RA, Kang SA, Spooner E, Carr SA, Sabatini DM. PRAS40 is an insulin-regulated inhibitor of the mTORC1 protein kinase. *Mol Cell*. 2007; 25: 903-15. doi: 10.1016/j.molcel.2007.03.003.
 186. Ho AL, Musí E, Ambrosini G, Nair JS, Deraje Vasudeva S, de Stanchina E, Schwartz GK. Impact of combined mTOR and MEK inhibition in uveal melanoma is driven by tumor genotype. *PLoS One*. 2012; 7: e40439. doi: 10.1371/journal.pone.0040439.
 187. Populo H, Soares P, Rocha AS, Silva P, Lopes JM. Evaluation of the mTOR pathway in ocular (uvea and conjunctiva) melanoma. *Melanoma Res*. 2010; 20: 107-17. doi: 10.1097/CMR.0b013e32832ccd09.
 188. Feng X, Degese MS, Iglesias-Bartolome R, Vaque JP, Molinolo AA, Rodrigues M, Zaidi MR, Ksander BR, Merlino G, Sodhi A, Chen Q, Gutkind JS. Hippo-independent activation of YAP by the GNAQ uveal melanoma oncogene through a trio-regulated rho GTPase signaling circuitry. *Cancer Cell*. 2014; 25: 831-45. doi: 10.1016/j.ccr.2014.04.016.
 189. Yu FX, Luo J, Mo JS, Liu G, Kim YC, Meng Z, Zhao L, Peyman G, Ouyang H, Jiang W, Zhao J, Chen X, Zhang L, et al. Mutant Gq/11 promote uveal melanoma tumorigenesis by activating YAP. *Cancer Cell*. 2014; 25: 822-30. doi: 10.1016/j.ccr.2014.04.017.
 190. Lyubasyuk V, Ouyang H, Yu FX, Guan KL, Zhang K. YAP inhibition blocks uveal melanogenesis driven by GNAQ or GNA11 mutations. *Mol Cell Oncol*. 2015; 2: e970957. doi: 10.4161/23723548.2014.970957.

CHAPTER 2

MDMX regulates transcriptional activity of p53 and FOXO

R.C. Heijkants¹, A.F.A.S Teunisse¹, D. de Jong¹, H. Mei², S. Kielbasa², K. Szuhai¹,
A.G. Jochemsen¹.

1) Department of Cell and Chemical Biology, Leiden University Medical Center, Leiden, The
Netherlands

2) Department of Biomedical Data Sciences, Leiden University Medical Center, Leiden, The
Netherlands

Abstract

Tumor suppressor p53 has an important role in cell-fate determination. In cancer cells p53 activity is frequently inhibited by high levels of MDMX and/or MDM2. MDM2 is an E3 ubiquitin ligase whose activity results in ubiquitin- and proteasome-dependent p53 degradation, while MDMX shields p53's transactivation domain. Interestingly, the oncogenic functions of MDMX appear more wide-spread than exclusively the inhibition of p53. The present study sets out to elucidate the MDMX controlled transcriptome. Therefore, we depleted MDMX from a high MDMX expressing uveal melanoma cell line and determined the effect on the transcriptome by RNAseq. Biological function analyses indicate the inhibition of the cell cycle- and stimulation of cell death- regulating genes upon selective MDMX depletion. Although the inhibition of p53 activity clearly contributes to the transcription regulation controlled by MDMX, it appeared that the regulation of multiple genes did not fully rely on p53 expression. Analysis of gene regulatory networks suggests a role for Forkhead box (FOX) transcription factors. Indeed, an increased level of FOXO1 protein was observed upon MDMX depletion, independent of p53 expression. The mechanism of the p53-independent oncogenic functions of MDMX could be partially explained by these p53-independent effects on the transcriptome possibly regulated by FOXO1. As an example, we demonstrate that MXD4 (also named MAD4) expression is controlled by MDMX in a p53-independent manner. Interestingly, we found that MXD4 depletion activates p53 potentially suggesting a backup system in which MXD4 promotes MDM2 activity upon MDMX depletion. In order to enhance p53 activating strategies the MXD4 is proposed as a potential new therapeutic target.

Introduction

The p53 protein is considered to be a master regulator in a cell, mainly due to its central role in cellular stress sensing and its ability to regulate the transcription of a plethora of genes involved in multiple biological processes including cell cycle regulation, apoptosis, metabolism and autophagy [1]. Upon various types of intra- and extracellular stress p53 is activated and stabilized, resulting in transcriptional regulation inducing cell cycle arrest, senescence or apoptosis [2, 3]. Because of its central and important function in cell-fate, p53 activity needs to be under tight control. This stringent control of p53 is provided by many proteins including the ubiquitin E3 ligase MDM2 and the structurally related MDMX. This was best demonstrated *in vivo* where knock out of MDM2 or MDMX in mice resulted in embryonic lethality, which was shown to be p53-dependent [3-7]. Although both MDM2 and MDMX are crucial for mouse embryonic development, in adult tissue MDM2 loss is always lethal whereas MDMX often has more mild effects, indicative of the differences in expression and functions between the two proteins [8-14]. MDM2 is an E3 ubiquitin ligase and has been shown to directly bind with its N-terminal hydrophobic pocket to the N-terminal α helix of p53 and subsequently ubiquitinate p53, which consequently is sent for proteasomal degradation [15-18]. MDMX was initially discovered as a novel p53 interactor with high sequence homology and great structural similarities with MDM2 [19-21]. Despite the high conservation of the acidic domain and the RING domain MDMX does not have any E3 ubiquitin ligase activity. However, MDMX can, via its RING finger, form a heterodimer with MDM2, enhancing MDM2's ubiquitin ligase activity [22-24]. MDMX directly inhibits transcriptional activation by p53 by tightly binding and thereby shielding its transactivation domain [17, 18]. Considering that the levels of MDM2 and MDMX are crucial for the level and/or activity of p53 in a cell, also the levels of MDM2 and MDMX are under stringent control. Upon certain stress, e.g. DNA damage, p53 has to be liberated from its inhibitors MDM2 and MDMX. One mechanism is the degradation of both proteins by increased MDM2-mediated ubiquitination via decreased de-ubiquitination by ubiquitin specific protease (USP) 7 [5, 18, 25]. Additionally, serine-threonine kinase ATM-mediated phosphorylation on MDM2 inhibits its ubiquitin ligase activity towards p53 [26]. As a result the p53 protein is activated and stabilized and can perform its tumor suppressor function. During the recovery phase after an insult, a cell needs to re-constrain p53 activity by MDM2 and MDMX. It has been demonstrated that both MDM2 and MDMX are transcriptional targets of p53 providing a negative feedback loop [27, 28].

Approximately 50% of all human cancers contain a genetically altered p53 gene, either a point mutation or a deletion leading to loss of expression, to render cancer cells re-

sistant to the tumor suppressor function of p53 [29, 30]. Despite the high frequency of p53 mutations the other half of the human cancers evolved alternative mechanisms to attenuate p53 signaling [31]. Amplifications of MDM2 or MDMX are frequently found in sarcoma, glioblastoma, retinoblastoma and breast cancer, providing an interesting therapeutic target, i.e. re-activation of wild-type p53 by inhibition of MDM2/MDMX-p53 interaction [32]. Nutlin-3 was the first small molecule compound reported to exploit MDM2 overexpression by disrupting the MDM2 and p53 interaction resulting in stabilization of p53, subsequently inducing cell cycle arrest and apoptosis [33]. Importantly, it has been demonstrated that this p53 activation by Nutlin-3 was not due to activation of the DNA damage response [34, 35]. Recently it has been shown that the abundance of a naturally occurring MDMX short transcript isoform (MDMX-S) can be promoted using anti-sense oligonucleotides resulting in a shift from the full length to the short RNA isoform leading to decreased MDMX protein levels [36]. MDMX has been shown to be a potent therapeutic target in retinoblastoma, melanoma [37] and wild-type p53 breast cancer [38]. MDMX depletion induced cell cycle arrest and apoptosis in cancer cells in a partly p53-independent manner [37, 39], which could imply that MDMX is not only a valuable therapeutic target in wild-type p53 cancer cells, but also in p53 mutated cells. Indeed in p53 mutated breast cancer cell lines expressing high levels of MDMX protein the expression of MDMX was shown to be essential for cell viability and tumor growth [40]. This could be, at least partly, explained by the p53-independent upregulation of CDK inhibitory protein p27 upon MDMX depletion [39]. Furthermore, high levels of MDMX inhibit the early DNA damage response, independently of p53 and MDM2, resulting in genome instability [41]. However, the exact mechanisms leading to the p53 independent oncogenic functions of MDMX remain unspecified. Here we set out to elucidate to which extent the transcriptome is controlled by MDMX in a wild-type p53 cell line and how transcription regulation by MDMX might explain both its p53-dependent and -independent functions.

Results

Regulation of transcriptional activity by MDMX

The effect of p53 reactivation on the transcriptome has been studied extensively in previous studies (reviewed by: [42]). Here we studied the regulation of the transcriptome by MDMX. For this purpose we used a wild-type p53 cell line (MEL202) derived from a primary uveal melanoma, a cancer which rarely has mutated p53 and frequently highly express MDMX to constrain p53 activity [43]. We had shown before that this cell line is dependent on MDMX expression for proliferation [39]. We generated five MEL202-derived cell lines; one cell line containing a doxycycline-

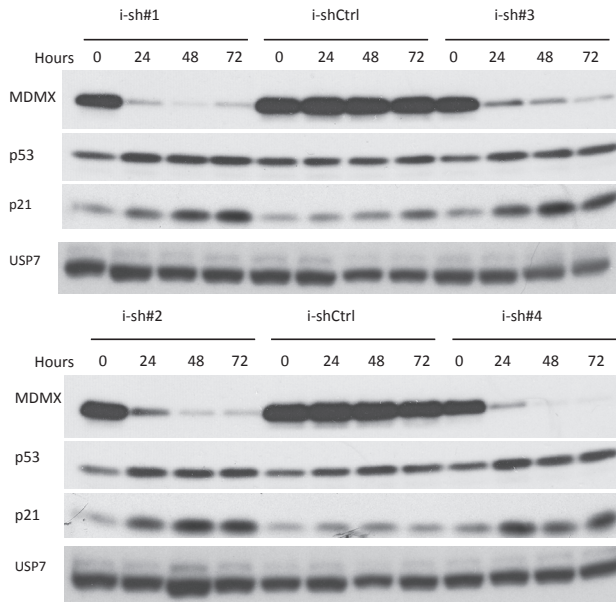
inducible control shRNA expression construct and four cell lines containing a distinct doxycycline-inducible MDMX targeting shRNA expression construct.

Efficiency and kinetics of knockdown was tested by incubating the cells with doxycycline for 24, 48 and 72 hrs and harvesting both RNA and protein. These initial experiments show that the depletion of MDMX was efficient from 24 hours onwards with all shRNA constructs used (Figure 1A). Based on known p53 targets p21 and MAD2L1 we determined the transcriptional kinetics upon MDMX depletion (Figure 1B). The increase of CDK inhibitor p21 expression was already present at 24 hours and did not increase dramatically in the later time points. Mitotic arrest deficient 2 like 1 (MAD2L1), a component of the mitotic spindle assembly checkpoint, repression was only modest at 24, but reached plateau at 48 hours.

Based on these results we have performed transcriptional profiling by RNA sequencing upon doxycycline-inducible MDMX knockdown using 4 different shRNAs and 1 inducible control shRNA incubated with doxycycline for 48 hours. Thorough analysis of the data resulted in the identification of 176 genes which were significantly upregulated at least $0.7\log_2$ fold upon MDMX depletion (Supplementary Table 1). Besides induction of expression, 70 genes were significantly down regulated with at least $-0.7\log_2$ fold upon MDMX depletion (Supplementary Table 2.). Gene ontology (GO) terms pathway analysis clearly showed that the upregulated genes promote cell death and apoptosis, while the down regulated genes are associated with genes involved in controlling the cell cycle (Supplementary Table 3).

To determine whether these effects are mediated via a specific transcription factor we employed the computational method iRegulon [44]. It turned out that of the 176 upregulated genes 66 have a p53 binding motive in their promotor regions (Supplementary Figure 1 and Supplementary Table 1) indicating that, despite the limited log fold changes, 37.5% of the upregulated genes could be explained by the p53 activation upon MDMX depletion. It appeared also from these analysis that the majority (114 of the 176, 65%) of the upregulated genes have a Forkhead Box (FOX) DNA binding motive, recognized by multiple FOX transcription factors. Interestingly, the genes containing a p53 DNA binding motive contained also a FOX motive in 89% of the cases. Analysis of the downregulated genes indicated enrichment for two known repressive transcription regulators, E2F4 and SIN3A. In total 61 of the 70 (87%) downregulated genes contained one or both repressive transcription regulators binding sites (Supplementary Figure 1 and Supplementary Table 2). We verified the transcriptional regulation of a number of these genes using qPCR (Figure 2A). Not only at the RNA level but also at protein level the upregulation of p21 (CDKN1A) and p53 upregulated

1A



B

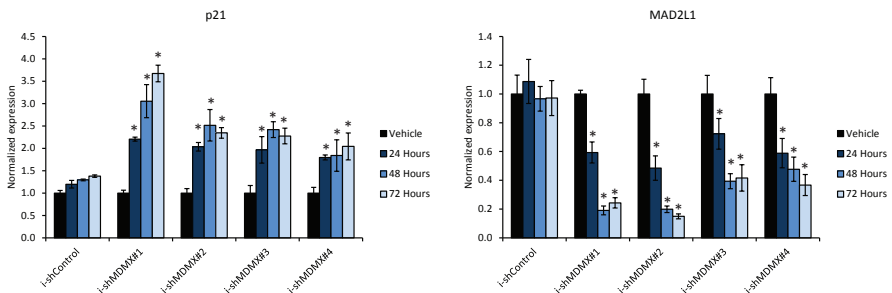


Figure 1. Kinetics of MDMX depletion in MEL202 cells upon doxycycline treatment. A) Protein expression analysis of i-shCtrl and i-shMDMX MEL202 cells harvested after different incubation periods with doxycycline. The cells containing the distinct MDMX targeting shRNA constructs (#1, 2, 3 and 4) show a clear reduction of MDMX protein upon doxycycline treatment (10 ng/ml). Simultaneously with MDMX depletion p53 levels slightly increase and also p21 levels rise, mostly at the later time points. B) Relative mRNA expression of p21 and MAD2L1 in i-shCtrl and i-shMDMX MEL202 cells harvested after different incubation periods with doxycycline (10 ng/ml). Expression of p21 is markedly increased upon MDMX depletion already after 24 hrs and only slightly increases at later time points. Repression of MAD2L1 upon MDMX depletion takes approximately 48 hours before reaching a plateau. Significant differences between the ish-Control and ish-MDMX knockdowns are indicated with an asterisk (*).

modulator of apoptosis (PUMA or BBC3) and downregulation of MAD2L1 could be confirmed (Figure 2B). Importantly, not only the sequence data was confirmed but also the expression of the transcription factors binding to the motives identified by iRegulon (p53 and FOXO1) were slightly increased upon MDMX depletion (Figure 2B). Importantly, both p53 and FOXO1 were found to interact with MDMX in MEL202 cells (Figure 2C). This interaction could be stabilized by the inhibition of the proteasome using MG132. Furthermore, the transcriptional regulation of the same down- and up-regulated MDMX target genes were also tested in a second uveal melanoma cell line (92.1) upon MDMX knockdown. In this cell line similar changes were observed as upon MDMX knockdown in MEL202 (Supplementary Figure 2A). These results indicate that the effects observed in the RNA sequencing are reliable and not cell line dependent.

p53-dependent and -independent effects

We and others have previously shown that depletion of MDMX can result in a p53-independent growth arrest. We, therefore, determined to what extent the observed MDMX induced effects on the transcriptome are p53-dependent. As an initial step we investigated whether non-genotoxic activation of p53 by Nutlin-3 would affect the expression of the same genes as observed upon MDMX depletion. As expected, we observed that the mRNA level of the known p53 target gene p21 (CDKN1A) is strongly induced upon Nutlin-3 treatment (Figure 2D). Similar effects were observed for cytoplasmic FMR1 interacting protein 2 (CYFIP2) and patched domain containing 4 (PTCHD4) (Figure 2C). Max dimerizing protein 4 (MXD4) and phosphoinositide-3-kinase interacting protein 1 (PIK3IP1) expression was also increased upon Nutlin-3 treatment, although the induction was much less compared to p21, CYFIP2 or PTCHD4. The mRNA levels of all genes downregulated upon MDMX knockdown that were tested (exonuclease 1 (EXO1), hyaluronan synthase 2 (HAS2), kinesin family member 23 (KIF23), MAD2L1 and minichromosome maintenance 10 replication initiation factor (MCM10)) were also repressed upon incubation with Nutlin-3 (Figure 2D). To investigate a putative cell line dependency of the regulation of these genes by p53 we investigated the effect of Nutlin-3 treatment in another uveal and in four cutaneous melanoma cell lines, of which 94.07 contain a p53-inactivating mutation. Nutlin-3 treatment of the uveal melanoma cell line 92.1 showed transcriptional regulation of these genes similar to the results in MEL202 (Supplementary Figure 3). p53 wild type cutaneous melanoma cell lines 04.01 and 06.24 showed upon Nutlin-3 treatment that p21, CYFIP1 and PTCHD4 are potent p53 targets, whereas PIK3IP1 and MXD4 expression levels hardly, if anything, changed (Supplementary Figure 3). It can be noted that, although p21, CYFIP1, PTCHD4 responded in every cell line, the levels of increase vary significantly per cell line. Nutlin-3 treatment of both cutaneous melanoma lines resulted in a strong decrease of mRNA levels of genes downregulated upon MDMX

2
A

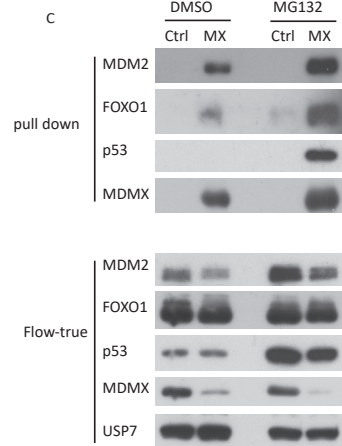
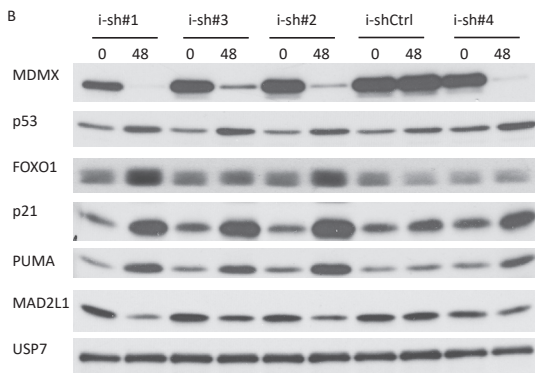
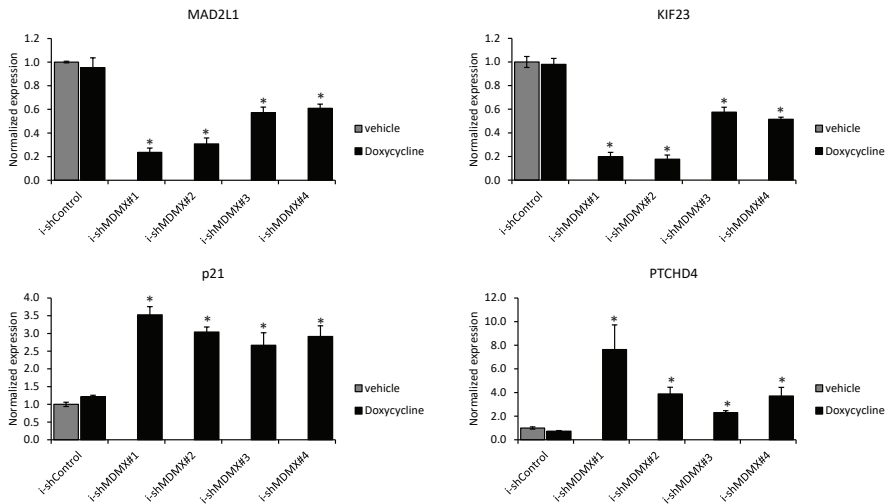
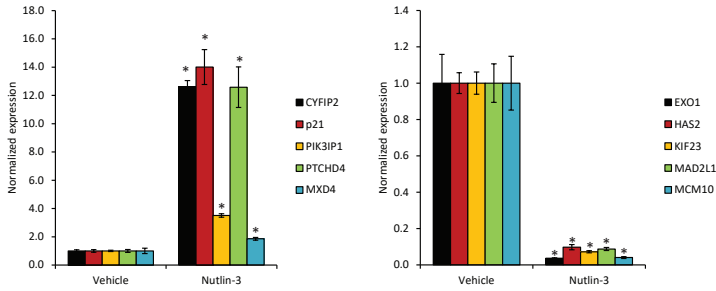


Figure 2. Verification of MDMX target genes. A) Relative Expression of MAD2L1, KIF23, p21 and PTCHD4 genes after 48 hours of doxycycline treatment of indicated cell lines. MAD2L1 and KIF23 are downregulated and p21 and PTCHD4 are upregulated upon MDMX knockdown. Significant differences in expression between doxycycline treated ish-Control cells and ish-MDMX cells is indicated with an asterisk (*). B) Analysis of protein expression after 48 hours doxycycline treatment shows a consistent repression of MAD2L1 level and an increase in p53, FOXO1, p21 and PUMA levels upon MDMX depletion. C) Pull-down of MDMX shows that both p53 and FOXO1 interact with MDMX. By inhibiting the proteasome, using MG132, this interaction is stabilized.

2 D



E

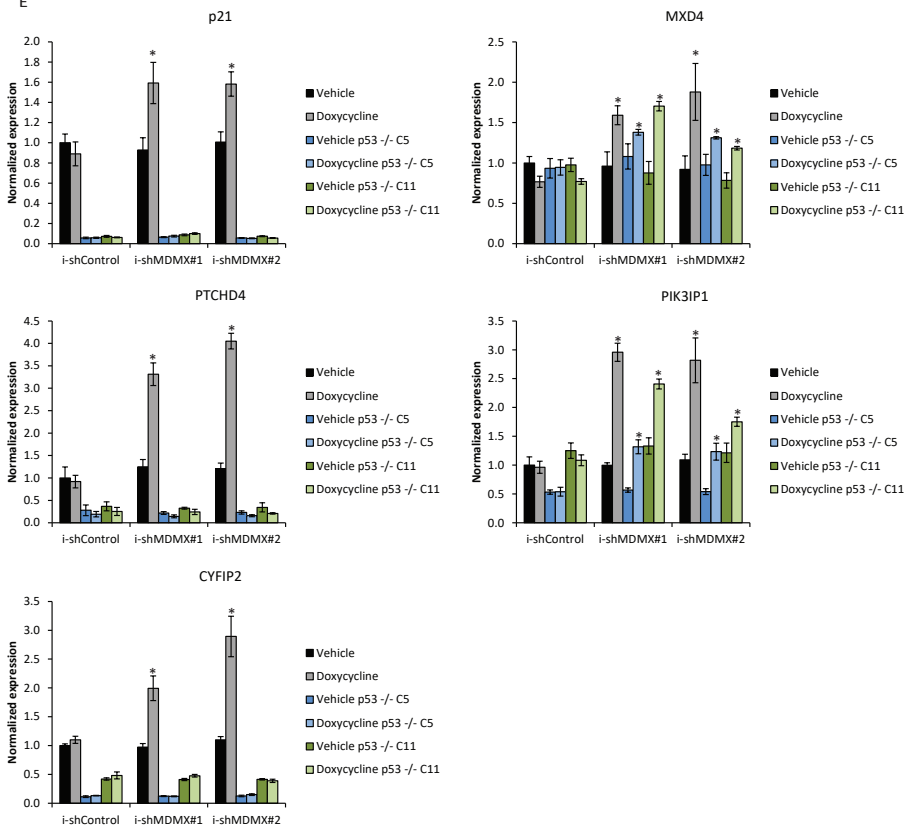


Figure 2. Verification of MDMX target genes. D) Relative mRNA expression of MDMX target genes in MEL202 cells upon 24 hour incubation with 4 μ M Nutlin-3. Significant differences in gene expression between vehicle and Nutlin-3 are indicated with an asterisk (*). E) Relative mRNA expression of MDMX target genes upon MDMX depletion (48 hrs doxycycline, 10 ng/ml) in both MEL202 wild-type and MEL202 p53 knockout cells. Gene expression which was significantly upregulated upon MDMX depletion is indicated with an asterisk (*).

depletion, except for HAS2; some transcriptional repression of HAS2 could only be found 06.24 (Supplementary Figure 3). Cutaneous melanoma cell line 94.07 has an inactivating mutation in p53, which indeed coincides with limited observed changes in the mRNA levels of the analysed genes upon Nutlin-3 treatment (Supplementary Figure 3). Together these results demonstrate that the p53 targets found upon MDMX knockdown are indeed bona fide p53 targets in melanoma in general.

As a second step to study the p53-dependency of the changes in the transcriptome upon MDMX depletion, we created MEL202 cells deficient of p53 using CRISPR/CAS9 technology [45, 46]. We selected two clones which fully lack any detectable p53 protein as a consequence of an adenine insertion (after nucleotide position 143 of the coding sequence) resulting in the mutation of ASP48 to GLU and simultaneously introducing an alternative reading frame resulting in an early translation stop after amino acid position 50 (Supplementary Figure 4A and B). This lack of p53 protein renders the cells, as expected, resistant for Nutlin-3 induced growth arrest (Supplementary Figure 4C). The p53 KO cells did not show any aberrations in their karyotype at chromosomal level compared with the parental cell line as determined by combined binary ratio fluorescence in situ hybridization (COBRA FISH) (Supplementary Figure 4D). From these cells doxycycline-inducible shMDMX or -inducible shCtrl cell lines were generated. With the use of these cell lines we could clearly demonstrate that the increased expression of p21, PTCHD4 and CYFIP2 upon MDMX depletion is fully p53-dependent (Figure 2E). Interestingly, also the basal levels of these genes are largely p53-dependent, indicating that there is some basal p53 activity in these cells. Although both PIK3IP1 and MXD4 were found to be direct p53 targets genes according to our iRegulon analysis, upon MDMX depletion the expression of both genes was increased independently of p53 expression (Figure 2E). Although the MDMX depletion triggered induction of these genes is p53-independent, the Nutlin-3 mediated increase of both MXD4 and PIK3IP1 expression occurred p53-dependent (Supplementary figure 5A), even though the basal levels of both PIK3IP1 and MXD4 were not affected by p53 knockout. We again analysed 92.1 cells to confirm these data, albeit with shp53/mediated p53 depletion instead of knock out. Also in these cells the expression of p21, PTCHD4 and CYFIP2 was found to be p53-dependently upregulated upon MDMX depletion, but increased expression of PIK3IP1 and MXD4 is p53-independent (Supplementary Figure 2A and B). IRegulon network analysis further indicated the involvement of FOXOs in the transcriptional changes upon MDMX depletion. The previous mentioned upregulation of FOXO1 was indeed found to be p53-independent (supplementary figure 5B). These data show that not all upregulated genes upon MDMX depletion are p53 target genes in these cell lines, possibly explaining the p53-independent growth stimulatory functions of MDMX.

Similarly, we found that in both MEL202 and 92.1 cell lines the transcriptional repression of genes upon MDMX knockdown in many cases is partially, but not fully dependent on p53 expression (Supplementary Figure 2A and Supplementary Figure 6).

MXD4 in uveal melanoma

To study the p53-independent functions of MDMX in greater detail we focussed on MXD4, which according to previous studies forms a transcription repressive complex with SIN3A. It has also previously been shown that SIN3A can interact with and protect p53 from MDM2 mediated ubiquitination and degradation [47, 48]. We hypothesized that upregulation of MXD4 upon MDMX depletion could function as a ‘rescue’ mechanism for the tumor cell to counteract the p53 activation. We propose a model in which the increased MXD4 levels sequester a proportion of SIN3A and thereby partly liberate p53 for MDM2-mediated ubiquitination resulting in its degradation. Supporting this model is our finding that MXD4 knockdown in MEL202 induced a p53-dependent growth arrest, indicating a p53 activating effect (Figure 3A and B). This suggestion is strengthened by the observation that the p53 target gene p21 is upregulated in MXD4 knockdown cells. Similarly, the p53 repressed genes MAD2L1 and KIF23 are slightly downregulated in MXD4 knockdown cells (Figure 3A). Interestingly, these effects on p53 target genes could be further enhanced by MDMX knockdown. As expected, these enhanced transcriptional effects correlated with a stronger growth reduction in a long term cell proliferation assay (Figure 3C).

To investigate whether MXD4 knockdown also boosts other p53 stabilizing and/or activating approaches, cells were treated with a low dose of Nutlin-3 (MDM2/X inhibitor), doxorubicin (topoisomerase 2 inhibitor) or XI-011 (inducer of MDMX depletion). In a three day cell viability assay neither MXD4 knockdown nor drug treatments had a strong effect on cell survival. However, the combination of MXD4 knockdown with either Nutlin-3, doxorubicin or XI-011 showed a synergistic reduction in cell survival (Figure 4A). These effects mostly correlate with an enhanced cell cycle arrest upon doxorubicin or XI-011 treatment (G1 and G2/M, respectively) (Figure 4B and C). Neither MXD4 knockdown nor the low concentration drug treatment affected MDMX levels, but did slightly increase p53 levels (Figure 4B). In accordance with the enhanced biological effects, the MXD4 knockdown increases the induction of PUMA by Nutlin-3 and XI-011, and the p21 induction by doxorubicin and XI-011 treatment. Likewise, MAD2L1 repression seems to be slightly more prominent in the MXD4 knockdown cells.

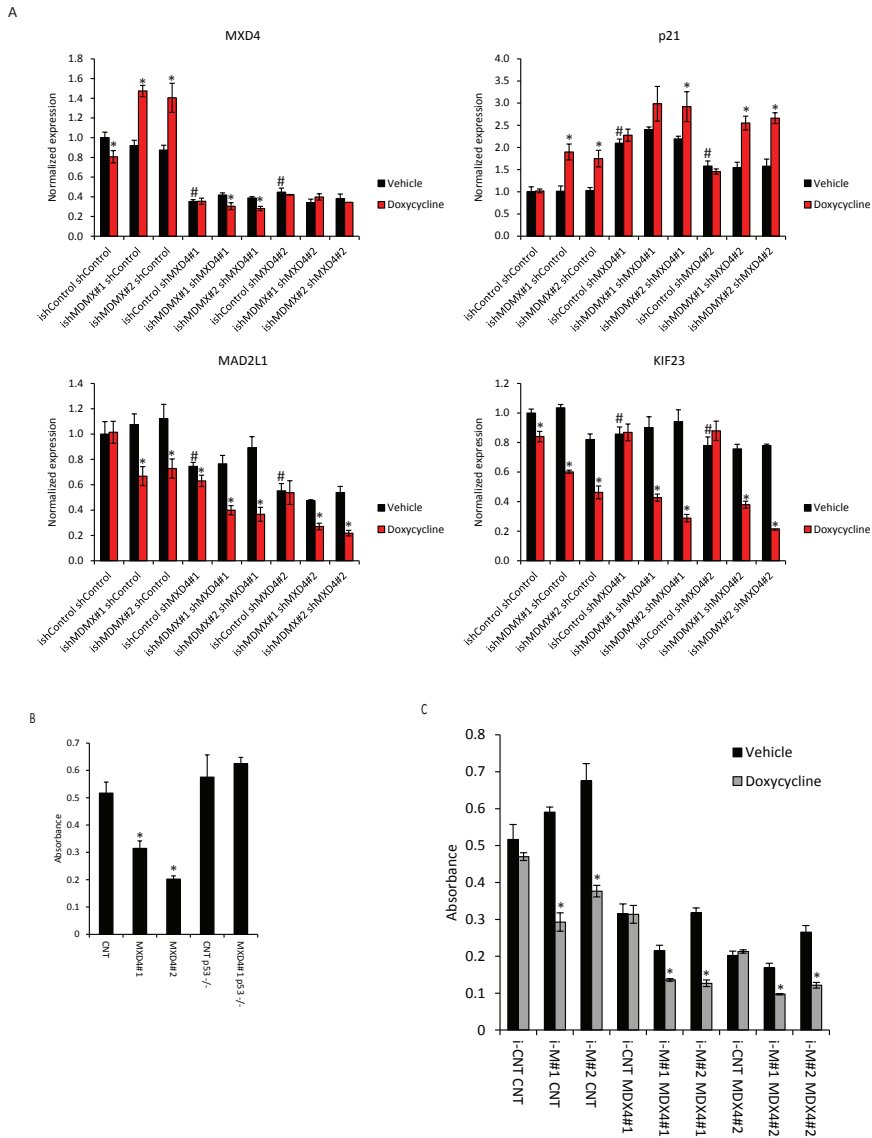


Figure 3. MXD4 knockdown activates p53, inhibits cell growth and enhances effect of MDMX knockdown in MEL202 cells. Relative mRNA expression of MXD4, p21, MAD2L1, PIK3IP1 and KIF23 upon MDMX knockdown in sh-Control and sh-MXD4 cells. Asterisk (*) indicates significant differences between vehicle and doxycycline treated cell line. Significant differences in normalized expression between sh-Control and shMXD4 targeting constructs in cells expressing ish-Control are indicated with a hashtag (#). B) Quantification of long term growth assay of MEL202 MXD4 knockdown cells in p53 wildtype and p53 knockout cells and C) MEL202 cells with either MXD4, MDMX or combined knockdown. Significant differences in absorbance between Control and sh-MXD4 (B) and between vehicle and doxycycline treated (C) is indicated with an asterisk (*).

Discussion

Our studies presented here make it evident that MDMX is affecting the transcription of genes which are implicated in cell cycle regulation and apoptosis. Further analysis of the downregulated MDMX target genes indicate that E2F4- and SIN3A-mediated transcription repression is involved. To discriminate whether SIN3A or E2F4 is essential for the repression of these target genes will be essentially impossible. First, because it has been shown that in SIN3A knock out cells E2F target genes are regulated [49] and, secondly, because previous studies actually showed that SIN3A forms a repressive complex with E2F4 [50, 51]. Most likely a large repressive complex is formed, containing multiple transcription repressive factors like HDACs, to ensure proper target gene repression.

Based on large meta-analysis performed by Fisher and colleagues our results suggest that depletion of MDMX liberates p53, resulting in increased levels of p21 protein, which in turn leads to the activation of the DP, RB-like, E2F4 and Muvb (DREAM) complex, resulting in the repression of target genes [52-54]. Of the 210 essential regulators of G2 phase and mitosis assigned to be regulated by the p53-p21-DREAM axis [53], we identify 23 genes down regulated upon MDMX depletion. The identification of the p53-p21-E2F4/SIN3A axis for 87% of the repressed genes seems to indicate that MDMX controls the transcriptional activity of p53 to control cell cycle progression. However, MDMX clearly has (wt)-p53 independent oncogenic functions [37, 39-41]. Such a p53-independent biological function could correlate with our observation that in distinct cell lines the repression of target genes upon MDMX depletion is not fully p53 dependent. It suggests that MDMX depletion is triggering E2F4/SIN3A-mediated target gene repression that is in part independent of p53.

The list of upregulated genes upon MDMX knockdown contains 66 genes that are potentially regulated directly by p53 of which multiple genes are among the most commonly found p53 activated genes, namely CDKN1A, zinc finger matrin-type 3 (ZMAT3), tumor protein p53 inducible nuclear protein 1 (TP53INP1), tetraspanin 11 (TSPAN11), ectodysplasin a2 receptor (EDA2R) and CYFIP2 [42], indicating that p53 transactivation is repressed by MDMX in our uveal melanoma cells as expected. Surprisingly, although the regulation of most verified genes identified as p53 targets upon MDMX depletion is highly dependent on p53 expression, the regulation of at least PIK3IP1 and MXD4 is not. Both genes were identified as p53-responsive genes in previous studies, but since a clear p53 DNA binding near the promoter region could not be found they were not assigned as true p53 target gene status [52]. Also in our hands the responsiveness of these genes to p53 activation upon Nutlin-3 treatment

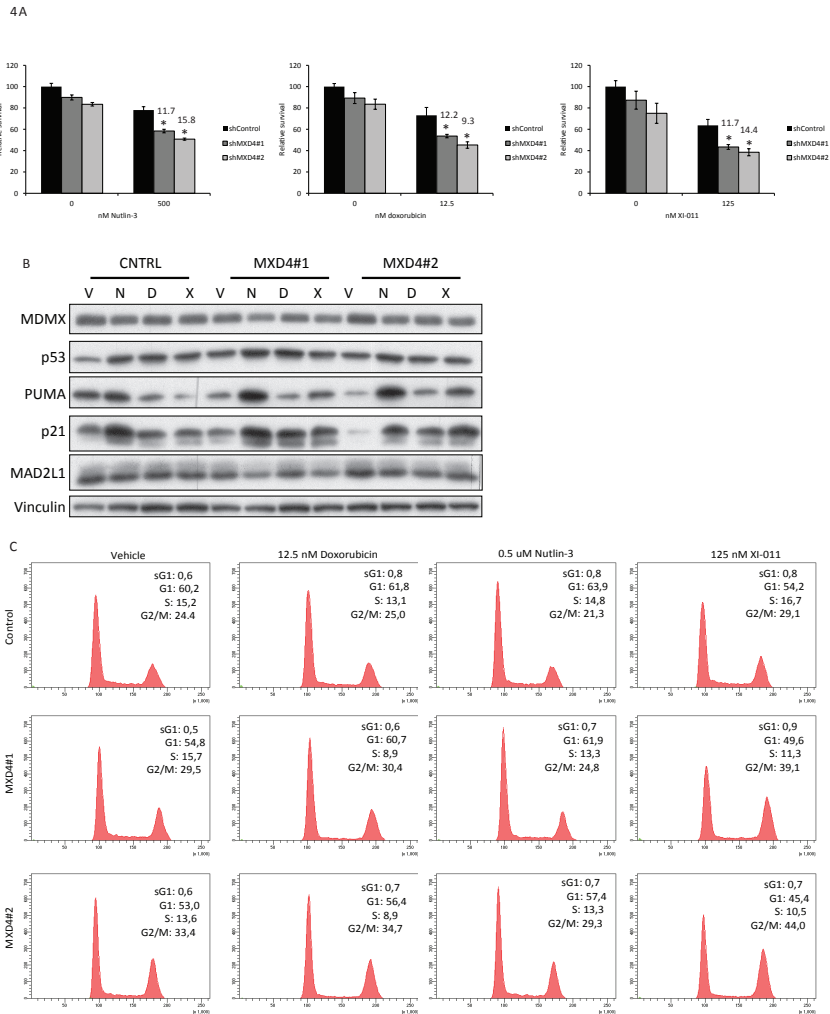


Figure 4. MXD4 knockdown sensitizes cells for p53 activation. A) Relative survival of MEL202 sh-Ctrl and shMXD4 cells treated for 72 hrs with 0.5 μ M Nutlin-3 (N), 12.5 nM Doxorubicin (D), 125 nM XI-011 (X) or vehicle (V). Numbers indicate the Excess over Bliss scores of the combination treated samples. An asterisk (*) indicates significant differences in relative survival comparing the combination treatment with both single treatments. Scores above 2.0 indicate synergism. B) Protein expression analysis of the cells treated as mentioned in A. While MDMX and p53 protein levels hardly change upon combination treatments compared to single treatment, levels of downstream p53 targets p21, PUMA and to a lesser extent MAD2L1 show a stronger response in the combination treated samples. Vinculin expression was assessed to show equal loading. C) Cell cycle profiles of cells treated as indicated at A. Doxorubicin-treated cells show an enhanced S-phase depletion when combined with MXD4 knockdown, while the profiles of the combined MXD4 knockdown + Nutlin-3 treated samples show intermediate phenotype compared to single treatments. Cells with combined MXD4 knockdown and XI-011 showed a clearly enhanced G2/M arrest.

is very weak. Interestingly, both PIK3IP1 and MXD4 contain, like 65% of all the up-regulated genes upon MDMX depletion, FOX transcription factor DNA binding sites. PIK3IP1 has been demonstrated to be a direct FOXO3 target [55]. We could verify that FOXO1 is stabilized upon MDMX depletion in a p53-independent manner. It could be hypothesized that MDMX, by the demonstrated binding of FOXO1, inhibits FOXO1 explaining, at least partly, the p53-independent oncogenic functions of MDMX.

The MXD4 (MAD4) protein has been described as an antagonist for c-MYC by competing with c-MYC for MAX dimerization [56-58]. Possibly relevant for our story is the observation that MXD4 is not only a c-MYC antagonist, but it can also form a transcriptional repressor complex with SIN3A [59]. SIN3A has also been reported to bind p53 and thereby protect it from MDM2-mediated ubiquitination and degradation [47, 48]. Since the reduced proliferation upon MXD4 knockdown is p53-dependent, we hypothesize that MXD4 can repress p53 activity by binding SIN3A, allowing enhanced MDM2-mediated degradation of p53. Indeed we observed a small increase in p53 protein level upon MXD4 knockdown, suggesting that MXD4 is involved in p53 stability. In addition, various p53 stabilizing and activating strategies could be enhanced upon MXD4 knockdown, i.e. upon MDMX depletion, MDM2/X inhibition via Nutlin-3, and treatment of the cells with doxorubicin or XI-011.

In conclusion, our data presented here suggest the existence a novel back-up loop in which a FOX transcription factor is released or activated upon MDMX depletion resulting in increased MXD4 expression. Subsequently, MXD4 competes with p53 for SIN3A binding, sensitizing p53 for MDM2-mediated degradation thereby blunting the p53 tumor suppressor response. Implicating that MXD4 is a potential novel target to boost current p53 activating strategies.

Acknowledgements

The authors like to acknowledge Prof S. van de Burg and Dr. E. Verdegaal for the kind donation of cell lines 94.07 04.01, 04.04 and 06.24. The authors like to acknowledge Dr. M. Goncalves for his assistance and the kind donation of the adenoviral expression vectors used during the establishment of p53 knockout cells.

References

1. Biegling KT, Mello SS, Attardi LD. Unravelling mechanisms of p53-mediated tumour suppression. *Nat Rev Cancer*. 2014; 14: 359-70. doi: 10.1038/nrc3711.
2. Riley T, Sontag E, Chen P, Levine A. Transcriptional control of human p53-regulated genes. *Nat Rev Mol Cell Biol*. 2008; 9: 402-12. doi: 10.1038/nrm2395.
3. Jones SN, Roe AE, Donehower LA, Bradley A. Rescue of embryonic lethality in Mdm2-deficient mice by absence of p53. *Nature*. 1995; 378: 206-8. doi: 10.1038/378206a0.
4. Montes de Oca Luna R, Wagner DS, Lozano G. Rescue of early embryonic lethality in mdm2-deficient mice by deletion of p53. *Nature*. 1995; 378: 203-6. doi: 10.1038/378203a0.
5. Okamoto K, Kashima K, Pereg Y, Ishida M, Yamazaki S, Nota A, Teunisse A, Migliorini D, Kitabayashi I, Marine JC, Prives C, Shiloh Y, Jochemsen AG, et al. DNA damage-induced phosphorylation of MdmX at serine 367 activates p53 by targeting MdmX for Mdm2-dependent degradation. *Mol Cell Biol*. 2005; 25: 9608-20. doi: 10.1128/MCB.25.21.9608-9620.2005.
6. Finch RA, Donoviel DB, Potter D, Shi M, Fan A, Freed DD, Wang CY, Zambrowicz BP, Ramirez-Solis R, Sands AT, Zhang N. mdmX is a negative regulator of p53 activity in vivo. *Cancer Res*. 2002; 62: 3221-5. doi: 10.1158/0008-5472.CCR-01-2000.
7. Parant J, Chavez-Reyes A, Little NA, Yan W, Reinke V, Jochemsen AG, Lozano G. Rescue of embryonic lethality in Mdm4-null mice by loss of Trp53 suggests a nonoverlapping pathway with MDM2 to regulate p53. *Nat Genet*. 2001; 29: 92-5. doi: 10.1038/ng714.
8. Francoz S, Froment P, Bogaerts S, De Clercq S, Maetens M, Doumont G, Bellefroid E, Marine JC. Mdm4 and Mdm2 cooperate to inhibit p53 activity in proliferating and quiescent cells in vivo. *Proc Natl Acad Sci U S A*. 2006; 103: 3232-7. doi: 10.1073/pnas.0508476103.
9. Marine JC, Francoz S, Maetens M, Wahl G, Toledo F, Lozano G. Keeping p53 in check: essential and synergistic functions of Mdm2 and Mdm4. *Cell Death Differ*. 2006; 13: 927-34. doi: 10.1038/sj.cdd.4401912.
10. Valentin-Vega YA, Okano H, Lozano G. The intestinal epithelium compensates for p53-mediated cell death and guarantees organismal survival. *Cell Death Differ*. 2008; 15: 1772-81. doi: 10.1038/cdd.2008.109.
11. Valentin-Vega YA, Box N, Terzian T, Lozano G. Mdm4 loss in the intestinal epithelium leads to compartmentalized cell death but no tissue abnormalities. *Differentiation*. 2009; 77: 442-9. doi: 10.1016/j.diff.2009.03.001.
12. Grier JD, Xiong S, Elizondo-Fraire AC, Parant JM, Lozano G. Tissue-specific differences of p53 inhibition by Mdm2 and Mdm4. *Mol Cell Biol*. 2006; 26: 192-8. doi: 10.1128/MCB.26.1.192-198.2006.
13. Ringshausen I, O'Shea CC, Finch AJ, Swigart LB, Evan GI. Mdm2 is critically and continuously required to suppress lethal p53 activity in vivo. *Cancer Cell*. 2006; 10: 501-14. doi: 10.1016/j.ccr.2006.10.010.
14. Moyer SM, Larsson CA, Lozano G. Mdm proteins: critical regulators of embryogenesis and homeostasis. *J Mol Cell Biol*. 2017. doi: 10.1093/jmcb/mjx004.
15. Barak Y, Oren M. Enhanced binding of a 95 kDa protein to p53 in cells undergoing p53-mediated growth arrest. *EMBO J*. 1992; 11: 2115-21. doi: 10.1101/110115.
16. Momand J, Zambetti GP, Olson DC, George D, Levine AJ. The mdm-2 oncogene product forms a complex with the p53 protein and inhibits p53-mediated transactivation. *Cell*. 1992; 69: 1237-45. doi: 10.1016/0092-8674(92)90323-8.
17. Kawai H, Wiederschain D, Yuan ZM. Critical contribution of the MDM2 acidic domain to p53 ubiquitination. *Mol Cell Biol*. 2003; 23: 4939-47. doi: 10.1128/MCB.23.17.4939-4947.2003.
18. Meulmeester E, Frenk R, Stad R, de Graaf P, Marine JC, Vousden KH, Jochemsen AG. Critical role for a central part of Mdm2 in the ubiquitylation of p53. *Mol Cell Biol*. 2003; 23: 4929-38. doi: 10.1128/MCB.23.17.4929-4938.2003.

19. Shvarts A, Steegenga WT, Riteco N, van Laar T, Dekker P, Bazuine M, van Ham RC, van der Hoven van Oordt W, Hateboer G, van der Eb AJ, Jochemsen AG. MDMX: a novel p53-binding protein with some functional properties of MDM2. *EMBO J.* 1996; 15: 5349-57. doi:
20. Marine JC, Jochemsen AG. Mdmx and Mdm2: brothers in arms? *Cell Cycle.* 2004; 3: 900-4. doi:
21. Bottger V, Bottger A, Garcia-Echeverria C, Ramos YF, van der Eb AJ, Jochemsen AG, Lane DP. Comparative study of the p53-mdm2 and p53-MDMX interfaces. *Oncogene.* 1999; 18: 189-99. doi: 10.1038/sj.onc.1202281.
22. Sharp DA, Kratowicz SA, Sank MJ, George DL. Stabilization of the MDM2 oncoprotein by interaction with the structurally related MDMX protein. *J Biol Chem.* 1999; 274: 38189-96. doi:
23. Gu J, Kawai H, Nie L, Kitao H, Wiederschain D, Jochemsen AG, Parant J, Lozano G, Yuan ZM. Mutual dependence of MDM2 and MDMX in their functional inactivation of p53. *J Biol Chem.* 2002; 277: 19251-4. doi: 10.1074/jbc.C200150200.
24. Linares LK, Hengstermann A, Ciechanover A, Muller S, Scheffner M. HdmX stimulates Hdm2-mediated ubiquitination and degradation of p53. *Proc Natl Acad Sci U S A.* 2003; 100: 12009-14. doi: 10.1073/pnas.2030930100.
25. Pereg Y, Shkedy D, de Graaf P, Meulmeester E, Edelson-Averbukh M, Salek M, Biton S, Teunisse AF, Lehmann WD, Jochemsen AG, Shiloh Y. Phosphorylation of Hdmx mediates its Hdm2- and ATM-dependent degradation in response to DNA damage. *Proc Natl Acad Sci U S A.* 2005; 102: 5056-61. doi: 10.1073/pnas.0408595102.
26. Stommel JM, Wahl GM. Accelerated MDM2 auto-degradation induced by DNA-damage kinases is required for p53 activation. *EMBO J.* 2004; 23: 1547-56. doi: 10.1038/sj.emboj.7600145.
27. Phillips A, Teunisse A, Lam S, Lodder K, Darley M, Emaduddin M, Wolf A, Richter J, de Lange J, Verlaan-de Vries M, Lenos K, Bohnke A, Bartel F, et al. HDMX-L is expressed from a functional p53-responsive promoter in the first intron of the HDMX gene and participates in an autoregulatory feedback loop to control p53 activity. *J Biol Chem.* 2010; 285: 29111-27. doi: 10.1074/jbc.M110.129726.
28. Pigolotti S, Krishna S, Jensen MH. Oscillation patterns in negative feedback loops. *Proc Natl Acad Sci U S A.* 2007; 104: 6533-7. doi: 10.1073/pnas.0610759104.
29. Hollstein M, Hergenbahr M, Yang Q, Bartsch H, Wang ZQ, Hainaut P. New approaches to understanding p53 gene tumor mutation spectra. *Mutat Res.* 1999; 431: 199-209. doi:
30. Hainaut P, Hollstein M. p53 and human cancer: the first ten thousand mutations. *Adv Cancer Res.* 2000; 77: 81-137. doi:
31. Vogelstein B, Lane D, Levine AJ. Surfing the p53 network. *Nature.* 2000; 408: 307-10. doi: 10.1038/35042675.
32. Gao J, Aksoy BA, Dogrusoz U, Dresdner G, Gross B, Sumer SO, Sun Y, Jacobsen A, Sinha R, Larsson E, Cerami E, Sander C, Schultz N. Integrative analysis of complex cancer genomics and clinical profiles using the cBioPortal. *Sci Signal.* 2013; 6: pl1. doi: 10.1126/scisignal.2004088.
33. Vassilev LT, Vu BT, Graves B, Carvajal D, Podlaski F, Filipovic Z, Kong N, Kammlott U, Lukacs C, Klein C, Fotouhi N, Liu EA. In vivo activation of the p53 pathway by small-molecule antagonists of MDM2. *Science.* 2004; 303: 844-8. doi: 10.1126/science.1092472.
34. Vassilev LT. MDM2 inhibitors for cancer therapy. *Trends Mol Med.* 2007; 13: 23-31. doi: 10.1016/j.molmed.2006.11.002.
35. de Lange J, Ly LV, Lodder K, Verlaan-de Vries M, Teunisse AF, Jager MJ, Jochemsen AG. Synergistic growth inhibition based on small-molecule p53 activation as treatment for intraocular melanoma. *Oncogene.* 2012; 31: 1105-16. doi: 10.1038/onc.2011.309.

36. Dewaele M, Tabaglio T, Willekens K, Bezzi M, Teo SX, Low DH, Koh CM, Rambow F, Fiers M, Rogiers A, Radaelli E, Al-Haddawi M, Tan SY, et al. Antisense oligonucleotide-mediated MDM4 exon 6 skipping impairs tumor growth. *J Clin Invest.* 2016; 126: 68-84. doi: 10.1172/JCI82534.
37. Gembarska A, Luciani F, Fedele C, Russell EA, Dewaele M, Villar S, Zwolinska A, Haupt S, de Lange J, Yip D, Goydos J, Haigh JJ, Haupt Y, et al. MDM4 is a key therapeutic target in cutaneous melanoma. *Nat Med.* 2012; 18: 1239-47. doi: 10.1038/nm.2863.
38. Haupt S, Buckley D, Pang JM, Panimaya J, Paul PJ, Gamell C, Takano EA, Lee YY, Hiddings S, Rogers TM, Teunisse AF, Herold MJ, Marine JC, et al. Targeting Mdmx to treat breast cancers with wild-type p53. *Cell Death Dis.* 2015; 6: e1821. doi: 10.1038/cddis.2015.173.
39. de Lange J, Teunisse AF, Vries MV, Lodder K, Lam S, Luyten GP, Bernal F, Jager MJ, Jochemsen AG. High levels of Hdmx promote cell growth in a subset of uveal melanomas. *Am J Cancer Res.* 2012; 2: 492-507. doi:
40. Jeffreena Miranda P, Buckley D, Raghu D, Pang JB, Takano EA, Vijayakumaran R, Teunisse AF, Posner A, Procter T, Herold MJ, Gamell C, Marine JC, Fox SB, et al. MDM4 is a rational target for treating breast cancers with mutant p53. *J Pathol.* 2017. doi: 10.1002/path.4877.
41. Carrillo AM, Bouska A, Arrate MP, Eischen CM. Mdmx promotes genomic instability independent of p53 and Mdm2. *Oncogene.* 2015; 34: 846-56. doi: 10.1038/onc.2014.27.
42. Fischer M. Census and evaluation of p53 target genes. *Oncogene.* 2017; 36: 3943-56. doi: 10.1038/onc.2016.502.
43. Jochemsen AG. Reactivation of p53 as therapeutic intervention for malignant melanoma. *Curr Opin Oncol.* 2014; 26: 114-9. doi: 10.1097/CCO.0000000000000033.
44. Janky R, Verfaillie A, Imrichova H, Van de Sande B, Standaert L, Christiaens V, Hulselmans G, Herten K, Naval Sanchez M, Potier D, Svetlichnyy D, Kalender Atak Z, Fiers M, et al. iRegulon: from a gene list to a gene regulatory network using large motif and track collections. *PLoS Comput Biol.* 2014; 10: e1003731. doi: 10.1371/journal.pcbi.1003731.
45. Maggio I, Stefanucci L, Janssen JM, Liu J, Chen X, Mouly V, Goncalves MA. Selection-free gene repair after adenoviral vector transduction of designer nucleases: rescue of dystrophin synthesis in DMD muscle cell populations. *Nucleic Acids Res.* 2016; 44: 1449-70. doi: 10.1093/nar/gkv1540.
46. Holkers M, Maggio I, Henriques SF, Janssen JM, Cathomen T, Goncalves MA. Adenoviral vector DNA for accurate genome editing with engineered nucleases. *Nat Methods.* 2014; 11: 1051-7. doi: 10.1038/nmeth.3075.
47. Murphy M, Ahn J, Walker KK, Hoffman WH, Evans RM, Levine AJ, George DL. Transcriptional repression by wild-type p53 utilizes histone deacetylases, mediated by interaction with mSin3a. *Genes Dev.* 1999; 13: 2490-501. doi:
48. Zilfou JT, Hoffman WH, Sank M, George DL, Murphy M. The corepressor mSin3a interacts with the proline-rich domain of p53 and protects p53 from proteasome-mediated degradation. *Mol Cell Biol.* 2001; 21: 3974-85. doi: 10.1128/MCB.21.12.3974-3985.2001.
49. McDonel P, Demmers J, Tan DW, Watt F, Hendrich BD. Sin3a is essential for the genome integrity and viability of pluripotent cells. *Dev Biol.* 2012; 363: 62-73. doi: 10.1016/j.ydbio.2011.12.019.
50. Dannenberg JH, David G, Zhong S, van der Torre J, Wong WH, Depinho RA. mSin3A corepressor regulates diverse transcriptional networks governing normal and neoplastic growth and survival. *Genes Dev.* 2005; 19: 1581-95. doi: 10.1101/gad.1286905.
51. Li H, Collado M, Villasante A, Matheu A, Lynch CJ, Canamero M, Rizzoti K, Carneiro C, Martinez G, Vidal A, Lovell-Badge R, Serrano M. p27(Kip1) directly represses Sox2 during embryonic stem cell differentiation. *Cell Stem Cell.* 2012; 11: 845-52. doi: 10.1016/j.stem.2012.09.014.

52. Fischer M, Grossmann P, Padi M, DeCaprio JA. Integration of TP53, DREAM, MMB-FOXO1 and RB-E2F target gene analyses identifies cell cycle gene regulatory networks. *Nucleic Acids Res.* 2016; 44: 6070-86. doi: 10.1093/nar/gkw523.
53. Fischer M, Quaas M, Steiner L, Engeland K. The p53-p21-DREAM-CDE/CHR pathway regulates G2/M cell cycle genes. *Nucleic Acids Res.* 2016; 44: 164-74. doi: 10.1093/nar/gkw927.
54. Fischer M, Steiner L, Engeland K. The transcription factor p53: not a repressor, solely an activator. *Cell Cycle.* 2014; 13: 3037-58. doi: 10.4161/15384101.2014.949083.
55. Schmidt-Strassburger U, Schips TG, Maier HJ, Kloiber K, Mannella F, Braunstein KE, Holzmann K, Ushmorov A, Liebau S, Boeckers TM, Wirth T. Expression of constitutively active FoxO3 in murine forebrain leads to a loss of neural progenitors. *FASEB J.* 2012; 26: 4990-5001. doi: 10.1096/fj.12-208587.
56. Grinberg AV, Hu CD, Kerppola TK. Visualization of Myc/Max/Mad family dimers and the competition for dimerization in living cells. *Mol Cell Biol.* 2004; 24: 4294-308. doi:
57. Hurlin PJ, Queva C, Koskinen PJ, Steingrimsson E, Ayer DE, Copeland NG, Jenkins NA, Eisenman RN. Mad3 and Mad4: novel Max-interacting transcriptional repressors that suppress c-myc dependent transformation and are expressed during neural and epidermal differentiation. *EMBO J.* 1996; 15: 2030. doi:
58. Rottmann S, Luscher B. The Mad side of the Max network: antagonizing the function of Myc and more. *Curr Top Microbiol Immunol.* 2006; 302: 63-122. doi:
59. Yang W, Yang X, David G, Dorsey JF. Dissecting the complex regulation of Mad4 in glioblastoma multiforme cells. *Cancer Biol Ther.* 2012; 13: 1339-48. doi: 10.4161/cbt.21814.
60. Chen PW, Murray TG, Uno T, Salgaller ML, Reddy R, Ksander BR. Expression of MAGE genes in ocular melanoma during progression from primary to metastatic disease. *Clin Exp Metastasis.* 1997; 15: 509-18. doi:
61. De Waard-Siebinga I, Blom DJ, Griffioen M, Schrier PI, Hoogendoorn E, Beverstock G, Danen EH, Jager MJ. Establishment and characterization of an uveal-melanoma cell line. *Int J Cancer.* 1995; 62: 155-61. doi:
62. Amirouchene-Angelozzi N, Frisch-Dit-Leitz E, Carita G, Dahmani A, Raymondie C, Liot G, Gentien D, Nemati F, Decaudin D, Roman-Roman S, Schoumacher M. The mTOR inhibitor Everolimus synergizes with the PI3K inhibitor GDC0941 to enhance anti-tumor efficacy in uveal melanoma. *Oncotarget.* 2016; 7: 23633-46. doi: 10.18632/oncotarget.8054.
63. Herold MJ, van den Brandt J, Seibler J, Reichardt HM. Inducible and reversible gene silencing by stable integration of an shRNA-encoding lentivirus in transgenic rats. *Proc Natl Acad Sci U S A.* 2008; 105: 18507-12. doi: 10.1073/pnas.0806213105.
64. Carlotti F, Bazuine M, Kekarainen T, Seppen J, Pognonec P, Maassen JA, Hoeben RC. Lentiviral vectors efficiently transduce quiescent mature 3T3-L1 adipocytes. *Mol Ther.* 2004; 9: 209-17. doi: 10.1016/j.ymthe.2003.11.021.
65. Chen X, Rinsma M, Janssen JM, Liu J, Maggio I, Goncalves MA. Probing the impact of chromatin conformation on genome editing tools. *Nucleic Acids Res.* 2016; 44: 6482-92. doi: 10.1093/nar/gkw524.
66. Szuhai K, Bezrookove V, Wiegant J, Vrolijk J, Dirks RW, Rosenberg C, Raap AK, Tanke HJ. Simultaneous molecular karyotyping and mapping of viral DNA integration sites by 25-color COBRA-FISH. *Genes Chromosomes Cancer.* 2000; 28: 92-7. doi:
67. Szuhai K, Tanke HJ. COBRA: combined binary ratio labeling of nucleic-acid probes for multi-color fluorescence in situ hybridization karyotyping. *Nat Protoc.* 2006; 1: 264-75. doi: 10.1038/nprot.2006.41.
68. Hof PV, Arindrarto W, Bollen S, Kielbasa S, Laros J, Mei H. (2017). BIOPET: Towards Scalable, Maintainable, User-Friendly, Robust and Flexible NGS Data Analysis Pipelines. 2017 17th IEEE/ACM International Symposium on Cluster, Cloud and Grid Computing (CCGRID), pp. 823-9.

Methods

Cell culture and viability assays

The UM cell lines MEL202 [60] and 92.1 [61] were cultured in a mixture of RPMI and DMEM-F12 (1:1 ratio), supplemented with 10% fetal calf serum (FCS) and antibiotics. Cutaneous melanoma lines 94.07 04.01, 04.04 and 06.24 were cultured in DMEM medium, supplemented with 10% FCS and antibiotics.

For short term growth assay the cells were seeded in triplicate, in 96-well format and incubated for 3 days with drugs as indicated. Cell survival was determined via the Cell Titre-Blue Cell Viability assay (Promega, Fitchburg, WI, USA); fluorescence was measured in a microplate reader (Victor, Perkin Elmer, San Jose, CA, USA). Excess over Bliss values were calculated to determine the synergism between two conditions as described by Amirouchene-Angelozzi N *et al.*[62].

For colony assays the cells were seeded in triplicate in 12-well plates and were incubated for 8 days. Cells were fixed for 5 minutes in 4% paraformaldehyde. DNA was stained using 30-minute incubation with 0.05% crystal violet. After washing and drying the relative number of cells was quantified by solubilizing the crystal violet in methanol and measuring absorbance at 545nm using a microplate reader (Victor3, Perkin Elmer).

Manipulation of cell lines

1. Establishment of inducible MDMX knockdown cell lines

Inducible shRNA knockdown lentiviral vectors were constructed as described previously [38, 63]. Production of lentivirus stocks by transfections into HEK293T cells essentially as described, but calcium phosphate was replaced with PEI [64]. Virus was quantitated by antigen capture ELISA measuring HIV p24 levels (ZeptoMetrix Corp., New York, NY, USA). Cells were transduced using MOI 2 in medium containing 8 µg/ml polybrene. Target sequences of shRNA constructs to deplete MDMX are: #1: 5'-GTGCAGAGGAAAGTTCCAC, #2: 5'- GAATCTCTGAAGCCATGT, #3: 5'- CAGTCCTCAGC-TATTCAT and #4: 5'- AGTCAAGACCAACTGAAGC. As a control shRNA the construct targeting 5'-GAATCTTGTTACATCAGCT was used.

2. Generation of p53 knockout MEL202-derived cells

MEL202 cells were transduced with puromycin-selectable lentiviral guideRNA expression construct (AA19_pLKO.1-puro.U6.sgRNA.Bvel-stuffer) [65], with targets the sequence: 5'-CCATTGTTCAATATCGTCCG-3' in exon 4 of the p53 gene. After selection on puromycin, Cas9 was temporarily expressed upon transduction with adenoviral

Cas9 expression construct (AdV^{D2}P.Cas9.F⁵⁰ [45]) or a control EGFP encoding adenoviral vector (20 IUs/cell). The EGFP-encoding adenoviral vector used differs from AdV.Δ2.donor^{S1/T-TS} [46] in that it has FRT sites flanking an expression cassette consisting of the human PGK1 gene promoter, the EGFP ORF and the bovine growth hormone polyadenylation signal. Cells were selected for p53 inactivity by continuous presence of 4 μM of Nutlin-3 (Cayman Chemical, Ann Arbor, MI, USA) after which single cell derived clones were established and p53 protein expression was analyzed. To determine the exact mutation genomic DNA of these clones was isolated which was used as a template for PCR (Fw primer: GAGACCTGTGGGAAGCGAAA and Rv-primer: GCTGCCCTGGTAGGTTTTCT), followed by Sanger sequencing using the forward primer. To investigate chromosomal abnormalities upon CRISPR/Cas9-mediated p53 knockout, karyotyping of the cell lines was performed by COBRA-FISH as described earlier [66, 67].

RNA sequencing

MEL202 cells with 4 MDMX targeting doxycycline inducible shRNA constructs and 1 control shRNA construct were treated for 48 hours with 10 ng/ml doxycycline; the cell line containing the control shRNA construct was also mock treated to investigate doxycycline induced effects.

RNA was isolated from three independent biological replicates. RNA was isolated using miRNeasy (Qiagen, Hilden, Germany) and treated with DNase (Qiagen) according to manufactures protocol. The quality of the samples was determined using a Bioanalyzer 6000 nanochip (Agilent), followed by ribosomalRNA depletion using Ribo-Zero (Epicentre, Madison, WI, USA) after which the libraries were constructed as described by the NEBNext Ultra Directional RNA Library Prep Kit for Illumina (NEB E7420S). Samples were pooled and sequenced on the HiSeq2500, run type paired-end 2x50bp + dual index on v4 reagents and flowcells. Read counts were extracted from the BAM files with FeatureCounts (version 1.5.3).

All RNAseq files were processed using the BIOPET Gentrapp pipeline version 0.7 developed at the LUMC [68]. This pipeline performs FASTQ pre-processing (including quality control, quality trimming and adapter clipping), RNAseq alignment, read and base quantification, and optionally transcript assembly. In this project, FastQC version 0.11.2 was used for checking raw read QC. Low quality read trimming was done using Sickle version 1.33 with default settings. Adapter clipping was performed using Cutadapt version 1.9.1 with default settings. The RNAseq reads alignment was performed using GSNAP version 2014-12-23 with setting "--npaths 1 --quiet-if-excessive". The reference genome used was GRCh38 without the alternative contigs. The gene

read quantification was performed using HTSeq-count version 0.6.1p1 with setting "--stranded=reverse". The gene annotations used for quantification were GENCODE version 23.

For statistical analysis of the read counts R (version 3.4.2) was used. Read counts were normalized using quantile normalization in the DeSeq package (Version 1.16.1). Differential expression analysis was performed with DeSeq. Gene regulatory network analysis was performed using iRegulon (44). Enriched biological processes (GO) were determined using String-DB version 10.5.

RNA isolation, cDNA synthesis and real-time quantitative PCR

RNA was isolated using the SV total RNA isolation kit (Promega), after which the reverse transcriptase reaction mixture as indicated by Promega was used to synthesize cDNA. qPCR was performed using SYBR green mix (Roche Diagnostics, Indianapolis, IN, USA) in a C1000 touch Thermal Cycler (Bio-Rad laboratories, Hercules, CA, USA). Relative expression of target genes was determined in three independent experiments compared to housekeeping genes CAPNS1 and SRPR. Per experiment the average relative expression was compared to the untreated set at 1. For primer sequences see supplementary table 4.

Western blot analysis

After incubation with drugs as indicated cells were harvested in Laemmli sample buffer. SDS-PAGE was used to separate equal amounts of protein which were blotted onto polyvinylidene fluoride transfer membranes (Millipore, Darmstadt, Germany). Followed by blocking in TBST (10 mM Tris-HCl pH8.0, 150 mM NaCl, 0.2% Tween 20) containing 10% milk. Membranes were incubated with the proper primary antibodies: USP7 (A300-033A, Bethyl Laboratories, Montgomery, TX, USA), MDMX (8C6, Millipore, Burlington, MA, USA), p53 (DO1, Santa Cruz Biotechnology, Dallas, TX, USA), p21 (CP74, Millipore), PUMA (G3, Santa Cruz Biotechnology), MDM2 (SMP14, Santa Cruz Biotechnology; 3G9, Millipore), MAD2L1 (C2C3, Genetex, Irving, CA, USA) or Vinculin (hVIN-1/V9131, Sigma-Aldrich, St Louis, MO, USA) and appropriate HRP-conjugated secondary antibodies (Jackson Laboratories, Bar Harbor, ME, USA). Chemoluminescence was used to visualize bands by exposure to X-ray film.

Flow cytometry

Cells were harvested for cell cycle analysis by trypsinization, washed twice in PBS and fixed in ice cold 70% ethanol. Following fixation, cells were washed in PBS containing 2% FCS and stained using PBS containing 2% FCS, 50 µg/ml RNase and 50 µg/ml

propidium iodide (PI). Flow cytometry analysis was performed using the BD LSR II system (BD Biosciences, San Diego, CA, USA).

Immuno-precipitations

MEL202 cells, 80-90% confluent, were incubated with 10 μ M MG132 for 5 hours to establish inhibition of the proteasome. Cells were washed twice with cold PBS and subsequently lysed in a low salt containing Giordano buffer (50mM Tris-HCl pH7.4, 150 mM NaCl, 0.1% Triton X-100 and 5 mM EDTA; supplemented with phosphatase- and protease inhibitors and 15% glycerol). 500 μ g of lysate was incubated with 30 μ l of 50% bead suspension of HDMX or control beads (Chromotek, Planegg-Martinsried, Germany) in a final volume of 800 μ l, tumbling for 16 hours at 4°C. After this incubation flow-through was collected. Beads were washed 3 times in lysis buffer according to manufactures instructions. Samples were eluted in 40 μ l Laemmli buffer, incubated at 98°C for 5 minutes. Samples were span through a 0.2 μ m nylon centrifugal filter (VWR, Radnor, PA, USA) to remove beads, elution's and flow-through (30 μ l with 15 μ l 3x Laemmli buffer incubated for 5 minutes at 98°C) were separated using SDS-PAGE and analysed as described above (Western blot analysis). Primary antibodies used for protein detection were C29H4 (Cell Signaling technology, Danvers, MA, USA) for FOXO1, a mix of SMP14 (Santa Cruz Biotechnology) and 3G9 (Millipore) was used for MDM2, DO1 (Santa Cruz Biotechnology) for p53, flow-through MDMX was detected using 8C6 (Millipore) and pull-down MDMX using MDMX-BL (Bethyl Laboratories). USP7 (A300-033A, Bethyl Laboratories) was detected to ensure equal loading of the flow-through.

Statistical analysis

Student's t-test was used to calculate the significance between two groups. P-values of 0.05 or less were considered to be significant.

Supplementary table 1. Upregulated genes upon MDMX knockdown

Gene ID	Log2FoldChange	iRegulon motive
PTCHD4	1.92	
PIK3IP1	1.59	FOX
CYFIP2	1.58	FOX
ACTA2	1.57	
CDKN1A	1.48	FOX
EDA2R	1.47	FOX
MIR34A	1.45	
C10orf10	1.35	FOX
BTG2	1.35	
TSPAN11	1.34	FOX
PTGER4	1.23	FOX
C10orf54	1.14	FOX
ZMAT3	1.13	FOX
MXD4	1.09	FOX
FAM212B	1.09	
COL16A1	1.08	FOX
CCDC18-AS1	1.07	
PLN	1.05	FOX
FOXN3-AS1	1.05	
DDIT4	1.04	FOX
p53INP1	1.04	FOX
TCP11L2	1.02	FOX
TXNIP	1.01	FOX
MYO15B	1.00	
DENND2A	1.00	FOX
PNRC1	0.99	FOX
MIR100HG	0.98	
DHX58	0.98	
SORBS2	0.97	FOX
ADAM19	0.95	FOX
ADAMTS6	0.95	FOX
COL24A1	0.95	FOX
TAP1	0.95	
ERBB4	0.94	FOX
YPEL2	0.94	FOX
FOXP2	0.94	FOX

Supplementary table 1. Upregulated genes upon MDMX knockdown (continued)

Gene ID	Log2FoldChange	iRegulon motive	
GAPDHP33	0.93		
RPS27L	0.93	FOX	p53
ARRDC3	0.93	FOX	p53
CASP4	0.93		
EFNA1	0.93	FOX	p53
AP1G2	0.92	FOX	p53
IL1RAPL1	0.92	FOX	
p53TG1	0.92		
PDGFC	0.92	FOX	
RASGRF2	0.92	FOX	
FILIP1	0.91	FOX	p53
FZD4	0.91	FOX	p53
SULF2	0.90	FOX	p53
TM7SF2	0.90		
SYTL2	0.90	FOX	
CFAP70	0.90		
L1CAM	0.89		
PHLDA3	0.89	FOX	p53
CFI	0.89		
LINC00518	0.89		
PLSCR4	0.88	FOX	
CTSO	0.88	FOX	
PPP1R9A	0.87	FOX	
S100B	0.87		
FEZ1	0.87	FOX	
NINJ1	0.86	FOX	p53
CDC42EP5	0.86	FOX	p53
P2RX6	0.86		
BTBD19	0.86		
JMY	0.85	FOX	
WDR66	0.85		
ADAMTS10	0.85	FOX	
LTBP4	0.85	FOX	
EPAS1	0.85		
GMPR	0.85	FOX	
KCNIP4-IT1	0.84		

Supplementary table 1. Upregulated genes upon MDMX knockdown (continued)

Gene ID	Log2FoldChange	iRegulon motive	
ITGB8	0.84	FOX	
KLHL30	0.84	FOX	
ALDH3B1	0.84	FOX	p53
DNASE1L1	0.84		
DRAM1	0.84		
FDXR	0.84	FOX	
JUN	0.84	FOX	
SATB1	0.84	FOX	p53
OPRL1	0.84	FOX	
DMD	0.83	FOX	p53
LACC1	0.83		
ABCA9	0.83	FOX	
RPS6KA2	0.82	FOX	
FSIP2	0.82		
FN1	0.82		
ABCA1	0.82	FOX	
RIMS2	0.82	FOX	p53
HSPB7	0.81	FOX	
C15orf52	0.81		p53
PLA2G4C	0.81		
PLK3	0.81	FOX	
MAML3	0.81	FOX	p53
ZNF630	0.81		
SFRP4	0.80		
PRSS23	0.80	FOX	p53
TSC22D1	0.80	FOX	
BBC3	0.80	FOX	p53
SESN1	0.80	FOX	p53
RND3	0.80	FOX	
MCF2L	0.80	FOX	p53
PCDHGA12	0.80		
SATB1-AS1	0.79		
SEMA3B	0.79	FOX	p53
ICAM5	0.79		
SLC4A3	0.78		p53
MDM2	0.78	FOX	p53

Supplementary table 1. Upregulated genes upon MDMX knockdown (continued)

Gene ID	Log2FoldChange	iRegulon motive	
March2	0.78		
ADAMTS13	0.78	FOX	
GADD45A	0.78	FOX	p53
ARSG	0.78	FOX	p53
C1RL	0.78		
PSMG3-AS1	0.78		
CALCOCO1	0.78		
KLF9	0.78	FOX	
ZNF610	0.77	FOX	
FAM214A	0.77		
KIF26B	0.77	FOX	
C1orf101	0.77	FOX	
LRRTM4	0.76	FOX	
ICA1	0.76	FOX	p53
GPR155	0.76	FOX	p53
RAB7B	0.76		
CUBN	0.76	FOX	
FHDC1	0.75	FOX	p53
DDB2	0.75		p53
LINC00346	0.75		
DOCK8	0.75		
JAG1	0.75	FOX	p53
ZRANB2-AS2	0.75		
SEMA6C	0.75	FOX	p53
ZNF536	0.75	FOX	
FBXO32	0.75	FOX	p53
FAM43A	0.75	FOX	
KLHL7-AS1	0.74		
ACER2	0.74		p53
ETFBKMT	0.74		
CD226	0.74	FOX	p53
PCDHA9	0.74		
DCLK1	0.74	FOX	
VPS37D	0.74		p53
DOK6	0.74	FOX	p53
EPHA2	0.74		p53

Supplementary table 1. Upregulated genes upon MDMX knockdown (continued)

Gene ID	Log2FoldChange	iRegulon motive	
NPAS3	0.73	FOX	
RHOJ	0.73	FOX	p53
LCA5L	0.73	FOX	
PBX1	0.73	FOX	
C1S	0.73		
CA8	0.73	FOX	
ITGAX	0.73		
PAR3B	0.73	FOX	p53
PBXIP1	0.72	FOX	
CNTN1	0.72	FOX	p53
NDRG1	0.72	FOX	
ASTN2	0.72	FOX	p53
HTR2B	0.72	FOX	p53
PLD1	0.72	FOX	p53
LRRC37A3	0.72	FOX	
PLK2	0.72		p53
LAMA4	0.72	FOX	
PQLC3	0.72		
ITGA3	0.71	FOX	p53
COL4A5	0.71	FOX	
GDPD1	0.71		
SV2B	0.71		
FAM227A	0.71		
C1orf116	0.71	FOX	p53
RCAN2	0.71	FOX	
EHHADH	0.71	FOX	p53
ZNF528	0.71		
FAP	0.71	FOX	p53
CRIM1	0.71	FOX	p53
LIMA1	0.70	FOX	p53
IGFBP7	0.70	FOX	p53
RRM2B	0.70	FOX	p53

Supplementary table 2. Downregulated genes upon MDMX knockdown

Gene ID	Log2FoldChange	iRegulon motive	
CEP128	-1.54		
LMNB1	-0.93	E2F4	SIN3A
KIF14	-0.93	E2F4	SIN3A
HLX	-0.92	E2F4	
IDH1	-0.90	E2F4	SIN3A
DTL	-0.88	E2F4	SIN3A
ANP32E	-0.87	E2F4	SIN3A
KIF4B	-0.87		
HAS2	-0.87	E2F4	
MTFR2	-0.87		
SCML1	-0.87	E2F4	
AURKB	-0.86	E2F4	SIN3A
CENPI	-0.85	E2F4	SIN3A
DCLRE1A	-0.85	E2F4	SIN3A
MDM4	-0.83	E2F4	
CDC25A	-0.83		SIN3A
AUNIP	-0.82		
SKA3	-0.81	E2F4	SIN3A
SPAG5	-0.80		SIN3A
KIF23	-0.80		SIN3A
SUV39H1	-0.79	E2F4	SIN3A
CHAF1A	-0.79	E2F4	SIN3A
ERCC6L	-0.79	E2F4	SIN3A
BRCA1	-0.78	E2F4	SIN3A
MCM7	-0.78	E2F4	SIN3A
MAD2L1	-0.78		SIN3A
MCM10	-0.78	E2F4	SIN3A
NUF2	-0.77	E2F4	SIN3A
WDR62	-0.77	E2F4	SIN3A
NMRK2	-0.77		
PBK	-0.77	E2F4	SIN3A
MCM3	-0.77		SIN3A
WDR76	-0.77	E2F4	SIN3A
SASS6	-0.76	E2F4	SIN3A
GSG2	-0.76		SIN3A

Supplementary table 2. Downregulated genes upon MDMX knockdown (continued)

Gene ID	Log2FoldChange	iRegulon motive
CHAF1B	-0.76	E2F4
ZNF114	-0.75	
CLSPN	-0.75	E2F4 SIN3A
FKBP5	-0.75	E2F4 SIN3A
MCM4	-0.75	E2F4 SIN3A
SKA1	-0.75	SIN3A
SKA2	-0.75	E2F4 SIN3A
GTSE1	-0.75	SIN3A
DBF4	-0.74	SIN3A
SMC4	-0.74	E2F4 SIN3A
KIF4A	-0.74	E2F4 SIN3A
SGO1	-0.73	
CCNB1	-0.73	SIN3A
RBM47	-0.73	E2F4 SIN3A
PSMC3IP	-0.73	E2F4 SIN3A
HIST1H2AM	-0.73	E2F4 SIN3A
PRR5L	-0.72	E2F4 SIN3A
MIS18A	-0.72	
E2F8	-0.72	E2F4 SIN3A
DEPDC1B	-0.72	E2F4 SIN3A
ERI1	-0.72	E2F4 SIN3A
SLC43A3	-0.72	E2F4
ATAD5	-0.71	E2F4 SIN3A
CDT1	-0.71	E2F4 SIN3A
MCM5	-0.71	E2F4 SIN3A
HIST1H1E	-0.71	E2F4 SIN3A
SFXN1	-0.71	E2F4
C1orf112	-0.71	E2F4 SIN3A
INCENP	-0.71	E2F4 SIN3A
RACGAP1	-0.71	E2F4 SIN3A
TRAIIP	-0.71	E2F4 SIN3A
DBF4B	-0.70	SIN3A
CEP72	-0.70	
GINS2	-0.70	E2F4
ORC6	-0.70	E2F4 SIN3A

Supplementary table 3.

Up-regulated genes top 5 GO biological processes

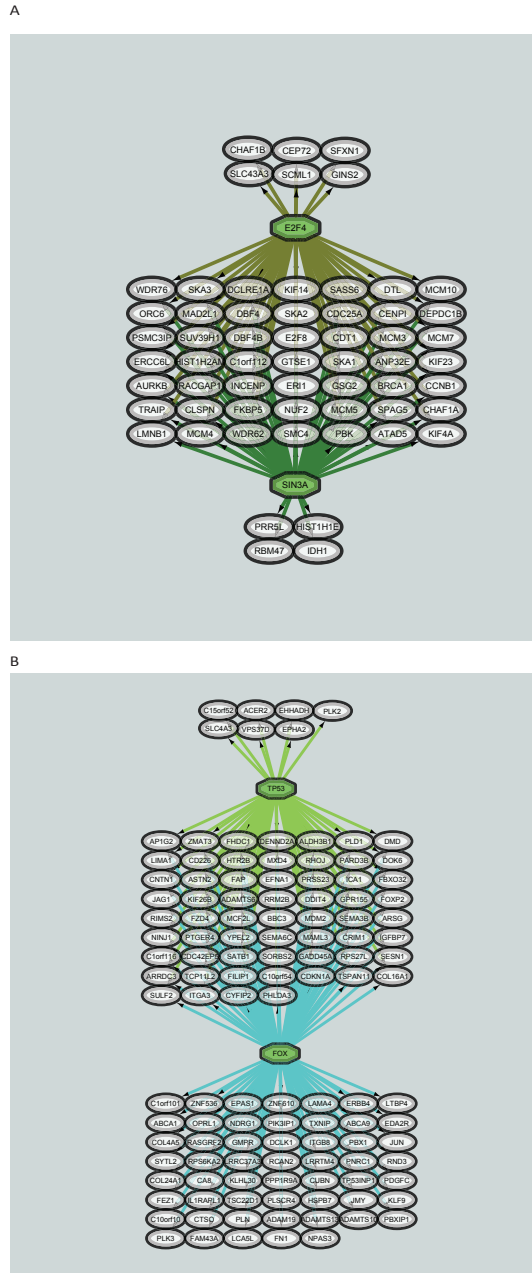
pathway ID	pathway description	count in gene set	false discovery rate
GO:0007155	cell adhesion	24	0.000647
GO:0010942	positive regulation of cell death	19	0.000647
GO:0043068	positive regulation of programmed cell death	18	0.000647
GO:0043065	positive regulation of apoptotic process	17	0.0023
GO:0042981	regulation of apoptotic process	27	0.0048

Down-regulated genes top 5 GO biological processes

pathway ID	pathway description	count in gene set	false discovery rate
GO:0007049	cell cycle	44	2.24E-32
GO:0000278	mitotic cell cycle	36	5.08E-29
GO:1903047	mitotic cell cycle process	34	6.14E-28
GO:0022402	cell cycle process	37	2.68E-27
GO:0007067	mitotic nuclear division	22	1.77E-19

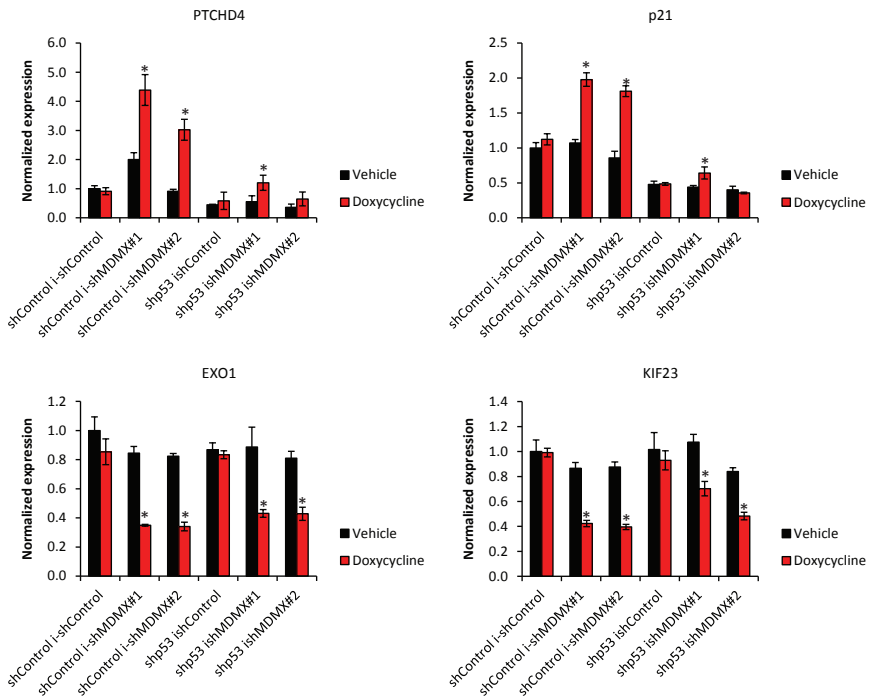
Supplementary table 4.

Primer name	Sequence
CYFIP2 F	CAGCCCAACCGAGTAGAGAT
CYFIP2 R	CTTCACCTCGCTGCAGAAC
PTCHD4 F	TATTTTGCTCCAGGCTGAGG
PTCHD4 R	ATGGCTCTGGCTGACTTGAC
PIK3IP1 F	TGGTGATCATCATTGCCATC
PIK3IP1 R	GCTGCATCTCCCTCTCACAT
p21 F	AGCAGAGGAAGACCATGTGGA
p21 R	AATCTGTCATGCTGGTCTGCC
exo1 F	AAGCGGGAATTGTGCAAG
exo1 R	TGAATACATCCCAAGCTGTC
KIF23 F	TGCTGCCATGAAGTCAGCGAGAG
KIF23 R	CCA GTGGGCGCACCTACAG
MXD4 F	GAGCTGAACTCCCTGCTGAT
MXD4 R	TTTCTCCCTGGCGAAGTC
HAS2 F	TTCAGAGCACTGGGACGAAG
HAS2 R	GACATCTCCCCAACACCTC
E2F7 F	AAGAGCGAGGTCGTAACCA
E2F7 R	CCAGCTTCTGTTTTGCACAG
mcm10 F	TCTTATTTGGAGAAGTTCACAAAGC
mcm10 R	AGGTCAAGAGCTTCACCCATAA
MAD2L1 F	AAGTGGTGAGGTCCTGGAAA
MAD2L1 R	TTCCAACAGTGGCAGAAATG
CAPNS1 F	ATGGTTTTGGCATTGACACATG
CAPNS1 R	GCTTGCCTGTGGTGTGCGC
SRPR F	CATTGCTTTTGCACGTAACCAA
SRPR R	ATTGTCTTGCATGCGGCC

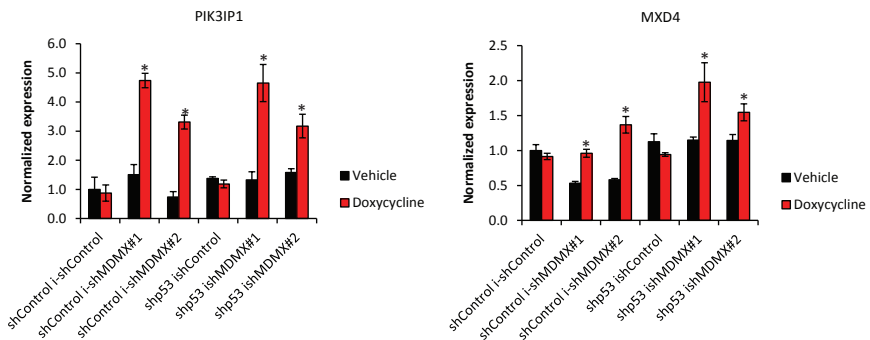


Supplementary figure 1. Gene regulatory network of genes transcriptionally affected upon MDMX knockdown. A) Gene regulatory network of genes downregulated upon MDMX depletion identifying the two major regulators E2F4 and SIN3A. B) Gene regulatory network of genes upregulated upon MDMX depletion identifying the two major regulators p53 and Forkhead box (FOX) transcription regulators.

S2A

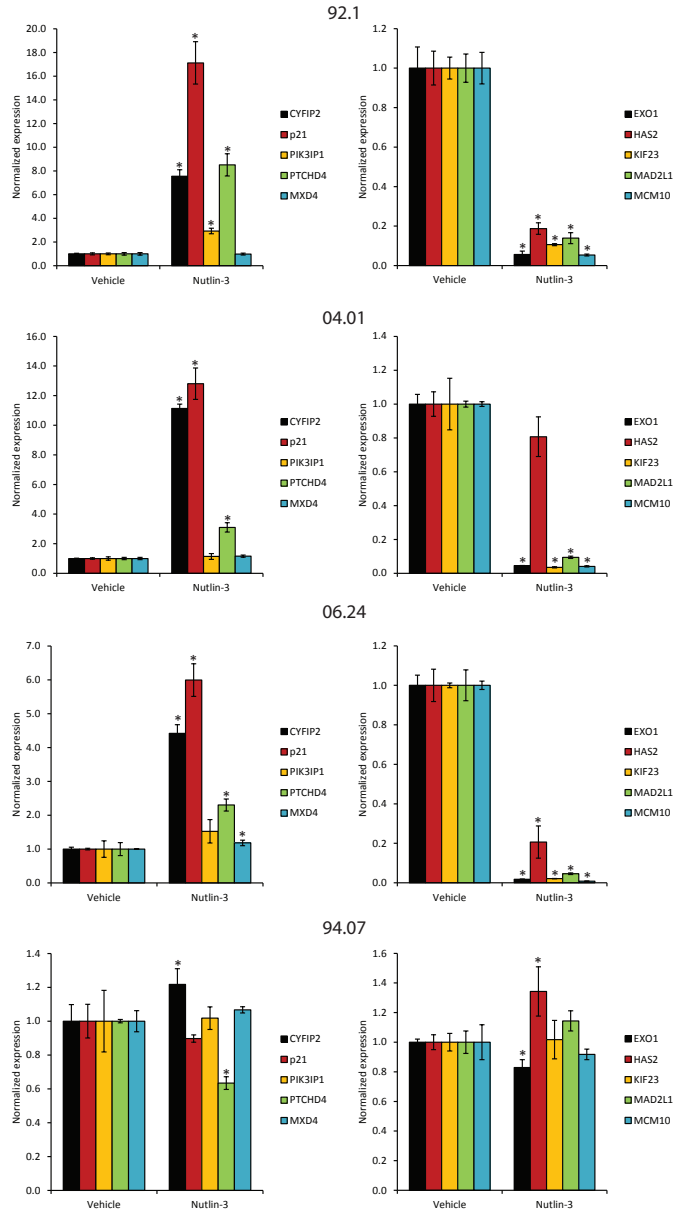


B

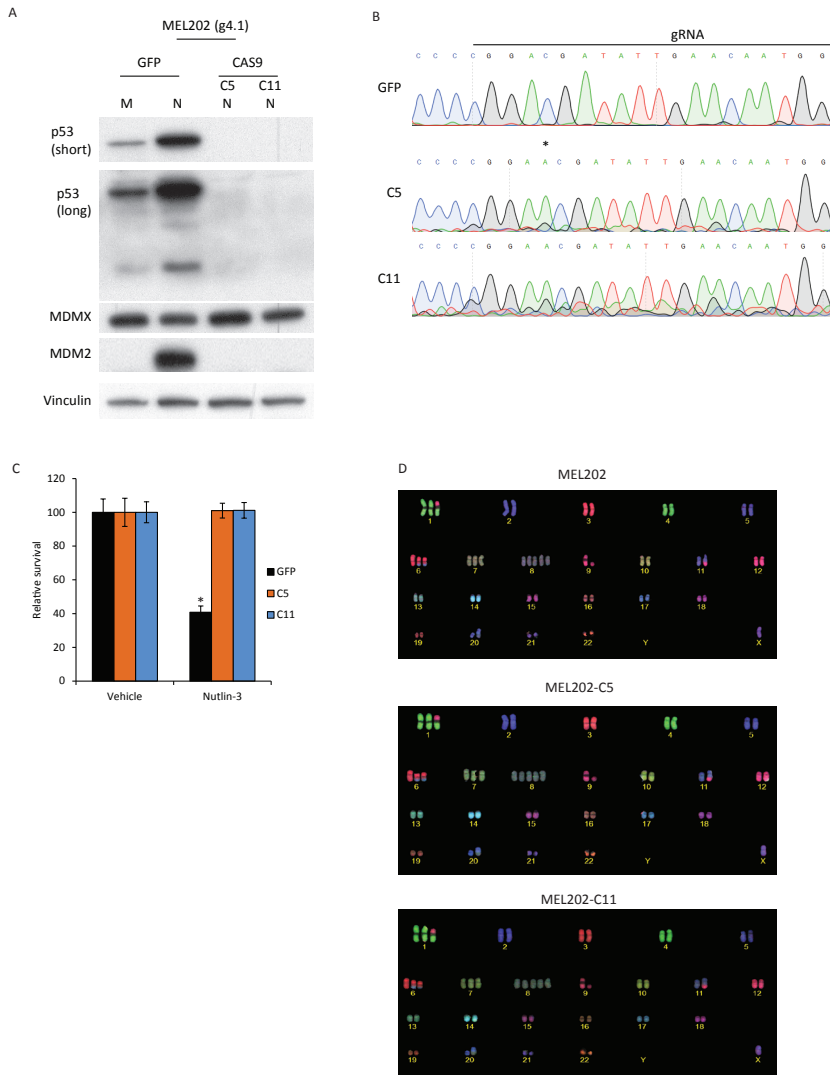


Supplementary figure 2. Transcriptional effects upon MDMX depletion in 92.1 cells. A) Relative mRNA expression of the downregulated genes EXO1 and KIF23, and the upregulated genes p21 and PTCHD4 upon MDMX depletion in 92.1/shCtrl and 92.1/shp53 cells. B) Relative mRNA expression of PIK3IP1 and MXD4 in 92.1 cells under conditions described in A. Significant differences in expression between vehicle and doxycycline treated cells are indicated with an asterisk (*).

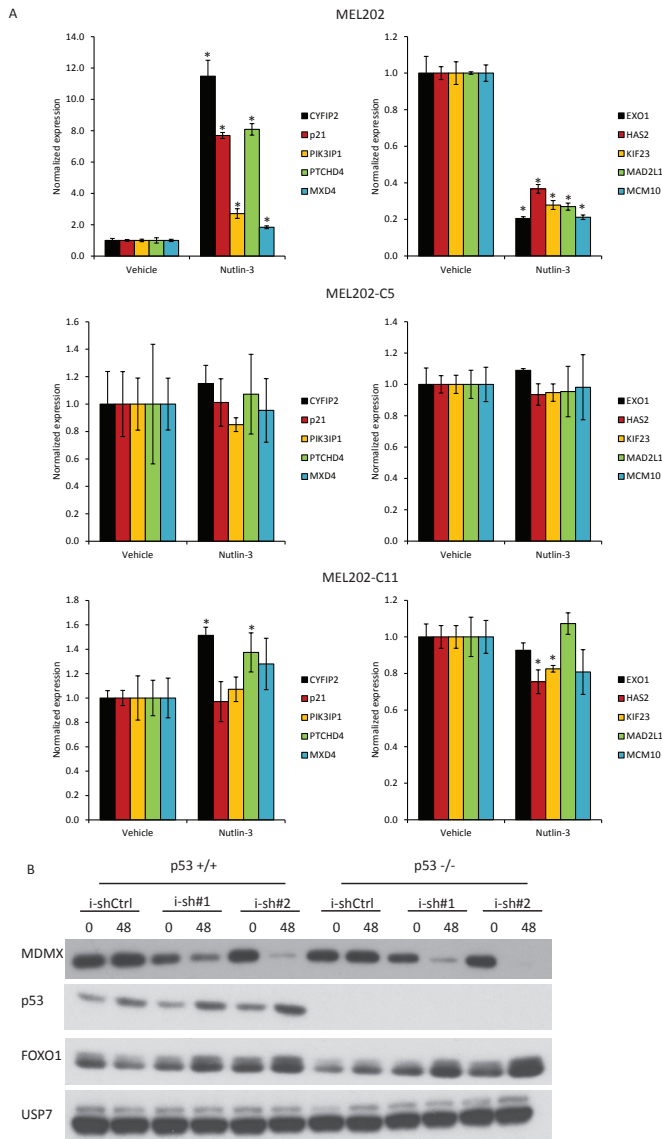
S3



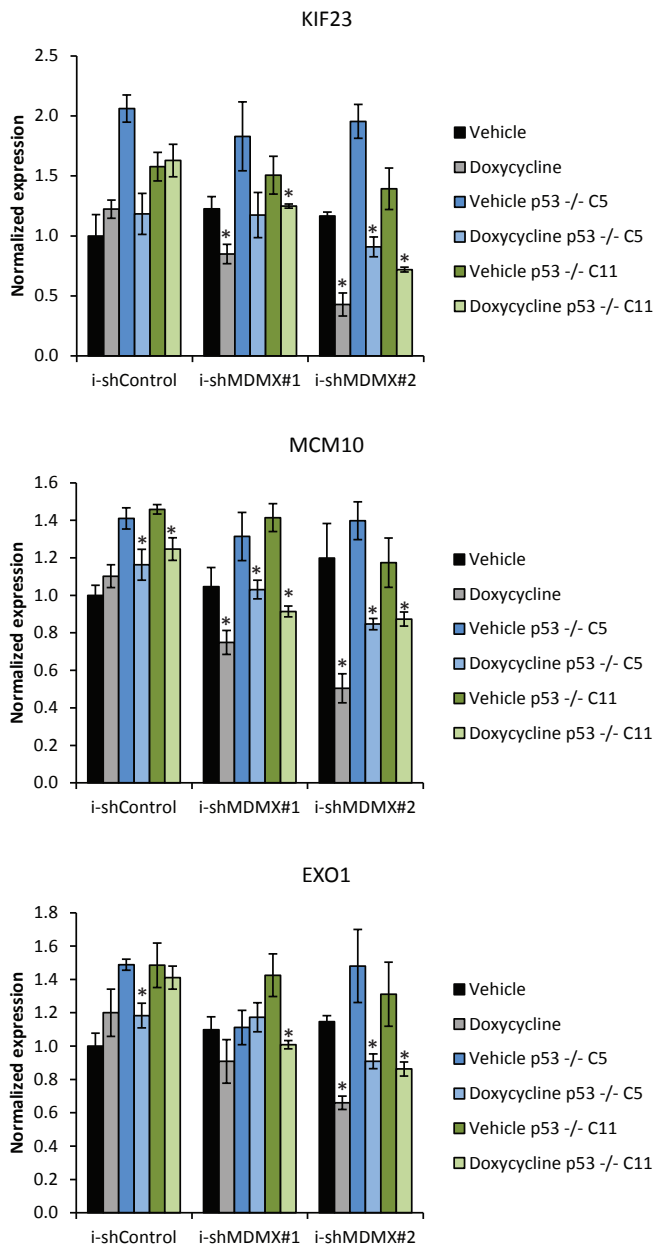
Supplementary figure 3. Effects of Nutlin-3 treatment on expression of 'MDMX target genes' in uveal and cutaneous melanoma cell lines. Relative mRNA expression of CYFIP2, p21, PIK3IP1, PTCHD4, MXD4, EXO1, HAS2, KIF23, MAD2L1 and MCM10 upon 24 hours of Nutlin-3 treatment in uveal melanoma cell line 92.1 and cutaneous melanoma cell lines 04.01, 06.24 and 94.07. Differences in expression between vehicle and Nutlin-3 treated cells found to be significant are indicated with an asterisk (*).



Supplementary figure 4. Generation of p53 knock-out MEL202 cells. A) Analysis of protein expression of MEL202 control cells and two distinct MEL202 p53 knockout cells treated for 24 hrs with DMSO (D) or 4 μ M Nutlin-3 (N). The p53 protein levels increased in the GFP control cells upon Nutlin-3 treatment, but remained undetectable in the p53 knockout cells. MDMX levels showed minor differences between clones. MDM2 levels increased upon Nutlin-3 treatment in the p53 knockout cells but remained undetectable in the p53 KO cells. B) Sanger sequencing of control and p53 knockout clones. Shown are the guide RNA sequence and the insertion of one adenine, highlighted by the asterisk (*). C) Relative survival of MEL202 control- and MEL202 p53 KO cells upon 4 μ M Nutlin-3 treatment for 72 hrs. Significant differences in relative survival between vehicle and Nutlin-3 treatment are indicated with an asterisk (*). D) COBRA-FISH analysis of chromosomal content of MEL202 control - and two distinct p53 knockout clones.



Supplementary figure 5. Effects of Nutlin-3 treatment on expression of ‘MDMX target genes’ in MEL202 control- and p53 knockout cells. A) Relative expression of EXO1, HAS2, KIF23, MAD2L1, MCM10, CYFIP2, p21, PTCHD4, PIK3IP1 and MXD4 in MEL202 control- and p53 knockout cells upon 24 hours of 4 μ M Nutlin-3. Significant differences in expression between vehicle and Nutlin-3 treated cells are indicated with an asterisk (*). B) Protein expression analysis upon MDMX knockdown (48 hrs doxycycline, 10 ng/ml) in MEL202 control- and p53 knockout cells. The cells containing the distinct MDMX targeting shRNA constructs show a clear reduction of MDMX protein upon doxycycline treatment. MDMX depletion results in a slight increase of p53 and FOXO1 protein levels. USP7 was analysed to show equal loading.



Supplementary figure 6. Repressing of transcription upon MDMX depletion is partly p53-independent. Relative mRNA expression of KIF23, MCM10 and EXO1 upon MDMX depletion (48 hour of 20 ng/ml doxycycline), in MEL202 control cells and MEL202 p53 knockout cells. Significant differences in expression between vehicle and doxycycline incubated samples is indicated with an asterisk (*).

CHAPTER 3

Targeting MDMX and PKC δ to improve current uveal melanoma therapeutic strategies

R.C. Heijkants, M. Nieveen, K.C.'t Hart, A.F.A.S Teunisse, A.G. Jochemsen.

Department of Cell and Chemical Biology, Leiden University Medical Centre, Leiden,
the Netherlands.

Abstract

Uveal melanoma (UM) is the most frequent ocular cancer in adults, accounting for ~5% of the total melanoma incidence. Although the primary tumour is well treatable, patients frequently develop metastases for which no curative therapy exists. Highly activated protein kinase C (PKC) is a common feature of UM and has shown potential as therapeutic intervention for UM patients. Unfortunately, PKC inhibition as single treatment appears to have only limited clinical benefit. Combining PKC inhibition with activation of p53, which is rarely mutated in UM, by MDM2 inhibitors has shown promising results *in vitro* and *in vivo*. However, clinical studies have shown strong adverse effects of MDM2 inhibition. Therefore, we investigated alternative approaches to achieve similar anti-cancer effects, but with potentially less adverse effects.

We studied the potential of targeting MDMX, an essential p53 inhibitor during embryonal development but less universally expressed in adult tissues compared to MDM2. Therefore, targeting MDMX is predicted to have less adverse effects in patients. Depletion of MDMX, like the pharmacological activation of p53, inhibits the survival of UM cells, which is enhanced in combination with PKC inhibition.

Also pan-PKC inhibitors elicit adverse effects in patients. Since the PKC family consists of 10 different isoforms it could be hypothesized that targeting a single PKC isoform would have less adverse effects compared to a pan-PKC inhibitor. Here we show that specifically depleting PKC δ inhibits UM cell growth, which can be further enhanced by p53 reactivation.

In conclusion, our data show that the synergistic effects of p53-activation by MDM2 inhibition and broad spectrum PKC inhibition on survival of UM cells can also largely be achieved by the presumably less toxic combination of depletion of MDMX and targeting a specific PKC isoform, PKC δ .

Introduction

Uveal melanoma (UM) is a collective name for a cancer arising from the melanocytes originating from the choroid (85%), iris (5%) or ciliary body (10%).[1] Primary tumors can be treated effectively, but approximately half of the patients develop metastasis within 15 years after primary tumor detection.[2, 3] Thus far no therapeutic intervention has been successful in treating metastatic UM. Due to the lack of effective therapy the median survival of patients with metastasized UM therefore ranges between 3 and 12 months.

UM is most frequently driven by activating mutations in the alpha subunits of G-proteins GNAQ (50%) or GNA11 (43%).[4-6] As a result, these G-proteins are locked in a GTP-bound state, continuously activating a number of signaling pathways, including the MAPK pathway. The latter is achieved via an important downstream effector of GNAQ and GNA11, Phospholipase C- β (PLC- β), which hydrolyzes phosphatidylinositol 4,5-bisphosphate (PIP2) to generate inositol 1,4,5-trisphosphate (IP3) and diacylglycerol (DAG).[7] These are both second messengers activating various protein kinase C (PKC) isoforms, which in turn fuel the continuous activation of the MAPK pathway. These findings have spurred studies to investigate the potential of PKC and MEK inhibitors in treating UM patients. UM cells containing a GNAQ or GNA11 mutation are indeed dependent on MAPK signaling and were shown to be sensitive to both MEK and PKC inhibition.[8, 9] However, preclinical *in vivo* studies showed that both MEK and PKC inhibition is needed to completely abolish MAPK signaling and thereby tumor growth.[9] Confirming these pre-clinical studies, phase I clinical trials show promising results, but only modest clinical benefit, for both PKC and MEK inhibitors as single agents.[10] Based on the pre-clinical studies a phase II clinical trial was conducted to assess combined PKC and MEK inhibition. This phase II clinical trial was terminated premature due to strong adverse effects [11]. Based on the clinical activity of PKC inhibitor Sotrastaurin/AEB071, progression free survival of 15 weeks in half of the patients[10], has encouraged us and others to explore whether the effect of Sotrastaurin can be boosted by interfering with additional oncogenic or tumor suppressor pathways. New insights into UM has stimulated studies combing PKC inhibition with CDK inhibition or targeting the PI3K/mTOR pathway.[11] An alternative interesting approach could be the activation of p53, which is essentially never mutated in UM. We have previously shown that UM frequently overexpress the p53 inhibitors MDM2 and/or MDMX.[12] Furthermore, we found that pharmacological activation of p53 or depletion of MDMX results in diminished UM cell growth and synergistically enhances DNA damage induced cell death.[13] Recently, it has been shown that the combination of an inhibitor of the MDM2-p53 interaction (CGM097[14]) with the broad PKC

inhibitor Sotrastaurin did not achieve synergistic inhibition of cell growth *in vitro*. [11] Even so, *in vivo* 4 out of 5 PDX models showed a significant additive effect when AEB071 was combined with the MDM2 inhibitor CGM097.

In this study we re-activated p53 by Nutlin-3 treatment and demonstrate that the combination of Nutlin-3 with Sotrastaurin does synergistically inhibit UM cell growth *in vitro*. Our data suggest these synergistic effects are due to a switch from a p53-induced cell cycle arrest to a pro-apoptotic response in combination with PKC inhibition. Detailed genetic studies showed that depletion of MDMX from UM cells enhances the efficacy of pan-PKC inhibition and, *vice versa*, PKC δ depletion sensitizes UM cells for p53 activation. Our results indicate that specifically targeting MDMX or PKC δ are potential new avenues for effectively treating UM patients in combination with PKC-inhibitor(s) or p53 reactivation, respectively.

Results

Synergistic growth inhibition upon PKC inhibition and p53 reactivation

We first examined whether p53 reactivation (Nutlin-3) in combination with PKC inhibition (Sotrastaurin) synergistically inhibits the growth of UM cells (Figure 1). In cell lines MEL270, MEL202, MM66, OMM2.5, OMM2.3 and MM28 combining Sotrastaurin with Nutlin-3 resulted in synergistic growth inhibition. So far the OMM1 cell line is the only exception of all GNAQ/11 mutated cell lines tested in which Sotrastaurin does not significantly enhance the Nutlin-3 effect. As expected, and shown before [9], MEL290 cells, lacking a GNAQ/11 mutation, are not responsive to Sotrastaurin and the combination of Nutlin-3 and Sotrastaurin is even antagonistic.

Combined Nutlin-3 and Sotrastaurin treatment promotes apoptosis

To assess target engagement of Sotrastaurin in the GNAQ/11 mutated UM cell lines we determined the levels of phosphorylated PKC δ/θ and phosphorylated MARCKS (Figure 2). The levels of these phosphorylated proteins almost disappeared or were significantly reduced upon Sotrastaurin treatment, confirming inhibition of the PKC activity. In GNAQ/11 wild-type cell line MEL290 neither phosphorylated PKC δ/θ nor could phospho-MARCKS not be detected, as has previously been reported.[9] Effectivity of Sotrastaurin was further confirmed by the reduced mRNA levels of *CDC25A*, *Survivin* and *Cyclin D1* in the treated cells (Supplementary Figure 1S), as has been reported before [8, 15]. Interestingly, in most cell lines Sotrastaurin also increased the levels of the pro-apoptotic protein PUMA. Treating cells with Nutlin-3 resulted in increased levels of p53 protein in all cell lines, with a concomitant increase in

expression of known target genes/proteins (e.g. p21, MDM2 and PUMA; Figure 2, Supplementary figure 1S). Furthermore, p53 reactivation repressed the expression of the pro-survival gene *Survivin* (Supplementary Figure 1S).

Combined Sotrastaurin/Nutlin-3 treatment slightly further increased the levels of the pro-apoptotic PUMA protein compared to single treatments while, in contrast, *CDC25A* and *Survivin* mRNA levels and p21 protein were reduced in most cell lines compared to single treatments. The mRNA levels of p21 were not reduced upon combinatory treatment, suggesting that the p21 protein reduction is regulated at a post transcriptional level. These results suggest that the pro-apoptotic response remains the same or is slightly increased in the combination treatment, but that the cell cycle arrest and pro-survival response is reduced, indicative of a shift from a cell cycle arrest to apoptosis.

To study whether the observed shift in biochemical response results in increased apoptosis, we investigated PARP cleavage as a marker for apoptosis because upon induction of apoptosis the PARP protein gets cleaved by activated caspases. Clear increased levels of cleaved PARP were detected in cell lines MEL270, OMM2.3 and OMM2.5 when treated with Nutlin-3/Sotrastaurin (Figure 3a) and to a lesser extent in OMM1 and MEL202 cells. In MM66 and MM28 cells Sotrastaurin treatment alone already resulted in PARP cleavage, which was not further enhanced by addition of Nutlin-3 (Figure 3a). However, in MM66 and MM28 the full-length PARP levels in the combined treated cells decreased, indicating that the percentage of cleaved PARP compared to full length still increased in the Nutlin-3/Sotrastaurin treated cells. Additionally, cleaved caspase 3 was increased in MM66 and MM28 cells further indicating the induction of apoptosis (Supplementary Figure 2a). No PARP cleavage was observed in MEL290 cells.

Since the main goal is to find better treatment for UM metastases, further experiments have been performed with metastasis-derived cell lines only. Flow cytometry analysis was performed to examine the effects of the drugs on the cell cycle progression and a possible induction of a subG1 fraction, indicative of cell death. The MM66 and OMM1 cells showed an arrest in the G1 phase upon p53 reactivation. This effect was not obvious in MM28 cells, possibly also because these cells grow very slowly and the population of untreated cells already contains 87% of cells in G1-phase (Figure 3b and Supplementary Figure 2Sb). Nutlin-3 treatment did slightly increase subG1 fraction in MM28 cells. Cell cycle profiles of OMM2.3 and OMM2.5 cells were only slightly affected by treatment with Nutlin-3. Sotrastaurin treatment induced an accumulation of cells in G1 phase in all cell lines. In MM66 and MM28 cell lines Sotrastaurin also

1

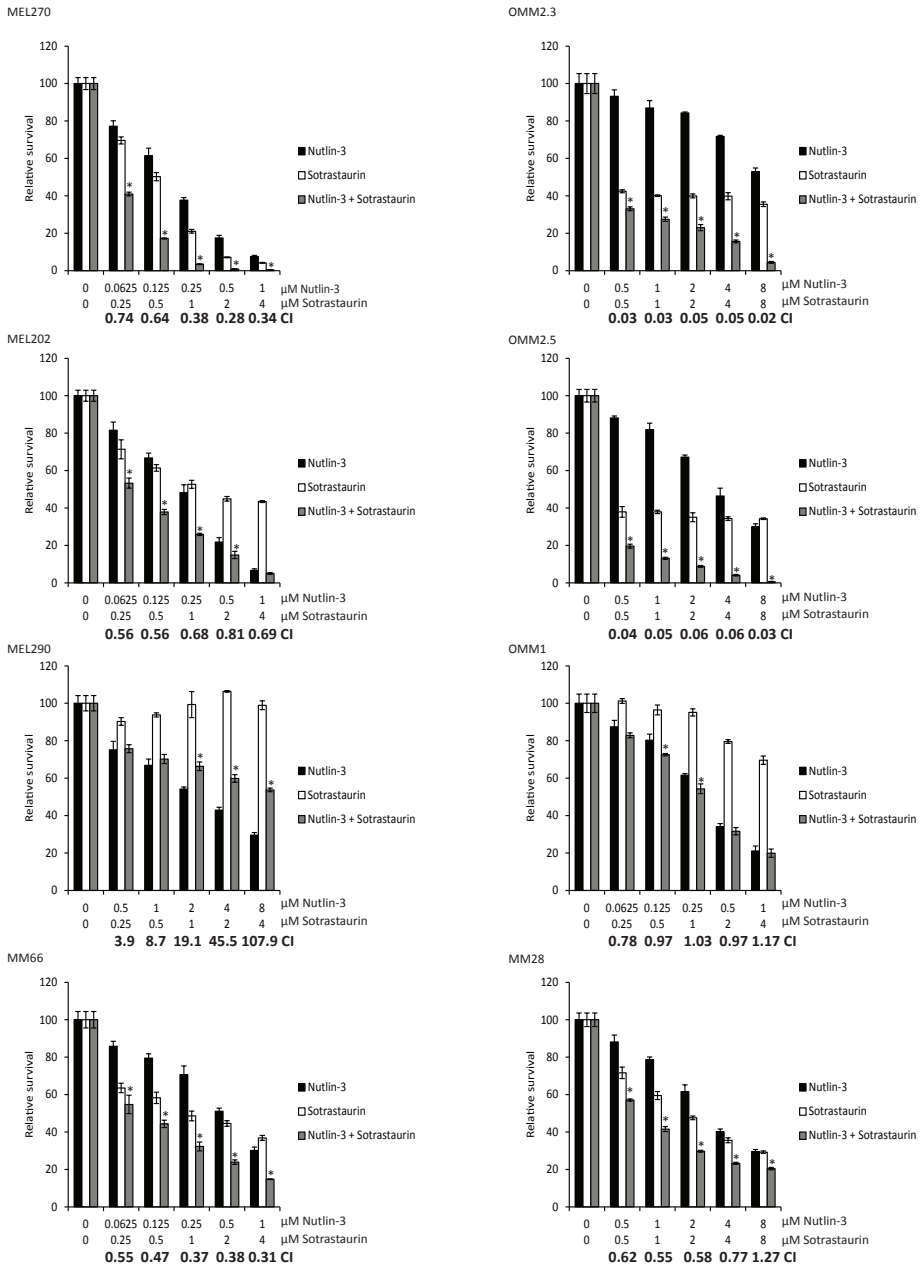


Figure 1. Synergistic growth inhibition by Sotrastaurin and Nutlin-3 in GNAQ/11 mutated UM cells. Various UM cell lines were treated for 72 hours with indicated concentrations Sotrastaurin and Nutlin-3 alone or in combination to determine the effect on cell viability. Data plotted are the normalized averages with the standard deviation as error bars. To determine putative synergism

the combination index (CI) values were calculated with the Compusyn software. CI values below 0.9 were considered to be synergistic, between 0.9 and 1.1 additive and above 1.1 to be antagonistic. Combinations which survival significantly differed compared to both single treatments are indicated with an asterisk (*).

2

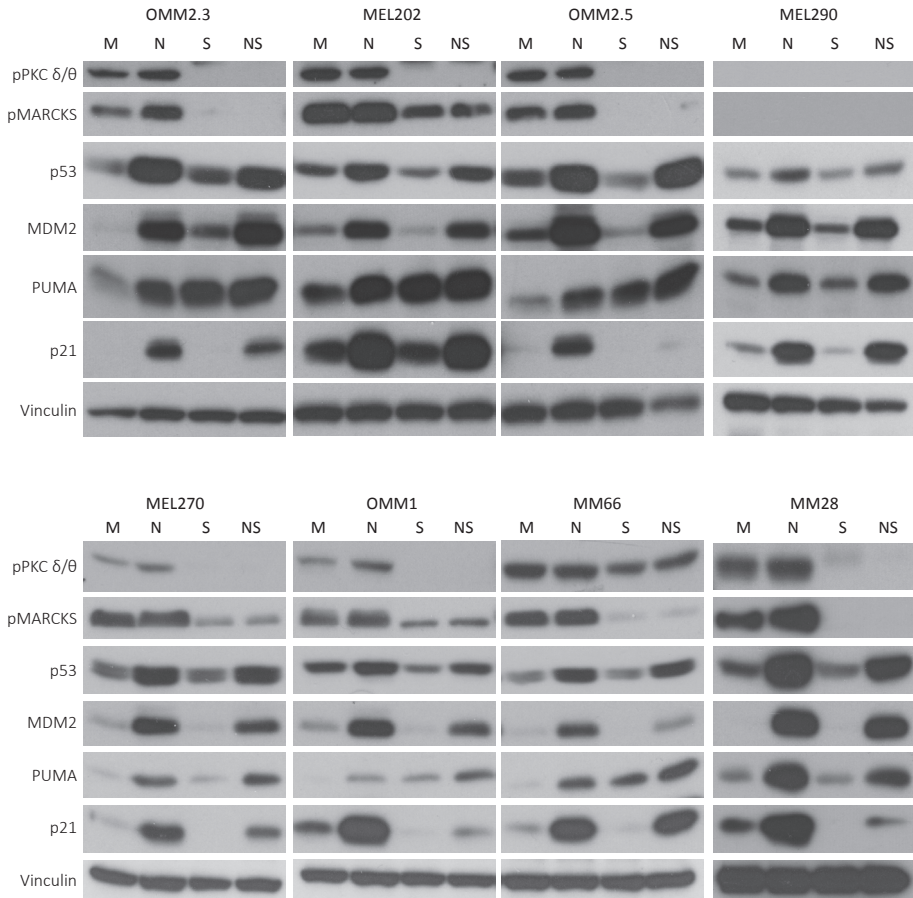


Figure 2. Biochemical response of uveal melanoma cell lines to Sotrastaurin and Nutlin-3. Cell lines OMM2.3, OMM2.5 and OMM1 and were treated with 8 μ M Nutlin-3 and 4 μ M Sotrastaurin. MEL290 was incubated with 2 μ M Nutlin-3 and 4 μ M Sotrastaurin, cell line MM28 with 8 μ M Nutlin-3 and 1 μ M Sotrastaurin, and cell lines MEL202, MEL270 and MM66 with 2 μ M Nutlin-3 and 0.5 μ M Sotrastaurin. All cell lines were incubated for 24 hours after which cells were harvested. Protein lysates were analyzed for the expression levels of phosphorylated PCK δ/θ , phosphorylated MARCKS, p53, MDM2, PUMA, p21 by Western blot. Expression of vinculin was analyzed to control for equal loading.

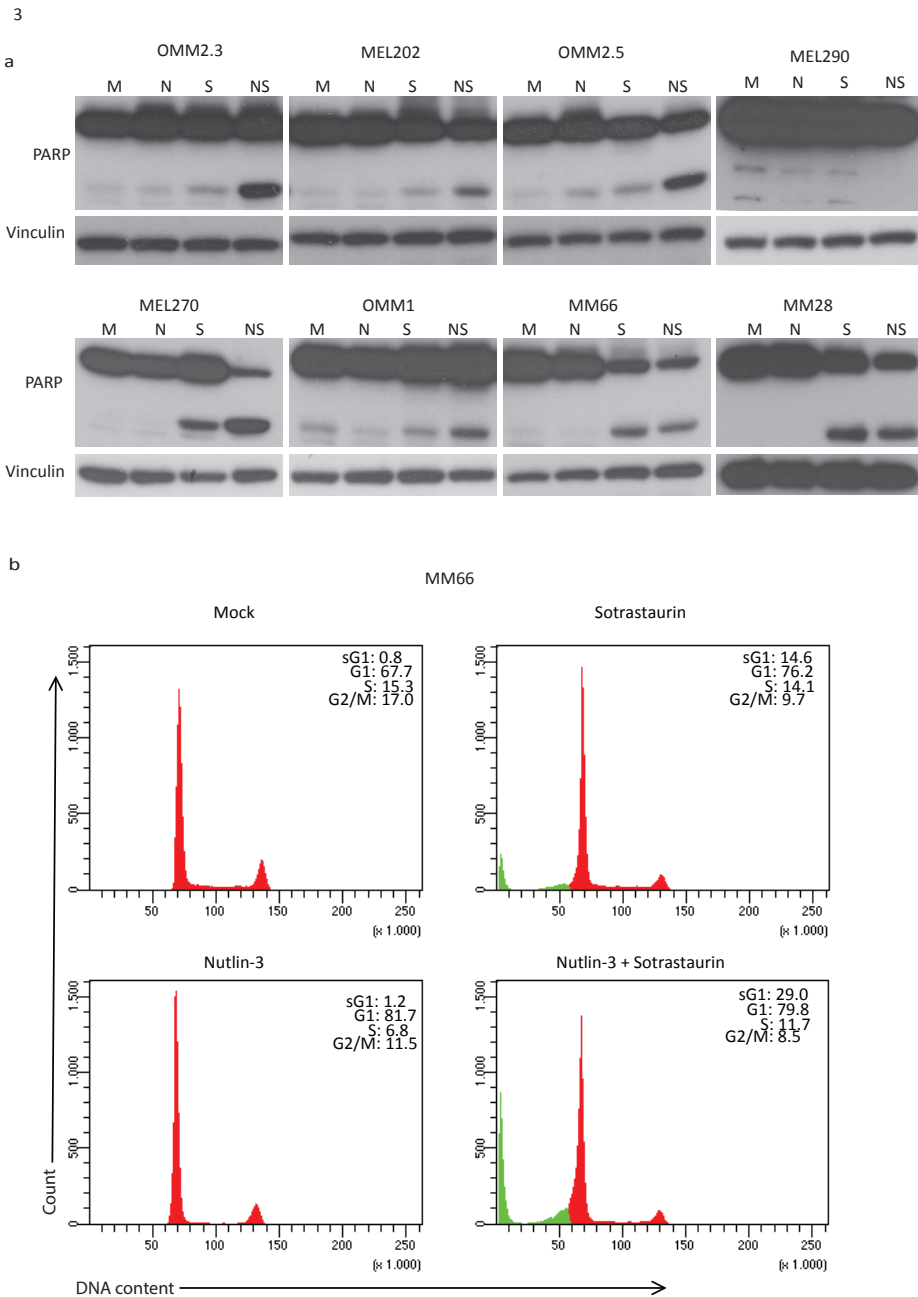


Figure 3. Induction of apoptosis upon combined p53 activation with PKC inhibition. (a) Cell lines OMM2.3, OMM2.5 and OMM1 and were treated with 8 μ M Nutlin-3 and 4 μ M Sotrastaurin. MEL290 was incubated with 2 μ M Nutlin-3 and 4 μ M Sotrastaurin, cell line MM28 with 8 μ M Nutlin-3 and 1 μ M Sotrastaurin. and cell lines MEL202, MEL270 and MM66 with 2 μ M Nutlin-3

and 0.5 μ M Sotrastaurin. All cell lines were incubated for 72 hours before harvesting. Protein lysates were analyzed for the expression levels of cleaved and full length PARP by Western blot. Expression of vinculin was analyzed to control for equal loading. (b) MM66 cells were incubated with 2 μ M Nutlin-3 and 0.5 μ M Sotrastaurin for 72 hours after which the cell cycle profiles were determined by flow cytometry after PI staining, showing an increase in the subG1 fraction upon combined treatment.

increased cells in subG1 (14.6% and 21.0%, respectively), in concordance with the analysis of PARP cleavage. Combining Nutlin-3 and Sotrastaurin slightly increased number of G1 cells in OMM2.5 and OMM2.3, but not in the other cell lines. Importantly, simultaneous p53 reactivation and PKC inhibition significantly increased the fraction of subG1 cells in all cell lines, most strikingly in MM28, MM66 and OMM2.5 cells. In conclusion, these results together with the PARP cleavage analysis indicate that the combination of Nutlin-3 and Sotrastaurin is more potent in the induction of apoptosis compared to the single treatments.

MDMX depletion enhances growth inhibitory effect of Sotrastaurin

Since 'specific' MDM2 inhibitors in the clinic have shown strong adverse effects [16], we determined whether specific targeting of MDMX could serve as an alternative for MDM2-inhibitor based therapies in UMs, especially in combination with Sotrastaurin. Therefore, we created OMM2.3- and MEL202- derived cell lines containing two distinct MDMX-targeting shRNAs (i-shMDMX) or control shRNA (i-shCtrl) under control of doxycycline inducible promoter. Inducing shRNA expression with doxycycline resulted in depletion of MDMX protein in the i-shMDMX containing cells with no effect in the i-shCtrl cells (Figure 4a and c). Concomitantly, depletion of MDMX activated p53 signaling with up-regulation of mRNA levels of p53 target genes *MDM2*, *CYFIP2*, *MAD2L1* and *KIF23* in MEL202 and *p21* in both OMM2.3 and MEL202 (Supplementary Figure 3Sa and b). Although OMM2.3 cells express rather low basal levels of MDMX protein, depletion of MDMX still resulted in growth inhibition (38-53% survival) in a long term growth assay (Figure 4b). Growth inhibition upon Sotrastaurin treatment was comparable in the OMM2.3-derived cell lines (~55% survival). Adding Sotrastaurin to MDMX-depleted cells further reduced cell survival to 21-28% (Figure 4b). MEL202 cells showed a 45-47% survival upon MDMX depletion and a 46-60% survival upon PKC inhibition. Combining MDMX depletion with PKC inhibition resulted in a further reduction of survival of ~30%, a reduction of ~20% compared to Sotrastaurin (Figure 4c and d). However, in both cell lines the Excess over Bliss scores did not suggest synergism. These results suggest that targeting MDMX could be further explored as an alternative for p53 activation by MDM2-inhibitors in obtaining enhanced UM growth inhibition by PKC inhibition with Sotrastaurin.

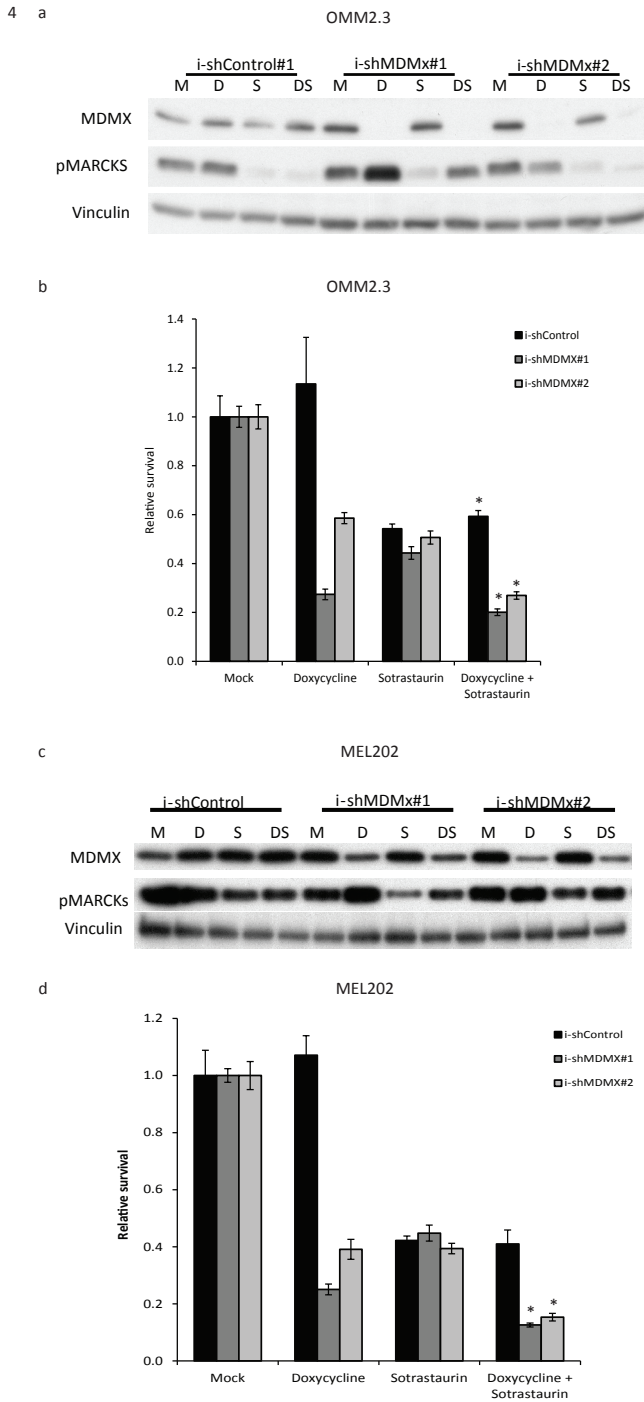


Figure 4.

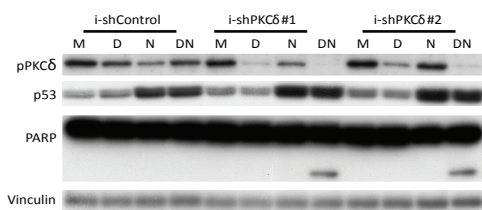
Figure 4. MDMX depletion inhibits UM cell growth and increases growth inhibition by Sotrastaurin treatment. (a, c) OMM2.3 and MEL202 i-shCtrl and i-shMDMX cells were incubated for 72 hours with 10 ng/ml doxycycline, 0.5 μ M Sotrastaurin or the combination before harvesting. The expression of MDMX and phosphorylated MARCKS was analyzed by Western blot. Vinculin expression was analyzed to control for equal loading). (b, d) OMM2.3 and MEL202 i-shCtrl and i-shMDMX cells were seeded in quadruplicate in 12-well plates and incubated for 8 days with indicated compounds (OMM2.3: 20 ng/ml doxycycline and 0.5 μ M Sotrastaurin; MEL202: 20 ng/ml doxycycline and 0.1 μ M Sotrastaurin). Cell survival was determined using crystal violet staining. Data plotted are the normalized averages with the standard deviation as error bars. Combinations which survival significantly differed compared to both single treatments are indicated with an asterisk (*).

PKC δ depletion sensitizes UM cells for p53 activation

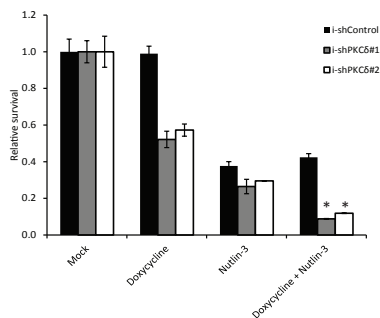
Previous studies have shown non-redundant and essential roles for various PKC isoforms in cancer cell growth. One of the PKC isoforms shown to be essential for UM cell growth and proliferation is PKC δ . [8, 17] To specifically target PKC δ in MEL202 and OMM2.5 cells we introduced lentiviral constructs which inducible express PKC δ -targeting shRNAs (i-shPKC δ ; two distinct target sequences) or control shRNA (i-shCtrl). Incubating the cells with doxycycline strongly reduced PKC δ levels, without effecting PKC isoforms α , β , λ , and ξ , in the i-shPKC δ cells without effect in the i-shCtrl cells (Figure 5a and Supplementary Figure 4Sa and C). Depletion of PKC δ reduced OMM2.5 cell survival to 52-57% (Figure 5b). OMM2.5 cells expressing i-shCtrl or i-shPKC δ shRNAs showed similar sensitivity to Nutlin-3 treatment with a survival of 29-38%. Combining PKC δ depletion with Nutlin-3 reduced cell survival to 9 - 12%, a reduction of \sim 17% for both inducible shRNA's compared to Nutlin-3 alone, which results in high synergistic Excess over Bliss values of 5.0 (Figure 5b). Interestingly, PARP cleavage could only be detected in the Nutlin-3 treated cells depleted for PKC δ , indicating the triggering of apoptosis (Figure 5a). Indeed, the induction of cell death was confirmed by flow cytometry analysis, which showed a strong increase in the fraction of subG1 cells in Doxycycline/Nutlin-3 treated i-shPKC δ cells, whereas single treatments mainly show a minor induction of subG1 and a G1 arrest (Figure 5c). Synergism was also observed in MEL202 cells when PKC δ depletion was combined with Nutlin-3 in a long term growth assay, with Excess over Bliss scores of 5.5 and 9.4 (Supplementary Figure 4b). Specificity of the PKC δ knockdown was demonstrated by the lack of change in PCK isoforms α , β , λ and ξ (Supplementary Figure 4c). Indicating PKC δ depletion alone is sufficient to replace pan-PKC inhibition for achieving synergist cell growth inhibitory effects in combination with p53 reactivation.

5

a



b



c

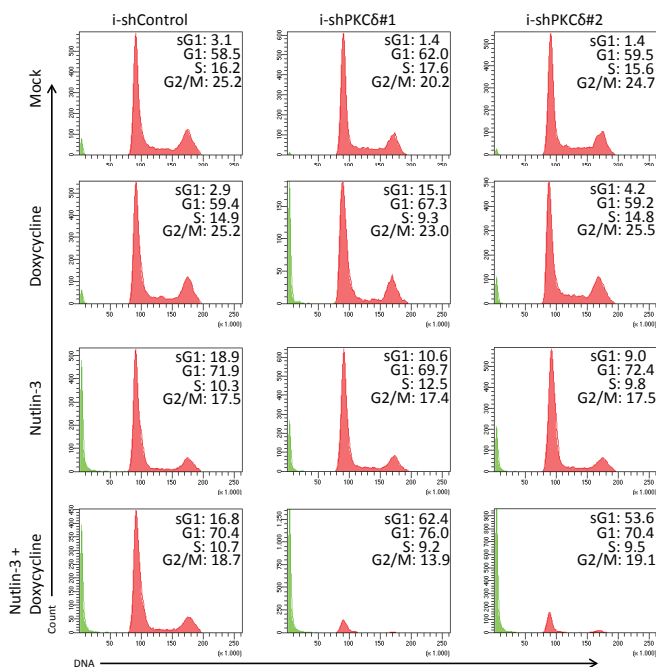


Figure 5. PKCδ depletion and Nutlin-3 synergize to induce apoptosis in UM cells. (a) OMM2.5 i-shCtrl and i-shPKCδ cells were incubated for 72 hours with 20 ng/ml doxycycline, 8 μM Nutlin-3 or the combination of compounds. Expression of phosphorylated PKCδ, p53 and PARP was determined using Western blot. Expression of vinculin was assessed to control for equal loading. (b) OMM2.5 i-shCtrl and i-shPKCδ cells were seeded into 96 wells plates and incubated with 20 ng/ml doxycycline and 4 μM Nutlin-3. After 5 days of incubation cell survival was determined by CTB measurement. Data plotted are the normalized averages with the standard deviation as error bars. Combinations which survival significantly differed compared to both single treatments are indicated with an asterisk (*). (c) Cell cycle profiles of OMM2.5 i-shCtrl and i-shPKCδ cells were determined after 72 hours of treatment with indicated drugs by flow cytometry after PI staining, showing an increase in the subG1 fraction upon combined treatment.

Discussion

UM is considered to be a rare disease with an incidence of approximately 6 per million, accounting for 5% of all melanoma cases.[18] Melanomas originating from the uvea are most commonly driven by activating mutations in G-proteins GNAQ (50%) or GNA11 (43%).[4, 5] These distinct mutations, among additional effects, hyper-activate protein kinase C (PKC) isoforms, which in turn feed into the MAPK pathway. This insight has spurred the development of several (pan-) PKC inhibitors, including Sotrastaurin. Despite the effectivity of Sotrastaurin *in vitro* on the growth of UM cell lines, in a phase I clinical trial only modest effects as single therapy were observed.[10] To enhance the effect of the PKC inhibitor a trial was started with Sotrastaurin in combination with a MEK inhibitor. Unfortunately, this clinical trial had to be terminated prematurely due to toxicity issues. The urge for novel therapeutic interventions has spiked the interested to combine PKC inhibition with compounds inspired by other key features of UM. One of these features is the lack of p53 mutations. UMs frequently show high levels of MDM2 and/or MDMX to constrain p53 tumor suppressor activity, opening the possibility to use MDM2/X inhibitors such as Nutlin-3 to reactivate p53. Previous studies have already shown that MDM2/X inhibitors have the potential to be used as therapeutic intervention for UM.[12, 13, 19]

During the course of our studies it has been reported that inhibition of p53 regulation by MDM2 using CGM097 further constrained *in vivo* tumor growth in UM PDX models when combined with PKC inhibition, although this combination did not result in synergistic growth inhibition *in vitro*. [11] In contrast, our results clearly show synergistic effects when p53 reactivation is combined with PKC inhibition with the same PKC inhibitor and also with an alternative inhibitor GF109203X (data not shown). This apparent controversy can possibly be explained by the use of distinct p53-reactivators. We have previously shown that Nutlin-3 not only prevents the MDM2/p53 complex, but also affects the MDMX/p53 interaction, which has not been investigated for the MDM2 inhibitor CGM097. It could suggest that only inhibiting the MDM2/p53 interaction might not be sufficient to fully unleash p53 and achieve a synergistic response, at least *in vitro*. Even so, functional MDM2 inhibition might not be the optimal way to go in patients, due to the previous reported adverse effects.[16, 20, 21] Therefore, we focused our studies on targeting MDMX, because mouse studies have indicated that depletion of MDMX has much less detrimental effects on the well-being of the organism, most likely because MDMX is less universal expressed in adult tissues. We demonstrate here that depletion of MDMX also enhanced the growth inhibitory effects of PKC inhibition. Furthermore, we have shown previously that MDMX has onco-

genic effects beyond inhibition of p53 [12, 19, 22, 23], so targeting MDMX might have more wide-ranging tumor growth inhibitory effects than merely p53 re-activation.

Unfortunately, to date, no small molecule compound specifically targeting MDMX is commercially available. It had been reported that the XI-011 compound decreases MDMX levels in tumor cells by blocking transcription of the *MDMX* gene.[24] However, we have shown previously that this compound not only affect MDMX levels but also clearly elicits a DNA damage response, making the mode-of-action of this compound rather complex.[12] Much more promising, Dewaele and colleagues recently showed the potential of stimulating the naturally occurring alternative splicing of *MDMX* by antisense oligonucleotides, thereby decreasing the amount of full length MDMX protein.[25] The depletion of MDMX resulted in inhibition of cutaneous melanoma growth, both *in vitro* and in PDX mouse models. These results combined with ours strongly suggest a potential therapeutic intervention to target metastasized UM.

Previous studies have demonstrated the non-redundant and often essential roles of different PKC isoforms in UM.[8, 17] We sought to determine whether an inhibition or depletion of a single PKC isoform could also be capable of enhancing MDM2/MDMX inhibition. Wu and colleagues showed in 2012 in two independent studies that PKC isoforms α , β , θ , ϵ and δ are essential for UM cell line viability.[8, 17] More recently it was reported that PKC ϵ and δ are responsible for the activation of RASGRP3 driving the RAS/MEK/ERK pathway. [26] In line with these studies we show that UM cell viability depends on PKC δ and therefore could provide a potential drug target, especially since PKC δ does not seem to be required for development and normal cell proliferation.[27, 28] Interestingly the depletion of a single PKC isoform not only reduced cell viability, but also synergistically enhanced the effects of Nutlin-3. Our data show that this reduced cell survival is due to the induction of cell death, most likely via apoptosis. The induction of cell death suggests an interesting therapeutic potential. Our study shows that combining an isoform-selective PKC inhibitor with MDMX-inhibition might be a new potent therapeutic intervention for UM metastases with limited adverse effects.

Acknowledgements

The authors like to thank Dr. Bruce Ksander, Dr. Martine Jager, Dr. Gré Luyten, Dr. Sergio Roman-Roman and Dr. Fariba Nemati for providing the cell lines.

References

1. Shah SU, Mashayekhi A, Shields CL, Walia HS, Hubbard GB, 3rd, Zhang J, Shields JA. Uveal metastasis from lung cancer: clinical features, treatment, and outcome in 194 patients. *Ophthalmology*. 2014; 121: 352-7. doi: 10.1016/j.ophtha.2013.07.014.
2. Augsburger JJ, Correa ZM, Shaikh AH. Effectiveness of treatments for metastatic uveal melanoma. *Am J Ophthalmol*. 2009; 148: 119-27. doi: 10.1016/j.ajo.2009.01.023.
3. Kivela T, Eskelin S, Kujala E. Metastatic uveal melanoma. *Int Ophthalmol Clin*. 2006; 46: 133-49. doi:
4. Van Raamsdonk CD, Bezrookove V, Green G, Bauer J, Gaugler L, O'Brien JM, Simpson EM, Barsh GS, Bastian BC. Frequent somatic mutations of GNAQ in uveal melanoma and blue naevi. *Nature*. 2009; 457: 599-602. doi: 10.1038/nature07586.
5. Van Raamsdonk CD, Griewank KG, Crosby MB, Garrido MC, Vemula S, Wiesner T, Obenaus AC, Wackernagel W, Green G, Bouvier N, Sozen MM, Baimukanova G, Roy R, et al. Mutations in GNA11 in uveal melanoma. *N Engl J Med*. 2010; 363: 2191-9. doi: 10.1056/NEJMoa1000584.
6. Chua V, Lapadula D, Randolph C, Benovic JL, Wedegaertner P, Aplin AE. Dysregulated GPCR Signaling and Therapeutic Options in Uveal Melanoma. *Mol Cancer Res*. 2017. doi: 10.1158/1541-7786.MCR-17-0007.
7. Kalinec G, Nazarali AJ, Hermouet S, Xu N, Gutkind JS. Mutated alpha subunit of the Gq protein induces malignant transformation in NIH 3T3 cells. *Mol Cell Biol*. 1992; 12: 4687-93. doi:
8. Wu X, Li J, Zhu M, Fletcher JA, Hodi FS. Protein kinase C inhibitor AEB071 targets ocular melanoma harboring GNAQ mutations via effects on the PKC/Erk1/2 and PKC/NF-kappaB pathways. *Mol Cancer Ther*. 2012; 11: 1905-14. doi: 10.1158/1535-7163.MCT-12-0121.
9. Chen X, Wu Q, Tan L, Porter D, Jager MJ, Emery C, Bastian BC. Combined PKC and MEK inhibition in uveal melanoma with GNAQ and GNA11 mutations. *Oncogene*. 2014; 33: 4724-34. doi: 10.1038/onc.2013.418.
10. Piperno-Neumann S, Kapiteijn E, Larkin J, Carvajal RD, Luke JJ, Seifert H, Roozen I, Zoubir M, Yang L, Choudhury S, Yerramilli-Rao P, Hodi FS, Schwartz GK. (2014). Phase I dose-escalation study of the protein kinase C (PKC) inhibitor AEB071 in patients with metastatic uveal melanoma. *ASCO annual meeting 2014: J. Clin. Oncol (abstr 9030)*.
11. Carita G, Frisch-Dit-Leitz E, Dahmani A, Raymondie C, Cassoux N, Piperno-Neumann S, Nemati F, Laurent C, De Koning L, Hailovic E, Jeay S, Wylie A, Emery C, et al. Dual inhibition of protein kinase C and p53-MDM2 or PKC and mTORC1 are novel efficient therapeutic approaches for uveal melanoma. *European Journal of Cancer*. 2016; 68: S31-S. doi:
12. de Lange J, Teunisse AF, Vries MV, Lodder K, Lam S, Luyten GP, Bernal F, Jager MJ, Jochemsen AG. High levels of Hdmx promote cell growth in a subset of uveal melanomas. *Am J Cancer Res*. 2012; 2: 492-507. doi:
13. de Lange J, Ly LV, Lodder K, Verlaan-de Vries M, Teunisse AF, Jager MJ, Jochemsen AG. Synergistic growth inhibition based on small-molecule p53 activation as treatment for intraocular melanoma. *Oncogene*. 2012; 31: 1105-16. doi: 10.1038/onc.2011.309.
14. Holzer P, Masuya K, Furet P, Kallen J, Valat-Stachyra T, Ferretti S, Berghausen J, Bouisset-Leonard M, Buschmann N, Pissot-Soldermann C, Rynn C, Ruetz S, Stutz S, et al. Discovery of a Dihydroisoquinoline Derivative (NVP-CGM097): A Highly Potent and Selective MDM2 Inhibitor Undergoing Phase 1 Clinical Trials in p53wt Tumors. *J Med Chem*. 2015; 58: 6348-58. doi: 10.1021/acs.jmedchem.5b00810.
15. Cerne JZ, Hartig SM, Hamilton MP, Chew SA, Mitsiades N, Poulaki V, McGuire SE. Protein kinase C inhibitors sensitize GNAQ mutant uveal melanoma cells to ionizing radiation. *Invest Ophthalmol Vis Sci*. 2014; 55: 2130-9. doi: 10.1167/iops.13-13468.

16. Biswas S, Killick E, Jochemsen AG, Lunec J. The clinical development of p53-reactivating drugs in sarcomas - charting future therapeutic approaches and understanding the clinical molecular toxicology of Nutlins. *Expert Opin Investig Drugs*. 2014; 23: 629-45. doi: 10.1517/13543784.2014.892924.
17. Wu X, Zhu M, Fletcher JA, Giobbie-Hurder A, Hodi FS. The protein kinase C inhibitor enzastaurin exhibits antitumor activity against uveal melanoma. *PLoS One*. 2012; 7: e29622. doi: 10.1371/journal.pone.0029622.
18. Chang AE, Karnell LH, Menck HR. The National Cancer Data Base report on cutaneous and noncutaneous melanoma: a summary of 84,836 cases from the past decade. The American College of Surgeons Commission on Cancer and the American Cancer Society. *Cancer*. 1998; 83: 1664-78. doi:
19. Gembarska A, Luciani F, Fedele C, Russell EA, Dewaele M, Villar S, Zwolinska A, Haupt S, de Lange J, Yip D, Goydos J, Haigh JJ, Haupt Y, et al. MDM4 is a key therapeutic target in cutaneous melanoma. *Nat Med*. 2012; 18: 1239-47. doi: 10.1038/nm.2863.
20. Andreeff M, Kelly KR, Yee K, Assouline S, Strair R, Popplewell L, Bowen D, Martinelli G, Drummond MW, Vyas P, Kirschbaum M, Iyer SP, Ruvolo V, et al. Results of the Phase I Trial of RG7112, a Small-Molecule MDM2 Antagonist in Leukemia. *Clin Cancer Res*. 2016; 22: 868-76. doi: 10.1158/1078-0432.CCR-15-0481.
21. Ray-Coquard I, Blay JY, Italiano A, Le Cesne A, Penel N, Zhi J, Heil F, Rueger R, Graves B, Ding M, Geho D, Middleton SA, Vassilev LT, et al. Effect of the MDM2 antagonist RG7112 on the P53 pathway in patients with MDM2-amplified, well-differentiated or dedifferentiated liposarcoma: an exploratory proof-of-mechanism study. *Lancet Oncol*. 2012; 13: 1133-40. doi: 10.1016/S1470-2045(12)70474-6.
22. Carrillo AM, Bouska A, Arrate MP, Eischen CM. Mdmx promotes genomic instability independent of p53 and Mdm2. *Oncogene*. 2015; 34: 846-56. doi: 10.1038/onc.2014.27.
23. Jeffreena Miranda P, Buckley D, Raghu D, Pang JB, Takano EA, Vijayakumar R, Teunisse AF, Posner A, Procter T, Herold MJ, Gamell C, Marine JC, Fox SB, et al. MDM4 is a rational target for treating breast cancers with mutant p53. *J Pathol*. 2017. doi: 10.1002/path.4877.
24. Wang H, Yan C. A small-molecule p53 activator induces apoptosis through inhibiting MDMX expression in breast cancer cells. *Neoplasia*. 2011; 13: 611-9. doi:
25. Dewaele M, Tabaglio T, Willekens K, Bezzi M, Teo SX, Low DH, Koh CM, Rambow F, Fiers M, Rogiers A, Radaelli E, Al-Haddawi M, Tan SY, et al. Antisense oligonucleotide-mediated MDM4 exon 6 skipping impairs tumor growth. *J Clin Invest*. 2016; 126: 68-84. doi: 10.1172/JCI82534.
26. Chen X, Wu Q, Depeille P, Chen P, Thornton S, Kalirai H, Coupland SE, Roose JP, Bastian BC. RasGRP3 Mediates MAPK Pathway Activation in GNAQ Mutant Uveal Melanoma. *Cancer Cell*. 2017; 31: 685-96 e6. doi: 10.1016/j.ccell.2017.04.002.
27. Leitges M, Mayr M, Braun U, Mayr U, Li C, Pfister G, Ghaffari-Tabrizi N, Baier G, Hu Y, Xu Q. Exacerbated vein graft arteriosclerosis in protein kinase Cdelta-null mice. *J Clin Invest*. 2001; 108: 1505-12. doi: 10.1172/JCI12902.
28. Miyamoto A, Nakayama K, Imaki H, Hirose S, Jiang Y, Abe M, Tsukiyama T, Nagahama H, Ohno S, Hatakeyama S, Nakayama KI. Increased proliferation of B cells and auto-immunity in mice lacking protein kinase Cdelta. *Nature*. 2002; 416: 865-9. doi: 10.1038/416865a.
29. Herold MJ, van den Brandt J, Seibler J, Reichardt HM. Inducible and reversible gene silencing by stable integration of an shRNA-encoding lentivirus in transgenic rats. *Proc Natl Acad Sci U S A*. 2008; 105: 18507-12. doi: 10.1073/pnas.0806213105.
30. Haupt S, Buckley D, Pang JM, Panimaya J, Paul PJ, Gamell C, Takano EA, Lee YY, Hiddingh S, Rogers TM, Teunisse AF, Herold MJ, Marine JC, et al. Targeting Mdmx to treat breast cancers with wild-type p53. *Cell Death Dis*. 2015; 6: e1821. doi: 10.1038/cddis.2015.173.

31. Carlotti F, Bazuine M, Kekarainen T, Seppen J, Pognonec P, Maassen JA, Hoeben RC. Lentiviral vectors efficiently transduce quiescent mature 3T3-L1 adipocytes. *Mol Ther.* 2004; 9: 209-17. doi: 10.1016/j.ymthe.2003.11.021.
32. Chou TC. Drug combination studies and their synergy quantification using the Chou-Talalay method. *Cancer Res.* 2010; 70: 440-6. doi: 10.1158/0008-5472.CAN-09-1947.
33. Amirouchene-Angelozzi N, Frisch-Dit-Leitz E, Carita G, Dahmani A, Raymondie C, Liot G, Gentien D, Nemati F, Decaudin D, Roman-Roman S, Schoumacher M. The mTOR inhibitor Everolimus synergizes with the PI3K inhibitor GDC0941 to enhance anti-tumor efficacy in uveal melanoma. *Oncotarget.* 2016; 7: 23633-46. doi: 10.18632/oncotarget.8054.

Methods

Cell culture and lentiviral transduction

Cell lines MEL270, MEL202, OMM2.3, MEL290, OMM2.5 and OMM1 were cultured in a mixture of RPMI and DMEM F12 (1:1 ratio), supplemented with 10% FCS and antibiotics. MM66 and MM28 were cultured in IMDM containing 20% FCS and antibiotics. Inducible shRNA knockdown lentiviral vectors were constructed as described previously.[29, 30] Production of lentivirus stocks by transfections into 293T cells essentially as described, but calcium phosphate was replaced with PEI.[31] Virus was quantitated by antigen capture ELISA measuring HIV p24 levels (ZeptoMetrix Corp., New York, NY, USA). Cells were transduced using MOI 2 in medium containing 8 μ g/ml polybrene. Target sequences to deplete MDMX or PKC δ and control sequences are shown in Table 1.

Western blot analysis

Cells were washed twice in ice cold PBS and lysed in Giordano buffer (50mM Tris-HCl pH7.4, 250 mM NaCl, 0.1% Triton X-100 and 5 mM EDTA; supplemented with phosphatase- and protease inhibitors). Equal protein amounts were separated using SDS-PAGE and blotted on polyvinylidene fluoride transfer membranes (Millipore, Darmstadt, Germany). After blocking the membranes in TBST (10 mM Tris-HCl pH8.0, 150 mM NaCl, 0.2% Tween-20) containing 10% non-fat dry milk, membranes were incubated with the proper primary antibodies (listed in a Table 2) and appropriate HRP-conjugated secondary antibodies (Jackson Laboratories, Bar harbor, MA, USA). Bands were visualized using chemoluminescence and autoradiography.

RNA isolation, cDNA synthesis and real-time quantitative PCR

RNA was isolated from cells using the SV total RNA isolation kit (Promega, Fitchburg, WI, USA), from which cDNA was synthesized using the reverse transcriptase reaction mixture as indicated by Promega. QPCR was performed using SYBR green mix (Roche, Basel, Switzerland) in a C1000 touch Thermal Cycler (Bio-Rad laboratories, Hercules, CA, USA). Relative expression of CDC25A, cyclin D1, survivin, p21 and MDM2 was determined over three independent experiments, compared to housekeeping genes CAPNS1 and SRPR. Relative expressions per experiment were compared and the untreated samples average was set at 1. Primer sequences are listed in Table 3.

Flow cytometry analysis

To analyze cell cycle profiles, the cells were harvested using trypsinization, washed with ice-cold PBS and fixed in ice-cold 70% ethanol. Cells were washed in PBS containing 2% FCS and resuspended in PBS containing 2% FCS, 50 μ g/ml RNAse and 50 μ g/

ml propidium iodide. Flow cytometry was performed using the BD LSR II system (BD Bioscience, San Diego, CA, USA). 10,000 cycling cells were analyzed and percentages G1, S and G2/M were determined and set to 100%. The subG1 population was determined as a percentage of the total population.

Cell growth and viability assays

Cells were seeded in triplicate, in 96-well format. Next day compounds were added and cells were incubated for 72 hours. Cell survival was determined using CellTiter-Blue Cell Viability assay (Promega); fluorescence was measured in a microplate reader (Victor3, Perkin Elmer, San Jose, CA, USA). Synergism between Sotrastaurin and Nutlin-3 was calculated using CompuSyn software (Paramus, NJ, USA). Sotrastaurin and Nutlin-3 were obtained from Selleck Chemicals (Houston, TX, USA) and Cayman Chemical (Ann Arbor, MI, USA), respectively.

Long term growth assay

Cells were seeded in triplicate in a 12-well plates and were incubated for 8 days. Cells were fixed for 5 minutes in 4% paraformaldehyde. DNA was stained using 30-minute incubation with 0.05% crystal violet. After washing and drying the relative number of cells was quantified by solubilizing the crystal violet in methanol and measuring absorbance at 545nm using a microplate reader (Victor3, Perkin Elmer).

Determining synergism

To determine the extent of synergism between Sotrastaurin and Nutlin-3 in UM cell lines Combination index (CI) values were calculated by comparing ranges of both single drugs (concentrations as indicated in the figure) to the combined treatment. Therefore, we used the CompuSyn program which uses the Chou-Talalay method.[32] CI values below 0.9 were considered to be synergistic, between 0.9 and 1.1 additive effects and above 1.1 to be antagonistic. Excess over Bliss (EoB) was used to determine the synergism between two conditions as described by Amirouchene-Angelozzi *N et al.*[33] when no two ranges of drugs were tested. EoB was used to determine the extent of synergism between MDMX depletion and Sotrastaurin and PKC δ depletion and Nutlin-3.

Statistical analysis

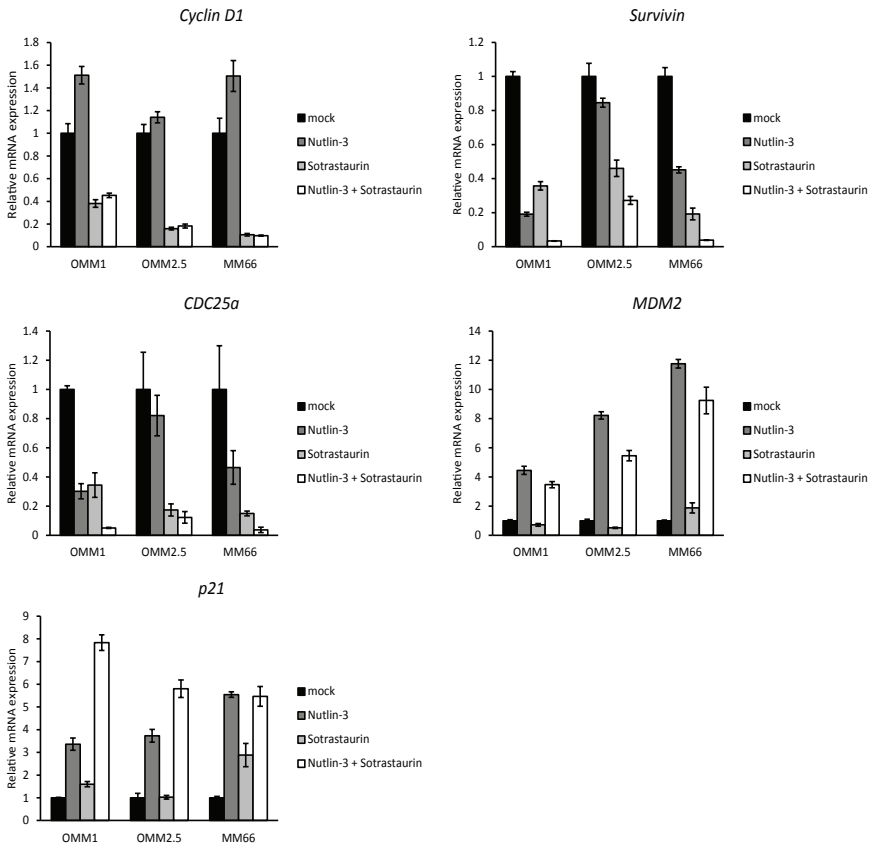
Differences between two groups were calculated using Student's t-test; P-values of 0.05 or less were considered to be significant.

Tables

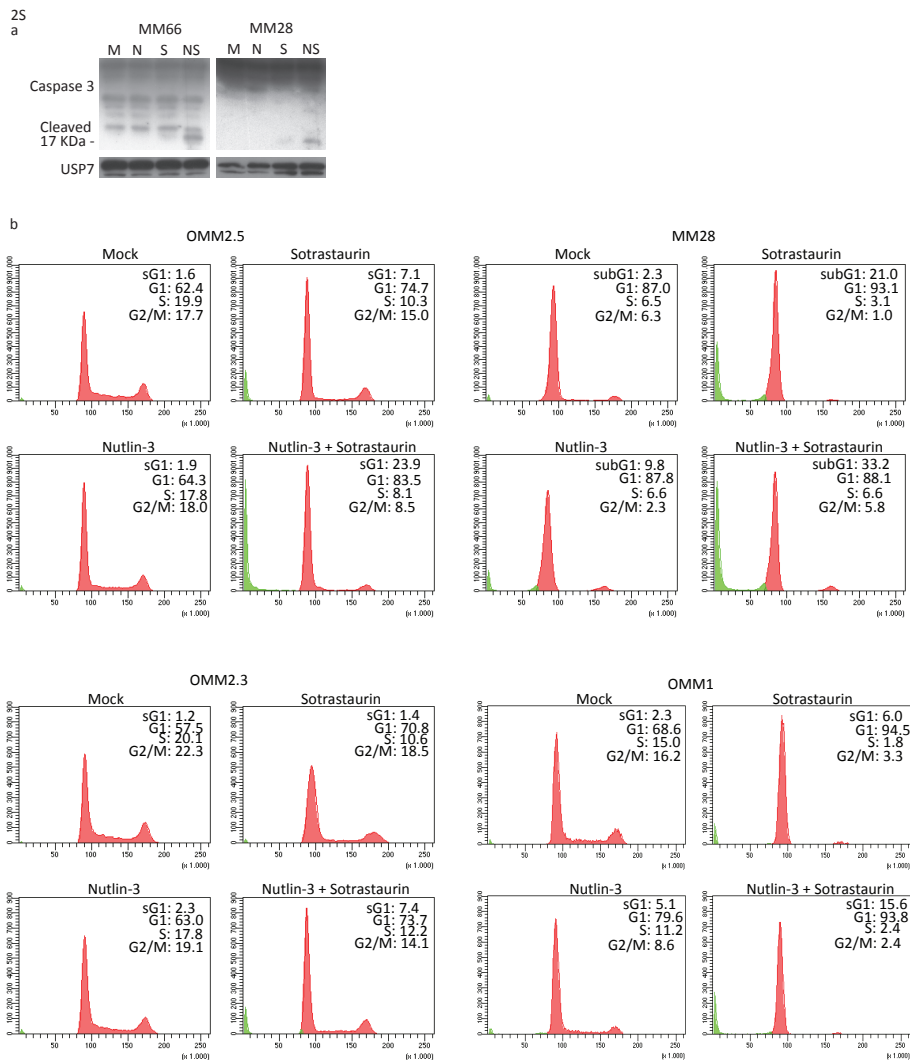
Table 1. shRNA target sequences

Target	shRNA sequence
Control	5'-GAATCTTGTTACATCAGCT-3'
PKC δ #1	5'-CAGAGCCTGTTGGGATATAC-3'
PKC δ #2	5'-CTTCGGAGGGAAATTGTAAT-3'
MDMX#1	5'-GTGCAGAGGAAAGTTCCAC-3'
MDMX#2	5'-GAATCTCTTGAAGCCATGT-3'

1S



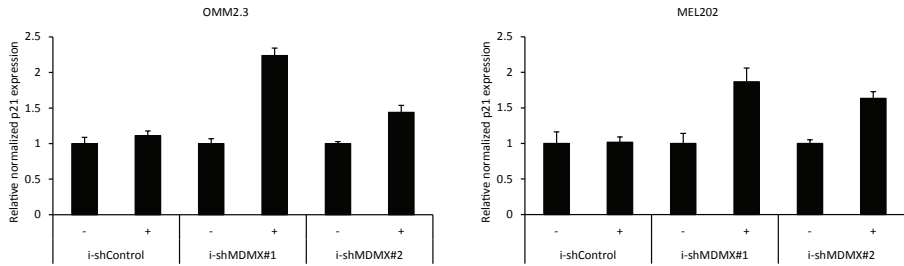
Supplementary Figure 1S. Analysis of gene transcription in response to Sotrastaurin and Nutlin-3. Cell lines OMM1, OMM2.5 (8 μ M Nutlin-3 and 4 μ M Sotrastaurin) and MM66 (2 μ M Nutlin-3 and 0.5 μ M Sotrastaurin) were incubated with Sotrastaurin and Nutlin-3 for 24 hours. Cells were harvested, RNA isolated, cDNA synthesized and expression of CDC25A, cyclin D1, Survivin, p21 and MDM2 was determined. Relative expression compared to untreated controls is plotted.



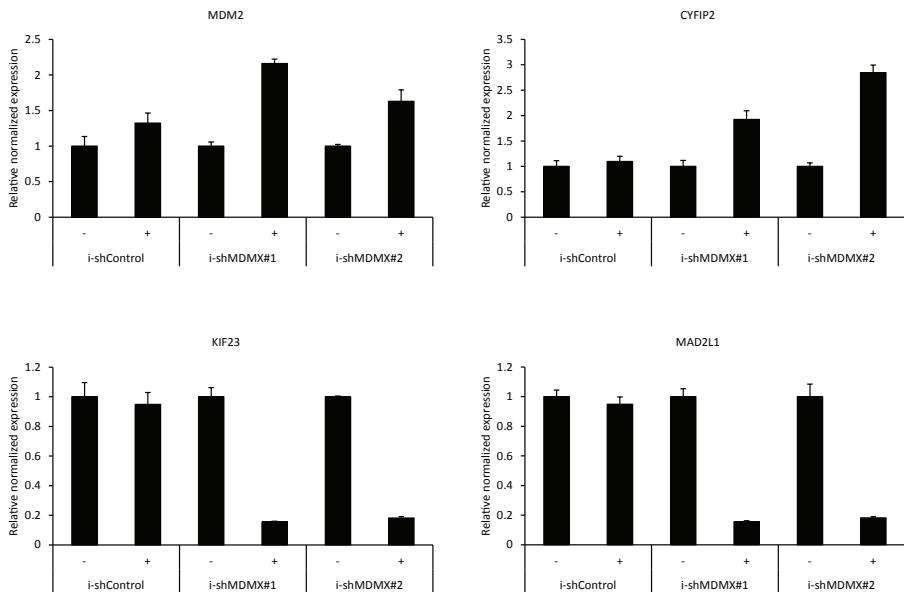
Supplementary Figure 2S. Induction of cell cycle arrest and cell death upon p53 activation and PKC inhibition. (a) MM66 and MM28 were incubated for 72 hours with Sotrastaurin (MM66: 4 μ M and MM28 1 μ M), 8 μ M Nutlin-3 or the combination. Expression of cleaved caspase 3 was determined by Western blot. Expression of UPS7 was assessed to control for equal loading. (b) After treating OMM2.5, OMM1, OMM2.3 (8 μ M Nutlin-3 and 4 μ M Sotrastaurin) and MM28 (8 μ M Nutlin-3 and 1 μ M Sotrastaurin) for 72 hours the cell cycle profiles were determined with flow cytometry using PI staining. Representative figures of three independent experiments with the percentage of each cell cycle phase (G1, S, G2/M and subG1) are shown.

35

a

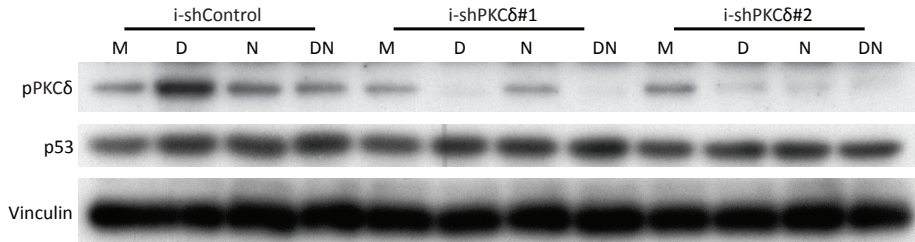


b

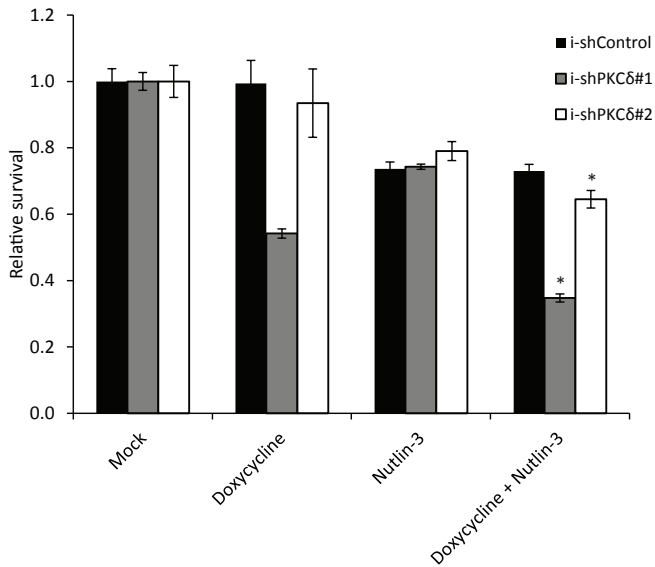


Supplementary Figure 3S. p21 expression in response to MDMX knockdown. (a) OMM2.3- and MEL202 i-shCtrl and i-shMDMX cells were incubated with 20 ng/ml doxycycline or solvent for 72 hours. Cells were harvested, RNA isolated, cDNA synthesized and expression levels of p21 mRNA was determined by qPCR. Relative expression compared to untreated is plotted. (b) Expression levels of known p53 target genes (MDM2, CYFIP2, MAD2L1 and KIF23) upon MDMX depletion in MEL202.

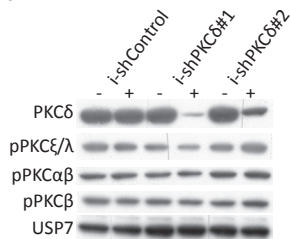
4S
a



b



c



Supplementary Figure 4S. PKC δ depletion sensitizes MEL202 cells for Nutlin-3. (a) MEL202 i-shCtrl and -i-shPKC δ cells were incubated for 72 hours with 20 ng/ml doxycline, 1 μ M Nutlin-3 or the combination. Expression of phosphorylated PKC δ , p53 and PARP was determined by Western blot. Expression of vinculin was assessed to control for equal loading. (b) MEL202 i-shCtrl and -i-shPKC δ cells were seeded in quadruplicate into 12-well plates and incubated for 8 days with 20

ng/ml doxycycline, 1 μ M Nutlin-3 or the combination. Cell survival was determined using crystal violet staining. Data plotted are the normalized averages with the standard deviation as error bars. Combinations which survival significantly differed compared to both single treatments are indicated with an asterisk (*). (c) MEL202 i-shCtrl and -i-shPKC δ cells were incubated for 72 hours with 20 ng/ml doxycycline. Expression of PKC δ , phosphorylated PKC α , β , λ , and ξ was determined by Western blot. Expression of USP7 was assessed to control for equal loading.

CHAPTER 4

Combined EZH2 and HDAC inhibition as novel therapeutic intervention for metastasized uveal melanoma

R. C. Heijkants, A. F. A. S. Teunisse, A. G. Jochemsen

Department of Cell and Chemical Biology, Leiden University Medical Centre, Leiden,
the Netherlands.

Summary

Purpose: Currently there is no effective therapeutic intervention available for patients with metastasized uveal melanoma (UM) resulting in poor prognosis. Loss of the tumor suppressor BAP1 is frequently found (80-90%) in metastasized UM. Expression of enhancer of zeste homolog 2 (EZH2), a methyltransferase and an essential component of the polycomb repressive complex 2 (PRC2), is frequently dysregulated in cancer. Like UM, mesotheliomas frequently lack BAP1 expression and it was found that loss of BAP1 expression sensitizes these cells for EZH2 inhibition. However, UM cell proliferation was reported not to be affected by EZH2 inhibition, independent of BAP1 expression. Here we continued studying the potential of EZH2 inhibition as therapeutic strategy for metastasized UM.

Methods: A panel of UM cell lines was used to determine the effects of EZH2 inhibition on both short and long term proliferation assays. Using the same cell lines the combination of EZH2 and histone deacetylase (HDAC) inhibition was assessed on cell proliferation, western blotting and flow cytometry.

Results: Here we demonstrate that UM cells are responsive to EZH2 inhibition in a long term growth assay. Furthermore, EZH2 inhibition sensitized UM cells for histone deacetylase inhibition even in a short term growth assay, correlating with increased induction of cell death.

Conclusions: EZH2 inhibition, opposed to what has been suggested previously, could still serve as a potential therapeutic intervention for metastasized UM when combined with other treatments opening new avenues for the treatment of metastasized UM patients.

Introduction

Uveal melanoma (UM) is an ocular malignancy originating from melanocytes located in the choroid (85%), iris (5%) or ciliary body (10%) [1, 2]. Primary tumors can usually be treated efficiently, however, approximately half of the patients within 15 years after primary tumor detection will develop metastases, for which no effective treatment exists to date [3, 4]. In addition to the driver mutations in the G-proteins GNAQ or GNA11, monosomy 3 and amplification of 8q are frequently observed genomic aberrations in UM [5, 6]. Particularly monosomy 3 strongly correlates with development of metastases and is, therefore, a robust marker for poor prognosis [7, 8]. The *BAP1* gene is located at chromosome 3 and in monosomy 3 tumors the remaining copy of *BAP1* is often found mutated leading to complete loss of BAP1 protein expression [9]. Indeed, mutations in *BAP1* have a strong predictive power for the occurrence of metastasis in UM and 80-90% of the UM metastases show loss of *BAP1* expression [9, 10]. Interestingly, a previous study reported upregulation of *enhancer of zeste (EZH)* 2 expression in mesothelioma upon *BAP1* loss [11].

EZH2 is frequently overexpressed and also mutated in various cancer types, including melanoma, and its high expression correlates with disease progression and aggression (Reviewed by [12]). *EZH2* is an essential component of the polycomb repressive complex 2 (PRC2) and functions as a methyltransferase, catalysing the tri-methylation of histone H3 at lysine 27 (H3K27me3) [13, 14]. This repressive tri-methylation mark of histone H3 is recognized by the PRC1 complex resulting in gene silencing [15, 16]. In this way *EZH2* controls the transcription of numerous genes [17]. In addition to the transcription repressive function of *EZH2* in the PRC2 complex, it has been demonstrated that *EZH2* is capable of promoting transcription, independently of PRC2 complex [18]. The switch from transcription repressor to activator appears to be mediated by the phosphorylation of serine 21. All in all, *EZH2* emerges as an important regulator of transcription in cancer cells.

Transformation of *BAP1* knockout myeloid cells was found to be *EZH2*-dependent and *EZH2* inhibition was demonstrated to be an effective treatment for *BAP1*-negative mesothelioma in a pre-clinical *in vivo* model [11]. Based upon these results a clinical trial with the *EZH2*-inhibitor Tazemetostat on patients with *BAP1*-negative malignant mesothelioma is ongoing (NCT02860286). These observations in malignant mesothelioma could be extrapolated to *BAP1*-negative metastasized UM, possibly providing an effective therapeutic intervention. However, a follow-up study addressing this matter reported that UM cell lines are insensitive to *EZH2* inhibition regardless of *BAP1* expression, disputing the generality of the observations made in malignant

mesothelioma [19]. However, it was argued that UM cell lines might need a prolonged exposure to EZH2 inhibition to observe growth inhibitory effects, especially because *BAP1*-negative UM cell lines generally have a very long doubling time [20]. This study focuses on the long term effects of EZH2 inhibition on UM cells and addresses the combinatory use of EZH2 inhibitor with histone deacetylase (HDAC) inhibition as potential therapeutic strategy for metastasized UM.

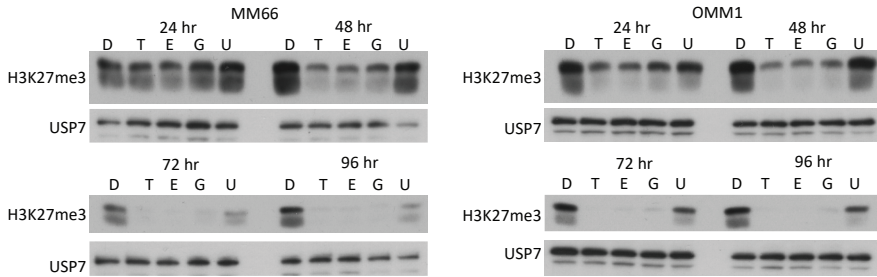
Results

EZH2 inhibition slows down uveal melanoma cell growth.

First, the biochemical effect of EZH2 inhibition, namely the reduction of H3K27me₃, was confirmed at different time points with all distinct EZH2 inhibitors tested in the current study (T: Tazemetostat, E: EPZ011989, G: GSK503 and U: UNC1999) compared to DMSO (D) treated cells (Fig. A). The reduction of H3K27me₃ after 24 hours incubation with EZH2 inhibitors is modest, but strong effects could be observed after 48, 72 and 96 hours. Although it must be noted that UNC1999 appears less potent since this drug is not able to completely abolish detectable H3K27me₃ in time, in contrast to the other EZH2 inhibitors (Fig. 1A). To assess the long term effects of EZH2 inhibition on growth of UM cells, cells were seeded into 6-well plates and cultured with or without exposure to two distinct EZH2 inhibitors (EPZ011989 or Tazemetostat), each condition in duplicate. When control (DMSO)-treated cells reached 80-90% confluency the cells from all conditions were counted to determine the effect of EZH2 inhibition on the growth, and all conditions were re-seeded in the same density as before to ensure equal conditions during this long term assays. Only minimal or no growth inhibition was observed within 5-9 days of treatment matching previous reported data of EZH2 inhibition in UM cells (Fig. 1B) [19]. Results of all cell counts show different dynamics per cell line upon EZH2 inhibition (Supplementary Fig. 1A). Interestingly, the *BAP1*-positive cells (OMM1, OMM2.5 and MM66) could still be sub-cultured with continuous EZH2 inhibition even though EZH2 inhibition resulted in clear growth retardation of OMM1 and MM66 cells. OMM2.5 was the only cell line tested whose growth was hardly affected by EZH2 inhibition, even after 40 days (Supplementary Fig. 1A).

Interestingly, two out of three *BAP1*-negative cells (MP38, MM28) completely stopped proliferating after 1 or 2 passages (Supplementary Fig. 1A). These data slightly hint towards a higher efficacy of EZH2 inhibition in *BAP1*-negative cells, although more *BAP1*-negative and positive cell lines need to be tested to confirm this result. However, supporting this possibility is that analysis of TCGA data indicates that *EZH2* mRNA expression is significantly upregulated in UM samples with a deleted *BAP1* allele

1
A



B

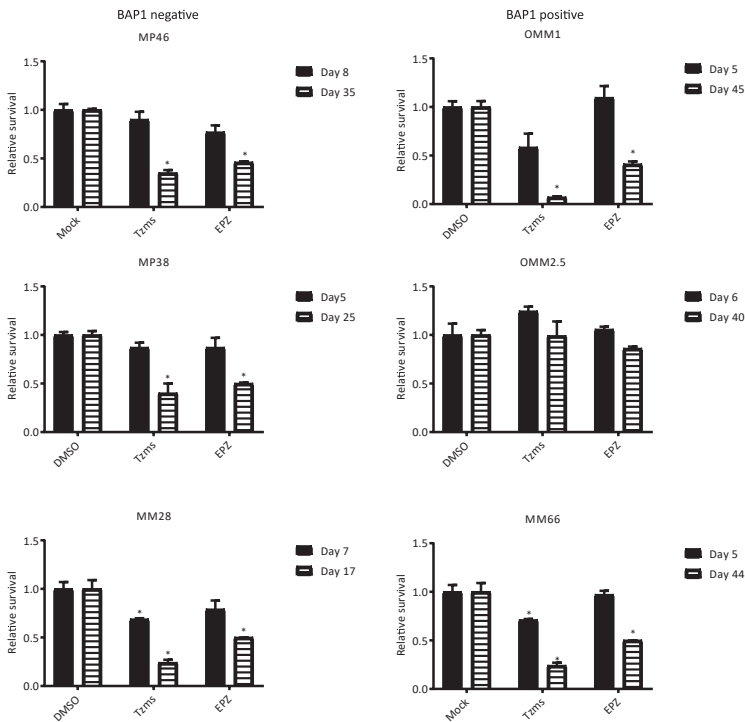


Figure 1. Effects of EZH2 inhibition on long-term growth of BAP1-positive and -negative uveal melanoma cell lines. **(A)** Time-course of four distinct EZH2 inhibitors (Tazemetostat (T; 6 μM), EZPO11989 (E; 6 μM), GSK503 (G; 6 μM), UNC1999 (U; 4 μM) and control (DMSO-treated) to investigate kinetics of H3K27me3 reduction; USP7 expression is analysed to show equal loading. **(B)** Early and last data points of proliferation assay of BAP1-positive (OMM1, OMM2.5 and MM66) and BAP1-negative (MM28, MP38 and MP46) uveal melanoma (UM) cells cultured in duplicate in the continuous presence of EZH2 inhibitors (2 μM Tzms (Tazemetostat) or 3 μM EPZ (EZPO11989)). When DMSO treated cells reached 80-90% confluency the cells from all wells/conditions were trypsinized and counted and re-seeded with the same initial density to continue the assay.

2
A

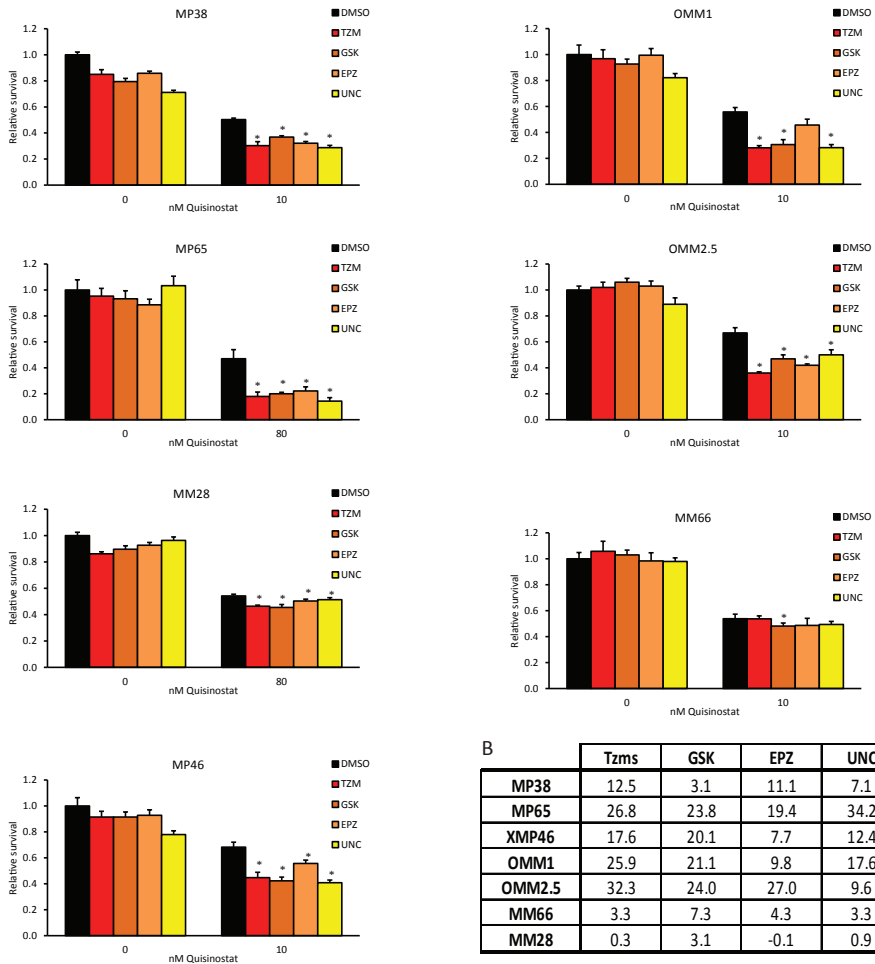


Figure 2. Synergistic effects of combined EZH2- and HDAC inhibition on uveal melanoma. **(A)** Indicated cell lines were treated with 4 distinct EZH2 inhibitors, Tazemetostat (Tzms; 4 μ M), GSK (GSK503; 4 μ M), EPZ011989 (EPZ; 4 μ M for MM28, MP65 and MM66; 6 μ M for MP38, MP46, OMM1 and OMM2.5), UNC1999 (UNC; 1 μ M for MM28, MP65, OMM1, OMM2.5 and MM66; 4 μ M for MP38 and MP46) or DMSO, the HDAC inhibitor Quisinostat or by a combination. Asterisk (*) indicates significant differences ($p \leq 0.05$) between Quisinostat-treated and the combined treated cells. **(B)** Excess over Bliss values were calculated to determine synergism.[39]

(Supplementary Fig. 1B) [21]. No such upregulation was found for SUZ12 expression, another member of the PRC2 complex, showing that the EZH2 upregulation was

not due to a general increase of all members of PRC2. In accordance with previous observations for mesothelioma cells [11], our results are supporting the argument that BAP1-negative UM cells are more sensitive to EZH2 inhibition, although the differences are clearly less dramatic in UM compared to mesothelioma.

Synergistic effects of concurrent HDAC and EZH2 inhibition.

Due to the lack of a rapid onset of growth arrest, EZH2 inhibition most likely will not be effective as single treatment for metastatic UM patients. It has previously been shown that dual inhibition of EZH2 and HDACs strongly reduced tumor cell survival and, therefore, has an interesting therapeutic potential [22-24]. For this reason we tested the broad spectrum HDAC inhibitor Quisinostat (JNJ-26481585), with known pre- and clinical effects in (uveal) melanoma cells and patients [25-27], in combination with four distinct EZH2 inhibitors. As mentioned before, EZH2 inhibition did not or hardly affect UM survival after an incubation of 5 days (Fig. 2A). Even so, all EZH2 inhibitors clearly enhanced the growth inhibition by Quisinostat in a synergistic manner in most cell lines (Excess over Bliss values ≥ 2) (Fig. 2A and B).

Combinatory inhibition of HDAC and EZH2 induces uveal melanoma cell death.

Analysis of protein lysates of tested cell lines showed a marked increase in H3K9/14-acetylation and a decrease of K27 tri-methylation upon Quisinostat or Tazemetostat, respectively (Fig. 3A). These changes in epigenetic markers show that both compounds efficiently affect activity of their designated target proteins. In most cell lines the combination stimulated cell death by apoptosis as indicated by increased PARP cleavage (Fig. 3A). Only MM66 did not show an increase in PARP cleavage in the combination compared to single Quisinostat treatment. MM28 hardly showed any PARP cleavage, suggesting resistance to apoptosis induction (Fig. 3A). Combination of Quisinostat with GSK503 yielded similar results in four cell lines tested (data not shown). Surprisingly, in both MM28 and MM66 the changes in epigenetic markers clearly indicate EZH2 and HDAC inhibition upon drug treatment, rendering the lack of synergism not due to inefficient target inhibition but to not yet identified differences between these cell lines. To verify increased cell death by the combined treatment, flow cytometry analyses have been performed. As expected, both EZH2 inhibitors Tazemetostat and GSK503 hardly affected the cell cycle profile correlating with the lack of effect on cell proliferation (Fig. 3B). Quisinostat on the other hand elicited a clear G1 phase cell cycle arrest, in accordance with our earlier and previous studies with other HDAC inhibitors [27, 28]. Importantly, combined treatment increased the fraction of subG1 cells in most cell lines (Fig. 3B), in agreement with the PARP cleavage analyses. As with the previous experiments hardly any differences were found between the single treat-

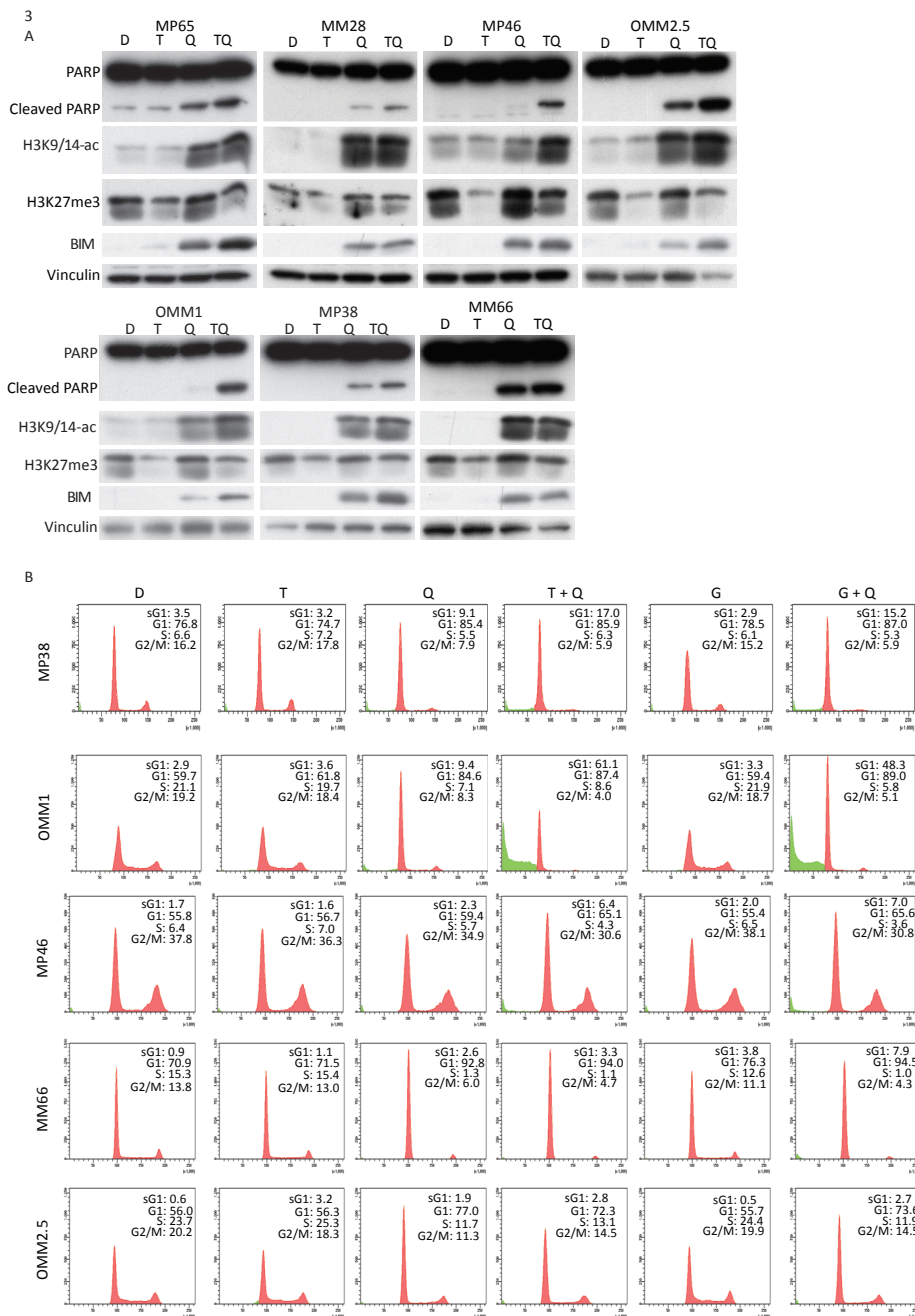


Figure 3. Induction of cell death upon concurrent inhibition of EZH2 and HDAC. **(A)** Biochemical effects of EZH2 and HDAC inhibition on BAP1-positive and -negative UM cells were assessed after 48 hours by Western blot. Tazemetostat (T; 4 μ M) reduced tri-methylated lysine 27 of histone 3 (H3K27me3) and Quisinstat (Q; 40 nM) treatment enhanced histone 3 acetylation (H3K9/14-

ac). Pro-apoptotic BIM protein levels and PARP cleavage were analysed as apoptotic markers and expression of vinculin was analysed to show equal loading. (B) Effects of EZH2 inhibition (T; Tazemetostat; 4 μ M) and G; GSK503; 4 μ M), HDAC inhibition (Q; Quisinostat; 40 nM) or combinations on the cell cycle profiles of UM cells after 48 hours.

ments and the combined-treated MM66 cells although a slightly increased subG1 phase is found in the Quisinostat/GSK503 combination.

To find an explanation for the increased cell death upon combinatory treatment expression of a number of genes involved in apoptosis was investigated, i.e. *BIM*, *NOXA* and *Survivin*.

These genes were chosen because it had been shown that *BIM* expression is strongly increased by combined HDAC and EZH2 inhibition [29] and both *NOXA* and *Survivin* have been reported to be responsive to HDAC inhibition [30, 31]. Indeed, Quisinostat is strongly increasing the mRNA levels of *BIM* and *NOXA* and in combination with EZH2-inhibition by Tazemetostat the levels are further enhanced, although this increase is not always statistically significant (Supplementary Fig 2). BIM protein levels were also investigated and indeed in most cell lines the combined Quisinostat/Tazemetostat treatment resulted in further increase in BIM levels (Figure 3A). As reported, HDAC inhibition strongly downregulates the expression of *Survivin*, which is not affected by addition of Tazemetostat. Since several reports that HDAC inhibition increases levels of FOXO proteins and the *BIM* gene is a known FOXO target, we investigated the expression of *FOXO1*, *FOXO3* and *FOXO4* mRNA. Also in these tested UM cell lines HDAC inhibition increased *FOXO1* and *FOXO3* mRNA levels and in 2/3 cell lines the increase is enhanced by concomitant EZH2 inhibition (Supplementary Fig 2). *FOXO4* mRNA levels were also increased upon HDAC inhibition in all UM cell lines tested, although less prominent, and was not further enhanced when HDAC and EZH2 inhibition was combined.

Thus, EZH2 inhibitors do not affect UM cell proliferation or survival at early time points but they still might sensitize UM cells for other therapeutic interventions, as illustrated here by HDAC inhibition. These effects are likely to be mediated in part by the upregulation of FOXO transcription factors.

Discussion

Despite ongoing developments with regard to novel therapeutic strategies to treat metastasized UM, no effective curative treatment is available. Typical for the onset of metastasis in UM is the loss of one chromosome 3 and inactivating mutations in the remaining *BAP1* gene [10, 32]. These events result in the absence of BAP1 expression in 80-90% of the metastasized UM cases [10]. The observation that cells lacking BAP1 expression would be more sensitive for EZH2 inhibition would, therefore, meet the need for a specific treatment of UM metastases. The data presented in this study suggest that UM cells are sensitive for EZH2 inhibition upon long-term treatment, seemingly in contrast to the conclusions drawn by Schoumacher *et al.*[19]. Same cell lines and partly the same compounds (Tazemetostat = EPZ6438) were used, but the apparent discrepancies can easily be explained by the long incubation time which EZH2 inhibitors need before affecting the cell growth. Furthermore, in general the *BAP1*-negative cells demonstrate a slightly more dramatic and faster response to EZH2 inhibition suggesting a potential enhancement of the treatment by *BAP1* loss. This could be, at least partially, explained by the observation that *BAP1*-negative UM tumors tend to have higher *EZH2* expression compared to *BAP1*-positive UM tumors.

Previous studies have already established the potency and interesting therapeutic potential of combined EZH2 and HDAC inhibition in various malignancies [22-24]. Moreover, HDAC inhibition as single treatment or in combination has already been demonstrated to be an interesting strategy for treating UM [27, 28, 33]. Although growth retardation by EZH2-inhibitors takes time, i.e. several replication rounds, at early time points EZH2-inhibition sensitizes the UM cells for HDAC inhibition. We show here for the first time that combined inhibition of EZH2 and HDAC results in a synergistic reduction in UM cell growth. Underlying these synergistic effects most likely is the induction of cell death in the combinatory treated cells. In accordance with previous studies, results in this study show increased levels of pro-apoptotic *BIM* and *NOXA* upon dual inhibition of EZH2 and HDACs, correlating with increased *FOXO1* and *FOXO3* mRNA levels, potentially underlying the increase in cell death and the synergism [29]. Although we cannot exclude additional pathways leading to the enhanced apoptosis, previous studies using HDAC inhibitors, including quisinostat, have shown that the increased cell death is at least partly dependent on the enhanced FOXO protein expression [34, 35]. Therefore, we propose that EZH2 inhibition in combination with other compounds, e.g. an HDAC inhibitor like Quisinostat, can provide a useful treatment alternative for metastasized UM.

Acknowledgements

The authors like to thank Dr. Bruce Ksander, Dr. Martine Jager, Dr. Gré Luyten, Dr. Sergio Roman-Roman and Dr. Fariba Nemati for providing the uveal melanoma cell lines. We thank Jinfeng Cao for the gift of GSK503 and UNC1999.

Competing financial interests

The authors declare no competing financial interests.

References

1. Shah SU, Mashayekhi A, Shields CL, Walia HS, Hubbard GB, 3rd, Zhang J, Shields JA. Uveal metastasis from lung cancer: clinical features, treatment, and outcome in 194 patients. *Ophthalmology*. 2014; 121: 352-7. doi: 10.1016/j.ophtha.2013.07.014.
2. Singh AD, Bergman L, Seregard S. Uveal melanoma: epidemiologic aspects. *Ophthalmol Clin North Am*. 2005; 18: 75-84, viii. doi: 10.1016/j.ohc.2004.07.002.
3. Augsburger JJ, Correa ZM, Shaikh AH. Effectiveness of treatments for metastatic uveal melanoma. *Am J Ophthalmol*. 2009; 148: 119-27. doi: 10.1016/j.ajo.2009.01.023.
4. Kivela T, Eskelin S, Kujala E. Metastatic uveal melanoma. *Int Ophthalmol Clin*. 2006; 46: 133-49. doi:
5. Horsman DE, White VA. Cytogenetic analysis of uveal melanoma. Consistent occurrence of monosomy 3 and trisomy 8q. *Cancer*. 1993; 71: 811-9. doi:
6. Kilic E, van Gils W, Lodder E, Beverloo HB, van Til ME, Mooy CM, Paridaens D, de Klein A, Luyten GP. Clinical and cytogenetic analyses in uveal melanoma. *Invest Ophthalmol Vis Sci*. 2006; 47: 3703-7. doi: 10.1167/iovs.06-0101.
7. Prescher G, Bornfeld N, Horsthemke B, Becher R. Chromosomal aberrations defining uveal melanoma of poor prognosis. *Lancet*. 1992; 339: 691-2. doi:
8. Prescher G, Bornfeld N, Hirche H, Horsthemke B, Jockel KH, Becher R. Prognostic implications of monosomy 3 in uveal melanoma. *Lancet*. 1996; 347: 1222-5. doi:
9. Harbour JW, Onken MD, Roberson ED, Duan S, Cao L, Worley LA, Council ML, Matatall KA, Helms C, Bowcock AM. Frequent mutation of BAP1 in metastasizing uveal melanomas. *Science*. 2010; 330: 1410-3. doi: 10.1126/science.1194472.
10. van Essen TH, van Pelt SI, Versluis M, Bronkhorst IH, van Duinen SG, Marinkovic M, Kroes WG, Ruivenkamp CA, Shukla S, de Klein A, Kilic E, Harbour JW, Luyten GP, et al. Prognostic parameters in uveal melanoma and their association with BAP1 expression. *Br J Ophthalmol*. 2014; 98: 1738-43. doi: 10.1136/bjophthalmol-2014-305047.
11. LaFave LM, Beguelin W, Koche R, Teater M, Spitzer B, Chramiec A, Papalexli E, Keller MD, Hricik T, Konstantinoff K, Micol JB, Durham B, Knutson SK, et al. Loss of BAP1 function leads to EZH2-dependent transformation. *Nat Med*. 2015; 21: 1344-9. doi: 10.1038/nm.3947.
12. Kim KH, Roberts CW. Targeting EZH2 in cancer. *Nat Med*. 2016; 22: 128-34. doi: 10.1038/nm.4036.
13. Margueron R, Reinberg D. The Polycomb complex PRC2 and its mark in life. *Nature*. 2011; 469: 343-9. doi: 10.1038/nature09784.
14. Di Croce L, Helin K. Transcriptional regulation by Polycomb group proteins. *Nat Struct Mol Biol*. 2013; 20: 1147-55. doi: 10.1038/nsmb.2669.
15. Shao Z, Raible F, Mollaaghababa R, Guyon JR, Wu CT, Bender W, Kingston RE. Stabilization of chromatin structure by PRC1, a Polycomb complex. *Cell*. 1999; 98: 37-46. doi: 10.1016/S0092-8674(00)80604-2.
16. Sparmann A, van Lohuizen M. Polycomb silencers control cell fate, development and cancer. *Nat Rev Cancer*. 2006; 6: 846-56. doi: 10.1038/nrc1991.
17. Yoo KH, Hennighausen L. EZH2 methyltransferase and H3K27 methylation in breast cancer. *Int J Biol Sci*. 2012; 8: 59-65. doi:
18. Xu K, Wu ZJ, Groner AC, He HH, Cai C, Lis RT, Wu X, Stack EC, Loda M, Liu T, Xu H, Cato L, Thornton JE, et al. EZH2 oncogenic activity in castration-resistant prostate cancer cells is Polycomb-independent. *Science*. 2012; 338: 1465-9. doi: 10.1126/science.1227604.
19. Schoumacher M, Le Corre S, Houy A, Mulugeta E, Stern MH, Roman-Roman S, Margueron R. Uveal melanoma cells are resistant to EZH2 inhibition regardless of BAP1 status. *Nat Med*. 2016; 22: 577-8. doi: 10.1038/nm.4098.

20. LaFave LM, Beguelin W, Koche R, Teater M, Spitzer B, Chramiec A, Papalexli E, Keller MD, Hricik T, Konstantinoff K, Micol JB, Durham B, Knutson SK, et al. Uveal melanoma cells are resistant to EZH2 inhibition regardless of BAP1 status Reply. *Nature Medicine*. 2016; 22: 578-9. doi: 10.1038/nm.4094.
21. Gao J, Aksoy BA, Dogrusoz U, Dresdner G, Gross B, Sumer SO, Sun Y, Jacobsen A, Sinha R, Larsson E, Cerami E, Sander C, Schultz N. Integrative analysis of complex cancer genomics and clinical profiles using the cBioPortal. *Sci Signal*. 2013; 6: pl1. doi: 10.1126/scisignal.2004088.
22. Grinshtein N, Riaseco CC, Marcellus R, Uehling D, Aman A, Lun X, Muto O, Podmore L, Lever J, Shen Y, Blough MD, Cairncross GJ, Robbins SM, et al. Small molecule epigenetic screen identifies novel EZH2 and HDAC inhibitors that target glioblastoma brain tumor-initiating cells. *Oncotarget*. 2016; 7: 59360-76. doi: 10.18632/oncotarget.10661.
23. Takashina T, Kinoshita I, Kikuchi J, Shimizu Y, Sakakibara-Konishi J, Oizumi S, Nishimura M, Dosaka-Akita H. Combined inhibition of EZH2 and histone deacetylases as a potential epigenetic therapy for non-small-cell lung cancer cells. *Cancer Sci*. 2016; 107: 955-62. doi: 10.1111/cas.12957.
24. Fiskus W, Wang Y, Sreekumar A, Buckley KM, Shi H, Jillella A, Ustun C, Rao R, Fernandez P, Chen J, Balusu R, Koul S, Atadja P, et al. Combined epigenetic therapy with the histone methyltransferase EZH2 inhibitor 3-deazaneplanocin A and the histone deacetylase inhibitor panobinostat against human AML cells. *Blood*. 2009; 114: 2733-43. doi: 10.1182/blood-2009-03-213496.
25. Venugopal B, Baird R, Kristeleit RS, Plummer R, Cowan R, Stewart A, Fourneau N, Hellemans P, Elsayed Y, McClue S, Smit JW, Forslund A, Phelps C, et al. A phase I study of quisinostat (JNJ-26481585), an oral hydroxamate histone deacetylase inhibitor with evidence of target modulation and antitumor activity, in patients with advanced solid tumors. *Clin Cancer Res*. 2013; 19: 4262-72. doi: 10.1158/1078-0432.CCR-13-0312.
26. van der Ent W, Burrello C, Teunisse AF, Ksander BR, van der Velden PA, Jager MJ, Jochemsen AG, Snaar-Jagalska BE. Modeling of human uveal melanoma in zebrafish xenograft embryos. *Invest Ophthalmol Vis Sci*. 2014; 55: 6612-22. doi: 10.1167/iovs.14-15202.
27. Heijkants R, Willekens S, Schoonderwoerd M, Teunisse A, Nieveen M, Radaelli E, Hawinkels H, Marine JC, Jochemsen A. Combined inhibition of CDK and HDAC as a promising therapeutic strategy for both cutaneous and uveal metastatic melanoma. *Oncotarget*. 2017; 9: 14. doi:
28. Landreville S, Agapova OA, Matatall KA, Kneass ZT, Onken MD, Lee RS, Bowcock AM, Harbour JW. Histone deacetylase inhibitors induce growth arrest and differentiation in uveal melanoma. *Clin Cancer Res*. 2012; 18: 408-16. doi: 10.1158/1078-0432.CCR-11-0946.
29. Huang JP, Ling K. EZH2 and histone deacetylase inhibitors induce apoptosis in triple negative breast cancer cells by differentially increasing H3 Lys(27) acetylation in the BIM gene promoter and enhancers. *Oncology Letters*. 2017; 14: 5735-42. doi: 10.3892/ol.2017.6912.
30. Gallagher SJ, Gunatilake D, Beaumont KA, Sharp DM, Tiffen JC, Heinemann A, Weninger W, Haass NK, Wilmott JS, Madore J, Ferguson PM, Rizos H, Hersey P. HDAC inhibitors restore BRAF-inhibitor sensitivity by altering PI3K and survival signalling in a subset of melanoma. *Int J Cancer*. 2017. doi: 10.1002/ijc.31199.
31. Feng W, Cai D, Zhang B, Lou G, Zou X. Combination of HDAC inhibitor TSA and silibinin induces cell cycle arrest and apoptosis by targeting survivin and cyclinB1/Cdk1 in pancreatic cancer cells. *Biomed Pharmacother*. 2015; 74: 257-64. doi: 10.1016/j.biopha.2015.08.017.
32. Robertson AG, Shih J, Yau C, Gibb EA, Oba J, Mungall KL, Hess JM, Uzunangelov V, Walter V, Danilova L, Lichtenberg TM, Kucherlapati M, Kimes PK, et al. Integrative Analysis Identifies Four Molecular and Clinical Subsets in Uveal Melanoma. *Cancer Cell*. 2017; 32: 204-20 e15. doi: 10.1016/j.ccell.2017.07.003.

33. Carol H, Gorlick R, Kolb EA, Morton CL, Manesh DM, Keir ST, Reynolds CP, Kang MH, Maris JM, Wozniak A, Hickson I, Lyalin D, Kurmasheva RT, et al. Initial testing (stage 1) of the histone deacetylase inhibitor, quisinostat (JNJ-26481585), by the Pediatric Preclinical Testing Program. *Pediatr Blood Cancer*. 2014; 61: 245-52. doi: 10.1002/pbc.24724.
34. Laporte AN, Poulin NM, Barrott JJ, Wang XQ, Lorzadeh A, Vander Werff R, Jones KB, Underhill TM, Nielsen TO. Death by HDAC Inhibition in Synovial Sarcoma Cells. *Mol Cancer Ther*. 2017; 16: 2656-67. doi: 10.1158/1535-7163.MCT-17-0397.
35. Pei Y, Liu KW, Wang J, Garancher A, Tao R, Esparza LA, Maier DL, Udaka YT, Murad N, Morrissy S, Sekercin H, Brabetz S, Qi L, et al. HDAC and PI3K Antagonists Cooperate to Inhibit Growth of MYC-Driven Medulloblastoma. *Cancer Cell*. 2016; 29: 311-23. doi: 10.1016/j.ccell.2016.02.011.
36. Chen PW, Murray TG, Uno T, Salgaller ML, Reddy R, Ksander BR. Expression of MAGE genes in ocular melanoma during progression from primary to metastatic disease. *Clin Exp Metastasis*. 1997; 15: 509-18. doi:
37. Luyten GP, Naus NC, Mooy CM, Hagemelijer A, Kan-Mitchell J, Van Drunen E, Vuzevski V, De Jong PT, Luijckx TM. Establishment and characterization of primary and metastatic uveal melanoma cell lines. *Int J Cancer*. 1996; 66: 380-7. doi: 10.1002/(SICI)1097-0215(19960503)66:3<380::AID-IJC19>3.0.CO;2-F.
38. Amirouchene-Angelozzi N, Nemati F, Gentien D, Nicolas A, Dumont A, Carita G, Camonis J, Desjardins L, Cassoux N, Piperno-Neumann S, Mariani P, Sastre X, Decaudin D, et al. Establishment of novel cell lines recapitulating the genetic landscape of uveal melanoma and preclinical validation of mTOR as a therapeutic target. *Mol Oncol*. 2014; 8: 1508-20. doi: 10.1016/j.molonc.2014.06.004.
39. Amirouchene-Angelozzi N, Frisch-Dit-Leitz E, Carita G, Dahmani A, Raymondie C, Liot G, Gentien D, Nemati F, Decaudin D, Roman-Roman S, Schoumacher M. The mTOR inhibitor Everolimus synergizes with the PI3K inhibitor GDC0941 to enhance anti-tumor efficacy in uveal melanoma. *Oncotarget*. 2016; 7: 23633-46. doi: 10.18632/oncotarget.8054.

Methods

Cell culture growth and viability assays

The UM cell lines MEL202, OMM2.5 and OMM1 were cultured in a mixture of RPMI and DMEM-F12 (1:1 ratio), supplemented with 10% fetal calf serum (FCS). Cell lines OMM2.5 and MEL202 were kindly provided by B Ksander [36]. OMM1 cells were kindly provided by GPM Luyten [37]. Establishment of the UM cell lines MM28, MM66, MP38, XMP46 and MP65 has been described [38] and these cells were maintained in IMDM containing 20% FCS. All media were supplemented with 100 U/ml penicillin and 100 µg/ml streptomycin. All cells were cultured in a humidified incubator at 37 °C and 5% CO₂.

For short term growth assay the cells were seeded in triplicate, in 96-well format and incubated for 5 days. Cell survival was determined via the Cell Titre-Blue Cell Viability assay (Promega, Fitchburg, WI, USA); fluorescence was measured in a microplate reader (Victor, Perkin Elmer, San Jose, CA, USA).

Tazemetostat, EPZ011989, GSK503, UNC1999 (all purchased from Selleck Chemicals, Houston, TX USA) and Quisinostat (Johnson and Johnson, New Brunswick, NJ, USA) were used at concentrations indicated in the figure legends.

Six UM cell lines were cultured in the continuous presence of EZH2 inhibitors (2 µM Tzms (Tazemetostat) or 3 µM EPZ (EPZ011989)). Cells were seeded sparsely in a 6-well format, ranging from 5×10^4 to 1.2×10^5 cells/well, depending on the cell line. When the confluency reached 80-90% in the DMSO treated cells all conditions were counted in duplicate, using a Bürker chamber, and re-seeded with the same initial density to continue the assay. Cells were provided with fresh medium/drugs every 2-3 days.

Western blot analysis

After incubation with drugs as indicated cells were harvested in Laemmli sample buffer. Bradford Ultra (Expedeon, San Diego, Ca USA) was used according to manufacturer's protocol to determine protein concentrations. Equal protein amounts were separated using SDS-PAGE and blotted onto polyvinylidene fluoride transfer membranes (Millipore, Darmstadt, Germany). After blocking in TBST (10 mM Tris-HCl pH8.0, 150 mM NaCl, 0.2% Tween 20) containing 10% milk, membranes were incubated with the following primary antibodies diluted in TBST/5% BSA (H3K27me3 (39155, Active Motif, Carlsbad, CA, USA), USP7 (A300-033A, Bethyl Laboratories, Montgomery, TX, USA), PARP (9542, Cell Signalling Technology, Beverly, MA, USA), Ac-H3 (06-599, Millipore), BIM (2819, Cell Signalling Technology, Beverly, MA, USA) or Vinculin (hVIN-1/V9131,

Sigma-Aldrich, St Louis, MO, USA)) and appropriate HRP-conjugated secondary antibodies (Jackson Laboratories, Bar Harbor, ME, USA). Bands were visualized using chemoluminescence and visualized by exposure to X-ray film.

Flow cytometry

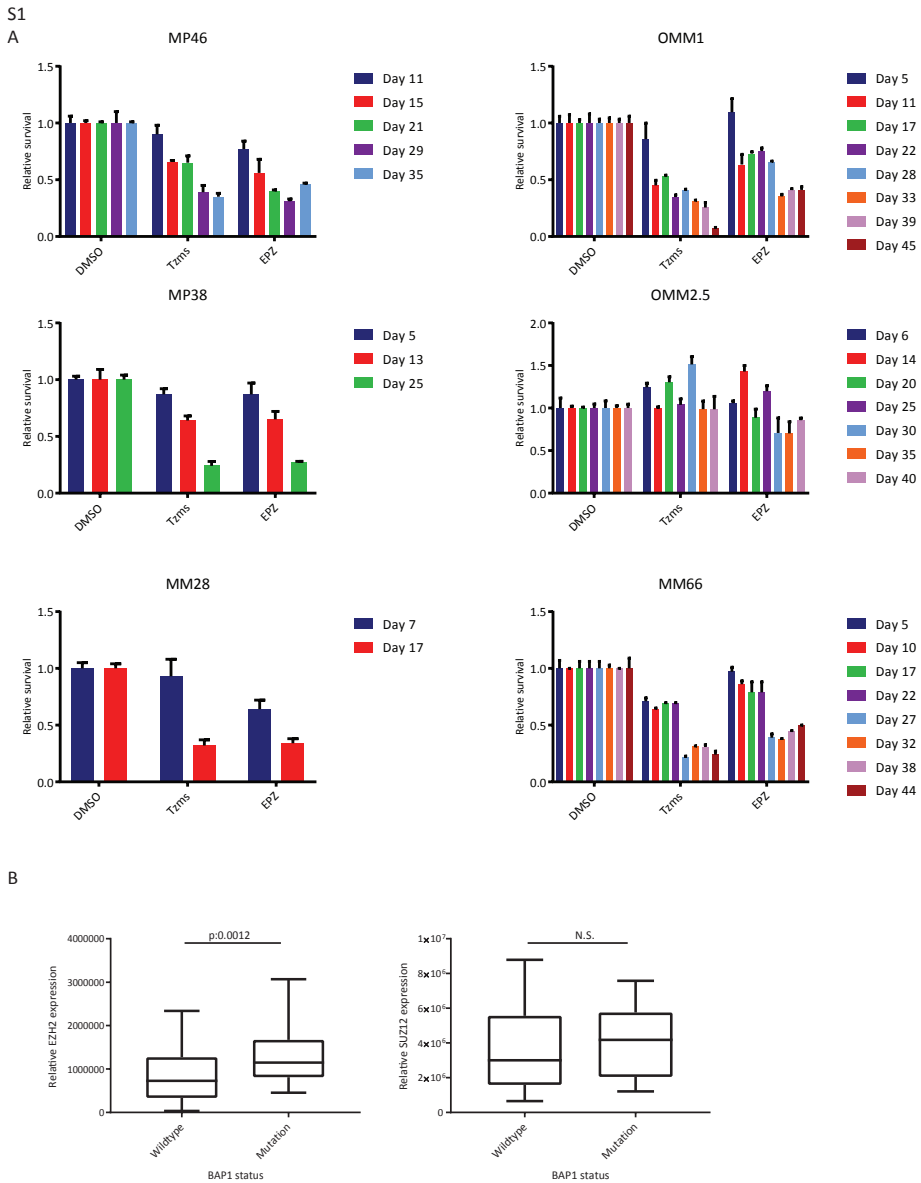
Cells were harvested for cell cycle analysis by trypsinization, washed twice in PBS and fixed in ice cold 70% ethanol. After fixation, cells were washed in PBS containing 2% FCS and resuspended in PBS containing 2% FCS, 50 µg/ml RNase and 50 µg/ml propidium iodide (PI). Flow cytometry analysis was performed using the BD LSR II system (BD Biosciences, San Diego, CA, USA).

Quantitative PCR

MM28, MP38 and MP46 cell were incubated for 48 hours with 4 µM Tazemetostat, 40 nM Quisinostat or a combination. The SV total RNA isolation kit (Promega, Fitchburg, WI, USA) was used to extract and purify RNA, from which cDNA was synthesized using the reverse transcriptase reaction mixture as indicated by Promega. SYBR green mix (Roche Diagnostics, Indianapolis, IN, USA) was used to perform qPCR in a C1000 touch Thermal Cycler (Bio-Rad laboratories, Hercules, CA, USA). Relative expression of target BIM (Fw: CATGCGGTATTCGGTTC and Rv: GCTTGCCATTGGTCTTTTT), NOXA (Fw: ACTGTTCGTGTTTCAGCTC and Rv: GTAGCACACTCGACTTCC), Survivin (Fw: AGCCCTTCTCAAGGACCA and Rv: CAGCTCCTTGAAGCAGAAGAA), FOXO1 (Fw: ATGTGTTGCCAACCAAAGC and Rv: TGCTTCTCTCAGTTCCTGCTG), FOXO3 (Fw: GCGTGCCCTACTTCAAGGAT and Rv: GCTCTTGCCAGTTCCTCAT) and FOXO4 (Fw: TGCCCAGATCTACGAGTGGA and Rv: GGGTTCAGCATCCACCAAGA) was determined corrected for the housekeeping genes CAPNS1 (Fw: ATGGTTTTGGCATTGACACATG and Rv: GCTTGCCCTGTGGTGTGCGC), RPS11 (Fw: AAGCAGCCGACCATCTTCA and Rv: CGGGAGCTTCTCCTTGCC) and SRPR (Fw: CATTGCTTTTGCACGTAACCAA and Rv: ATTGTCTTGCATGCGGCC). Per cell line the average relative expression was determined by setting the untreated at 1.

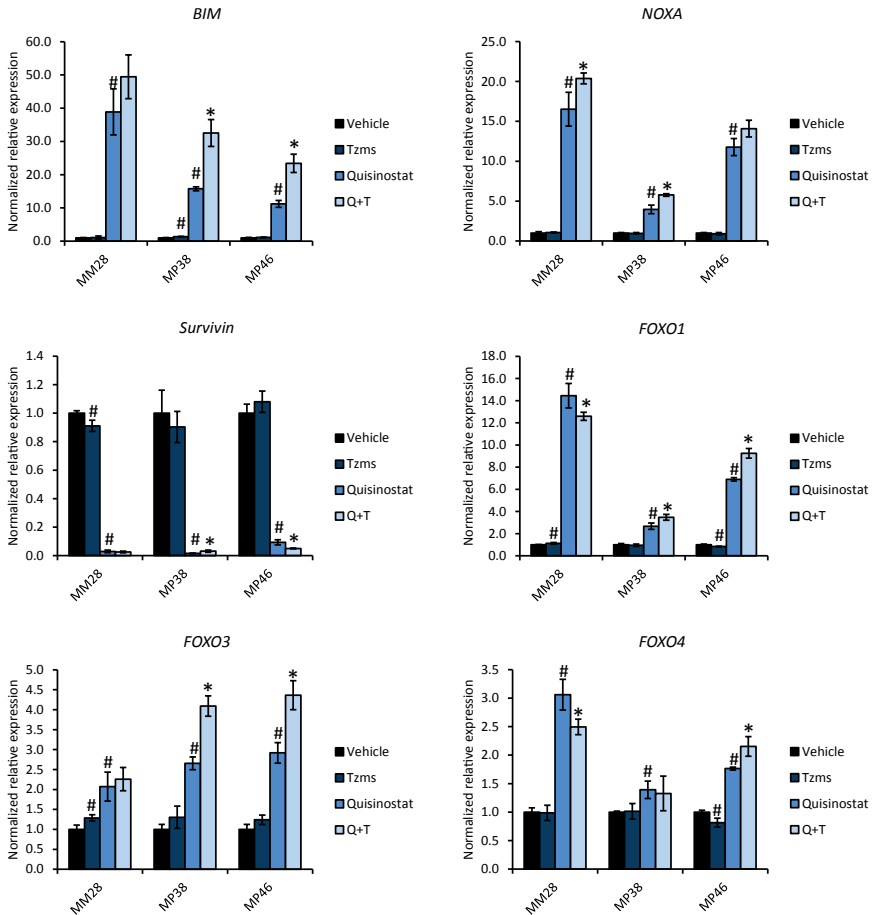
Statistical analysis

To determine significance of changes between two groups a student's t-test was used. P values of 0.05 or lower were considered to be significant.



Supplementary figure 1. Effects of EZH2 inhibition on long-term and in combination with HDAC inhibition on BAP1-positive and -negative uveal melanoma cell lines. **(A)** Extended version of Fig. 1B, showing all time points at which control reached 80-90% confluency and the relative cell survival in the corresponding EZH2 inhibitor treated cells was determined. Long-term growth assays were stopped when cells no longer proliferate or after 40-45 days. **(B)** Comparison of *EZH2* and *SUZ12* expression between UM tumors with diploid or a shallow deleted BAP1.[21]

S2



Supplementary figure 2. Effects of combined EZH2 and HDAC inhibition on *BIM*, *NOXA*, *Survivin*, *FOXO1*, *FOXO3* and *FOXO4* mRNA levels. Normalized relative expression of *BIM* and *NOXA* upon 48 hours incubation of 4 μ M Tazemetostat (Tzms), 40 nM Quisinostat (Q) or combined. Hashtag (#) indicates significant differences between vehicle and Tazemetostat or Quisinostat treated samples. Asterisk (*) indicates significant differences between the combined treated samples compared to both single treatments.

CHAPTER 5

Combined inhibition of CDK and HDAC as a promising therapeutic strategy for both cutaneous and uveal metastatic melanoma

R.C. Heijkants¹, K. Willekens^{2,3}, M.J.A. Schoonderwoerd⁴, A.F.A.S Teunisse¹,
M.C. Nieveen¹, E. Radaelli⁵, L.J.A.C. Hawinkels⁴, J.C. Marine^{2,3} and A.G.
Jochemsen¹

1) Department of Molecular Cell Biology, Leiden University Medical Center, 2300 RC Leiden,
the Netherlands.

2) Laboratory for Molecular Cancer Biology, VIB Center for Cancer Biology, Leuven, Belgium.

3) Department of Oncology, KU Leuven, Leuven, Belgium.

4) Department of Gastroenterology-Hepatology, Leiden University Medical Center, 2300 RC
Leiden, the Netherlands.

5) Mouse Histopathology Core Facility, VIB Center for the Biology of Disease, KU Leuven,
Leuven, Belgium.

Abstract

Very little to no improvement in overall survival has been seen in patients with advanced non-resectable cutaneous melanoma or metastatic uveal melanoma in decades, highlighting the need for novel therapeutic options. In this study we investigated as a potential novel therapeutic intervention for both cutaneous and uveal melanoma patients a combination of the broad spectrum HDAC inhibitor quisinostat and pan-CDK inhibitor flavopiridol. Both drugs are currently in clinical trials reducing time from bench to bedside. Combining quisinostat and flavopiridol shows a synergistic reduction in cell viability of all melanoma cell lines tested, irrespective of their driver mutations. This synergism was also observed in BRAF^{V600E} mutant melanoma that had acquired resistance to BRAF inhibition. Mechanistically, loss of cell viability was, at least partly, due to induction of apoptotic cell death. The combination was also effectively inducing tumor regression in a preclinical setting, namely a patient-derived tumor xenograft (PDX) model of cutaneous melanoma, without increasing adverse effects. We propose that the quisinostat/flavopiridol combination is a promising therapeutic option for both cutaneous and uveal metastatic melanoma patients, independent of their mutational status or (acquired) resistance to BRAF inhibition.

Introduction

Melanoma is an aggressive type of cancer which originates from melanocytes, affecting about 132,000 new patients in 2016 in the US alone [1]. Although melanoma is found predominantly as a cutaneous disease, melanomas from the uveal tract in the eye, uveal melanoma (UM), account for ~5.3% of total melanoma incidence [2]. UM is genetically distinct from cutaneous melanoma (CM). CM is most commonly driven by oncogenic mutations in NRAS or BRAF [3]; the latter spurred the development of mutant-specific BRAF inhibitors. Although most patients with BRAF mutations initially respond well to BRAF inhibition, resistance and relapse inevitably occurs within 6 to 8 months [4]. Besides BRAF inhibitors, immunotherapy has proven to be an effective treatment in CM cases [5]. In contrast, UM is in most cases driven by an activating mutation in one of the G-proteins GNA11 or GNAQ [6, 7]. It has been shown that the continuous activation GNA11 or GNAQ exerts its oncogenic capacity, among others, through the activation of the MAPK pathway via protein kinase C (PKC) signaling [8-10]. This insight has incited the use of PKC inhibitors as treatment for UM, but these inhibitors only have limited clinical effects [11]. Despite these ongoing developments there still is a lack of curative treatment for metastasized UM and CM, rendering metastasized melanoma a lethal disease. Our effort to search for novel therapeutic interventions for metastatic melanoma focuses on drugs in clinical development to reduce the time from bench to bedside.

A number of studies have shown promising results using histone deacetylase (HDAC) inhibitors, both in pre-clinical studies and clinical trials, as potential therapeutic intervention for both CM and UM [12-15]. One of these HDAC inhibitors is quisinostat (also known as JNJ-26481585), a second generation broad spectrum HDAC inhibitor. Quisinostat has proven its efficacy against several tumor types, including melanoma, in pre-clinical studies [16-19] and is currently being tested in phase 2 clinical trials [20, 21]. The antitumor-response observed with HDAC inhibitors is often limited to induction of a G1 cell cycle arrest. Although this effect can block tumor outgrowth [21], finding drug(s) that can synergize with HDAC inhibitors and promote cancer cell killing would greatly increase their clinical impact. In breast cancer cells HDAC inhibition induced the degradation of cyclin D1 protein, which could implicate that HDAC inhibition would sensitize cells for CDK inhibition [22]. Indeed, in neuroblastoma cell lines HDAC inhibition combined with CDK inhibition induces apoptosis [23]. In this study we aimed at potentiating the effect of quisinostat by combining the treatment with pan-cyclin-dependent kinase (CDK) inhibition using flavopiridol (also known as alvocidib). Flavopiridol is FDA approved and is currently being tested in clinical trials, predominantly as therapeutic intervention for lymphoma and acute myeloid leuke-

mia. Flavopiridol strongly inhibits CDK9 activity, but also affects activities of CDK1, CDK2, CDK4, CDK6, CDK7 and CDK12 [24-27]. By inhibiting CDK12, CDK9 and CDK7 flavopiridol inhibits the phosphorylation of serine 2 and 5 within the RNA pol 2 CTD repeats and, thereby, transcription initiation and elongation [26]. Via the inhibition of CDK1, CDK2, CDK4 and CDK6 flavopiridol induces cell cycle arrests [24, 25]. Interestingly, flavopiridol has been shown to induce stable disease in 7 out of 16 patients with previously untreated metastatic malignant melanoma. Unfortunately, flavopiridol failed to achieve significant clinical benefit according to objective response criteria [28].

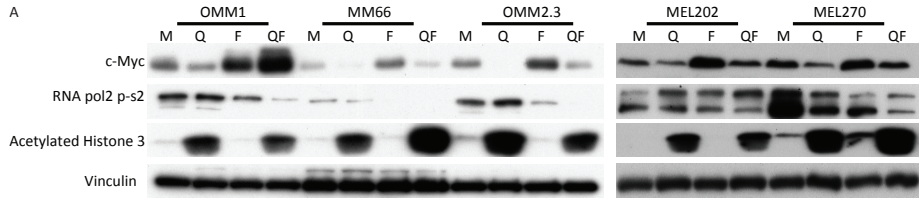
Here we show that single treatment with quisinostat or flavopiridol slows down the growth of UM and CM cells, while combined treatment synergistically inhibits growth and, importantly, decreases survival. Whereas single treatment only induced cell cycle arrest, the combination of quisinostat and flavopiridol induced apoptosis of melanoma cells and did so irrespective of their BRAF or NRAS status. Furthermore, melanoma cells with acquired resistance to BRAF inhibition remained as sensitive to the combination as their BRAF sensitive counterparts. The combination also effectively prevented tumor growth *in vivo*, in a patient derived xenograft (PDX) model of CM. In conclusion, we propose that combining quisinostat with flavopiridol should be explored as a first or second line therapeutic option for patients with metastatic UM and CM, respectively.

Results

Synergistic reduction of UM cell proliferation by simultaneous CDK and HDAC inhibition.

We first evaluated whether quisinostat and flavopiridol were capable of eliciting their expected biochemical responses in UM cells (Figure 1A). Consistent with quisinostat being an effective inhibitor of HDACs, an increase in acetylation of histone 3 was observed in all UM cell lines exposed to this drug. One of the main targets of flavopiridol is CDK9, which phosphorylates RNA pol2-CTD at Serine 2. Accordingly, reduced phosphorylation of RNA pol2-Ser2 was seen in all but one (MEL202) of the tested UM cell lines exposed to flavopiridol. Counterintuitively, it has been reported that treatment of cells with relatively low concentrations of flavopiridol actually increases the expression of c-Myc at both the RNA and protein level [29]. Indeed, we also find that in all UM cell lines flavopiridol increases c-Myc expression at RNA and protein levels (Figure 1A and Supplementary Figure S1). These data are consistent with flavopiridol being an inhibitor of CDK activity in UM cell lines. The flavopiridol-mediated increase

1



B

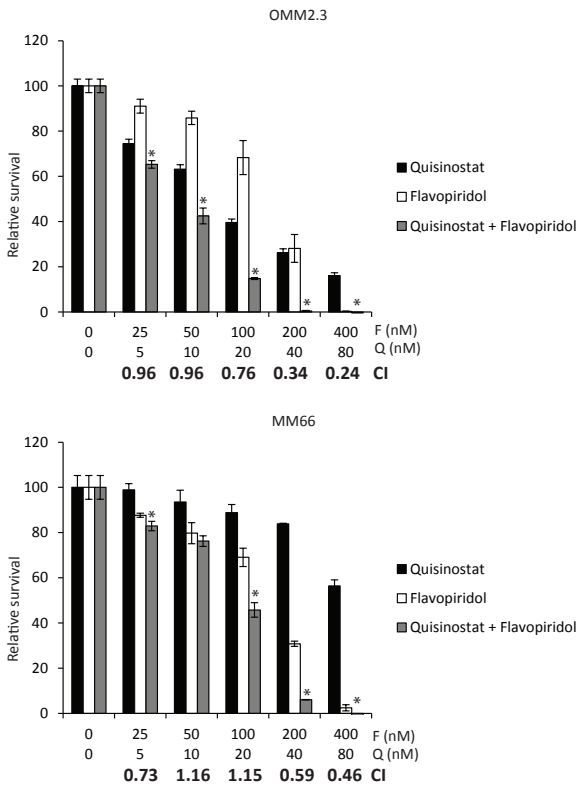


Figure 1. Simultaneous quisinstat and flavopiridol treatment synergistically inhibits growth of UM cell lines. A. UM cell lines OMM1, MM66, OMM2.3, MEL202 and MEL270 were treated with 20 nM quisinstat and 100 nM flavopiridol for 24 hours after which cells were harvested. Protein lysates were analyzed for the expression levels of c-Myc, RNA pol2-CTD Ser2 phosphorylation and acetylated histone 3 by Western blot. Expression of vinculin was analyzed to control for equal loading. B. UM cells OMM2.3 and MM66 were treated for 72 hours with indicated concentrations quisinstat and flavopiridol, either alone or in combination to determine effects on cell viability. To determine putative synergism the combination index (CI) values were calculated. Combinations with a significant ($p < 0.05$) lower relative survival compared to both single treatments are indicated with a *.

in c-Myc is largely reversed by the addition of quisinostat in most cell lines, as indeed quisinostat in most cases reduces c-Myc levels.

We next examined the effect of quisinostat and/or flavopiridol on UM cell proliferation. In all UM cell lines both quisinostat and flavopiridol reduced relative cell survival in a dose-dependent manner at nanomolar concentrations (Figure 1B and Supplementary Figure S2). Furthermore, a combination of these drugs resulted in an additive (CI: 1.1-0.9) or synergistic (CI: 0.9<) growth inhibitory effect in all cell lines.

Cell cycle arrest and apoptosis upon CDK and HDAC inhibition in UM cells.

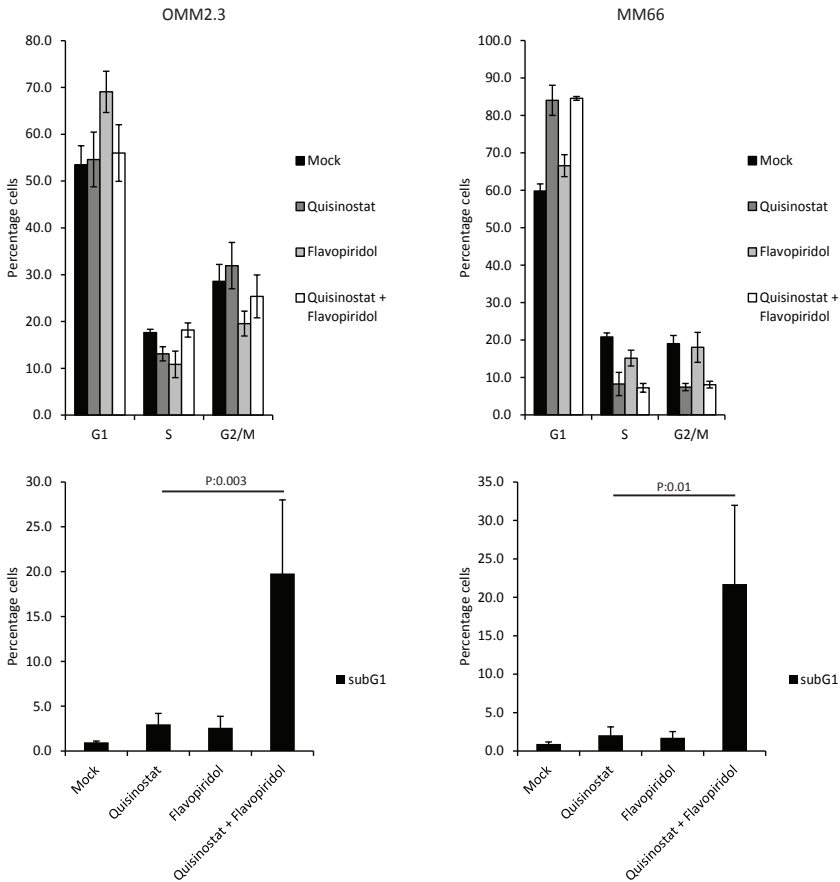
Flow cytometry was used to study the effects of the respective drugs on cell cycle progression. In agreement with previous reports, quisinostat induced a G1 cell cycle arrest in MM66, OMM1, MEL202 and MEL270 cells (Figure 2A and Supplementary Figure S3). The increase in G1 population was approximately 20% in these cell lines, concordant with a reduction of both the S- and G2/M- phase populations. However, no G1 arrest was observed upon quisinostat treatment in OMM2.3, although a small decrease in the number of S-phase cells could be observed (Figure 2A). Flavopiridol, due to its ability to inhibit multiple CDKs, has been reported to affect tumor cells at distinct stages during the cell cycle [23, 30]. We observed no obvious changes in the cell cycle profiles of MM66, OMM1 and MEL202 upon flavopiridol treatment, whereas in OMM2.3 cells flavopiridol treatment resulted in a G1 cell cycle arrest and in MEL270 cells in a G2/M cell cycle arrest (Figure 2A and Supplementary Figure S3). In spite of these partly distinct responses to the single compound treatments, the combination of drugs resulted in a significant increase in the subG1 population in all tested UM cell lines, indicating that combined treatment induced cell death (Figure 2 and Supplementary Figure S3). To further explore this increase in subG1, we immunoblotted for PARP. PARP is cleaved by activated caspase 3/7 during apoptosis and can therefore be used as a marker for apoptosis. An increase in cleaved PARP was observed in all cell lines treated with combined quisinostat and flavopiridol (Figure 2B), but not by single treatments. These data show that combining quisinostat and flavopiridol synergistically induce cell death via the induction of apoptosis in UM cell lines.

Synergistic effects of CDK and HDAC inhibition in cutaneous melanoma cells.

Since both quisinostat and flavopiridol are indirectly targeting a plethora of biological processes instead of specific oncogene-driven growth and -proliferation pathways, we explored whether the synergy is uveal specific or could also be observed in CM. We investigated whether these drugs elicit their biochemical effects in the following BRAF^{V600E} mutated cell lines: 93.05, A375, 634, MM249 and SK-MEL28. Furthermore,

2

A



B

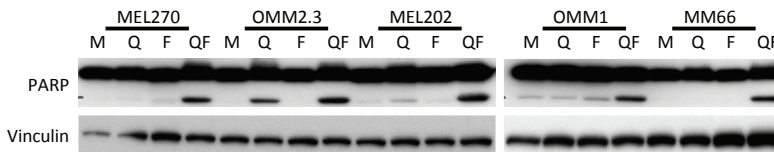


Figure 2. The combination of quisinostat and flavopiridol induces apoptosis in UM cell lines. A. OMM2.3 and MM66 cells were treated for 48 hours with 20 nM quisinostat and 100 nM flavopiridol after which cell were harvested to determine the cell cycle profiles by flow cytometry after PI staining. The percentages of each cell cycle phase (G1, S, G2/M and subG1) are the averages of three independent experiments. **B.** UM cell lines MEL270, OMM2.3, MEL202, OMM1 and MM66 were treated with 20 nM quisinostat and 100 nM flavopiridol for 48 hours. Protein lysates were analyzed by Western blot to investigate PARP cleavage. Expression of vinculin was analyzed to control for equal loading.

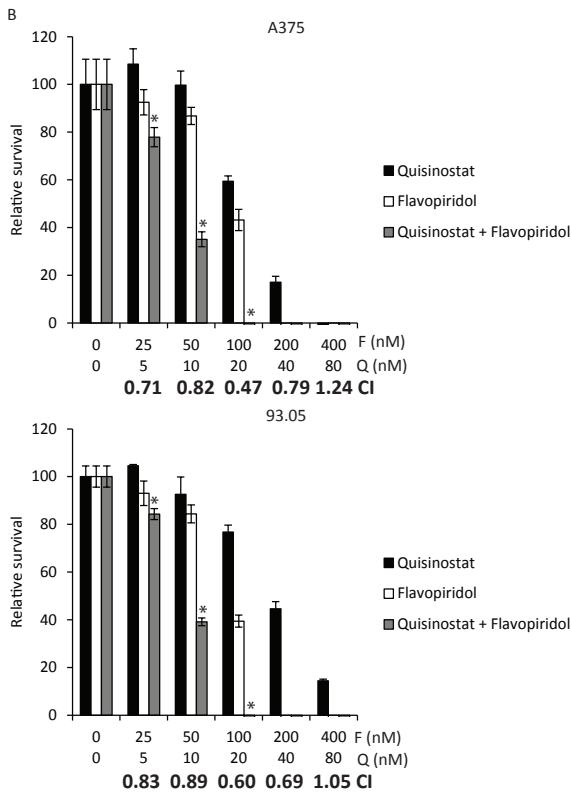
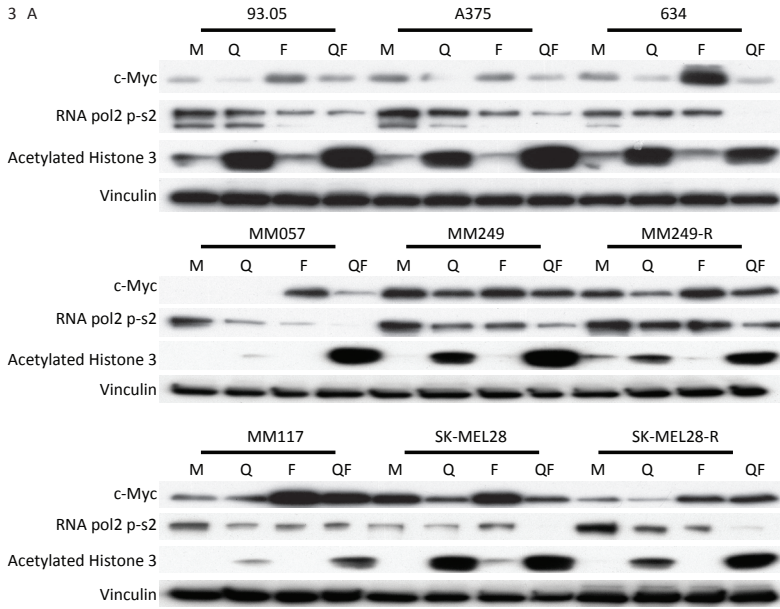


Figure 3.

Figure 3. Simultaneous quisinostat and flavopiridol treatment results in synergistic growth inhibition of CM cell lines. A. CM cell lines 93.05, A375, 634 (20 nM quisinostat and 100 nM flavopiridol), MM57, SK-MEL28, SK-MEL28R (20 nM quisinostat and 150 nM flavopiridol), MM117, M249 and M249-R (40 nM quisinostat and 200 nM flavopiridol) were treated for 24 hours with indicated concentrations of compounds. Protein lysates were analyzed by Western blotting to investigate levels of c-Myc, RNA pol2-CTD Ser2 phosphorylation and acetylated histone 3. Expression of vinculin was analyzed to control for equal loading. B. A375 and 93.05 cells were treated with quisinostat and/or flavopiridol with indicated concentrations for 72 hours to determine effect on cell viability. To determine putative synergism the combination index (CI) values were calculated. Combinations with a significant ($p < 0.05$) lower relative survival compared to both single treatments are indicated with a *.

NRAS^{Q61L} mutated cell line MM057 and NRAS/BRAF wild-type cell line MM117 were also exposed to these drugs. Treatment with quisinostat increased acetylated histone 3 levels, indicating that quisinostat is efficiently inhibiting HDACs in all cell lines (Figure 3A). Flavopiridol exposure resulted in reduced abundance of RNA pol2-CTD Ser2 phosphorylation in most cell lines but not in 634 and SK-MEL28. c-Myc protein levels were increased upon treatment with flavopiridol in most cell lines. Similar to UM the increase in c-Myc levels was seen at both protein and mRNA levels (Supplementary Figure S1). These data indicate that, like in UM, flavopiridol is actively inhibiting CDKs in CM cell lines. However, the molecular responses upon quisinostat and flavopiridol treatment seemed to vary between cell lines. As observed in UM cell lines, in some CM cell lines concurrent HDAC and CDK inhibition could affect the molecular responses; reversal of flavopiridol induced c-Myc increase, more pronounced drop of RNA pol2-S2 and further increase of acetylated histone 3.

We determined the effect of quisinostat and flavopiridol on the growth/survival of CM cells using cell proliferation assays (Figure 3B and Supplementary Figure S4). The combination of quisinostat and flavopiridol resulted in an additive (CI: 1.1-0.9) or synergistic (CI: 0.9>) growth inhibitory effect in all CM cell lines tested. Despite the fact that the IC50's differed per cell line, all IC50's were in the nanomolar range (Table 2). The first line therapy for CM patients carrying the BRAF^{V600E} mutation (~45% of all patients) consists of concurrent BRAF^{V600E}/MEK inhibition or immunotherapy, to which resistance occurs. Therefore, we investigated whether two cell lines that acquired resistance to BRAF inhibition *in vitro*, MM249-R and SK-MEL28-R were still responsive to HDAC/CDK inhibition. Striking responses to both drugs were observed in both the BRAF^{V600E} inhibitor resistant and - sensitive parental cell lines (Figure 3A). Furthermore, the BRAF^{V600E} inhibitor resistant and - sensitive parental cell lines had similar IC50's for both drugs (Table 2). Importantly, like their parental cell lines, the

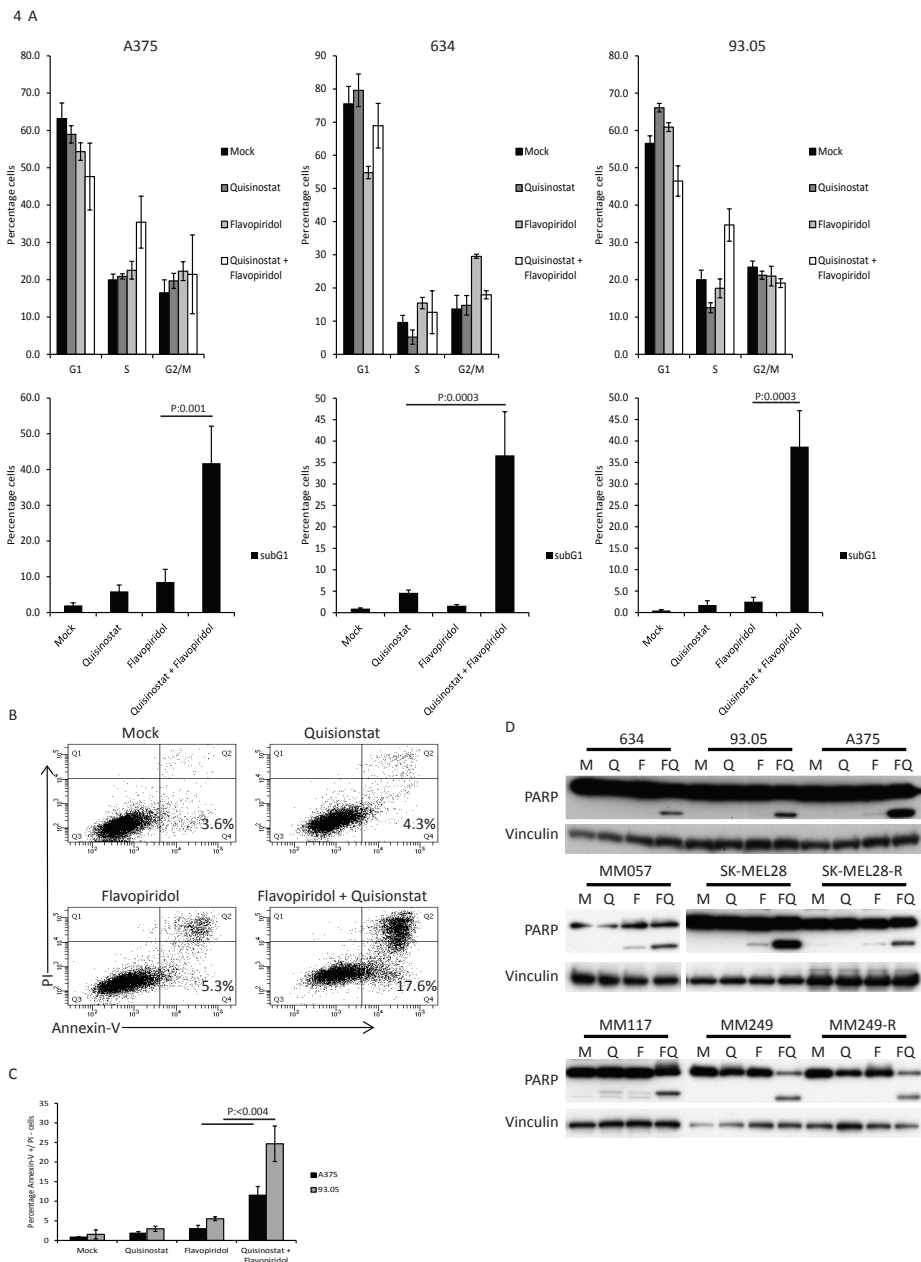


Figure 4. The combination of quisinstat and flavopiridol induces apoptosis in CM cell lines. A. A375, 634 and 93.05 were treated with 20 nM quisinstat and 100 nM flavopiridol for 48 hours after which cells were harvested to determine the cell cycle profiles by flow cytometry upon PI staining. The shown percentages of each cell cycle phase (G1, S, G2/M and subG1) are the averages of three independent experiments. **B.** CM cell lines 93.05, A375, 634 (20 nM Quisinstat and

100 nM Flavopiridol), MM57, SK-MEL28, SK-MEL28-R (20 nM Quisinostat and 150 nM Flavopiridol), MM117, M249 and M249-R (40 nM Quisinostat and 200 nM Flavopiridol) were treated with indicated concentration of drugs for 24 hours. Protein lysates were analyzed by Western blotting to investigate PARP cleavage. Expression of vinculin was analyzed to control for equal loading. C. The percentage of early apoptotic cells was assessed using Annexin V and PI staining, of which a representative experiment is shown using 93.05 cells. D. PI-negative and Annexin V-positive cells were considered to be early apoptotic. Percentages shown are averages of three independent experiments.

resistant cell lines showed synergistic or additive CI values upon concurrent treatment with flavopiridol and quisinostat (Supplementary Figure S4).

Concurrent CDK and HDAC inhibition results in cell cycle arrest and apoptosis in CM cells.

To study the mechanism underlying the synergistic growth inhibitory effect observed in response to concurrent inhibition of CDK and HDAC we determined the consequences of quisinostat and flavopiridol exposure on the cell cycle progression of CM cell lines 93.05, 634 and A375 (Figure 4A). Quisinostat induced a minor G1 arrest in 93.05 cells, slightly reduced S-phase in 634 but did not affect A375 cells. Flavopiridol treatment induced a G2/M arrest in 634, but no clear effect in A375 and 93.05. These results show again that different cell lines show distinct responses to quisinostat or flavopiridol treatment. Interestingly, combining both drugs increased the subG1 population in all three cell lines, indicating enhanced cell death (Figure 4A). To study whether this is, at least partly, a consequence of induction of apoptosis, 93.05 and A375 cells were stained with Annexin V-FITC and Propidium Iodide (PI) upon treatment and analyzed by flow cytometry. The results showed that the 'early' apoptotic fraction (Annexin V-positive, PI-negative) was increased when quisinostat and flavopiridol were combined (Figure 4B and C). To study whether this induction of apoptosis is observed in all different CM cell lines upon combined treatment, PARP cleavage was investigated by immunoblotting. A marked increase in cleaved PARP was evidenced in all cell lines upon quisinostat/flavopiridol exposure (Figure 4D). Given that these cell lines carry different driver mutations, these data show that the induction of apoptosis in response to this combination is independent on the BRAF or NRAS mutational status.

Concurrent CDK and HDAC inhibition results in growth inhibition *in vivo*.

To assess the potential clinical relevance of the quisinostat/flavopiridol combination, we tested its efficacy *in vivo* using a PDX preclinical mouse model of melanoma (MEL002). We used a BRAF wild type cutaneous melanoma tumor as a model as patients with this type of melanoma generally have limited therapeutic options. Once

tumors reached a size of 200mm², drug injections were given intraperitoneally every other day for 28 days. After 28 days, treatment with flavopiridol alone had significantly reduced tumor growth (Figure 5A and Supplementary Figure S5). Quisinstat monotherapy resulted in stable disease. The combined flavopiridol and quisinstat treatment resulted in a decrease in tumor volume significant greater than observed with flavopiridol monotherapy. 3/6 tumors from the combined treatment group showed a slight tumor regression (0.3, 0.2 and 0.2 fold) compared to day 0 (Figure 5A). In agreement with the reduced tumor volume, IHC staining for proliferation marker Ki-67 showed significantly reduced cell proliferation upon quisinstat treatment (Figure 5B and C). In flavopiridol treated tumors, either alone or in combination with quisinstat, a strong variation in numbers of Ki-67 positive cells between tumors was observed (Figure 5C), possibly indicating that the tumor growth inhibition is the result of a complex mix of arrests at distinct cell cycle phases.

To evaluate whether quisinstat and flavopiridol affected their respective targets *in vivo* the levels of acetylated histone 3, c-Myc and phosphorylated RNA pol2 CTD were assessed (Figure 5D). We could detect an increase in acetylated histone 3 upon quisinstat treatment, demonstrating the efficacy of quisinstat *in vivo*. Although flavopiridol treatment *in vivo* did not affect RNA pol2-Ser2 phosphorylation or c-Myc protein levels, combination-treated tumors tended to have higher levels of acetylated histone 3, a trend also visible in most *in vitro* treated CM cell lines. Complete histopathological examination of two mice per treatment group showed minimal and moderate toxicity upon treatment (Supplementary Figure S6). Most severe adverse effect found was necrosis of the lymph nodes induced by flavopiridol, which has been described before [31]. Importantly, when these two broad spectrum drugs were combined no increase in severity of the adverse events was found. Suggesting these drugs can be combined in order to enhance clinical benefits, without enhancing adverse effects.

Discussion

Despite recent advancements in the clinic, both metastasized uveal and cutaneous melanomas remain difficult to cure. For CM, advances have been made with respect to the optimization of mutated BRAF-targeting therapies [4], with or without MEK inhibitors, and immunotherapy has made it in some cases to first-line treatment [5]. Even so, a large proportion of CM patients does not respond to these therapies or eventually develop resistance. For metastasized UM no effective treatment is available in the clinic [32, 33].

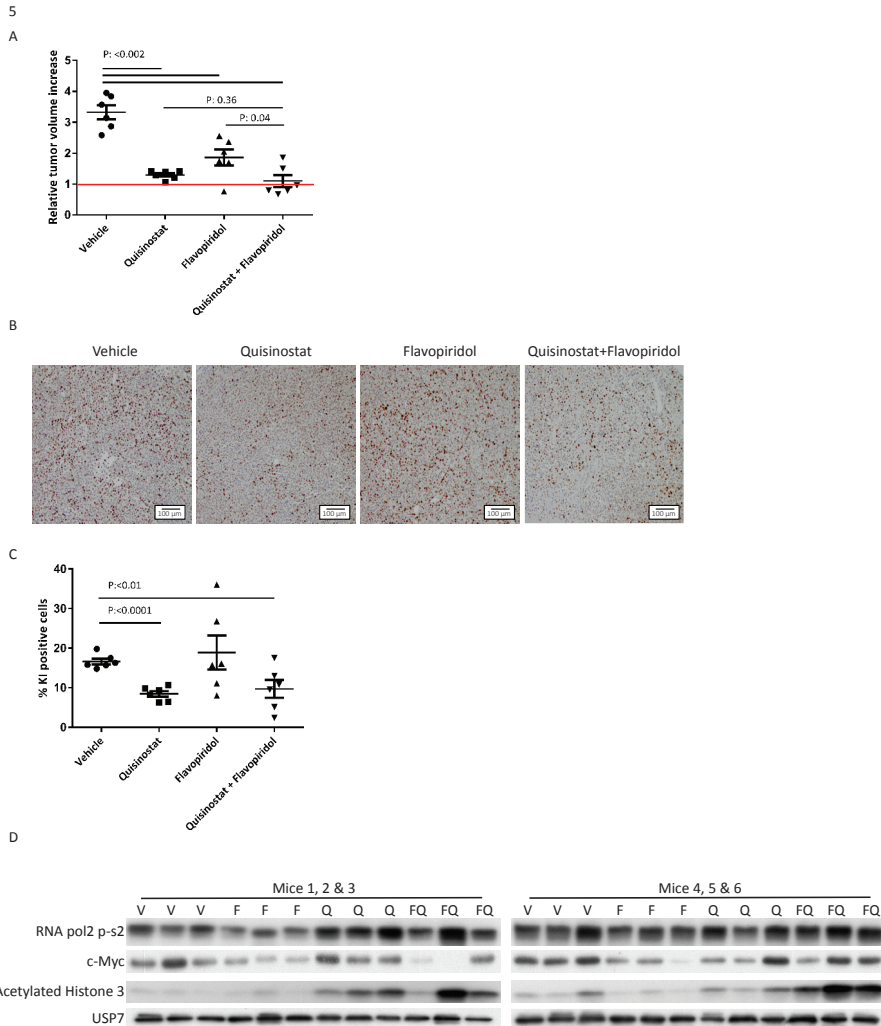


Figure 5. Growth inhibitory and molecular effects of HDAC and CDK inhibition on cutaneous melanoma MEL002 PDX model. A. Animals were transplanted with pieces from a patient biopsy. When tumors reached 200mm³ mice were injected intraperitoneally with vehicle, flavopiridol (5 mg/kg), quisinostat (20 mg/kg) or the combination of flavopiridol and quisinostat. Relative tumor increase of the vehicle treated group was on average 3.3-fold, whereas treatment with flavopiridol (5 mg/kg) or quisinostat (20 mg/kg) as single agent resulted in an average tumor increase of 1.9- and 1.3-fold, respectively. Combined therapy resulted in an average tumor increase of 1.1 fold. Out of the six tumors treated with the combination of compounds, three show regression compared to day 0 with a tumor growth of 0.7, 0.8 and 0.8 fold. B. Ki-67 staining was performed to determine the percentage of proliferating cells; representative pictures are shown in. C. Quantification of Ki-67 staining was performed with ImmunoRatio software. D. Protein lysates were analyzed by Western blotting to investigate levels of RNA pol2-CTD Ser2 phosphorylation, c-Myc and acetylated histone 3. Expression of USP7 was analyzed to control for equal loading.

To find a novel general therapeutic intervention for most, if not all, melanoma patients, we focused on compounds targeting pathways broadly deregulated in most cancer cells. This study focusses on the HDAC inhibitor quisinostat and the CDK inhibitor flavopiridol, both currently in clinical trials for various types of cancer. This implicates that promising pre-clinical results with these compounds can be implemented in the clinic relatively quickly, as toxicity of both single agents has already been assessed.

Our results show that, in agreement with previous studies, both the HDAC inhibitor quisinostat and the CDK inhibitor flavopiridol exert their respective anticancer functions independent of the type of driver mutations [16, 17, 28, 30, 34]. Quisinostat induces a G1 cell cycle arrest in tested UM cell lines, consistent with previous published results from Landreville *et al.* [12]. Despite the ability of quisinostat to inhibit HDACs in both CM and UM cell lines, our results suggest that CM and UM cell lines respond partly distinct to this compound. Whereas 80% (4/5) of tested UM cell lines show a G1 cell cycle arrest, only 1 out of 3 CM cell lines (BRAF mutant) tested showed only a modest increase (10%) in the G1 population. Differences in response to quisinostat can be attributed to potential differences in expression of various HDACs or variation in other effector protein expression. Regardless of the differences in mechanism of action of quisinostat between these different cell lines, it appears that all cell lines are growth inhibited by quisinostat with IC50s in the low nanomolar range.

According to previous studies the anticancer effects of flavopiridol are even more widespread, due to its ability to inhibit multiple CDK's, hampering both transcription (by inhibition of CDK9, CDK12 and CDK7) and the cell cycle, at multiple phases (via the inhibition of CDK1, CDK1, CDK4 and CDK6) [27, 29, 30, 34]. Apart from these well described targets, it has been reported recently that flavopiridol inhibits glycogen phosphorylase, reducing the available glucose for glycolysis of cancer cells [35]. Succeeding this report, it has been demonstrated that flavopiridol reduces various components of the glycolytic pathway in glioblastoma cell lines, limiting glycolysis, which could be a new perspective to flavopiridol [36]. Despite these broad ranges of molecular effects by flavopiridol, the drug is well tolerated in patients while inducing tumor regression [37]. Regardless of these wide-spread effects, nearly all melanoma cell lines responded similar to flavopiridol treatment at a molecular level, i.e. the reduction of RNA pol2 CTD Ser2 phosphorylation and the increase in c-Myc protein levels. The increase in c-Myc was mediated by enhanced gene transcription, rather than post transcriptional regulation, which is associated with low concentrations of flavopiridol [29]. In combination with quisinostat, these low flavopiridol concentrations have synergistic effects via the induction of apoptosis, potentially reducing adverse effects. Although the underlying mechanism of the induction of apoptosis remains

elusive it could be hypothesized that both drugs influence each other in a positive manner; for example, the observed further reduction of RNA pol2 CTD phosphorylation in the presence of quisinostat. Based upon literature showing that both CDK9 and HDAC inhibition decrease expression of the anti-apoptotic protein MCL-1 and thereby stimulate apoptosis [18, 38-43] one could propose that the combination treatment further reduces MCL-1 levels. It must be noted that concentrations of flavopiridol used to achieve these effects on MCL-1 expression tend to be in the micromolar range whereas in this study cells were exposed to flavopiridol in a nanomolar range. Probably therefore we could not detect consistent changes in MCL-1 levels using our experimental design (data not shown). However, it could be that MCL-1 will play an important role when high concentrations are used in a more (pre-) clinical setting. Similarly, expression levels of other Bcl-2 family members reported to be affected by quisinostat and/or flavopiridol were not significantly or consistently affected under our experimental settings.

In our study combined flavopiridol and quisinostat treatment significantly reduced tumor growth in a cutaneous melanoma PDX model. Quisinostat increased the level of acetylated histone 3 concomitant with a strongly reduced tumor cell proliferation. Strikingly, in the tumors treated with flavopiridol, either alone or in combination with quisinostat, the number of Ki-67 positive cells is highly variable, possibly indicating that the growth retardation induced by flavopiridol is a complex mixture of arrests at various cell cycle phases as discussed above. At a molecular level we could not confirm activity of flavopiridol in the treated tumors, although dose and regimen was comparable to previous studies [44, 45]. This could implicate that the molecular effects of flavopiridol are more transiently *in vivo* compared to *in vitro*, possibly caused by clearance of flavopiridol from the body, which only takes hours in humans [46]. Treatment with flavopiridol did inhibit the tumor growth and resulted in tumor regression in 50% of the mice treated with both quisinostat and flavopiridol. Interestingly, these beneficial effects could be achieved without enhancing adverse effects induced by these two broad spectrum drugs. In order to achieve similar synergistic effects *in vivo* compared to *in vitro*, our data suggest that a different treatment regime and/or dosage of flavopiridol should be used. Based on the results presented in this study it could be hypothesized that increasing the effect of flavopiridol could potentially synergistically enhance the effects of quisinostat, possibly resulting in tumor regression *in vivo*.

In conclusion, our data show that the combination of quisinostat and flavopiridol treatment inhibits melanoma cell viability synergistically by inducing apoptosis, independent of driver mutations and acquired BRAF inhibitor resistance. Simultane-

ous HDAC and CDK inhibition could be a potential therapeutic intervention for those melanoma patients that have relapsed on BRAFi treatment, since BRAFi-sensitive and BRAFi-resistant cell lines respond equally effective to this combination of compounds. It seems unlikely that one mutation or epigenetic change is able to induce resistance to this combination, since quisinostat and flavopiridol inhibits multiple HDACs and CDKs. Therefore, we propose this novel therapeutic intervention as treatment option for patients with metastasized UM. Moreover, combined quisinostat/flavopiridol treatment could be used as first-line treatment in CM patients that have a BRAF wild type tumor. Lastly, since the combination treatment has shown promising results in BRAF inhibitor-resistant cells, also relapsed patients under BRAF inhibitor treatment could benefit from our optimized combinatorial treatment regimen. This treatment could be implemented in the clinic rather easily since both quisinostat and flavopiridol are already in clinical trials.

Conflict of Interest

The authors declare no conflict of interest.

Acknowledgements

The authors like to thank Dr. Bruce Ksander, Dr. Martine Jager, Dr. Gré Luyten, Dr. Sergio Roman-Roman and Dr. Fariba Nemati for providing the uveal melanoma cell lines. We thank Dr. Sjoerd van de Burg and Dr. Els Verdegaal for providing the cutaneous melanoma cell lines 634 and 93.05. We thank Dr. Alfred Vertegaal for donating the c-Myc antibody. Johnson & Johnson kindly provided the Quisinostat. We thank O. Van Goethem for her excellent technical assistance with the *in vivo* work.

This work was supported in part by a grant from the Dutch Cancer Society (UL-2013-5757).

References

1. Society AAC. (2016). Cancer Fact & Figures 2016.
2. Chang AE, Karnell LH, Menck HR. The National Cancer Data Base report on cutaneous and noncutaneous melanoma: a summary of 84,836 cases from the past decade. The American College of Surgeons Commission on Cancer and the American Cancer Society. *Cancer*. 1998; 83: 1664-78. doi:
3. Cancer Genome Atlas N. Genomic Classification of Cutaneous Melanoma. *Cell*. 2015; 161: 1681-96. doi: 10.1016/j.cell.2015.05.044.
4. Chapman PB, Hauschild A, Robert C, Haanen JB, Ascierto P, Larkin J, Dummer R, Garbe C, Testori A, Maio M, Hogg D, Lorigan P, Lebbe C, et al. Improved survival with vemurafenib in melanoma with BRAF V600E mutation. *N Engl J Med*. 2011; 364: 2507-16. doi: 10.1056/NEJMoa1103782.
5. Franklin C, Livingstone E, Roesch A, Schilling B, Schadendorf D. Immunotherapy in melanoma: Recent advances and future directions. *Eur J Surg Oncol*. 2017; 43: 604-11. doi: 10.1016/j.ejso.2016.07.145.
6. Van Raamsdonk CD, Bezrookove V, Green G, Bauer J, Gaugler L, O'Brien JM, Simpson EM, Barsh GS, Bastian BC. Frequent somatic mutations of GNAQ in uveal melanoma and blue naevi. *Nature*. 2009; 457: 599-602. doi: 10.1038/nature07586.
7. Van Raamsdonk CD, Griewank KG, Crosby MB, Garrido MC, Vemula S, Wiesner T, Obenauf AC, Wackernagel W, Green G, Bouvier N, Sozen MM, Baimukanova G, Roy R, et al. Mutations in GNA11 in uveal melanoma. *N Engl J Med*. 2010; 363: 2191-9. doi: 10.1056/NEJMoa1000584.
8. Chen X, Wu Q, Tan L, Porter D, Jager MJ, Emery C, Bastian BC. Combined PKC and MEK inhibition in uveal melanoma with GNAQ and GNA11 mutations. *Oncogene*. 2014; 33: 4724-34. doi: 10.1038/onc.2013.418.
9. Wu X, Li J, Zhu M, Fletcher JA, Hodi FS. Protein kinase C inhibitor AEB071 targets ocular melanoma harboring GNAQ mutations via effects on the PKC/Erk1/2 and PKC/NF-kappaB pathways. *Mol Cancer Ther*. 2012; 11: 1905-14. doi: 10.1158/1535-7163.MCT-12-0121.
10. Wu X, Zhu M, Fletcher JA, Giobbie-Hurder A, Hodi FS. The protein kinase C inhibitor enzastaurin exhibits antitumor activity against uveal melanoma. *PLoS One*. 2012; 7: e29622. doi: 10.1371/journal.pone.0029622.
11. Piperno-Neumann S, Kapiteijn E, Larkin J, Carvajal RD, Luke JJ, Seifert H, Roozen I, Zoubir M, Yang L, Choudhury S, Yerramilli-Rao P, Hodi FS, Schwartz GK. (2014). Phase I dose-escalation study of the protein kinase C (PKC) inhibitor AEB071 in patients with metastatic uveal melanoma. ASCO annual meeting 2014: J. Clin. Oncol (abstr 9030).
12. Landreville S, Agapova OA, Matattal KA, Kneass ZT, Onken MD, Lee RS, Bowcock AM, Harbour JW. Histone deacetylase inhibitors induce growth arrest and differentiation in uveal melanoma. *Clin Cancer Res*. 2012; 18: 408-16. doi: 10.1158/1078-0432.CCR-11-0946.
13. Child F, Ortiz-Romero PL, Alvarez R, Bagot M, Stadler R, Weichenthal M, Alves R, Quagliano P, Beylot-Barry M, Cowan R, Geskin LJ, Perez-Ferriols A, Hellems P, et al. Phase II multicentre trial of oral quisinostat, a histone deacetylase inhibitor, in patients with previously treated stage IB-IVA mycosis fungoides/Sezary syndrome. *Br J Dermatol*. 2016; 175: 80-8. doi: 10.1111/bjd.14427.
14. van der Ent W, Burrello C, Teunisse AF, Ksander BR, van der Velden PA, Jager MJ, Jochemsen AG, Snaar-Jagalska BE. Modeling of human uveal melanoma in zebrafish xenograft embryos. *Invest Ophthalmol Vis Sci*. 2014; 55: 6612-22. doi: 10.1167/iovs.14-15202.
15. Hornig E, Hept MV, Graf SA, Ruzicka T, Berking C. Inhibition of histone deacetylases in melanoma-a perspective from bench to bedside. *Exp Dermatol*. 2016; 25: 831-8. doi: 10.1111/exd.13089.
16. Arts J, King P, Marien A, Floren W, Belien A, Janssen L, Pilatte I, Roux B, Decrane L, Gilissen R, Hickson I, Vreys V, Cox E, et al. JNJ-26481585, a novel "second-generation" oral histone deacetylase inhibi-

- tor, shows broad-spectrum preclinical antitumoral activity. *Clin Cancer Res.* 2009; 15: 6841-51. doi: 10.1158/1078-0432.CCR-09-0547.
17. Carol H, Gorlick R, Kolb EA, Morton CL, Manesh DM, Keir ST, Reynolds CP, Kang MH, Maris JM, Wozniak A, Hickson I, Lyalin D, Kurmasheva RT, et al. Initial testing (stage 1) of the histone deacetylase inhibitor, quisinostat (JNJ-26481585), by the Pediatric Preclinical Testing Program. *Pediatr Blood Cancer.* 2014; 61: 245-52. doi: 10.1002/pbc.24724.
 18. Stuhmer T, Arts J, Chatterjee M, Borawski J, Wolff A, King P, Einsele H, Leo E, Bargou RC. Preclinical anti-myeloma activity of the novel HDAC-inhibitor JNJ-26481585. *Br J Haematol.* 2010; 149: 529-36. doi: 10.1111/j.1365-2141.2010.08126.x.
 19. Fedyanin M, Tjulandin S, Cheporov S, Vladimirov V, Moiseenko V, Orlov S, Manikhas G, Cakana A, Azarova V, Karavaeva O, Vostokova N, Baranovskiy S. Phase I dose of oral quisinostat, in combination with gemcitabine (G) and cisplatin (Cis) or paclitaxel (P) and carboplatin (Carbo) in patients (pts) with non-small cell lung cancer or ovarian cancer (OC). *Annals of Oncology.* 2016; 27: 387P-P. doi: 10.1093/annonc/mdw368.30.
 20. Venugopal B, Baird R, Kristeleit RS, Plummer R, Cowan R, Stewart A, Fournau N, Hellemans P, Elsayed Y, McClue S, Smit JW, Forslund A, Phelps C, et al. A phase I study of quisinostat (JNJ-26481585), an oral hydroxamate histone deacetylase inhibitor with evidence of target modulation and antitumor activity, in patients with advanced solid tumors. *Clin Cancer Res.* 2013; 19: 4262-72. doi: 10.1158/1078-0432.CCR-13-0312.
 21. Demuth R. (2017). NewVac Reports Primary Endpoint Met in Phase II Clinical Trial of Quisinostat in Combination with Paclitaxel and Carboplatin in Platinum-Resistant Ovarian Cancer. (PR Newswire: PR Newswire).
 22. Alao JP, Stavropoulou AV, Lam EW, Coombes RC, Vigushin DM. Histone deacetylase inhibitor, trichostatin A induces ubiquitin-dependent cyclin D1 degradation in MCF-7 breast cancer cells. *Mol Cancer.* 2006; 5: 8. doi: 10.1186/1476-4598-5-8.
 23. Huang JM, Sheard MA, Ji L, Sposto R, Keshelava N. Combination of vorinostat and flavopiridol is selectively cytotoxic to multidrug-resistant neuroblastoma cell lines with mutant TP53. *Mol Cancer Ther.* 2010; 9: 3289-301. doi: 10.1158/1535-7163.MCT-10-0562.
 24. Senderowicz AM. Small molecule modulators of cyclin-dependent kinases for cancer therapy. *Oncogene.* 2000; 19: 6600-6. doi: 10.1038/sj.onc.1204085.
 25. Kaur G, Stetler-Stevenson M, Sebers S, Worland P, Sedlacek H, Myers C, Czech J, Naik R, Sausville E. Growth inhibition with reversible cell cycle arrest of carcinoma cells by flavone L86-8275. *J Natl Cancer Inst.* 1992; 84: 1736-40. doi:
 26. Chao SH, Fujinaga K, Marion JE, Taube R, Sausville EA, Senderowicz AM, Peterlin BM, Price DH. Flavopiridol inhibits P-TEFb and blocks HIV-1 replication. *J Biol Chem.* 2000; 275: 28345-8. doi: 10.1074/jbc.C000446200.
 27. Bosken CA, Farnung L, Hintermair C, Merzel Schachter M, Vogel-Bachmayr K, Blazek D, Anand K, Fisher RP, Eick D, Geyer M. The structure and substrate specificity of human Cdk12/Cyclin K. *Nat Commun.* 2014; 5: 3505. doi: 10.1038/ncomms4505.
 28. Burdette-Radoux S, Tozer RG, Lohmann RC, Quirt I, Ernst DS, Walsh W, Wainman N, Colevas AD, Eisenhauer EA. Phase II trial of flavopiridol, a cyclin dependent kinase inhibitor, in untreated metastatic malignant melanoma. *Invest New Drugs.* 2004; 22: 315-22. doi: 10.1023/B:DRUG.0000026258.02846.1c.
 29. Garcia-Cuellar MP, Fuller E, Mathner E, Breitingner C, Hetzner K, Zeitlmann L, Borkhardt A, Slany RK. Efficacy of cyclin-dependent-kinase 9 inhibitors in a murine model of mixed-lineage leukemia. *Leukemia.* 2014; 28: 1427-35. doi: 10.1038/leu.2014.40.

30. Carlson BA, Dubay MM, Sausville EA, Brizuela L, Worland PJ. Flavopiridol induces G1 arrest with inhibition of cyclin-dependent kinase (CDK) 2 and CDK4 in human breast carcinoma cells. *Cancer Res.* 1996; 56: 2973-8. doi:
31. Arguello F, Alexander M, Sterry JA, Tudor G, Smith EM, Kalavar NT, Greene JF, Jr., Koss W, Morgan CD, Stinson SF, Siford TJ, Alvord WG, Klabansky RL, et al. Flavopiridol induces apoptosis of normal lymphoid cells, causes immunosuppression, and has potent antitumor activity *In vivo* against human leukemia and lymphoma xenografts. *Blood.* 1998; 91: 2482-90. doi:
32. Kivela T, Eskelin S, Kujala E. Metastatic uveal melanoma. *Int Ophthalmol Clin.* 2006; 46: 133-49. doi:
33. Augsburger JJ, Correa ZM, Shaikh AH. Effectiveness of treatments for metastatic uveal melanoma. *Am J Ophthalmol.* 2009; 148: 119-27. doi: 10.1016/j.ajo.2009.01.023.
34. Carlson B, Lahusen T, Singh S, Loaiza-Perez A, Worland PJ, Pestell R, Albanese C, Sausville EA, Senderowicz AM. Down-regulation of cyclin D1 by transcriptional repression in MCF-7 human breast carcinoma cells induced by flavopiridol. *Cancer Res.* 1999; 59: 4634-41. doi:
35. Oikonomakos NG, Schnier JB, Zographos SE, Skamnaki VT, Tsitsanou KE, Johnson LN. Flavopiridol inhibits glycogen phosphorylase by binding at the inhibitor site. *J Biol Chem.* 2000; 275: 34566-73. doi: 10.1074/jbc.M004485200.
36. Cimini A, d'Angelo M, Benedetti E, D'Angelo B, Laurenti G, Antonosante A, Cristiano L, Di Mambro A, Barbarino M, Castelli V, Cinque B, Cifone MG, Ippoliti R, et al. Flavopiridol: An Old Drug With New Perspectives? Implication for Development of New Drugs. *J Cell Physiol.* 2017; 232: 312-22. doi: 10.1002/jcp.25421.
37. Awan FT, Jones JA, Maddocks K, Poi M, Grever MR, Johnson A, Byrd JC, Andritsos LA. A phase 1 clinical trial of flavopiridol consolidation in chronic lymphocytic leukemia patients following chemoimmunotherapy. *Ann Hematol.* 2016; 95: 1137-43. doi: 10.1007/s00277-016-2683-1.
38. Yeh YY, Chen R, Hessler J, Mahoney E, Lehman AM, Heerema NA, Grever MR, Plunkett W, Byrd JC, Johnson AJ. Up-regulation of CDK9 kinase activity and Mcl-1 stability contributes to the acquired resistance to cyclin-dependent kinase inhibitors in leukemia. *Oncotarget.* 2015; 6: 2667-79. doi: 10.18632/oncotarget.2096.
39. Gojo I, Zhang B, Fenton RG. The cyclin-dependent kinase inhibitor flavopiridol induces apoptosis in multiple myeloma cells through transcriptional repression and down-regulation of Mcl-1. *Clin Cancer Res.* 2002; 8: 3527-38. doi:
40. Ma Y, Cress WD, Haura EB. Flavopiridol-induced apoptosis is mediated through up-regulation of E2F1 and repression of Mcl-1. *Mol Cancer Ther.* 2003; 2: 73-81. doi:
41. Rahmani M, Aust MM, Benson EC, Wallace L, Friedberg J, Grant S. PI3K/mTOR inhibition markedly potentiates HDAC inhibitor activity in NHL cells through BIM- and MCL-1-dependent mechanisms *in vitro* and *in vivo*. *Clin Cancer Res.* 2014; 20: 4849-60. doi: 10.1158/1078-0432.CCR-14-0034.
42. Khan DH, Gonzalez C, Cooper C, Sun JM, Chen HY, Healy S, Xu W, Smith KT, Workman JL, Leygue E, Davie JR. RNA-dependent dynamic histone acetylation regulates MCL1 alternative splicing. *Nucleic Acids Res.* 2014; 42: 1656-70. doi: 10.1093/nar/gkt1134.
43. Chen S, Dai Y, Pei XY, Grant S. Bim upregulation by histone deacetylase inhibitors mediates interactions with the Bcl-2 antagonist ABT-737: evidence for distinct roles for Bcl-2, Bcl-xL, and Mcl-1. *Mol Cell Biol.* 2009; 29: 6149-69. doi: 10.1128/MCB.01481-08.
44. Kwak MS, Yu SJ, Yoon JH, Lee SH, Lee SM, Lee JH, Kim YJ, Lee HS, Kim CY. Synergistic anti-tumor efficacy of doxorubicin and flavopiridol in an *in vivo* hepatocellular carcinoma model. *J Cancer Res Clin Oncol.* 2015; 141: 2037-45. doi: 10.1007/s00432-015-1990-6.

45. Yang G, Sun H, Kong Y, Hou G, Han J. Diversity of RGD radiotracers in monitoring antiangiogenesis of flavopiridol and paclitaxel in ovarian cancer xenograft-bearing mice. *Nucl Med Biol.* 2014; 41: 856-62. doi: 10.1016/j.nucmedbio.2014.08.008.
46. Dickson MA, Rathkopf DE, Carvajal RD, Grant S, Roberts JD, Reid JM, Ames MM, McGovern RM, Lefkowitz RA, Gonen M, Cane LM, Dials HJ, Schwartz GK. A phase I pharmacokinetic study of pulse-dose vorinostat with flavopiridol in solid tumors. *Invest New Drugs.* 2011; 29: 1004-12. doi: 10.1007/s10637-010-9447-x.
47. Amirouchene-Angelozzi N, Nemati F, Gentien D, Nicolas A, Dumont A, Carita G, Camonis J, Desjardins L, Cassoux N, Piperno-Neumann S, Mariani P, Sastre X, Decaudin D, et al. Establishment of novel cell lines recapitulating the genetic landscape of uveal melanoma and preclinical validation of mTOR as a therapeutic target. *Mol Oncol.* 2014; 8: 1508-20. doi: 10.1016/j.molonc.2014.06.004.
48. Dewaele M, Tabaglio T, Willekens K, Bezzi M, Teo SX, Low DH, Koh CM, Rambow F, Fiers M, Rogiers A, Radaelli E, Al-Haddawi M, Tan SY, et al. Antisense oligonucleotide-mediated MDM4 exon 6 skipping impairs tumor growth. *J Clin Invest.* 2016; 126: 68-84. doi: 10.1172/JCI82534.
49. Hawinkels LJ, Verspaget HW, van Duijn W, van der Zon JM, Zuidwijk K, Kubben FJ, Verheijen JH, Hommes DW, Lamers CB, Sier CF. Tissue level, activation and cellular localisation of TGF-beta1 and association with survival in gastric cancer patients. *Br J Cancer.* 2007; 97: 398-404. doi: 10.1038/sj.bjc.6603877.
50. Tuominen VJ, Ruotoistenmaki S, Viitanen A, Jumppanen M, Isola J. ImmunoRatio: a publicly available web application for quantitative image analysis of estrogen receptor (ER), progesterone receptor (PR), and Ki-67. *Breast Cancer Res.* 2010; 12: R56. doi: 10.1186/bcr2615.

Methods

Cell culture

The UM cell lines MEL270, MEL202, OMM2.3 and OMM1 were cultured in a mixture of RPMI and DMEM-F12 (1:1 ratio), supplemented with 10% fetal calf serum (FCS) and antibiotics. OMM1 was provided by Gré Luyten (LUMC, Leiden, The Netherlands) and MEL270, MEL202, OMM2.3 were a kind gift of Bruce Ksander (Schepens Eye Research Institute, Boston, MA, USA). Establishment of the UM cell line MM66 has been described [47], was kindly provided by Sergio Roman-Roman (Curie Institute, Paris, France) and were cultured in IMDM containing 20% FCS and antibiotics. The CM cell lines A375, 634 and 93.05 were cultured in DMEM/high glucose supplemented with 10% FCS and antibiotics. M117 and M057 CM cell lines were cultured in DMEM-F10 with 8% FCS. SK-MEL28 was maintained in RPMI plus 10% FCS plus antibiotics. DMEM/high glucose containing 5% FCS/antibiotics was used to maintain the M249 CM cells. Medium for the BRAF inhibition resistant derivatives of SK-MEL28 and M249 was supplemented with 1 μ M PLX-4032 (Selleck Chemicals, Houston, TX, USA). All cell lines were cultured for no more than 20 passages after thawing and were checked regularly for mycoplasma.

Western blot analysis

Cells were rinsed twice with ice-cold PBS and lysed in Giordano buffer (50 mM Tris-HCl pH7.4, 250 mM NaCl, 0.1% Triton X-100 and 5 mM EDTA; supplemented with phosphatase- and protease inhibitors). Equal protein amounts were separated using SDS-PAGE and blotted onto polyvinylidene fluoride transfer membranes (Millipore, Darmstadt, Germany). After blocking the membranes in TBST (10 mM Tris-HCl pH8.0, 150 mM NaCl, 0.2% Tween 20) containing 10% milk, membranes were incubated with the proper primary antibodies (listed in Table 1) and appropriate HRP-conjugated secondary antibodies (Jackson Laboratories, Bar Harbor, ME, USA). Bands were visualized using chemoluminescence and visualized by exposure to X-ray film.

Cell growth and viability assays and calculation of synergism

Cells were seeded in triplicate, in 96-well format and incubated for 72 hours. Cell survival was determined via the CellTitre-Blue Cell Viability assay (Promega, Fitchburg, WI, USA); the fluorescence was measured in a microplate reader (Victor, Perkin Elmer, San Jose, CA, USA). Synergism between flavopiridol and quisinostat was calculated using Compusyn software (Paramus, NJ, USA). Combination Index (CI) values below 0.9 were considered to be synergistic, between 0.9 and 1.1 additive effects and above 1.1 to be antagonistic. Flavopiridol was obtained from Selleck Chemicals (Houston, TX, USA) and Quisinostat was kindly provided by Johnson & Johnson.

Flow cytometry

For cell cycle analysis the cells were harvested by trypsinization, washed twice in PBS and fixed in ice cold 70% ethanol. After fixation, cells were washed in PBS containing 2% FCS and resuspended in PBS containing 2% FCS, 50 µg/ml RNase and 50 µg/ml propidium iodide (PI). Flow cytometry analysis was performed using the BD LSR II system (BD Biosciences, San Diego, CA, USA). To determine presence of apoptotic cells by Annexin V staining, cells were harvested and washed twice in PBS, resuspended in Annexin V-binding buffer in presence of FITC-labelled Annexin V (Sigma-Aldrich, Saint Louis, MO, USA) and PI, following incubation for 10 minutes at room temperature. Cells staining negative for PI, but positive for Annexin V were considered to be apoptotic. Cells staining positive for both PI and Annexin V were considered to be late apoptotic or necrotic and, therefore, excluded from the analysis.

RNA isolation, cDNA synthesis and real-time quantitative PCR

RNA was isolated using the SV total RNA isolation kit (Promega), after which cDNA was synthesized using the reverse transcriptase reaction mixture as indicated by Promega. qPCR was performed using SYBR green mix (Roche Diagnostics, Indianapolis, IN, USA) in a C1000 touch Thermal Cycler (Bio-Rad laboratories, Hercules, CA, USA). In three independent experiments relative expression of c-Myc (fw: GCCACGTCTC-CACACATCAG, rev: TGGTGCATTTTCGGTTGTTG), compared to housekeeping genes CAPNS1 (fw: ATGGTTTTGGCATTGACACATG, rev: GCTTGCCTGTGGTGTCGC) and SRPR (fw: CATTGCTTTTGCACGTAACCAA, rev: ATTGTCTTGCATGCGCC) was determined. Average relative expression per experiment was compared to the untreated set at 1.

Patient derived xenograft mouse model

Tumor pieces of cutaneous melanoma tumor model MEL002 (BRAF wild type) were transplanted interscapular in NMRI nude mice as described by M. Dewaele *et al.* [48]. When tumor volume reached 200mm³ 6 animals per group were treated intraperitoneally, with either vehicle, quisinostat (20mg/kg), flavopiridol (5mg/kg) or the combination every other day for 28 days. Bodyweight was measured to monitor the animals. During the treatment tumor volume was assessed every other day using a caliper and calculated (tumor volume mm³= (width² x length)/2). At the end of the experiment all animals were sacrificed and tumors were removed, general necropsy was performed on 2 mice per group. Immunohistochemical (IHC) staining to assess tumor cell proliferation were performed as described by Hawinkels *et al.* [49] using primary antibody Ki-67 1:500 diluted (AB9260, Millipore). Three to five representative pictures were taken per tumor of which an average percentage of Ki-67 positive cells was determined per tumor using the ImmunoRatio web application as described by Tuominen *et al.* [50]. Tumor pieces were lysed using the TissueLyser LT (Quiagen,

Hilden, Germany) according to manufacturer's protocol in RIPA lysis buffer (150 mM NaCl, 1% NP-40, 0.25% deoxycholate, 0.1% SDS, 50 mM Tris-HCl pH 8.0, 2 mM EDTA; supplemented with phosphatase- and protease inhibitors) followed by western blot analysis, as described above.

Statistical analysis

Differences between two groups were calculated using Student's t-test. To determine the difference in tumor growth over time between groups in the PDX model a two way ANOVA was used. P-values of ≤ 0.05 were considered to be significant.

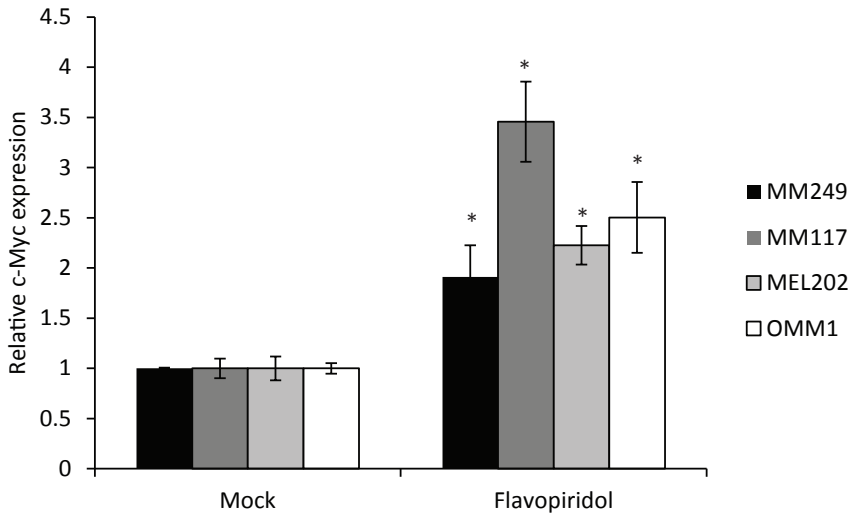
Table 1. List of antibodies used for Western blot.

Protein	Name/Cat#	Company
Vinculin	hVIN-1/ V9131	Sigma-Aldrich
PARP	9542	Cell Signaling Technology
RNA pol2 p-S2	AB5095	Abcam
c-Myc	AB32072	Abcam
Acetylated histone 3	31994	Millipore

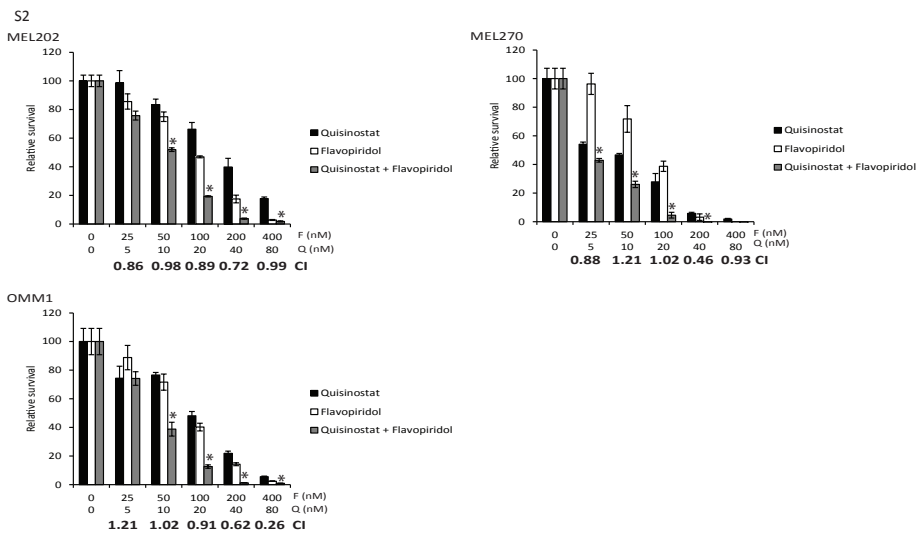
Table 2. IC50's for quisinostat and flavopiridol per cell line.

cell line	Quisinostat		Flavopiridol	
	IC50 nM	stdev	IC50 nM	stdev
MEL270	5.9	1.8	82.7	14.4
MEL202	24.8	6.4	68.4	10.3
OMM2.3	16.4	1.9	91.3	14.2
OMM1	18.6	2.8	71.3	3.1
MM66	93.0	21.7	99.8	19.3
634	14.8	2.7	133.6	21.0
93.05	36.2	7.3	66.8	7.0
A375	20.8	8.7	65.9	4.5
MM249	23.8	2.0	143.9	6.3
MM249R	17.5	3.1	128.6	24.5
SK-MEL28	30.7	4.4	113.1	6.1
SK-MEL28-R	28.4	6.2	92.6	10.5
MM117	14.8	1.5	178.2	17.8
MM057	66.8	9.5	97.5	18.4

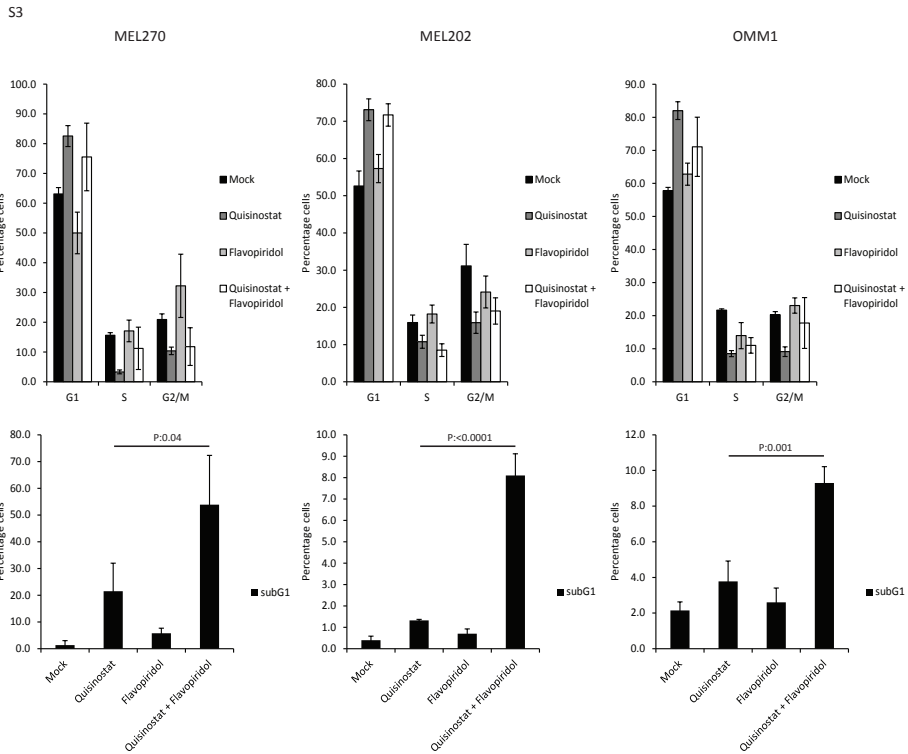
S1



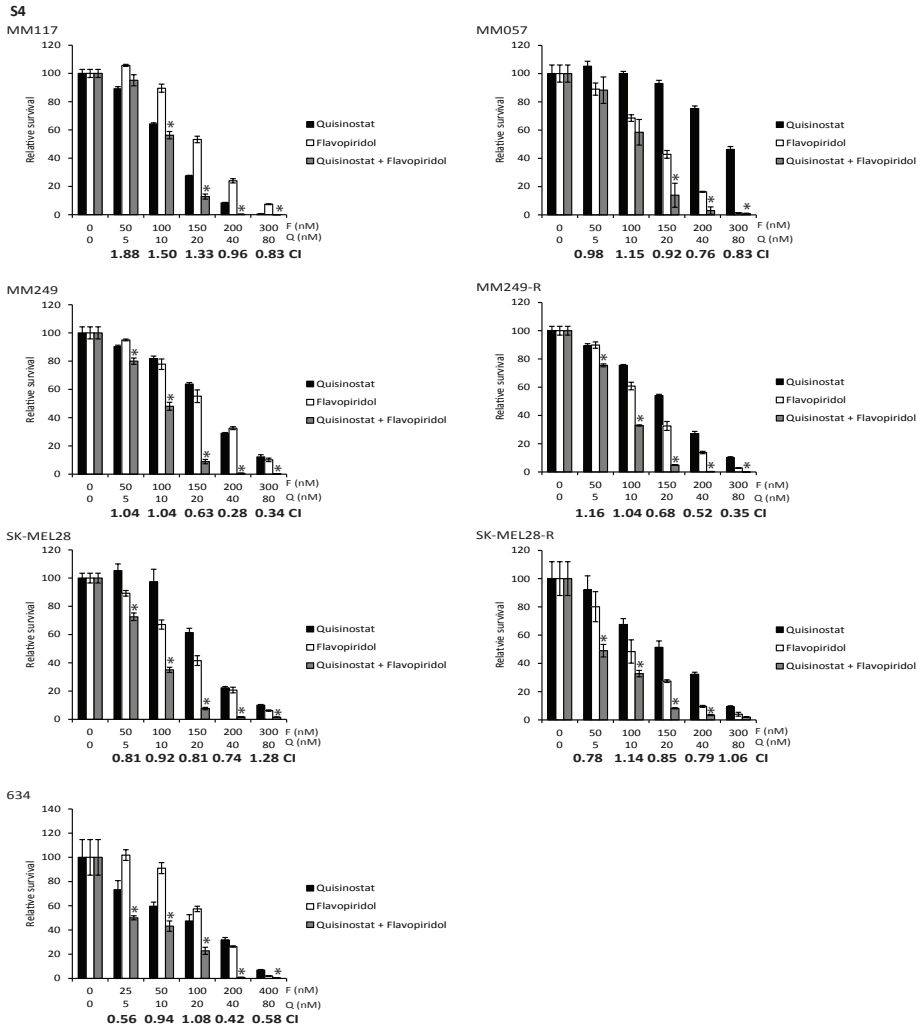
Supplementary Figure S1. Increase in c-Myc mRNA expression upon flavopiridol treatment. CM cells MM249 and MM117 and UM cells MEL202 and OMM1 were treated for 8 hours with flavopiridol (200, 150, 100 and 100nM, respectively). Cells were harvested, RNA isolated, cDNA was synthesized and expression of c-Myc mRNA was determined. Relative expression compared to untreated controls is plotted, when the difference was found to be significant ($p < 0.05$) compared to the control this was indicated with a *.



Supplementary Figure S2. Synergistic growth inhibition of CDK and HDAC inhibition on UM cells. UM cells were treated with the indicated concentrations of flavopiridol and quisinostat, alone or in combination. After 72h the cell viability was determined. To determine the extent of synergism the combination index (CI) was used. Combinations with a significant ($p < 0.05$) lower relative survival compared to both single treatments are indicated with a *.

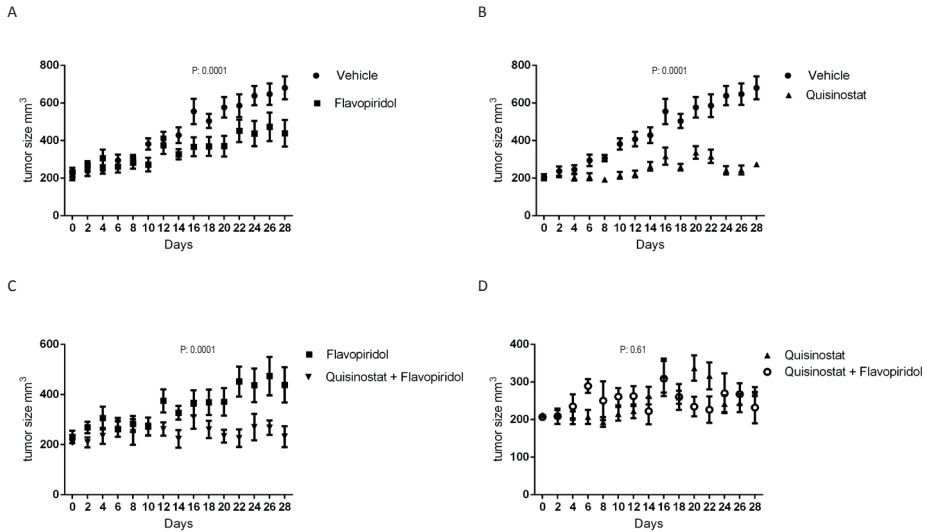


Supplementary Figure S3. Effect of CDK and HDAC inhibition on the cell cycle progression of uveal melanoma cells. MEL270, MEL202 and OMM1 cells were treated for 48 hours with 20 nM quisinostat and 100 nM flavopiridol after which cells were harvested to determine the cell cycle profiles by flow cytometry upon PI staining. The shown percentages of each cell cycle phase (G1, S, G2/M and subG1) are averages of three independent experiments.



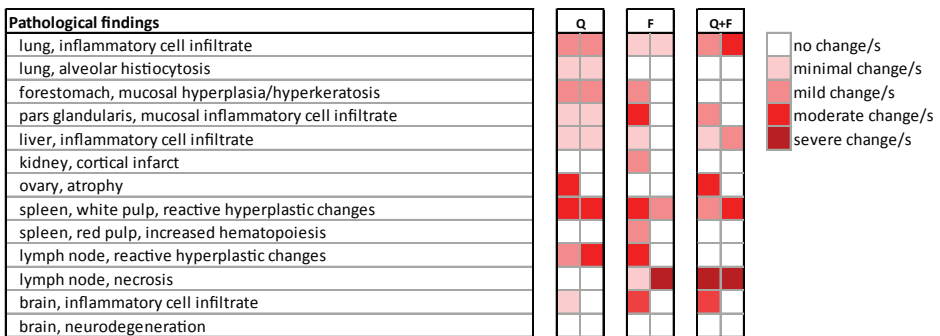
Supplementary Figure S4. Synergistic growth inhibition of CDK and HDAC inhibition on CM cells. CM cells were treated with the indicated concentrations of flavopiridol and quisinostat, alone or in combination. After 72h the cell viability was determined. To determine the extent of synergism the combination index (CI) was used. Combinations with a significant ($p < 0.05$) lower relative survival compared to both single treatments are indicated with a *.

S5



Supplementary Figure S5. Growth inhibitory effect of HDAC and CDK inhibition on MEL002 PDX model in time. Animals were transplanted with tumor pieces. When tumors reached 200 mm³ mice were injected I.P. every other day for 28 days. A. Mice were treated with flavopiridol (5 mg/kg), B. quisinostat (20 mg/kg) or C. Mice treated with flavopiridol compared to combination treated mice. D. Mice treated with quisinostat compared to combination treated mice. Tumor volume was assessed by caliper.

S6



Supplementary Figure S6. Lesion heat map of histopathological examination. Complete histopathological examination was performed on two animals treated with either quisinostat (Q), flavopiridol (F) or both (Q+F).

CHAPTER 6

General discussion

Oncogenic functions of MDMX in uveal melanoma

Malignant cells often highly express MDMX and/or MDM2 as means to dampen p53 activity [1]. MDM2 is an E3 ubiquitin ligase whose activity results in ubiquitin-dependent p53 degradation, while MDMX shields the transactivation domain of p53. However, the oncogenic functions of MDMX are not limited to the inhibition of p53 activity [2, 3]. Chapter 2 reports which genes are transcriptionally controlled by MDMX and to what degree this regulation is p53-dependent. The data presented indicate that MDMX regulates cell cycle progression, at least partially via the p53-p21-DREAM (DP, RB-like, E2F4 and MubB) axis, and apoptosis via p53 and FOXO's. It has been generally accepted for some time now that p53 promotes the expression of p21 and thereby induces transcriptional repression by the DREAM complex [4, 5]. However, to what level this particular indirect p53 activity could be inhibited by MDMX had not yet been studied. The observation that MDMX depletion, which only minimally effects p21 expression, is capable of inducing this transcriptional repression has never been reported before. Although possibly not very surprising, since MDMX is known to inhibit p53 transcriptional activity [6, 7], it further strengthens the proposition that MDMX could serve as alternative therapeutic target, since its inhibition provokes a similar downstream effect as inhibition of MDM2. While having a comparable therapeutic potential as MDM2 inhibition, MDMX is less commonly expressed and not always essential for cell survival in the adult tissue [8-14]. Therefore, it could well be that targeting MDMX has less adverse effects in patients compared to inhibition of MDM2, potentially making it the preferred way of reactivating p53.

In chapter 2 we established that the downregulated cell cycle controlling genes upon MDMX knockdown could indeed be regulated via the p53-p21-DREAM axis. However, the transcriptional repression is, at least partly, p53-independent, suggesting the existence of another transcription factor under the control of MDMX. Not only repressed, but also some of the upregulated genes show clear p53 independency. Although 38% of the upregulated genes were identified as direct p53 target genes the results demonstrate that MXD4 (also named MAD4) and PIK3IP1 expression is controlled by MDMX in a p53-independent manner. The major DNA binding consensus site identified in 65% of the up-regulated genes is the Forkhead-Boxes DNA binding site. Indeed, FOXO1 levels are slightly increased upon MDMX depletion in a p53-independent manner. Inhibition of FOXO1 activity could explain the p53-independent function of MDMX. Mechanistically it remains unsolved as yet how MDMX inhibits FOXO1. It is known that MDM2 is capable of directly binding and ubiquitinating FOXO1, 3 and 4 [15, 16]. Preliminary data show that reduced MDMX expression results in increased nuclear localization of FOXO1 (data not shown). If the inhibition of FOXO1 is the result of a direct interaction with MDMX, the development of specific compounds antago-

nizing this interaction could lead to new therapeutic option for tumors overexpressing MDMX.

Interestingly, MXD4 affects p53 activity potentially suggesting a novel back-up mechanism (see Figure 1). This back-up mechanism would include that upon MDMX depletion MXD4 is upregulated, mediated by FOXO1, and competes with p53 for SIN3A. By forming a complex with SIN3A, which is known to be involved in transcription repression, MXD4 could be part of a potential pathway leading to the p53-independent gene repression mentioned earlier. Interestingly, SIN3A might not only potentially enable p53-independent repression, it can also form a transcription repressive complex which not only includes E2F4 but also p27 [17, 18]. The latter protein was previously described as being stabilized upon MDMX depletion, independently of p53 [2]. Based on these earlier studies and the data described in chapter 2 a larger picture is emerging in which MDMX is controlling a large repressive complex via the regulation of SIN3A and E2F4 and inhibition of MXD4 transcription. Furthermore, releasing p53 from SIN3A allows MDM2 to bind p53 and to target p53 for ubiquitination-mediated degradation [19]. This pathway would imply a p53-independent back-up mechanism

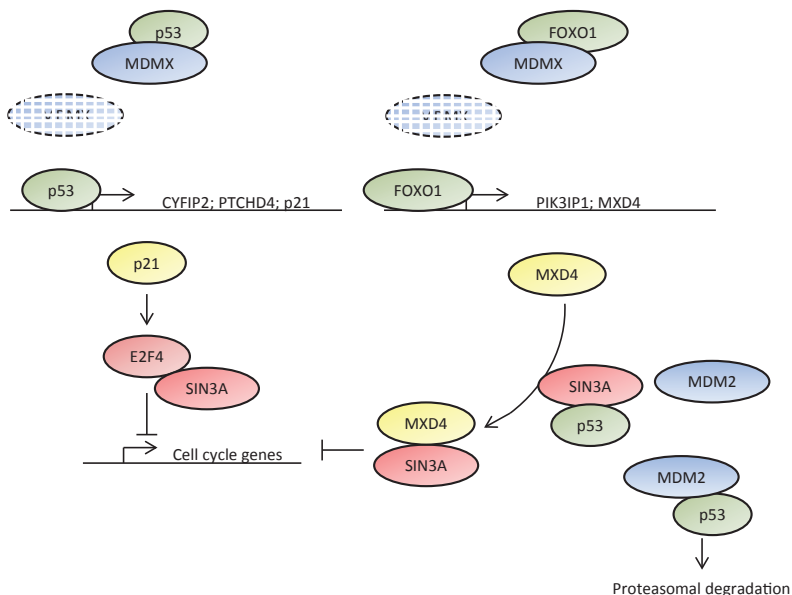


Figure 1. Working model of MDMX's oncogenic functions. In this model MDMX inhibits both p53 and FOXO1 which prevents target gene transcription. Upon MDMX depletion both transcription factors bind DNA and promote transcription resulting in, among other effects, the repression on cell cycle regulatory genes. Simultaneously, FOXO mediated upregulation of MXD4 transcription could prime p53 for MDM2 mediated degradation by competing with p53 for SIN3A binding.

in which a cell with high levels of MDMX rewires towards more MDM2 mediated p53 inhibition once MDMX is depleted. Not only does this SIN3A/MXD4 mediated 'back-up' mechanism clarify the p53-independent transcription repression upon MDMX depletion, it could also provide new therapeutic targets. Depletion of MXD4 resulted in p53 stabilization, possibly due to an increased SIN3A binding attenuating MDM2 binding to p53. MXD4 depletion resulted in a slight, p53-dependent, growth inhibition and it synergized with p53 activating and stabilizing drugs, showing that to fully unleash p53 and further exploit current p53 activating strategies a way to target MXD4 should be elucidated.

In conclusion, the data presented in chapter 2 show that p53-independent oncogenic functions of MDMX could be partially explained by the p53-independent effects on the transcriptome. In addition to a better understanding of the oncogenic functions of MDMX in melanoma, a possible new route to potentiate current anti-cancer strategies in various malignancies was uncovered.

MDMX as enhancer of current therapeutic interventions for metastasised uveal melanoma

The feasibility and clinical advantages of p53 reactivation by MDM2 inhibition have been established [20]. Unfortunately, clinical studies have shown strong adverse, on target, effects in patients upon MDM2 inhibition [21]. Although both MDM2 and MDMX are essential for restraining p53 during embryonic development [22-26], in adult cells and tissue MDM2 loss is always lethal whereas MDMX loss can be compatible with life [8-13]. The lack of general expression of MDMX compared to MDM2 would indicate potentially less adverse effects when targeting an MDMX expressing cancer. The therapeutic potential of MDMX targeting has been established by our lab and others for various cancer types, partly independent of p53 status [2, 3, 27, 28]. It has become evident and generally accepted that using a monotherapy on a cancer will in general not result in a durative and curative response [29]. Therefore, combinations of drugs are tried in more studies in order to hit a cancer cell from multiple angles at the same time, making acquired resistance less likely to occur. Interestingly, in melanoma concurrent targeting of MDMX and BRAF has proven to be an effective combination [3].

In uveal melanoma an activating mutation in GNAQ or GNA11 is the main driver towards malignancy. Constitutive active GNAQ/GNA11 activates a number of signalling pathways, including the proliferation stimulating MAPK pathway. An essential node in this cascade is the activation of protein kinase c (PKC) isoforms, which has been

recognized as a valuable therapeutic target for uveal melanoma, e.g. by means of the PKC inhibitor Sotrastaurin/AEB071 [30].

In chapter 3 it is described that combined p53 activation and PKC inhibition result in synergistic growth inhibition of uveal melanoma cells. In our studies the dual MDM2/X inhibitor Nutlin-3 was used, whereas the MDM2 inhibitor CGM097 was used in another study describing the beneficial effects of combining p53 reactivation with PKC inhibition [31]. Interestingly, in the latter study no synergistic effects upon concurrent PKC inhibition and p53 reactivation could be demonstrated *in vitro*, in contrast to our results, suggesting that full release of p53 from both MDM2 and MDMX is essential for synergism. Depletion of MDMX, like the pharmacological activation of p53 by MDM2 inhibitors, attenuates the proliferation and survival of UM cells, which is further enhanced by a combination with PKC inhibition. Thus, MDMX inhibition in combination with existing therapeutic interventions for uveal melanoma could serve as a promising therapeutic intervention, stressing the need for the development of specific MDMX inhibitors, which thus far has been proven very difficult.

Replacing pan-PKC inhibition for PKC δ targeting

Activated protein kinase C (PKC) isoforms is a common feature of UM and has shown potential as therapeutic intervention for UM patients [30]. Unfortunately, pan-PKC inhibition as single treatment appears to have only limited clinical benefit and elicits adverse effects in patients [32]. Combining PKC inhibition with activation of p53, which is rarely mutated in UM, by MDM2 inhibitors has shown promising results in pre-clinical studies. Therefore, alternative approaches were investigated to achieve similar anti-cancer effects, but with potentially less adverse effects. Since the PKC family consists of 10 different isoforms it can be hypothesized that targeting a single PKC isoform would have less adverse effects compared to a pan-PKC inhibitor. It has been demonstrated that, despite the great structural homology between the different PKC isoforms, especially within a certain subclass, they appear to have separate and non-redundant functions. Furthermore, it has been observed that all PKC isoforms tested (α , β , θ , ϵ and δ) are essential for uveal melanoma cell viability [30, 33], emphasising that specific targeting of a single PKC isoform could yield an effective treatment. PKC ϵ and PKC δ were shown to be responsible for the activation of RASGRP3, a guanine nucleotide exchange factor promoting the GTP loading of RAS. So, activation of RASGRP3 serves as a RAS activator driving the RAS/MEK/ERK pathway in uveal melanoma [34]. In chapter 3 it is confirmed that uveal melanoma cell viability depends on PKC δ expression and, therefore, could be regarded a potential drug target, especially interesting since PKC δ does not seem to be required for development and normal cell proliferation [35, 36]. As mentioned above, it is unlikely that the specific targeting

of a single signalling molecule will result in a curative response it was investigated whether PKC δ depletion would also enhance the effect of MDM2/MDMX inhibition. Like pan-PKC inhibition, the specific depletion of PKC δ resulted in synergistic growth inhibition of UM cells in combination with p53 reactivation.

In conclusion, the data presented in chapter 3 show that the synergistic effects of p53-activation by MDM2/MDMX inhibition and broad spectrum PKC inhibition on survival of UM cells can largely be achieved by the presumably less toxic combination of depletion of MDMX and targeting a specific PKC isoform, PKC δ . Although PKC δ appears to be a promising therapeutic target until recently no small molecule compound specifically targeting this kinase had been described. The functional non-redundancy between the various isoforms suggests the opportunity for developing a selective inhibitor. Recently, the development of a selective PKC δ inhibitor (B106) has been described [35], but our experiments with this inhibitor indicate that the growth inhibitory effect is not dependent on PKC activity in uveal melanoma cells (data not shown). The approach to develop this inhibitor was to design the structure of B106 on the reported Rottlerin's capability to selectively bind PKC δ compared to PKC α and to combine this with parts of the kinase inhibitor Staurosporin. However, it has now been widely accepted that Rottlerin does actually not bind PKCs and Staurosporin is considered to be one of the most α -selective kinase inhibitors commercially available. An alternative approach to selectively target PKC δ , or members of the novel-PKC family, could very well consist of modifying a known pan-PKC inhibitor such as Sotrastaurin or GF109203X. These selective pan-PKC inhibitors have a strong structural overlap with the α -selective Staurosporin with regard to the 'head' domain of these compounds, suggesting that the selectivity of the compounds has to be acquired from the 'tail' residues. A valid approach for the development of a selective PKC δ inhibitor would be to chemically modify the tail region of either GFX or Sotrastaurin and determine the specificity using *in vitro* kinase assays.

Deviating from the hypes

Finding curative therapeutic intervention has been the focus of many decades of cancer research. A few success stories, such as Imatinib (targeting the BCR/ABL fusion gene) and Rituximab (targeting CD20), catalysed the targeted therapies hype. Although great results were expected based on these successes, the median increase in survival was 2.1-2.5 months based on 71 drugs approved to treat cancer by the FDA between 2002 and 2014 [37]. According to the ASCO guidelines, regarding improve in quality of life and overall survival, only 42% of these drugs had a meaningful clinical impact. It should be noted that many of the 71 approved drugs contain an overlapping mode of action [37]. When a certain company has developed an approved and

profitable therapy, even if only with a modest improvement in overall survival, other pharmacological companies will develop compounds with a similar mode of action to ensure a piece of the market and the profit. Thereby, they are pushing drug prices to incredible height without really improving the quality of the therapy and patient survival. This is particularly illustrated by the 50 molecules which entered clinical trials for targeting vascular endothelial growth factor (VEGF) as a means of targeting angiogenesis, or the 25 molecules in clinical trials for the targeting of mitosis in solid tumours, the latter with an average response rate of just 1% [38]. These duplication efforts are even further illustrated by the observation that 9 big pharmaceutical companies have a 74% overlap in their molecules with regard to the expected mode of action [37].

This focus on targeted therapies, with only limited clinical benefit, has almost blinded funding agencies, academia and companies. It is nowadays accepted that targeted therapies tend to work efficiently for 'single cause' diseases, but not really for more complex malignancies such as cancer due to tumor heterogeneity [39]. The most recent big breakthrough in cancer treatment is the development of immune checkpoint targeting drugs, discussed in the introduction of this thesis. These developments are currently changing the whole cancer research field, like targeted therapies did a few decades ago. Although promising in some cancer type, stratification of patients appears to be crucial for the success of a treatment, like for targeted therapies [40]. It appears that immunotherapies are most efficient in tumours with a high mutational load. Cutaneous melanomas have a high mutation load in contrast to uveal melanomas. Indeed, uveal melanoma patients did not benefit from immunotherapy in the form of Ipilimumab [41, 42]. It appears that with regard to metastasized uveal melanoma a therapeutic intervention should not come from current immunotherapy nor targeted therapy strategies. Therefore, the remainder of this discussion will be on the use of therapeutics not fitting within targeted- nor immunotherapy, but which are already in clinical trials, to reduce the time from bench to bedside.

EZH2 and HDAC as therapeutic intervention

In uveal melanoma BAP1 expression is frequently lost due to mutation and loss of the second allele [43-45]. In UM 80-90% of the metastases show loss of BAP1 expression resulting in strong predictive power for BAP1 mutations for the occurrence of metastasis [45, 46]. Interestingly, upregulation of Enhancer of Zeste (EZH) 2 expression in mesothelioma cells upon BAP1 loss has been reported [47]. EZH2 is an essential component of the polycomb repressive complex 2 (PRC2), which mediates the tri-methylation of histone H3 at lysine 27 [48, 49]. EZH2 controls the expression of numerous genes by promoting the repressive tri-methylation of histone H3 thereby

reducing transcription [50]. An EZH2 dependency was found in myeloid cells for BAP1 knockout induced transformation and *in vivo* it was demonstrated for BAP1-negative mesothelioma that EZH2 inhibition is an effective treatment for BAP-1 negative cancers [47]. A clinical trial was initiated for patients with BAP1-negative mesothelioma using the EZH2-inhibitor Tazemetostat (identifier: NCT02860286). In a later report, EZH2 inhibition did not appear to affect both BAP-1 positive and negative UM cell proliferation. However, in chapter 4 it is demonstrated that UM cells are responsive to long term EZH2 inhibition.

Nevertheless, it appears that for most cell lines tested the time until onset of growth inhibition was over a week. Furthermore, only 2 of the cell lines tested completely stopped proliferating, meaning that most cell lines tested could be sub-cultured with continuous EZH2 inhibition. These relatively slow and mild effects *in vitro* are far from optimal for translation to a clinical setting, in which a patient with metastasised uveal melanoma generally only has a few months to live. Therefore, it was investigated whether EZH2 inhibition would sensitize UM cells for other compounds, known to be effective in uveal melanoma patients. Concurrent inhibition of EZH2 and HDAC has already been shown to effectively reduced tumor cell survival in various different cancer types [51-53]. Therefore this combination could be considered as an interesting novel strategy, which should be further studied in clinical trials, for multiple malignancies. Importantly, HDAC inhibitors have already been described as a potential therapeutic intervention for uveal melanoma [54, 55]. Indeed it was found that also UM cell lines are sensitized for HDAC inhibition upon EZH2 inhibition due to the induction of cell death. Others have showed that, in KRAS mutated lung cancer cells, EZH2 inhibition sensitized for MEK and PI3K/AKT inhibitor [56]. Furthermore, EZH2 is involved in the transcriptional repression of various DNA repair-related genes, which result in higher sensitivity to chemotherapeutic agents when cells are treated with an EZH2 inhibitor [57-59]. These studies indicate that in addition to the dual inhibition of HDACs and EZH2, other compounds could well synergize with EZH2 inhibition and be a promising therapeutic intervention for metastasised uveal melanoma. Future research has to elucidate which combinations are the most potent and feasible.

Combining HDAC and CDK inhibition as therapeutic strategy

As described previously, overall survival has hardly improved for patients with advanced unresectable cutaneous melanoma or metastatic uveal melanoma in the last decades. This lack of improvement is highlighting the need for novel therapeutic options. In chapter 5 the potential of the combination of another compound with the HDAC inhibitor (Quisinostat) described in chapter 4 was investigated. Both drugs

assessed in this chapter are currently in clinical trials reducing time from bench to bedside.

Encouraging results using histone deacetylase (HDAC) inhibitors indicate a potential therapeutic intervention for uveal and cutaneous melanoma [12–15]. HDAC inhibition often induces a G1 cell cycle arrest in cancer cells. Although this cell cycle arrest can prevent further outgrowth of a tumor [21], finding drug combinations that synergistically induce cancer cell killing would greatly increase the clinical impact of HDAC inhibitors. For example, apoptosis is induced when both CDKs and HDACs are inhibited in neuroblastoma cell lines [23]. This study aimed at potentiating the effect of HDAC inhibitor Quisinostat by combining the therapy with CDK inhibition using Flavopiridol. Flavopiridol is currently tested in clinical trials, mainly as treatment strategy for acute myeloid leukaemia and lymphoma. Interestingly, stable disease in 7/16 patients with previously untreated metastatic malignant melanoma was induced by Flavopiridol. Unfortunately, according to objective response criteria Flavopiridol failed to achieve significant clinical benefit [28]. Data presented in chapter 5 show that single treatment with Flavopiridol or Quisinostat slows down the growth of UM and CM cells, while concurrent treatment inhibits cell growth synergistically and reduces survival.

Concurrent Flavopiridol and Quisinostat treatment shows a synergistic reduction in melanoma cell survival independent of mutations driving the malignancy. These synergistic effects were also observed in BRAF mutant melanoma cells that had acquired resistance to BRAF inhibition *in vitro*. Induction of apoptosis could at least partly explain the mechanism behind the observed synergism. However, the molecular mechanism underlying this induction of cell death remains undetermined. In a cutaneous melanoma PDX model combined Flavopiridol and Quisinostat treatment induced tumor regression, without enhancing adverse effects. However, the observed combinatory effects did not measure up to the expected results based on the *in vitro* assays. This can most likely be attributed to the lack of clear Flavopiridol activity on a molecular level. Flavopiridol is known to be cleared from the human body in hours [60]. Future research on this drug combination should mainly focus on reaching and maintaining proper CDK inhibition by Flavopiridol in order to reach maximum synergism and thus clinical benefit. When that can be achieved the Flavopiridol/Quisinostat combination could be a promising treatment strategy for metastasized uveal and cutaneous melanoma patients, regardless of earlier received treatments.

Considerations for drug combinatory studies

When two drugs are combined they can influence each other's respective outcome in either a synergistic, additive or antagonistic manner. When synergy between two

drugs occurs this indicates a potential novel therapeutic intervention. However, resolving the underlying mechanism driving the observed synergism could be extremely difficult, especially when the compounds are targeting a number of related molecules, as for instance described in chapter 5. These difficulties arise from the numerous possibilities on how both drugs might influence each other. This complexity is illustrated by a list of basic motives with only 3 theoretical nodes which already results in 21 possible explanations for synergism, let alone when more general pathways or cellular processes are influenced [61].

The other option upon combining drugs is the occurrence of antagonism. Synergism only tends to occur in a minority of drug combinations when systematically tested [62]. There appears to be a bias in both published literature and this thesis towards synergistic drug combinations rather the antagonistic ones based on a PubMed search for ‘antagonism’ or ‘synergism’ in combination with cancer’. This search yielded six times more hits for synergism in cancer compared to antagonism in cancer, although according to unbiased screening there should be at least ten times more antagonistic combinations compared to synergistic ones. Although these combinations clearly do not contain a therapeutic benefit, they could reveal potential mechanism of drugs resistance. To mechanistically explain antagonism appears to be easier compared to synergism as there are far less theoretical explanations for the occurrence of antagonism compared to synergism [61]. For example, it has been shown that p53 reactivation in combination with CDK1/2 inhibition results synergistically in growth inhibition of melanoma cells [63]. However, preliminary data from our lab show that the pan-CDK inhibitor Flavopiridol has an antagonistic effect on p53 activation (data not shown). Which could actually make sense since Flavopiridol’s main target is the block of transcription by CDK9 inhibition, which would antagonize p53-induced transcription upon activation. So, despite Flavopiridol’s lack of synergistic capabilities with p53 the results could help understanding which drugs or CDK inhibitors could provide useful therapeutic enhancers of p53 activation therapies and which will not.

For the studies described in this thesis the ‘educated guess’ methodology was used to find novel synergistic combinations to inhibit uveal melanoma cell growth. Illustrated by the concurrent targeting of two main hallmarks of uveal melanoma, namely PKC activity and high expression of MDMX/2. Furthermore, knowledge of BAP1 and EZH2 was applied to combine EZH2 and HDAC inhibition, of which the latter had been shown to elicit metastasis regression in uveal melanoma patients. The observed HDAC inhibition induced cell cycle arrest directed us towards the combination with CDK inhibition. Although these combinations work synergistically *in vitro* and hold

true potential it could easily be doubted whether these combinations are the best combinations possible.

An alternative approach consists of performing unbiased synthetic lethal screens to find genes and pathways synergising with a particular drug. The question remains which drugs to select for these approaches. One might select drugs based on their availability in the clinic, proven clinical efficacy, or their ability to induce a growth arrest *in vitro* so the synergism will be clear. However, it could also be considered to select a drug for this screening based on the lack of activity. Especially the lack of strong adverse effects could be considered a pro due to the reduced likeness of enhancing adverse effects in the combination. A prominent downside of this approach could well be that the ideal pathway or molecule identified by these screens cannot -yet- be targeted by a specific small molecule compound. Another drawback could be that no interest exists from the industry to commercialize a certain treatment option.

A last option would be to put all scientific interest aside and, much like the Quisino-stat/Flavopiridol combination, focus on drugs already in clinical trials and preferably FDA approved. Also here it boils down to which drugs to investigate. In such a setting it could be wise to test only those compounds the companies are willing to bring forward into clinical trials. Finding a cure for metastasised uveal melanoma following this approach has the great advantage of a relatively short time from bench to bedside. The obvious downside of this approach is that again the combination with strongest effects and with the least adverse side effects could be missed.

Clinical relevance and concluding remarks

When studies, like described in this thesis, are being performed one should always wonder what the true question is that needs to be answered. Whether or not there is a scientific interest in a certain molecule or pathway or just simply the need to find a curative treatment for patients who have none or have run out of treatment options. Regardless of the fact that finding a curative treatment for all metastasised uveal melanoma patients is most likely impossible due to great inter- and intra-tumor variation, the identification of the 'best possible' drug (combination) will require the 'brains' of the educated guess approach, the unbiasedness of the second and unconditional support of pharmacological industries. Concluding that none of the above mentioned approaches is either good or wrong as long as they are fitting with the question needing to be answered.

To date no effective therapy exists for metastasized uveal melanoma. It is therefore that all potential effective or prognosis improving therapeutic strategies need to be

evaluated properly in order to obtain an effective therapy for this deadly malignancy. Findings in this thesis provide several potential new therapeutic interventions mainly based on drugs already in clinical trials in order to reduce time from bench to bedside. However, in all cases of suggested drug combinations additional research needs to be performed, in a (pre-) clinical setting, to show the true potential of these combinations.

References

1. Gao J, Aksoy BA, Dogrusoz U, Dresdner G, Gross B, Sumer SO, Sun Y, Jacobsen A, Sinha R, Larsson E, Cerami E, Sander C, Schultz N. Integrative analysis of complex cancer genomics and clinical profiles using the cBioPortal. *Sci Signal*. 2013; 6: pl1. doi: 10.1126/scisignal.2004088.
2. de Lange J, Teunisse AF, Vries MV, Lodder K, Lam S, Luyten GP, Bernal F, Jager MJ, Jochemsen AG. High levels of Hdmx promote cell growth in a subset of uveal melanomas. *Am J Cancer Res*. 2012; 2: 492-507. doi:
3. Gembarska A, Luciani F, Fedele C, Russell EA, Dewaele M, Villar S, Zwolinska A, Haupt S, de Lange J, Yip D, Goydos J, Haigh JJ, Haupt Y, et al. MDM4 is a key therapeutic target in cutaneous melanoma. *Nat Med*. 2012; 18: 1239-47. doi: 10.1038/nm.2863.
4. Fischer M. Census and evaluation of p53 target genes. *Oncogene*. 2017; 36: 3943-56. doi: 10.1038/onc.2016.502.
5. Fischer M, Quaas M, Steiner L, Engeland K. The p53-p21-DREAM-CDE/CHR pathway regulates G2/M cell cycle genes. *Nucleic Acids Res*. 2016; 44: 164-74. doi: 10.1093/nar/gkv927.
6. Marine JC, Jochemsen AG. Mdmx and Mdm2: brothers in arms? *Cell Cycle*. 2004; 3: 900-4. doi:
7. Bottger V, Bottger A, Garcia-Echeverria C, Ramos YF, van der Eb AJ, Jochemsen AG, Lane DP. Comparative study of the p53-mdm2 and p53-MDMX interfaces. *Oncogene*. 1999; 18: 189-99. doi: 10.1038/sj.onc.1202281.
8. Francoz S, Froment P, Bogaerts S, De Clercq S, Maetens M, Doumont G, Bellefroid E, Marine JC. Mdm4 and Mdm2 cooperate to inhibit p53 activity in proliferating and quiescent cells in vivo. *Proc Natl Acad Sci U S A*. 2006; 103: 3232-7. doi: 10.1073/pnas.0508476103.
9. Marine JC, Francoz S, Maetens M, Wahl G, Toledo F, Lozano G. Keeping p53 in check: essential and synergistic functions of Mdm2 and Mdm4. *Cell Death Differ*. 2006; 13: 927-34. doi: 10.1038/sj.cdd.4401912.
10. Valentin-Vega YA, Okano H, Lozano G. The intestinal epithelium compensates for p53-mediated cell death and guarantees organismal survival. *Cell Death Differ*. 2008; 15: 1772-81. doi: 10.1038/cdd.2008.109.
11. Valentin-Vega YA, Box N, Terzian T, Lozano G. Mdm4 loss in the intestinal epithelium leads to compartmentalized cell death but no tissue abnormalities. *Differentiation*. 2009; 77: 442-9. doi: 10.1016/j.diff.2009.03.001.
12. Grier JD, Xiong S, Elizondo-Fraire AC, Parant JM, Lozano G. Tissue-specific differences of p53 inhibition by Mdm2 and Mdm4. *Mol Cell Biol*. 2006; 26: 192-8. doi: 10.1128/MCB.26.1.192-198.2006.
13. Ringshausen I, O'Shea CC, Finch AJ, Swigart LB, Evan GI. Mdm2 is critically and continuously required to suppress lethal p53 activity in vivo. *Cancer Cell*. 2006; 10: 501-14. doi: 10.1016/j.ccr.2006.10.010.
14. Moyer SM, Larsson CA, Lozano G. Mdm proteins: critical regulators of embryogenesis and homeostasis. *J Mol Cell Biol*. 2017. doi: 10.1093/jmcb/mjx004.
15. Brenkman AB, de Keizer PL, van den Broek NJ, Jochemsen AG, Burgering BM. Mdm2 induces monoubiquitination of FOXO4. *PLoS One*. 2008; 3: e2819. doi: 10.1371/journal.pone.0002819.
16. Fu W, Ma Q, Chen L, Li P, Zhang M, Ramamoorthy S, Nawaz Z, Shimojima T, Wang H, Yang Y, Shen Z, Zhang Y, Zhang X, et al. MDM2 acts downstream of p53 as an E3 ligase to promote FOXO ubiquitination and degradation. *J Biol Chem*. 2009; 284: 13987-4000. doi: 10.1074/jbc.M901758200.
17. Dannenberg JH, David G, Zhong S, van der Torre J, Wong WH, Depinho RA. mSin3A corepressor regulates diverse transcriptional networks governing normal and neoplastic growth and survival. *Genes Dev*. 2005; 19: 1581-95. doi: 10.1101/gad.1286905.

18. Li H, Collado M, Villasante A, Matheu A, Lynch CJ, Canamero M, Rizzoti K, Carneiro C, Martinez G, Vidal A, Lovell-Badge R, Serrano M. p27(Kip1) directly represses Sox2 during embryonic stem cell differentiation. *Cell Stem Cell*. 2012; 11: 845-52. doi: 10.1016/j.stem.2012.09.014.
19. Zilfou JT, Hoffman WH, Sank M, George DL, Murphy M. The corepressor mSin3a interacts with the proline-rich domain of p53 and protects p53 from proteasome-mediated degradation. *Mol Cell Biol*. 2001; 21: 3974-85. doi: 10.1128/MCB.21.12.3974-3985.2001.
20. Vassilev LT, Vu BT, Graves B, Carvajal D, Podlaski F, Filipovic Z, Kong N, Kammlott U, Lukacs C, Klein C, Fotouhi N, Liu EA. In vivo activation of the p53 pathway by small-molecule antagonists of MDM2. *Science*. 2004; 303: 844-8. doi: 10.1126/science.1092472.
21. Biswas S, Killick E, Jochemsen AG, Lunec J. The clinical development of p53-reactivating drugs in sarcomas - charting future therapeutic approaches and understanding the clinical molecular toxicology of Nutlins. *Expert Opin Investig Drugs*. 2014; 23: 629-45. doi: 10.1517/13543784.2014.892924.
22. Jones SN, Roe AE, Donehower LA, Bradley A. Rescue of embryonic lethality in Mdm2-deficient mice by absence of p53. *Nature*. 1995; 378: 206-8. doi: 10.1038/378206a0.
23. Montes de Oca Luna R, Wagner DS, Lozano G. Rescue of early embryonic lethality in mdm2-deficient mice by deletion of p53. *Nature*. 1995; 378: 203-6. doi: 10.1038/378203a0.
24. Okamoto K, Kashima K, Pereg Y, Ishida M, Yamazaki S, Nota A, Teunisse A, Migliorini D, Kitabayashi I, Marine JC, Prives C, Shiloh Y, Jochemsen AG, et al. DNA damage-induced phosphorylation of MdmX at serine 367 activates p53 by targeting MdmX for Mdm2-dependent degradation. *Mol Cell Biol*. 2005; 25: 9608-20. doi: 10.1128/MCB.25.21.9608-9620.2005.
25. Finch RA, Donoviel DB, Potter D, Shi M, Fan A, Freed DD, Wang CY, Zambrowicz BP, Ramirez-Solis R, Sands AT, Zhang N. mdmx is a negative regulator of p53 activity in vivo. *Cancer Res*. 2002; 62: 3221-5. doi:
26. Parant J, Chavez-Reyes A, Little NA, Yan W, Reinke V, Jochemsen AG, Lozano G. Rescue of embryonic lethality in Mdm4-null mice by loss of Trp53 suggests a nonoverlapping pathway with MDM2 to regulate p53. *Nat Genet*. 2001; 29: 92-5. doi: 10.1038/ng714.
27. Carrillo AM, Bouska A, Arrate MP, Eischen CM. Mdmx promotes genomic instability independent of p53 and Mdm2. *Oncogene*. 2015; 34: 846-56. doi: 10.1038/onc.2014.27.
28. Jeffreena Miranda P, Buckley D, Raghu D, Pang JB, Takano EA, Vijayakumar R, Teunisse AF, Posner A, Procter T, Herold MJ, Gamell C, Marine JC, Fox SB, et al. MDM4 is a rational target for treating breast cancers with mutant p53. *J Pathol*. 2017. doi: 10.1002/path.4877.
29. Maughan T. The Promise and the Hype of 'Personalised Medicine'. *New Bioeth*. 2017; 23: 13-20. doi: 10.1080/20502877.2017.1314886.
30. Wu X, Li J, Zhu M, Fletcher JA, Hodi FS. Protein kinase C inhibitor AEB071 targets ocular melanoma harboring GNAQ mutations via effects on the PKC/Erk1/2 and PKC/NF-kappaB pathways. *Mol Cancer Ther*. 2012; 11: 1905-14. doi: 10.1158/1535-7163.MCT-12-0121.
31. Carita G, Frisch-Dit-Leitz E, Dahmani A, Raymondie C, Cassoux N, Piperno-Neumann S, Nemati F, Laurent C, De Koning L, Halilovic E, Jeay S, Wylie A, Emery C, et al. Dual inhibition of protein kinase C and p53-MDM2 or PKC and mTORC1 are novel efficient therapeutic approaches for uveal melanoma. *European Journal of Cancer*. 2016; 68: S31-S. doi:
32. Piperno-Neumann S, Kapiteijn E, Larkin J, Carvajal RD, Luke JJ, Seifert H, Roozen I, Zoubir M, Yang L, Choudhury S, Yerramilli-Rao P, Hodi FS, Schwartz GK. (2014). Phase I dose-escalation study of the protein kinase C (PKC) inhibitor AEB071 in patients with metastatic uveal melanoma. ASCO annual meeting 2014: J. Clin. Oncol (abstr 9030)).

33. Wu X, Zhu M, Fletcher JA, Giobbie-Hurder A, Hodi FS. The protein kinase C inhibitor enzastaurin exhibits antitumor activity against uveal melanoma. *PLoS One*. 2012; 7: e29622. doi: 10.1371/journal.pone.0029622.
34. Chen X, Wu Q, Depeille P, Chen P, Thornton S, Kalirai H, Coupland SE, Roose JP, Bastian BC. RasGRP3 Mediates MAPK Pathway Activation in GNAQ Mutant Uveal Melanoma. *Cancer Cell*. 2017; 31: 685-96 e6. doi: 10.1016/j.ccell.2017.04.002.
35. Miyamoto A, Nakayama K, Imaki H, Hirose S, Jiang Y, Abe M, Tsukiyama T, Nagahama H, Ohno S, Hatakeyama S, Nakayama KI. Increased proliferation of B cells and auto-immunity in mice lacking protein kinase Cdelta. *Nature*. 2002; 416: 865-9. doi: 10.1038/416865a.
36. Leitges M, Mayr M, Braun U, Mayr U, Li C, Pfister G, Ghaffari-Tabrizi N, Baier G, Hu Y, Xu Q. Exacerbated vein graft arteriosclerosis in protein kinase Cdelta-null mice. *J Clin Invest*. 2001; 108: 1505-12. doi: 10.1172/JCI12902.
37. Fojo T, Mailankody S, Lo A. Unintended consequences of expensive cancer therapeutics-the pursuit of marginal indications and a me-too mentality that stifles innovation and creativity: the John Conley Lecture. *JAMA Otolaryngol Head Neck Surg*. 2014; 140: 1225-36. doi: 10.1001/jamaoto.2014.1570.
38. Komlodi-Pasztor E, Sackett DL, Fojo AT. Inhibitors targeting mitosis: tales of how great drugs against a promising target were brought down by a flawed rationale. *Clin Cancer Res*. 2012; 18: 51-63. doi: 10.1158/1078-0432.CCR-11-0999.
39. Jamal-Hanjani M, Quezada SA, Larkin J, Swanton C. Translational implications of tumor heterogeneity. *Clin Cancer Res*. 2015; 21: 1258-66. doi: 10.1158/1078-0432.CCR-14-1429.
40. Reck M, Rodriguez-Abreu D, Robinson AG, Hui R, Czoszi T, Fulop A, Gottfried M, Peled N, Tafreshi A, Cuffe S, O'Brien M, Rao S, Hotta K, et al. Pembrolizumab versus Chemotherapy for PD-L1-Positive Non-Small-Cell Lung Cancer. *N Engl J Med*. 2016; 375: 1823-33. doi: 10.1056/NEJMoa1606774.
41. Schinzari G, Rossi E, Cassano A, Dadduzio V, Quirino M, Pagliara M, Blasi MA, Barone C. Cisplatin, dacarbazine and vinblastine as first line chemotherapy for liver metastatic uveal melanoma in the era of immunotherapy: a single institution phase II study. *Melanoma Res*. 2017; 27: 591-5. doi: 10.1097/CMR.0000000000000401.
42. Heppt MV, Steeb T, Schlager JG, Rosumeck S, Dressler C, Ruzicka T, Nast A, Berking C. Immune checkpoint blockade for unresectable or metastatic uveal melanoma: A systematic review. *Cancer Treat Rev*. 2017; 60: 44-52. doi: 10.1016/j.ctrv.2017.08.009.
43. Prescher G, Bornfeld N, Horsthemke B, Becher R. Chromosomal aberrations defining uveal melanoma of poor prognosis. *Lancet*. 1992; 339: 691-2. doi:
44. Prescher G, Bornfeld N, Hirche H, Horsthemke B, Jockel KH, Becher R. Prognostic implications of monosomy 3 in uveal melanoma. *Lancet*. 1996; 347: 1222-5. doi:
45. Harbour JW, Onken MD, Roberson ED, Duan S, Cao L, Worley LA, Council ML, Matatall KA, Helms C, Bowcock AM. Frequent mutation of BAP1 in metastasizing uveal melanomas. *Science*. 2010; 330: 1410-3. doi: 10.1126/science.1194472.
46. van Essen TH, van Pelt SI, Versluis M, Bronkhorst IH, van Duinen SG, Marinkovic M, Kroes WG, Ruivenkamp CA, Shukla S, de Klein A, Kilic E, Harbour JW, Luyten GP, et al. Prognostic parameters in uveal melanoma and their association with BAP1 expression. *Br J Ophthalmol*. 2014; 98: 1738-43. doi: 10.1136/bjophthalmol-2014-305047.
47. LaFave LM, Beguelin W, Koche R, Teater M, Spitzer B, Chramiec A, Papalexi E, Keller MD, Hricik T, Konstantinoff K, Micol JB, Durham B, Knutson SK, et al. Loss of BAP1 function leads to EZH2-dependent transformation. *Nat Med*. 2015; 21: 1344-9. doi: 10.1038/nm.3947.
48. Margueron R, Reinberg D. The Polycomb complex PRC2 and its mark in life. *Nature*. 2011; 469: 343-9. doi: 10.1038/nature09784.

49. Di Croce L, Helin K. Transcriptional regulation by Polycomb group proteins. *Nat Struct Mol Biol.* 2013; 20: 1147-55. doi: 10.1038/nsmb.2669.
50. Yoo KH, Hennighausen L. EZH2 methyltransferase and H3K27 methylation in breast cancer. *Int J Biol Sci.* 2012; 8: 59-65. doi:
51. Grinshtein N, Riaseco CC, Marcellus R, Uehling D, Aman A, Lun X, Muto O, Podmore L, Lever J, Shen Y, Blough MD, Cairncross GJ, Robbins SM, et al. Small molecule epigenetic screen identifies novel EZH2 and HDAC inhibitors that target glioblastoma brain tumor-initiating cells. *Oncotarget.* 2016; 7: 59360-76. doi: 10.18632/oncotarget.10661.
52. Takashina T, Kinoshita I, Kikuchi J, Shimizu Y, Sakakibara-Konishi J, Oizumi S, Nishimura M, Dosaka-Akita H. Combined inhibition of EZH2 and histone deacetylases as a potential epigenetic therapy for non-small-cell lung cancer cells. *Cancer Sci.* 2016; 107: 955-62. doi: 10.1111/cas.12957.
53. Fiskus W, Wang Y, Sreekumar A, Buckley KM, Shi H, Jillella A, Ustun C, Rao R, Fernandez P, Chen J, Balusu R, Koul S, Atadja P, et al. Combined epigenetic therapy with the histone methyltransferase EZH2 inhibitor 3-deazaneplanocin A and the histone deacetylase inhibitor panobinostat against human AML cells. *Blood.* 2009; 114: 2733-43. doi: 10.1182/blood-2009-03-213496.
54. Carol H, Gorlick R, Kolb EA, Morton CL, Manesh DM, Keir ST, Reynolds CP, Kang MH, Maris JM, Wozniak A, Hickson I, Lyalin D, Kurmasheva RT, et al. Initial testing (stage 1) of the histone deacetylase inhibitor, quisinostat (JNJ-26481585), by the Pediatric Preclinical Testing Program. *Pediatr Blood Cancer.* 2014; 61: 245-52. doi: 10.1002/pbc.24724.
55. Landreville S, Agapova OA, Matatall KA, Kneass ZT, Onken MD, Lee RS, Bowcock AM, Harbour JW. Histone deacetylase inhibitors induce growth arrest and differentiation in uveal melanoma. *Clin Cancer Res.* 2012; 18: 408-16. doi: 10.1158/1078-0432.CCR-11-0946.
56. Riquelme E, Behrens C, Lin HY, Simon G, Papadimitrakopoulou V, Izzo J, Moran C, Kalhor N, Lee JJ, Minna JD, Wistuba, II. Modulation of EZH2 Expression by MEK-ERK or PI3K-AKT Signaling in Lung Cancer Is Dictated by Different KRAS Oncogene Mutations. *Cancer Res.* 2016; 76: 675-85. doi: 10.1158/0008-5472.CAN-15-1141.
57. Yang Q, Nair S, Laknaur A, Ismail N, Diamond MP, Al-Hendy A. The Polycomb Group Protein EZH2 Impairs DNA Damage Repair Gene Expression in Human Uterine Fibroids. *Biol Reprod.* 2016; 94: 69. doi: 10.1095/biolreprod.115.134924.
58. Gao SB, Li KL, Qiu H, Zhu LY, Pan CB, Zhao Y, Wei SH, Shi S, Jin GH, Xue LX. Enhancing chemotherapy sensitivity by targeting PcG via the ATM/p53 pathway. *Am J Cancer Res.* 2017; 7: 1874-83. doi:
59. Yamaguchi H, Du Y, Nakai K, Ding M, Chang SS, Hsu JL, Yao J, Wei Y, Nie L, Jiao S, Chang WC, Chen CH, Yu Y, et al. EZH2 contributes to the response to PARP inhibitors through its PARP-mediated poly-ADP ribosylation in breast cancer. *Oncogene.* 2017. doi: 10.1038/onc.2017.311.
60. Dickson MA, Rathkopf DE, Carvajal RD, Grant S, Roberts JD, Reid JM, Ames MM, McGovern RM, Lefkowitz RA, Gonen M, Cane LM, Dials HJ, Schwartz GK. A phase I pharmacokinetic study of pulse-dose vorinostat with flavopiridol in solid tumors. *Invest New Drugs.* 2011; 29: 1004-12. doi: 10.1007/s10637-010-9447-x.
61. Yin N, Ma W, Pei J, Ouyang Q, Tang C, Lai L. Synergistic and antagonistic drug combinations depend on network topology. *PLoS One.* 2014; 9: e93960. doi: 10.1371/journal.pone.0093960.
62. Severyn B, Liehr RA, Wolicki A, Nguyen KH, Hudak EM, Ferrer M, Caldwell JS, Hermes JD, Li J, Tudor M. Parsimonious discovery of synergistic drug combinations. *ACS Chem Biol.* 2011; 6: 1391-8. doi: 10.1021/cb2003225.
63. Lu M, Breysens H, Salter V, Zhong S, Hu Y, Baer C, Ratnayaka I, Sullivan A, Brown NR, Endicott J, Knapp S, Kessler BM, Middleton MR, et al. Restoring p53 Function in Human Melanoma Cells by

Inhibiting MDM2 and Cyclin B1/CDK1-Phosphorylated Nuclear iASPP. *Cancer Cell*. 2016; 30: 822-3.
doi: 10.1016/j.ccell.2016.09.019.

APPENDIX

Dutch summary

Curriculum Vitae

List of publications

Acknowledgements

Nederlandse samenvatting

1. Innovatieve nieuwe functies van MDMX

1.1. Kanker

Een ziekte waar steeds meer mensen mee geconfronteerd worden is kanker. Dit is een ziekte van het ongecontroleerd en ongeremd delen van lichaamscellen. De oorzaak hiervan is een opeenstapeling van fouten in het erfelijk materiaal, het DNA, mutaties genoemd. Deze mutaties kunnen ervoor zorgen dat bepaalde eiwitten veranderen van eigenschappen. Zo kunnen specifieke eiwitten die celgroei en celdeling stimuleren door toedoen van mutaties altijd 'aan' staan. Op deze manier wordt een cel tot delen aangezet, terwijl dit eigenlijk niet de bedoeling is. Hoewel het essentieel is voor het ontwikkelen van kanker dat cellen over zo'n ongelimiteerd 'groeisignaal' beschikken, is dit op zichzelf niet voldoende voor het ontstaan van kanker. Er zijn, voor zover bekend, gemiddeld zes mutaties nodig om van een normale cel te veranderen in een kwaadaardige cel.

1.2. p53

Cellen beschikken over verschillende mechanismen voor het ontdekken van DNA schade en stress, die onder andere ontstaan gedurende het ontsporen van een normale cel tot een kwaadaardige cel. Op het moment dat er te veel schade en of stress wordt gedetecteerd, wordt een proces van geprogrammeerde celdood, genaamd apoptose, in werking gezet om het ontstaan van ontspoorde cellen te voorkomen. Naast het constante 'groeisignaal' moet een kankercel dus ook resistent worden voor onder andere apoptose om volledig te ontsporen en ongeremd en ongecontroleerd te kunnen blijven delen. Centraal in de herkenning van stresssituaties van een cel staat het eiwit p53. P53 is een zogenoemde transcriptie factor die op het moment van detectie van stress zorgt voor de genregulatie van eiwitten die een cel in eerste instantie doen stoppen met delen om de geïdentificeerde stressor te verwijderen. Wanneer de stresssituatie niet verbetert of de schade onherstelbaar blijkt, treedt apoptose in werking. Niet alleen ophoping van DNA schade, maar ook kankercel stimulerende mutaties kunnen zorgen voor activatie van p53. Doordat p53 een centrale rol vervult in de reactie op stress en groei stimulerende mutaties, is het gen dat codeert voor p53 vaak gemuteerd in kanker. Dergelijke inactiverende mutaties worden in ongeveer de helft van alle tumoren gevonden, wat p53 het meest frequent gemuteerde eiwit in kanker maakt. Kankercellen zonder een p53 mutatie maken gebruik van andere strategieën om p53 functie (of activiteit) te onderdrukken.

Eén zo'n strategie die kankercellen gebruiken voor het onderdrukken van p53 is het hoog tot expressie brengen van één of twee p53 remmers, genaamd MDM2 en MDMX. Deze twee eiwitten hebben als taak om in een gezonde cel p53 activiteit onder controle te houden, zodat het apoptose programma niet wordt geactiveerd en de cel onderdeel blijft uitmaken van het lichaam. Hoewel deze twee eiwitten structureel veel op elkaar lijken, verschillen ze wel in de manier waarop ze p53 remmen. MDM2 is een zogeheten ubiquitine ligase, dat ervoor zorgt dat het p53 eiwit snel wordt afgebroken. MDMX beschikt niet over deze ubiquitine ligase activiteit, maar kan wel zodanig aan p53 binden dat deze niet meer voor de inductie van een groei-stop of apoptose kan zorgen. Door MDM2 en/of MDMX hoog tot expressie te brengen kan een cel zonder p53 mutaties toch kwaadaardig worden.

1.3. Nieuwe functies van MDMX

In hoofdstuk 2 is getracht om verder de functie van MDMX te bepalen door te onderzoeken van welke genen de expressie wordt gecontroleerd door deze p53 remmer. De resultaten lieten zien dat MDMX de expressie van celdeling-stimulerende genen verhoogt, terwijl het de expressie van genen betrokken bij apoptose juist verlaagt. Deze resultaten correleren goed met de eerder beschreven oncogene functies van MDMX, waaronder de onderdrukking van p53 activiteit. Uit eerder onderzoek is echter gebleken dat MDMX ook bijdraagt aan tumorgroei en -ontwikkeling op een manier onafhankelijk van p53 remming. Inderdaad, de resultaten beschreven in hoofdstuk 2 laten zien dat een deel van de waargenomen effecten van MDMX op genregulatie onafhankelijk is van p53. Verdere diepgaande analyses van de genexpressie data suggereerden dat MDMX ook de functie van een familie van andere eiwitten beïnvloedt, de FOXO eiwitten. Deze eiwitten zijn, net zoals p53, transcriptiefactoren die een belangrijke rol spelen bij het aan- of uitzetten van genen. Een belangrijke observatie is dat MDMX, naast p53, ook aan FOXO1 kan binden. Dit zou kunnen betekenen dat MDMX niet alleen in staat is om de activiteit van p53 te remmen, maar ook van andere transcriptiefactoren zoals FOXO1. Met deze hypothese zouden mogelijk een deel van de p53-onafhankelijke oncogene effecten van MDMX verklaard kunnen worden, wat zou bijdragen aan het beter begrijpen van kanker.

Het steeds beter begrijpen van MDMX, en daarmee kanker, zou op de lange termijn kunnen leiden tot nieuwe medicijnen of therapeutische strategieën. Om deze hypothese te testen is een p53-onafhankelijk en MDMX/FOXO-gereguleerd gen, coderend voor MXD4, in meer detail bestudeerd. Resultaten suggereerden een nog niet eerder beschreven 'back-up' mechanisme waarmee een kankercel MDMX verlies zou kunnen compenseren met p53 inhibitie door MDM2. Verdere experimenten toonden aan dat MXD4 depletie in kankercellen leidt tot een verhoogde gevoeligheid voor p53-

activerende medicijnen. Deze resultaten bieden perspectief voor de toekomst van p53-activerende medicijnen en mogelijke nieuwe manieren om deze nog effectiever te laten zijn.

2. Nieuwe therapeutische strategieën voor uvea melanoom

2.1. Melanoom

Huidmelanoom is een dodelijke variant van huidkanker die ontstaat uit pigmentproducerende cellen genaamd melanocyten. Primaire melanomen kunnen vaak goed behandeld worden door middel van chirurgische verwijdering. Patiënten hebben daardoor ook een grote overlevingskans. Zodra uitzaaiingen optreden verkleint de kans op overleving echter drastisch wegens het gebrek aan effectieve therapieën. Een grote stap leek gemaakt met de ontdekking van een zeer specifieke activerende mutatie van het gen BRAF, dat in ongeveer de helft van alle melanoom patiënten voorkomt. Voor deze gemuteerde vorm van BRAF is vervolgens een medicijn ontwikkeld, wat de tumoren erg effectief deed verdwijnen. Echter, zoals vaak bij soortgelijke gepersonaliseerde medicatie, vindt de tumor na een paar maanden een andere manier om overleven en verder te groeien onafhankelijk van het gemuteerde BRAF. Een sprong voorwaarts werd gemaakt met de ontdekkingen van verschillen manieren om een patiënt zijn of haar eigen immuunsysteem kwaadaardige cellen aan te laten vallen. Deze vorm van therapie, ook wel immunotherapie genoemd, lijkt erg effectief en leidt zelfs tot genezing van sommige patiënten. Hoewel er gedurende de afgelopen decennia vooruitgang is geboekt in het verbeteren van behandelmethodes, blijft melanoom door het ontstaan van resistentie een lethale ziekte waarvoor nieuwe behandelmethodes gevonden dienen te worden.

2.2. Uvea melanomen

Een subgroep van melanoom is het uvea melanoom (UM). Deze vorm van melanoom beslaat ongeveer 5% van het totaal aantal melanomen en ontstaat uit melanocyten uit specifieke structuren in het oog, namelijk het vaatvlies, straallichaam en de iris. Net zoals huidmelanomen zijn uvea melanomen goed te behandelen tot het moment waarop uitzaaiingen plaatsvinden. Zodra metastases worden gedetecteerd, daalt de gemiddelde levensverwachting naar 2 tot 7 maanden. Er is inmiddels veel duidelijkheid over verschillende classificaties waarin een tumor kan vallen, die bepalend zijn voor het al dan niet ontstaan van metastases. Een cruciale gebeurtenis hiervoor lijkt het verlies van één van de twee kopieën van chromosoom 3. Als het andere kopie daarnaast een gemuteerd BAP1 gen bevat, resulteert dit in verlies van BAP1 expressie en een verhoogde kans op de ontwikkeling van uitzaaiingen. Hoewel het dus steeds

beter te voorspellen wordt welke patiënten metastases gaan ontwikkelen, blijft het behandelen hiervan nagenoeg onmogelijk. Dit komt omdat deze metastases tot nu toe ongevoelig lijken voor alle therapieën, met een korte levensverwachting voor de patiënt tot gevolg. Dit proefschrift focust zich daarom verder op het verbeteren van bestaande methodes en het vinden van nieuwe strategieën om patiënten met uitgezaaide UM te behandelen.

2.3. Verbetering van de huidige behandelmethodes voor gemetastaseerde uvea melanomen

2.3.1. Huidige therapieën

Zoals hierboven beschreven heeft iedere kanker mutaties nodig die voor een continue 'groeisignaal' zorgen. De mutaties die verantwoordelijk zijn voor dit signaal in UM focussen zich in een specifiek deel van de G-eiwitten GNAq of GNA11. Doordat deze eiwitten permanent 'aan' staan, wordt er constant een groei-stimulerende signaal-transductie-cascade geactiveerd. Een onmisbare stap in deze cascade is de activatie van zogeheten Protein Kinase C (PKC) eiwitten. Uit eerder onderzoek is gebleken dat de remming van de activiteit van deze eiwitten een goede strategie is om de groei van UM cellen te stoppen. Het toedienen van deze remmers in de kliniek aan patiënten met uitgezaaid UM leidt echter slechts tot een stop van tumorgroei voor gemiddeld 15 weken in de helft van de patiënten. Hoewel deze resultaten veelbelovend zijn, is er in hoofdstuk 3 gezocht naar nieuwe manieren waarop de groei-remmende effecten van PKC remmers versterkt kunnen worden.

2.3.2. Combinatie met p53 activatie

Hoewel p53 mutaties zeer frequent zijn, varieert het per kankersoort in welke hoeveelheid p53 mutaties aanwezig zijn. In 90% van de eierstoktumoren worden p53 mutaties gevonden, terwijl deze nog nooit zijn gevonden in UM. Deze tumoren gebruiken vaak MDM2 en/of MDMX om p53 te onderdrukken, wat een interessante therapeutische mogelijkheid biedt. Het is namelijk mogelijk om met een 'drug' (Nutlin-3) de remming van p53 door MDMX/MDM2 te voorkomen en daarmee p53 te reactiveren. Door deze MDM2/MDMX inhibitie te combineren met PKC remming werd er een synergistische remming van overleving van verschillende UM cellijnen gevonden. Hieraan lag een omslag van groei-stop naar apoptose ten grondslag. Deze resultaten impliceren dat PKC remming en de bijbehorende positieve effecten in de kliniek versterkt kunnen worden door middel van p53 activatie.

2.3.3. MDMX/PKC δ

De combinatie van p53 activatie en PKC remming is erg effectief in het laboratorium, maar in de kliniek zouden er problemen kunnen ontstaan. Het is namelijk bekend dat

de remming van MDM2 sterke bijwerkingen tot gevolg heeft, die in eerdere klinische studies al tot een vroegtijdige stop van deze studies hebben geleid. Deze sterke bijwerkingen zijn het gevolg van de belangrijke p53-remmende rol die MDM2 heeft in gezonde cellen van het volwassen lichaam. MDMX komt in het volwassen lichaam beduidend minder hoog tot expressie dan MDM2, waardoor het waarschijnlijk is dat specifiek het voorkomen van p53 remming door MDMX in minder bijwerkingen resulteert dan de remming van MDM2 functie. In hoofdstuk 3 is daarom onderzocht of het specifiek remmen van MDMX dezelfde PKC inhibitie-versterkende effecten vertoont als Nutlin-3. Omdat er nog geen specifieke remmer van MDMX bestaat, is er gebruik gemaakt van een 'genetische truc' die leidt tot afwezigheid van MDMX. De resultaten uit hoofdstuk 3 laten zien dat depletie van MDMX de effecten van PKC inhibitie inderdaad versterkt.

Omdat ook PKC remmers vervelende bijwerkingen hebben in patiënten, vroegen we ons af of PKC remming nader gespecificeerd kon worden. De klinisch gebruikte PKC remmers onderdrukken namelijk de activiteit van alle verschillende vormen van deze eiwitten. In overeenstemming met eerder gepubliceerde data laten de resultaten in hoofdstuk 3 duidelijk zien dat afwezigheid van alleen PKC δ voldoende is om de groei van UM cellen te stoppen. Belangrijk in dit hoofdstuk is het bewijs dat p53 activatie synergistisch kan worden versterkt met de depletie van specifiek PKC δ . Concluderend, p53 activatie gecombineerd met PKC inhibitie is een synergistische werkende combinatie in de remming van UM groei, waarvan de potentiële bijwerkingen beperkt kunnen worden door de therapieën specifiek te richten op MDMX en PKC δ .

2.4. Nieuwe strategieën voor de behandeling van uitgezaaide uvea melanomen

2.4.1. EZH2- en HDAC-remming

Naast het optimaliseren van de bestaande therapieën richt dit proefschrift zich ook op het vinden van compleet nieuwe strategieën die gebruik maken van al goedgekeurde medicijnen. De nieuwe strategie bestudeerd in hoofdstuk 4 is gebaseerd op literatuur waarin beschreven wordt dat tumoren zonder expressie van een bepaald gen (BAP1) extra gevoelig zijn voor inhibitie van het eiwit Enhancer of Zeste 2 (EZH2). EZH2 is een onderdeel van het Polycomb Repressive Complex 2, een groep eiwitten die samen de dichtheid van het DNA bepaalt door modificaties aan te brengen op histonen, de eiwitten waarop DNA zit 'opgerold'. Het ontstaan van UM metastases hangt samen met de afwezigheid van expressie van BAP1, met als gevolg dat 80-90% van alle UM metastases geen BAP1 expressie hebben. Deze resultaten tezamen suggereerden dat EZH2 remming een goede therapie zou zijn voor de behandeling van UM metastases. Echter, de resultaten uit een vervolgstudie lieten zien dat UM cellen, onafhankelijk

van BAP1 expressie, ongevoelig waren voor EZH2 inhibitie. In deze studie werden de effecten van EZH2 remming op UM groei tot maximaal 5 dagen bestudeerd. Omdat UM cellen, en zeker die cellen die geen BAP1 meer tot expressie brengen, heel langzaam delen werd het mogelijk geacht dat de effecten van EZH2 remming op langere termijn pas meetbaar zouden zijn.

En inderdaad, de data uit hoofdstuk 4 laten duidelijk zien dat UM cellen wel gevoelig zijn voor EZH2 remming. Deze groei-remmende effecten van EZH2 inhibitie waren echter pas meetbaar na een week of langer. De groeiremming die op lange termijn werd geobserveerd leek sterker te zijn in de BAP1-negatieve cellen, wat selectiviteit voor de metastase suggereert. Dit kon worden gecorreleerd aan de observatie dat de expressie van EZH2 hoger is in BAP1-negatieve tumoren, welke uitzaaiende tumoren of al ontstane metastases vertegenwoordigen.

Een opvallende observatie was dat de het moleculaire effect van EZH2 remming, een vermindering van een histon modificatie, al zichtbaar was na 24-48 uur, terwijl er dan nog geen groeiremming waar te nemen is. De resultaten in hoofdstuk 4 laten zien dat de combinatie van EZH2 remming met de inhibitie van andere histon-modificerende eiwitten, histon-deacetylases (HDACs), leidt tot een synergistische reductie van de overleving van UM cellen. EZH2 remming op korte termijn heeft geen effect op UM groei terwijl HDAC inhibitie leidt tot stop van celdeling. Echter, de combinatie resulteerde niet alleen in een celdelingstop, maar ook in celdood. Het veroorzaken van celdood kan de synergistische afname van de overleving van UM cellen verklaren. De belangrijkste conclusies uit hoofdstuk 4 zijn dat EZH2 wel degelijk effect heeft op de groei UM cellen en dat deze effecten mogelijk sterker zijn in BAP1-negatieve cellen. Het duurt echter lang, dat wil zeggen meerdere celdelingen, voordat EZH2 inhibitie in een verminderde groei van deze cellen resulteert, terwijl in combinatie met HDAC inhibitie wel op korte termijn celdood geïnduceerd kan worden. Daarom wordt in hoofdstuk 4 een combinatie van EZH2 en HDAC-remmers gesuggereerd als potentiële nieuwe therapeutische strategie voor het behandelen van gemetastaseerde UM.

2.4.2. Gecombineerde HDAC en CDK inhibitie

Hierboven zijn de experimenten besproken waarin EZH2 inhibitie wordt gecombineerd met HDAC remming om de groei en overleving van UM cellen te verminderen. Zoals al genoemd leidt HDAC inhibitie tot een celcyclus-stop van UM cellen. Het doel van de resultaten beschreven in hoofdstuk 5 was om dit effect van een HDAC remmer te versterken. Er is voor dit onderzoek gekozen voor de HDAC inhibitor Quisinostat, een experimenteel medicijn dat veelbelovende resultaten liet zien in een fase 1 klinische

studie met melanoom patiënten en ook wordt getest op patiënten met ander type tumoren.

Er is gekozen om Quisinostat te combineren met een remmer van Cyclin-Dependent Kinases (CDKs), genaamd Flavopiridol. CDKs spelen een belangrijke rol in het gecontroleerd laten verlopen van de celcyclus, maar zijn ook essentieel voor de regulatie van expressie van genen. Een goede progressie van de celcyclus is afhankelijk van een strikte volgorde en tijdige activatie en in-activatie van verschillende CDKs. In neuroblastoma cellijnen was al aangetoond dat de remming van CDKs de effecten van HDAC inhibitie kunnen versterken. Zowel Flavopiridol als Quisinostat kunnen alleen al wel een groeistop veroorzaken in UM cellen, maar de combinatie van deze medicijnen remt synergistisch de groei en leidt tot celdood.

CDKs en HDACs zijn niet specifiek ontregeld in UM cellen; deze eiwitten dragen in de meeste kankers op één of andere manier bij aan tumorprogressie. Omdat deze combinatie van medicijnen erg effectief bleek voor UM cellen, werd besloten deze ook te testen op huidmelanoom cellen. En inderdaad, ook huidmelanoom cellen bleken erg gevoelig voor de combinatie van CDK en HDAC remming. Zoals eerder besproken bestaat de huidige behandeling van BRAF-gemuteerde melanoom uit het specifiek remmen van dit geactiveerde onco-eiwit. Hoewel dit vaak erg effectief is voor een paar maanden, ontwikkelt de kanker bijna zonder uitzondering resistentie. Naast de diverse melanoom typen, gedreven door verschillende activerende mutaties, hebben we gekeken of het effect van deze combinatie anders is voor BRAF-gevoelige en -resistente cellen. Alle geteste melanoom cellen bleken zeer gevoelig voor de gecombineerde CDK- en HDAC-inhibitie.

Om de effectiviteit van gecombineerde CDK- en HDAC-remming in een meer klinische setting te testen is er gebruik gemaakt van een muismodel. In dit model groeit een menselijke huidmelanoom subcutaan (onderhuids) in muizen. Deze muizen met tumoren werden behandeld met óf alleen Quisinostat, óf alleen met Flavopiridol óf met de combinatie óf werden niet behandeld. Flavopiridol remde de groei van de tumoren terwijl Quisinostat alleen de groei al bijna volledig kon voorkomen. Daarom was er weinig toename in effectiviteit van de combinatie van remmers waar te nemen. Bovendien waren de moleculaire effecten van Flavopiridol in de tumorcellen van behandelde muizen niet goed detecteerbaar, hetgeen suggereert dat om synergistische effecten te zien er een hogere concentratie of toedieningsfrequentie van Flavopiridol gekozen dient te worden. Een belangrijk aspect om rekening mee te houden bij het bestuderen van synergistische combinaties is de aanwezigheid van negatieve bijwerkingen. Het gebeurt namelijk regelmatig dat niet alleen de anti-kanker-effecten

versterkt worden door een combinatie van medicijnen zoals onderzocht is in het laboratorium, maar in een patiënt ook de negatieve effecten synergistisch worden versterkt. Echter, een aantal muizen behandeld met Quisinostat, Flavopiridol of de combinatie hiervan werden uitgebreid onderzocht door een patholoog en er bleek amper verschil te zijn tussen de behandelingen. Dus, de combinatie van CDK en HDAC remmers zou een relatief veilige en veelbelovende nieuwe strategie kunnen zijn voor de behandeling van verschillende soorten melanoom, ook die met ontwikkelde BRAF resistentie.

3. Algemene conclusies en klinische implicaties

De studies beschreven in dit proefschrift dragen bij aan het beter begrijpen van kanker en bieden nieuwe perspectieven voor het behandelen van gemetastaseerde UM patiënten. Het ontrafelen van de functies van MDMX heeft geleid tot nieuwe inzichten en kan in de toekomst leiden tot nieuwe therapeutische strategieën. In het bijzonder zal de mogelijke regulatie van FOXO transcriptie factoren door MDMX tot vervolg onderzoek leiden, met potentieel interessante klinische mogelijkheden. De huidige strategieën om gemetastaseerde UM te behandelen zijn niet effectief en worden gekenmerkt door bijwerkingen. Dit proefschrift geeft diverse mogelijkheden om de huidige therapieën te verbeteren en compleet nieuwe strategieën die in overweging genomen kunnen worden. Echter voor de optimalisatie van de huidige therapieën dienen nieuwe medicijnen ontwikkeld te worden, hetgeen nog tijd, geld en vervolg studies gaat kosten om te realiseren. Ook de nieuwe strategieën gebaseerd op bestaande medicijnen dienen nog beter te worden bestudeerd voordat ze als vervanging van de huidige therapieën kunnen dienen.

Curriculum Vitae

Renier Heijkants was born in Amersfoort, the Netherlands, on May 20th, 1989. In 2006 he graduated from the Dongemond College in Raamsdonksveer and started his studies on Biomedical Laboratory Research at Avans Hogeschool Breda. As part of this education he performed an internship in the group of Jos Jonkers, under the supervision of Marco Koudijs, at the NKI-AVL in Amsterdam in 2009. Later that year he started his second internship in the group of Marcel Tijsterman at the Leiden University Medical Center in Leiden, under the supervision of Bennie Lemmens. After receiving his Bachelor of Applied Sciences degree in 2010, Renier decided to continue his education in Leiden. He successfully completed the pre-master programme and started his Master's studies on Biomedical Sciences in Leiden in 2011. The first internship performed for these studies was executed in the group of David Glover at Cambridge University in Cambridge (UK) in 2012, under the supervision of Zoltan Lipinszki. His final internship was performed in 2013 in the group of Peter ten Dijke, under the supervision of Luuk Hawinkels. In that same year the Master's degree was obtained and he started his PhD in the group of A.G. Jochemsen, which resulted in the research described in this thesis.

List of publications

Heijkants R.C., Teunisse A.F.A.S, de Jong D, Mei H, Kielbasa S, Szuhai K, Jochemsen A.G. MDMX regulates transcriptional activity of p53 and FOXO.

Manuscript in preparation

Heijkants R.C., Teunisse A.F.A.S, Jochemsen A.G.

Inhibition of EZH2 affects uveal melanoma cells proliferation, and survival in combination with HDAC inhibitors.

Submitted manuscript

Heijkants R.C., Teunisse A.F.A.S, de Vries J, Ovaa H, Jochemsen A.G.

Selective PKC δ inhibitor B106 elicits uveal melanoma growth inhibitory effects independent of activated PKC isoforms.

Accepted for publication in ACS Chemical Biology.

Cao J, Pontes K.C.S, **Heijkants R.C.**, Brouwer N.J, Groenewoud A, Jordanova E, Marinkovic M, van Duinen S, Teunisse A.F.A.S, Snaar-Jagalska E, Jochemsen A.G, Jager M.J.

Overexpression of EZH2 in conjunctival melanoma offers a new therapeutic target
J Pathol. 2018 Aug. 245(4):433-444

Heijkants R.C., Hart 't K, Nieveen M, Teunisse A.F.A.S, Jochemsen A.G.

Targeting MDMX or PKC δ to enhance current anti uveal melanoma strategies.

Oncogenesis. 2018 Mar 29. 7(3):33

Heijkants R.C., Willekens K, Schoonderwoerd M.J.A, Teunisse A.F.A.S, Nieveen M, Hawinkels L.J, Marine J.C, Jochemsen A.G.

Combining CDK and HDAC inhibition synergistically kills melanoma cells.

Oncotarget. 2017 Dec 15. 9(5):6174-6187.

Paauwe M, **Heijkants R.C.**, Oudt C.H, van Pelt G.W, Cui C, Theuer C.P, Hardwick J.C, Sier C.F, Hawinkels L.J.

Endoglin targeting inhibits tumor angiogenesis and metastatic spread in breast cancer.

Oncogene. 2016 Aug 4. 35(31): 4069-4079.

Cao J, **Heijkants R.C**, Jochemsen A.G, Dogrusöz M, de Lange M.J, van der Velden P.A, van der Burg S.H, Jager M.J, Verdijk R.M.

Targeting of the MAPK and AKT pathways in conjunctival melanoma shows potential synergy.

Oncotarget. 2016 Jul 22. 22;8(35):58021-58036.

Hawinkels L.J, de Vinuesa A.G, Paauwe M, Kruithof-de Julio M, Wiercinska E, Pardali E, Mezzanotte L, Keereweer S, Braumuller T.M, **Heijkants R.C**, Jonkers J, Löwik C.W, Goumans M.J, ten Hagen T.L, ten Dijke P.

Activin Receptor-like Kinase 1 Ligand Trap Reduces Microvascular Density and Improves Chemotherapy Efficiency to Various Solid Tumors.

Clin Cancer Res. 2016 Jan 1. 22(1): 96-106.

Dankwoord

Dan is het nu tijd voor het meest gelezen stuk van ieder proefschrift. Hiervoor denk ik met plezier terug aan een mooie tijd, aan al die lieve en aardige mensen die ik de afgelopen jaren heb leren kennen en aan iedereen die heeft meegeholpen aan de totstandkoming van dit boekje. Ik ben zo veel mensen erg dankbaar dat het onmogelijk is om iedereen persoonlijk te bedanken, dus ik zal het proberen bondig te houden zonder te kort te doen aan de enorme waardering die ik heb voor iedereen.

Allereerst, AG bedankt voor alles! Bedankt dat ik onder jouw vleugel een 'volwassen' wetenschapper mocht worden. Ik had me geen betere copromotor kunnen wensen die met zijn uiterst kritische blik, no-nonsense commentaar, constante stroom ideeën en energie mij altijd heeft kunnen motiveren. Dat we buiten het lab om ook goed met elkaar overweg konden is iets wat ik al die jaren ook zeer heb gewaardeerd.

Peter, bedankt dat je mijn promotor wilde zijn. Ik heb jouw input en begeleiding erg gewaardeerd. Ook wil ik graag mijn begeleidingscommissie, Martine en Alfred, bedanken voor het in de gaten houden van mijn progressie gedurende mijn PhD traject. Daarnaast wil ik deze gelegenheid gebruiken om iedereen van andere afdelingen/instituten, waar ik met veel plezier mee heb samengewerkt om tot mooie publicaties en hoofdstukken te komen, te bedanken (Chris, Karen, Luuk, Mark en Cao).

Iedereen met wie ik gedurende mijn PhD het lab heb gedeeld verdient een enorm groot compliment. De sfeer op het lab was zeker een bepalende factor waardoor ik iedere dag met plezier naar mijn werk kwam. Amina, jij verdient zeker een speciale vermelding. Jij stond altijd voor me klaar en hebt in mijn afrondende fase vele 'laatste' proeven afgemaakt zodat ik me kon richten op de totstandkoming van dit proefschrift. Dit is iets wat ik enorm waardeer. Maaike, wij gingen samen het PKC stuk 'eventjes' afmaken, waarnaast we ook nog aan diverse andere projecten hebben gewerkt. Ik wil je graag bedanken voor deze fijne samenwerking. Daarnaast wil ik graag alle studenten, die ik voornamelijk kennis heb laten maken met het FACS apparaat (Joyce, Valentina, Mouraya, Valerie en Daan), bedanken voor de mooie tijd. Een speciaal dankwoord voor 'mijn' studenten Kelly en Manon is op zijn plaats. Jullie vielen onder mijn directe begeleiding en hebben altijd vol enthousiasme mijn eindeloze ideeën en suggesties verwerkt in jullie projecten. Ik vond het erg leuk en leerzaam om jullie begeleider te zijn, bedankt hiervoor.

Graag wil ik ook mijn collega's van het 'oude' MCB bedanken voor een fantastische tijd en alle hulp die ik van jullie gehad heb tijdens mijn experimenten. Dat ik hele mooie

en bijzondere collega's had blijkt wel uit de fantastische borrels, LUMC zomerfeesten, voetbaltoernooien, hardloopwedstrijden, surfavonden, MCB dagjes uit, housewarmings en reizen die we samen hebben gemaakt. Roman, Danielle, Frauke, Maarten T, Timo, Vera, Marjolein, Amiet, Tobias, Aleks, Karo, Ivo, Joost, Minnie, Tamara, Jessie, Sumit, Fredrik en Matty bedankt voor deze fantastische avonturen! Madelon, jou zou ik graag nog in het bijzonder willen bedanken voor alle kopjes koffie door de jaren heen, waarbij we alles konden bespreken en relativeren zelfs nu jij in het verre Glasgow woont. Op momenten waarop dat nodig was stonden twee collega's altijd voor mij klaar. Edwin en David bedankt dat jullie er altijd voor me waren en dat jullie mijn paranimfen willen zijn. Zonder enige twijfel had mijn PhD periode er zonder jullie heel anders uitgezien en ik ben jullie erg dankbaar voor de mooie tijd en herinneringen die we samen hebben gemaakt.

Om aan het lab te ontsnappen kon ik altijd terecht bij mijn vrienden van het eerste uur Maarten W, Tim en Lucas. Hoewel ik er in de laatste periode van mijn PhD niet erg meer aan toe kwam wil ik jullie toch graag heel erg bedanken voor de nodige afleiding. Ook afspraakjes met 'de beertjes' waren voor mij van grote waarde gedurende dit traject, Christian, Stefanie, Juna, Martijn, Lisanne, Lizanne, Arjan, Hazal, Roel, Kathy en Ishan super bedankt! Daarnaast wil ik ook de familie Cuijpers bedanken voor de leuke uitjes en weekenden.

Lieve familie. Papa en Mama, Marike en Peter, Ceciel en Wouter. Wat ben ik jullie enorm dankbaar dat jullie er altijd voor mij waren. In goede en in slechte tijden vormen jullie altijd een veilige plek om alles te bespreken. Ook al snapten jullie niet altijd het onderwerp, de proef of andere stress situatie, ik kon toch altijd rekenen op jullie steun. Dit is voor mij van onschatbare waarde geweest de afgelopen jaren.

En dan als allerlaatste mijn allerliefste Sabine. Ik kan zonder overdrijven stellen dat dit hele traject doorlopen zonder jou nooit was gelukt. Wat hebben we samen veel meegemaakt tijdens onze PhD en, hoewel het niet altijd zo voelde, zijn we er allebei sterker en slimmer uitgekomen. Bedankt dat je er altijd voor mij bent om mijn hart te luchten en bovendien om mee te lachen. BEDANKT!

List of Abbreviations

Combination index	CI
Combined binary ratio fluorescence in situ hybridization	COBRA-FISH
Cutaneous melanoma	CM
Cyclin dependent kinase	CDK
Cysteinyl Leukotriene Receptor 2	CYSLTR2
Cytoplasmic FMR1 interacting protein 2	CYFIP2
Cytotoxic T-lymphocyte antigen-4	CTLA-4
Diacylglycerol	DAG
DP, RB-like, E2F4 and Muvb	DREAM
Ectodysplasin a2 receptor	EDA2R
Enhancer of zeste homolog 2	EZH2
Excess over bliss	EoB
Exonuclease 1	EXO1
EZP011989	EPZ
Fetal calf serum	FCS
Forkhead box	FOX
Gene ontology	GO
Glutamic acid	E
Glutamine	Q
Histone deacetylase	HDAC
Hyaluronan synthase 2	HAS2
Immunohistochemical	IHC
Inositol 1,4,5-trisphosphate	IP3
Kinesin family member 23	KIF23
Max dimerizing protein 4	MXD4
MDMX short transcript isoform	MDMX-S
Mechanistic target of rampamycin kinase	MTOR
Minichromosome maintenance 10 replication initiation factor	MCM10
Mitotic arrest deficient 2 like 1	MAD2L1
Mouse double minute	MDM
Myristolated alanine rich protein kinase c substrate	MARCKS
p53 reactivation and induction of massive apoptosis	PRIMA
p53 upregulated modulator of apoptosis	PUMA
Patched domain containing 4	PTCHD4
Patient-derived tumor xenograft	PDX
Phosphatidylinositol 3 kinase	PI3K
Phosphatidylinositol 4,5-bisphosphate	PIP2

Phosphoinositide-3-kinase interacting protein 1	PIK3IP1
Phospholipase C Beta 4	PLCB4
Poly(ADP-ribose) polymerase 1	PARP
Polycomb repressive complex 2	PRC2
Propidium iodide	PI
Protein kinase C	PKC
RAS Guanyl Releasing Protein 3	RASGRP3
Receptor tyrosine kinase	RTK
Splicing factor 3B subunit 1	SF3B1
Tazemetostat	TZMS
Tetraspanin 11	TSPAN11
Tri-methylation histone 3 at lysine 27	H3K27me3
Tumor protein p53 inducible nuclear protein 1	TP53INP1
Ubiquitin specific protease	USP
Uveal melanoma	UM
Valine	V
Vascular endothelial growth factor	VEGF
Zinc finger matrin-type 3	ZMAT3